



CK06-06
D/V CHIKYU SHAKEDOWN CRUISE
OFFSHORE SHIMOKITA
LABORATORY OPERATION REPORT



CK06-06

D/V *Chikyu* Shakedown Cruise

Offshore Shimokita

Laboratory Operation Report



January 2007

**Science and Planning Department
Center for Deep Earth Exploration**

Edited by

Kan Aoike

Science and Planning Department
Center for Deep Earth Exploration

Contents

I. Introduction.....	1
1.1. Objectives of Laboratory System Integration Test.....	1
1.2. Scientific Objectives.....	2
1.3. Summary of Drilling Operations.....	4
1.4. Geologic Background.....	6
II. Overview of LSIT.....	9
2.1. Staffing.....	9
2.2. Core Flow, Measurements and Experiments.....	12
2.2.1. Outline of Laboratory Operation and Core Flow.....	12
2.2.2. Core Processings and Measurements.....	15
2.2.3. Discrete Sample Measurements.....	16
2.2.4. Additional Experiments.....	17
2.3. Conditions and Procedures of Instrumental Analyses.....	18
2.3.1. Routine Core measurements.....	18
2.3.2. Routine Discrete Sample (Solid and Gas) Measurements.....	22
2.3.3. Interstitial Water Chemistry.....	28
2.4. Technical Remarks on Measurement Results.....	31
2.4.1. Bulk Density.....	31
2.4.2. Total Organic Carbon and Total Inorganic Carbon.....	32
2.4.3. Chloride.....	32
2.4.4. Paleomagnetic Polarity.....	32
2.5. Summary of LSIT.....	34
III. Preliminary Scientific Results.....	35
3.1. Recovery of Methane Hydrates.....	35
3.2. Lithostratigraphy.....	36
3.2.1. Lithologic Units.....	36
3.2.2. Age Model.....	40
3.3. A Constraint to Late Quaternary Volcanic Activities of Northeast Japan.....	43
3.4. Implications for Late Quaternary Paleoenvironmental Variation of Northeast Japan Forearc Region.....	44
3.4.1. Two Major Clays.....	44

3.4.2. Periodic Paleoenvironmental Variations.....	46
References.....	48
IV. Curatorial Report.....	49
4.1. Summary.....	49
4.2. Core Recovery.....	50
4.3. Sample Request.....	51
4.4. Samples.....	52
4.5. Inventory.....	54
4.6. Shipments.....	54
4.7. Residue Distribution.....	55
4.8. Action Items for Curator and Superintendents.....	56
4.9. Problems Encountered.....	56
4.9.1. Partial Loss of Sample.....	56
4.9.2. Bent Core Liner.....	57
4.9.3. Twisted and Broken Liner.....	58
4.9.4. Handling of Carbonate Nodule.....	60
4.9.5. Pebble.....	60
4.10. Other Problems.....	61
Appendix.....	63
V. Laboratory Data management Report.....	65
5.1. Goals.....	65
5.2. Targets and Methods.....	65
5.2.1. J-CORES System.....	65
5.2.2. Web Directory to Collect Raw Data.....	65
5.2.3 Material Registration.....	66
5.2.4. Visual Core Description.....	66
5.2.5. Biostratigraphy.....	66
5.2.6. Provisional Archiving System of X-ray CT Scanning Image.....	66
5.2.7. The Other Instrumental Measurements in the Laboratory.....	67
5.2.8. Wireline Logging Data.....	67
5.2.9. Mud Logging Data.....	68
5.2.10. Drilling Parameters.....	68
5.3. Results.....	68

5.3.1. Data Quantities.....	68
5.3.2. Server Hardware Troubles.....	69
5.3.3. J-CORES Software Issues.....	69
5.3.4. Limitation of the Provisional Archiving system of X-ray CT Scanning Image.....	70
5.4. Summary.....	70
VI. Shipboard Scientific Party Report	
6.1. Routine Sampling.....	71
6.2. Methane-hydrate Sampling.....	71
6.3. Sample Preparations.....	71
6.4. pH and Alkalinity Measurement.....	72
Appendix.....	73
1. Core Photo Images	
2. X-ray CT Images	
3. Onboard Measurement Results	
4. Visual Core Description	

I. Introduction

1.1. Objectives of Laboratory System Integration Test

The D/V *Chikyu* Shakedown Cruise, CK06-06, was carried out in offshore Shimokita area from 6 August to 26 October 2006 to implement System Integration Tests (SIT) for deepwater riser drilling, piston coring, extended shoe coring, and rotary coring, as well as various shipboard systems relevant to drilling operations and laboratory measurement. The shakedown cruise took place in an extensively surveyed area offshore of the Shimokita Peninsula, on the northeast coast of Honshu, Japan (Fig. 1.1). Laboratory activities included a wide array of experiments related to processing, curating, measuring of cores, as well as collection and processing of data from discrete samples. All laboratory work was based on operations conducted under actual conditions using cores during the drilling SIT, and this operation was termed a “Laboratory System Integration Test (LSIT)”. The LSIT includes following operational items:

- i) core processing with instrumental analyses, visual core description (VCD) and sampling,
- ii) discrete sample processing and instrumental analyses,
- iii) cuttings processing and instrumental analyses,
- iv) biostratigraphic analyses
- v) curation,
- vi) data integration with J-CORES,
- vii) collecting samples for scientific purposes proposed by the scientific party, and
- viii) evaluation of laboratory setup.

By conducting these items, the major goals to be achieved in LSIT were:

- 1) to carry out processing/measurements on core and discrete samples in order to demonstrate the ability to meet IODP operation standards and minimum measurement requirements using real core and cuttings samples.

- 2) to familiarize laboratory staff with all analytical equipment onboard, including use of database system.
- 3) to investigate and establish efficient workflows and analytical procedures through routine measurements and experiments.
- 4) to identify issues, items and areas that should be solved/improved/developed over the coming months prior to IODP operations.
- 5) to obtain data for scientific use.

Five technical staff from USIO and 22 scientists from Japanese and foreign geological communities (Japan: 11, foreign countries: 16) were invited as technical/scientific advisors in order to assist in evaluation and critical observation of the laboratory operation. These advisors and observers came on board in relays during this cruise. Additionally, a scientific party focused mainly on subseafloor microbiology and geochemistry, as discussed later in this document, was organized internally by JAMSTEC and related institutions; 8 members came rotated on board over the course of the LSIT.

1.2. Scientific Objectives

Although this shakedown cruise was not designed as a scientific investigation, a scientific party (Chief scientist: Ken Takai, XBR/JAMSTEC) was organized prior to the cruise to utilize recovered cores for scientific purposes. The scientific goals of this cruise were primarily dedicated to deep biosphere and subseafloor ocean initiatives (some targets originally considered prior to the cruise were not attained during the coring SIT). Although available samples are restricted to relatively shallow formations, major scientific objectives to be achieved using the cores are:

- 1) to obtain functionally active microbial cultures, cells or molecular signatures from the cored formations,
- 2) to distinguish the depth-dependent microbial populations of dead, dormant and living cells,
- 3) to construct microbial metagenomic libraries from the subseafloor biosphere for the first time,

- 4) to estimate the resource potential and magnitude of subseafloor methane hydrate deposits,
- 5) to resolve the mechanisms of generation, transportation and enrichment of methane associated with either lithological and hydrogeologic properties, and
- 6) to retrieve paleoenvironmental records and paleomes (ancient biomolecular assemblages).

Based on the litho-stratigraphy suggested by previous scientific coring, exploration drilling and CDEX site surveys, two scientific target areas were the major focus investigation; (a) near-surface anoxic sulfate-reducing, methane-oxidation zone energized by input of methane (approx. 0-70 mbsf) and (b) bottom-simulating reflector (BSR) zone associated with formation of methane hydrate (approx. 100-400 mbsf). Intensive sampling of whole round core (WRC) samples (see IV. Curatorial Report) for interstitial fluid chemistry and microbiology was conducted onboard, immediately following delivery of core to the laboratory. Any bulk methane hydrate deposits were also sampled as WRC and were stored in liquid nitrogen. The cores were then subjected to routine onboard instrumental sampling and measurement procedures required for investigation of the, broad, multidisciplinary aspects of ocean drilling science such as chronological stratigraphy, geochemistry, sedimentology and paleoenvironmental analysis. The first onshore sampling party will be held at the Kochi Core Center at a time to be determined through consultation between the scientific party and the science services group at CDEX.

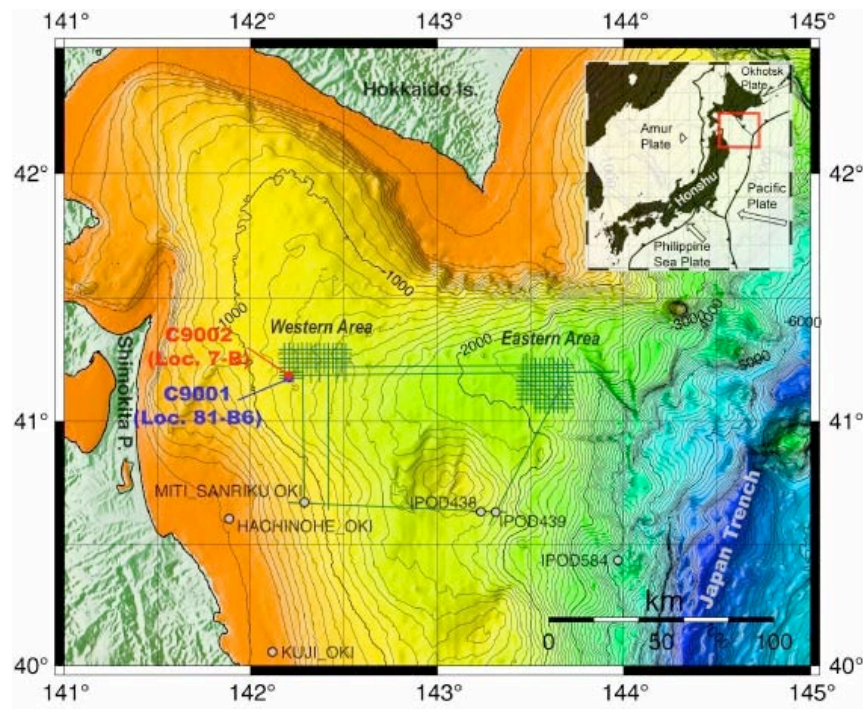


Fig. 1.1. Index map showing the Drilling/Coring SIT site offshore of the Shimokita peninsula, with bathymetry, seismic survey tracklines and existing borehole locations. HPCS coring locations C9001 and C9002 were drilled in late November 2005. Inset map shows the tectonic plate configuration around the Japanese Islands (after Taira, 2001) and the location of the detailed map (red square).

1.3. Summary of Drilling Operations

CK06-06 cruise was carried out from 6 August to 26 October 2006. The cruise met with many difficulties such as severe sea conditions and mechanical troubles; the planned operations were forced to delay considerably. In particular, a very strong low pressure that hit the area on from 6 to 7 October caused a harsh situation that LMRP (Lower Marine Riser Package, the upper portion of the Blowout Preventer system) was seriously damaged. Consequently, the situation compelled to abandon further drilling. In the last results, the coring operation test was conducted by riserless drilling with the HPCS (Hydraulic Piston Coring System) and ESCS (Extended Shoe Coring System) at a pilot hole, C9001C, 1180 m in water depth, penetrating to 365 mbsf and recovering 40 cores (386 m in total length), not reaching the initial target depth, 520 mbsf. The riser

drilling test at the main hole, C9001D, finished at a depth of 647 mbsf, far shallow to that originally targeted at 2200 mbsf. Cuttings samples, however, were obtained from intervals between 527 - 647 mbsf. Despite of this drilling result, five major SIT items, that is, 1) casing and cementing, 2) running riser and BOP (Blowout Preventer), 3) conducting EDS (Emergency Disconnect Sequence), 4) running CDEX coring systems, and 5) conducting wireline logging operations, were successfully completed in the essential parts. Results of the drilling operations in this cruise are outlined below. Detailed technical reports on the drilling operations and the SIT are provided separately from CDEX.

C9001B (pilot hole)

Position: 41°10.6254'N, 142°12.095'E

Start Hole: 09:00, 15 August 2006

End Hole: 06:25, 16 August 2006

Time on Hole: 21.4 hours

Water Depth: 1180 mbsf

Penetration: 540 mbsf (no coring; conducted for flow check)

C9001C (pilot hole)

Position: 41°10.6380'N, 142°12.081'E

Start Hole: 11:30, 18 August 2006

End Hole: 16:00, 23 August 2006

Time on Hole: 124.5 hours (5.2 days)

Seafloor: 1208.47 mbrf

Total Depth: 1573.80 mbrf

Elevation (distance between rig floor and draft): 28.0 m

Water Depth: 1180.47 m

Penetration: 365.33 m (Plan: 520 mbsf)

Coring Totals:

HPCS coring I: 0 ~ 301.66 mbsf

33 cores; Cored: 301.66 m; Recovered: 326.54 m; Recovery: 108 %

ESCS coring: 301.66 ~ 339.66 mbsf (conducted for SIT)

3 cores; Cored: 38.00 m; Recovered: 25.63 m; Recovery: 67 %

(Loss of core at the interval of 338-340 mbsf, Core 36X)

HPCS coring II: 339.66 ~ 365.33 mbsf

3 cores; Cored: 25.67 m; Recovered: 26.81 m; Recovery: 104 %

(Loss of tool at the hole bottom; finished in abandonment of hole)

Total coring:

40 cores; Cored: 365.33 m; Recovered: 385.90 m; Recovery: 106 %

(See Table 1 in V. Curatorial Report for details)

C9001D (main hole)

Position: 41°10.5984'N, 142°12.0328'E

Start Hole: 03:00, 28 August 2006

End Hole: 19:00 25 October 2006

Time on Hole: 1408 hours (58.7 days)

Seafloor: 1208 mbrf

Total Depth: 1855 mbrf

Elevation (distance between rig floor and draft): 28.0 m

Water Depth: 1180 m

Penetration: 647 mbsf (Plan: 2220 mbsf)

Jetting-in: 0 ~ 522 mbsf (set 36" and 20' casings)

Mud Logging: 522 ~ 647 mbsf

Duration: 6:35, 05 October 2006 ~ 12:35, 05 October 2006

1.4. Geological Background

This area is a place affected strongly by the Oyashio current, one of the major cold currents, and collaterally by a warm branch current of the Tsushima current flowing through the Tsugaru Strait. As for the geological setting, the drill site is located in a forearc basin formed by the subduction of the Pacific Plate (~8 cm/year, WNW plate motion vector: Seno et al., 1994) beneath northeastern Honshu, Japan (Fig. 1.1), forming the northernmost segment of the Japan Trench. The Hadaka Trough, a sedimentary basin formed by subsidence in the drilling area, originates just offshore southwest Hokkaido and extends to the Japan Trench. Along the coastal area of the Shimokita Peninsula, both sedimentary and volcanic rocks younger than late Cretaceous lie scattered on Triassic to early Cretaceous sedimentary rocks or Cretaceous granites.

Miocene deposits, which are the uppermost in this section, unconformably overlie the folded older strata.

Anomalous bottom-simulating reflectors (BSR) suggesting the occurrence of methane hydrates are observed at several locations in the Northeast Japan forearc basin, as shown in many seismic profiles including those obtained by CDEX. The BSRs in this region, situated around 400-600 mbsf, are associated with pull-up and pull-down reflection features, and chimney-like vertical blanking zones. These features strongly suggest dense but heterogeneous accumulation of methane hydrates in sediments around 600 mbsf, and generation and migration of methane-bearing fluids throughout the area.

II. Overview of LSIT

System setup of the Laboratory Area has been ongoing since the ship was delivered (July, 2005) and the first LSIT was conducted during the Hydraulic Piston Coring System (HPCS) coring test cruise in 2005 (Figure 1). Processing of ~127 meters of core was conducted at that time. The LSIT of this cruise was expected to be the first trial to handle cores obtained during riser drilling, however, as a result of mechanical problems and weather delays, the only core samples that we obtained were collected in riserless mode with HPCS and ESCS (Extended Shoe Coring System) and the total recovered core length was 386 m (365 m penetration) at Hole C9001C. Cuttings samples were obtained from 25 intervals from 527 to 647 mbsf at Hole C9001D during riser drilling test SIT.

2.1. Staffing

Laboratory staffs from CDEX and Marin Works Japan (MWJ) embarked in alternate shifts at intervals of two to three weeks. In addition to them, invited technical/scientific advisors were onboard generally for one week. The scientific party members from JAMSTEC and related institutions were onboard for one to three weeks during the former half of the cruise. Shipboard participant are listed in Table 2.1. CDEX and MWJ staffing for the laboratory in each phase by was generally as follows:

- Lab Manager: 2 persons (CDEX)
- Lab Technician: 5 persons x 2 teams (MWJ)
- Curator: 1 person (CDEX and MWJ)
- Database Specialist: 1 person (CDEX and MWJ)
- Supervisor: 0 ~ 1 person (CDEX)

Additionally, the invited advisors and the scientific party members was as follows:

- USIO staff: 5 persons
- Invited Advisor: 11 persons from Japan and 16 persons from foreign countries
- Scientific Party: 8 persons.

Table 2.1a. Shipboard participants of CDEX and MWJ.

Name	Affiliation	Role	Duration
Kan Aoike	CDEX	Lab Manager / Prime Investigator / VCD	25 Aug. – 15 Sep., 6 Oct. – 26 Oct.
Daniel Curewitz	CDEX	Lab Manager	6 Aug. – 25 Aug.
Takamitsu Sugihara	CDEX	Lab Manager	6 Aug. – 25 Aug.
Philippe Gaillot	CDEX	Lab Manager	25 Aug. – 15 Sep.
Hideki Masago	CDEX	Lab Manager	15 Sep. – 6 Oct.
Moe Kyaw Thu	CDEX	Lab Manager	15 Sep. – 6 Oct.
Lallan P. Gupta	CDEX	Curator	6 Aug. – 25 Aug.
Satoshi Hirano	MWJ	Curator	25 Aug. – 15 Sep.
Kyoma Takahashi	CDEX	Database Specialist	25 Aug. – 8 Sep.
Yhoshihiro Shiga	CDEX	Database Specialist	6 Aug. – 23 Aug., 8 Sep – 22 Sep.
Yohei Arakawa	MWJ	Database Specialist	9 Aug. – 25 Aug., 22 Sep. – 13 Oct.
Kazuhiro Sugiyama	MWJ	Lab Technician / Cruise Leader	
Toshikatsu Sugawara	MWJ	Lab Technician / Cruise Leader	
Hiroaki Muraki	MWJ	Lab Technician / Cruise Leader	
Kazuhiro Hayashi	MWJ	Lab Technician / Cruise Leader	
Toshikatsu Kuramoto	MWJ	Lab Technician / Cruise Leader	
Soichi Moriya	MWJ	Lab Technician	
Takahiro Suzuki	MWJ	Lab Technician	
Yoshiki Kido	MWJ	Lab Technician	
Tomomi Kondo	MWJ	Lab Technician	
Yoshifumi Noiri	MWJ	Lab Technician	
Toru Fujiki	MWJ	Lab Technician	
Shunsuke Miyabe	MWJ	Lab Technician	
Tomoko Maruyama	MWJ	Lab Technician	
Ryo Kurihara	MWJ	Lab Technician	
Hideki Mukoyoshi	MWJ	Lab Technician	
Tomoyuki Tanaka	MWJ	Lab Technician	
Lena Maeda	MWJ	Lab Technician	
Masahiro Nishimura	MWJ	Lab Technician	
Masumi Ishimori	MWJ	Lab Technician	
Kentaro Shiraishi	MWJ	Lab Technician	
Shin'ichi Kuramoto	CDEX	Supervisor	1 Oct. – 5 Oct.
Masahiro Shiraki	CDEX	Supervisor	30 Aug. – 9 Sep.
Kazushi Kuroki	CDEX	Supervisor	6 Aug. – 24 Aug.

Table 2.1b. Shipboard participants as technical/scientific advisor.

Name	Affiliation	Specialty/Role	Duration
John Firth	IODP-USIO	Curation	9 Sep. – 14 Sep.
Steven Prinz	IODP-USIO	Curation	6 Aug. – 18 Aug.
Phi Rumford	IODP-USIO	Curation	9 Sep. – 14 Sep.
Keith Gentry	IODP-USIO	Curation	6 Aug. – 24 Aug.
Rachel Culberson	IODP-USIO	Curation	9 Sep. – 14 Sep.
Hiroki Hayashi	Shimane Univ.	Paleontology / VCD	25 Aug. – 9 Sep.
Noritoshi Suzuki	Tohoku Univ.	Paleontology / VCD	24 Aug. – 31 Aug.
Toshiaki Maruyama	Yamagata Univ.	Paleontology	11 Aug. – 18 Aug.
Yoshiakki Aita	Utsunomiya Univ.	Paleontology	18 Aug. – 24 Aug.
Hiroshi Nishi	Hokkaido Univ.	Paleontology	9 Sep. – 15 Sep.
Gaku Kimura	Univ. of Tokyo	Structural Geology	11 Aug. – 17 Aug.
Juichiro Ashi	Univ. of Tokyo	Physical Properties	25 Aug. – 30 Aug.
Nobuo Morita	Waseda Univ.	Geophysics	18 Aug. – 23 Aug.
Hirokuni Oda	AIST	Paleomagnetism	24 Aug. – 30 Aug.
Saneatsu Saito	IFREE, JAMSTEC	Logging	15 Sep. – 21 Sep.
Masataka Kinoshita	IFREE, JAMSTEC	Logging	22 Sep. – 29 Sep.
Hyesu Yun	Chungnam National Univ.	Paleontology	18 Aug. – 23 Aug.
Seigfried Lallemand	Univ. of Cergy	Structural Geology	21 Sep. – 1 Oct.
Elizabeth J. Screaton	Univ. of Florida	Hydrogeology	11 Aug. – 17 Aug.
Demian Saffer	Pennsylvania State Univ.	Physical Properties	21 Sep. – 1 Oct.
Achim J. Kopf	Bremen Univ.	Physical Properties	9 Sep. – 15 Sep.
Harold J. Tobin	New Mexico Tech	Geophysics	28 Aug. – 5 Oct.
Michael Underwood	University of Missouri	Sedimentology	9 Sep. – 15 Sep.
Christian Wilson	British Geological Survey	Geology	5 Oct.- 13 Oct.
Meixun Zhao	Tonghi Univ.	Geochemistry	24 Aug. - 30 Aug.
Jong-Gwon Yum	NCIURF, Seoul Nat. Univ.	Geochemistry	24 Aug. – 30 Aug.
Gary Acton	Univ. of California, Davis	Paleomagnetism	24 Aug. – 30 Aug.

Table 2.1c. Shipboard participants of the scientific party

Name	Affiliation	Role	Duration
Fumio Inagaki	XBR, JAMSTEC	Microbiology	6 Aug. – 26 Aug.
Hitoshi Tomaru	XBR, JAMSTEC	Interstitial water chemistry	6 Aug. – 26 Aug.
Hiroyuki Imachi	XBR, JAMSTEC	Microbiology	10 Aug. – 26 Aug.
Rika Takeuchi	XBR, JAMSTEC	Interstitial water chemistry	18 Aug. – 26 Aug.
Tatsuhiko Sakamoto	IFREE, JAMSTEC	Sedimentology / VCD	24 Aug. – 1 Oct.
Weiren Lin	KCC, JAMSTEC	Geophysics	15 Sep. – 22 Sep.
Noriaki Masui	KCC, JAMSTEC	Microbiology	15 Sep -
Shigeki Ogihara	Univ. of Tokyo	Interstitial water chemistry	6 Aug. – 18 Aug.

2.2. Core Flow, Measurements and Experiments

2.2.1. Outline of Laboratory Operation and Core Flow

All experimental instruments available were run in order to examine the operational and analytical procedures and to evaluate those in terms of data quality, machine calibration and standardization, and preparation/operation methodology. These observations and the data collected will be used to assess and meet the upcoming QA/QC requirements for IODP operations, and comprise the main part of LSIT. We operated as if the shakedown cruise were an IODP operation, and carried out all IODP minimum measurements, some IODP standard measurements that are available as of now and some supplemental measurements unique to Chikyu as routine measurement items. Experiments for acquiring basic data needed to meet QA/QC requirements, and for developing/maturing procedures were also conducted on various instruments. After the riser-mode drilling at Hole C9001D, discrete samples, as well as cuttings samples were processed in similar fashion. All data obtained from routine measurements were registered to the database, J-CORES (see Chapter V. Laboratory Data Management Report).

Throughout the cruise, human resources and working hours were restricted by both operational needs (technical and mechanical personnel for the SIT operation took priority) and by labor regulations. Despite this, particular samples for scientific purposes required immediate processing following core retrieval. Accordingly, we adopted an unorthodox core flow (Figure 2.1 and 2.2) and divided the cruise roughly into three periods so that core and sample processing would run smoothly and staff could work effectively under the circumstances:

- Pre-A Period (before coring of Hole C9001C)

Preparation for core processing, 16 hour-operation with two shifts.

- A Period (while coring of Hole C9001C)

Routine core processing/measurements from the Core Cutting Area to X-ray CT imaging were conducted. Safety gas monitoring, sampling for microbiology, interstitial water chemistry and biostratigraphy, and particular chemical measurements on interstitial water were performed in parallel with the sampling and basic measurement/curation operations. Each sample for microbiology and

interstitial water analysis was taken as a whole-round core after X-ray CT image acquisition. In reality, X-ray CT imaging continued into the beginning of B period. 24-hour operation with two shifts.

- B Period (after coring of Hole C9001C)

Routine core processing/measurement from physical properties measurement with Multi-sensor Core Logger (MSCL), including visual core description (VCD) and collection of shipboard discrete samples, were carried out. Routine processing/measurements on discrete samples were performed mainly in the latter half of the B period. Alongside routine measurements, experiments for setup, verification, standardization, calibration and/or acquisition of basic data on some instruments were conducted using standard and/or surplus samples. 16 hour-operation with two shifts.

- C Period (after riser drilling of Hole C9001D)

Routine processing/measurement on discrete samples and verification experiments for some instruments to prepare for or meet QA/QC standards were continued. Cuttings samples were also used in some analyses. 16 hour-operation with two shifts.

Core Flow, Measurement and Sampling for CK06-06: A Period

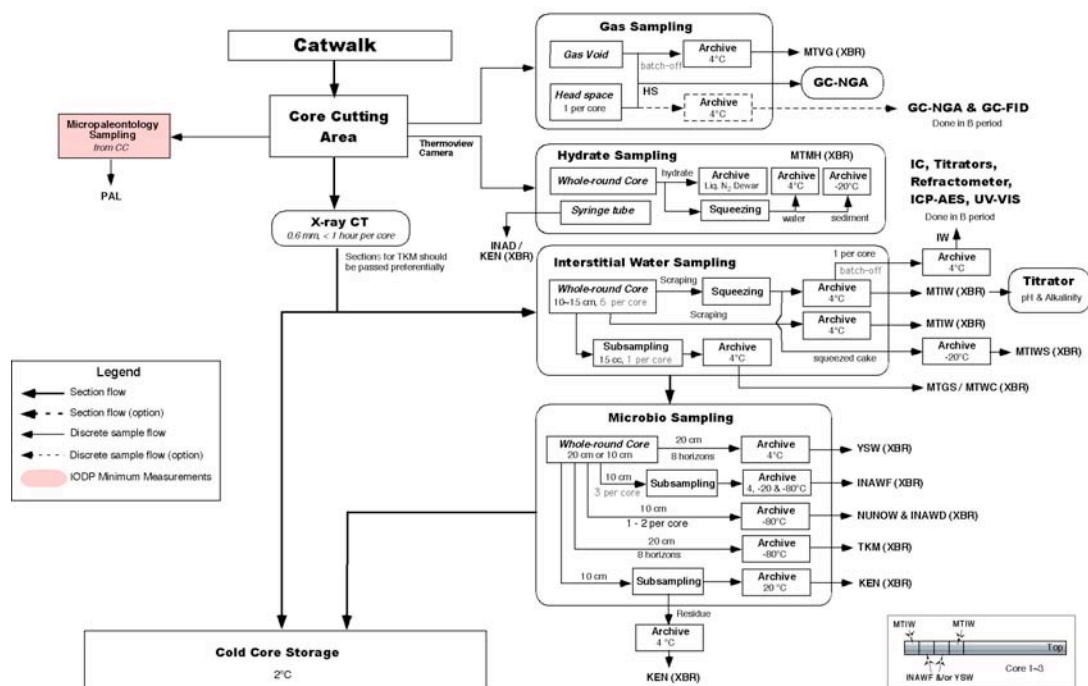


Figure 2.1. Core flow and measurements in A Period. Codes, such as PAL or MTIW indicate scientists' or shipboard samples.

Core Flow, Measurement and Sampling for CK06-06: B Period

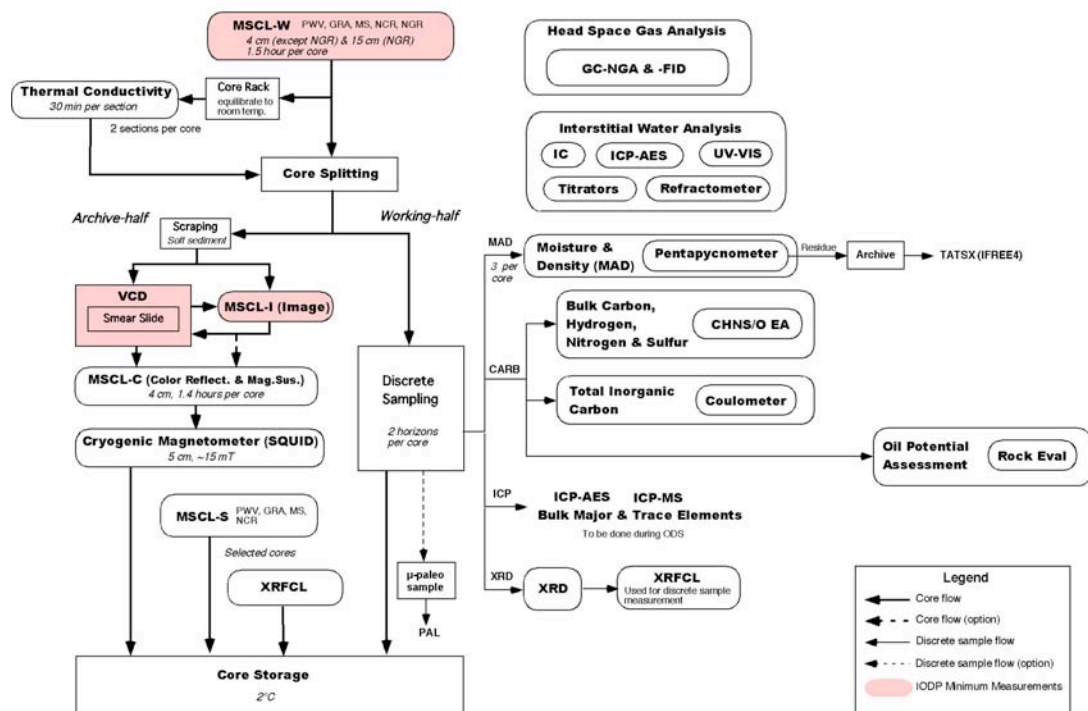


Figure 2.2. Core flow and measurements in B Period.

2.2.2. Core Processings and Measurements

The shipboard routine processing and measurement items performed for Hole C9001C cores are as follows (* indicates IODP minimum measurement):

1) Core Cutting

Each 9.5 m long core was partitioned into 1.4 m long sections at the Core Cutting Area.

2) Sampling for Biostratigraphy and Age Determination*

Routine sample were taken from each core catcher (CC). Processing for microfossil extraction and age determination was performed onboard by the invited micropaleontologists.

3) Safety Gas Monitoring

Routine sampling was conducted from the bottom of the top section of each core and/or gas void. Gas analysis was done using Gas Chromatograph Natural Gas analyzer (GC-NGA).

4) X-ray Computed Tomography imaging

All sections (except CCs and high-priority methane hydrate whole round cores) were imaged at 0.625 mm intervals.

5) Whole-round Core (WRC) sampling

WRC samples were taken for scientific use such as interstitial water chemistry and microbiological analyses. Shipboard samples for interstitial water analyses were batched from shipboard scientists' samples.

6) Multi-Sensor Core Logger –Whole-round Core Type (MSCL-W) measurement

All sections (except CCs and any missing WRC) were subjected to Gamma Ray Attenuation (GRA)*, Magnetic Susceptibility (MS)*, P-wave velocity (PWV), and Non-Contact electric Resistivity (NCR) at 4 cm intervals, as well as Natural Gamma-ray Radiation (NGR)* at 15 cm intervals.

7) Thermal Conductivity measurement

Two sections from every every core were subject to TC analysis.

8) Core Splitting

Cores from 1H to 39H were split using a thin wire after liner cutting with diamond blades in the horizontal mode. Core 40H was cut using diamond

blades in the vertical mode.

9) Visual Core Description (VCD)*

Description using tablet PCs with the J-CORES VCD application (Live-VCD) was performed as the first trial for real cores by several invited geologists and a CDEX Lab Manager. Smear Slides were made as appropriate for microscopic description.

10) Discrete Sample collection

One or two shipboard samples for each measurement item from every core.

11) Multi-Sensor Core Logger –Digital Photo Image scanning*

For all sections.

12) Multi-Sensor Core Logger –Reflectance, Spectrophotometry and Colorimetry measurement

For all sections except CCs at 4 cm intervals

13) Cryogenic Magnetometer (SQUID) –Paleomagnetic Polarity measurement

For all sections except CCs at 4 cm intervals.

14) Moisture and Density (MAD) measurement*

Samples from two horizons from every core were collected, weighed with Electric Balance System and subjected to volumetric measurement with Pentapycnometer.

2.2.3. Discrete Sample Measurements

Equipment used for shipboard analyses on discrete samples, including cuttings samples from C9001D, and analyzed items are as follows:

Solid Samples

1) Pentapycnometer

Porosity, bulk and grain densities of sediment

2) CHNS/O Elemental Analyzer

Bulk carbon, nitrogen, sulfur and total organic carbon contents

3) Rock Eval

Geochemistry on types and maturity of organic matters in sediments

4) Coulometer (Total Inorganic Carbon Analysis)

Total inorganic carbon content

5) X-ray Diffractometer (XRD)

Mineralogical composition

6) X-ray Fluorescence Core Logger (XRFCL)

Bulk chemical composition of sediment. Used as XRF analyzer for discrete sample measurement.

Head Space Gas

1) Gas Chromatograph –Natural Gas Analyzer (GC-NGA)

Hydrocarbons (~C12), hydrogen sulfur and carbon dioxide concentrations

2) Gas Chromatograph –Flame Ionization Detector (GC-FID)

Methane and ethane concentrations

Interstitial Water

1) Titrator

pH and chlorine concentration

2) Ultraviolet-Visible Light (UV-VIS) Spectrophotometer

Ammonia concentration

3) Ion Chromatograph Analyzer

Anion composition

4) Inductively-Coupled Plasma Atomic Emission Spectrometer (ICP-AES)

Metal composition

5) Refractometer

Salinity

Experiments for verifying/standardizing/calibrating analytical procedures were conducted on most instruments listed above before commencement of each routine measurement.

2.2.4. Additional Experiments

Verification experiments were conducted on several instruments after completion of each routine measurement. Major instruments for which such experiments were conducted were as follows:

1) X-ray CT Scanner

Verification on relation between CT values and densities

2) Pentapycnometer

Verification on data stability under several room temperature settings and under rough and calm sea conditions

3) Electric Balance

Verification of data stability

4) GC-NGA and GC-FID

Verification of sample preparation procedures

In addition to instruments used for routine measurements, the following instruments were also operated mainly for the purpose of setup and/or verification experiments:

1) Multi-Sensor Core Logger–Split-half core type (MSCL-S)

2) Kappabridge (Anisotropy of Magnetic Susceptibility Analyzer)

3) Spinner Magnetometer

4) Gas Chromatograph –Electron Capture Detector (GC-ECD)

5) Inductively-Coupled Plasma Mass Spectrometer (ICP-MS)

6) Fluorescent Microscope

2.3. Conditions and Procedures of Instrumental Analyses

2.3.1. Routine Core Measurements

1) X-ray Computed Tomography Scanner

X-ray CT images

X-ray CT images were acquired for whole-round core sections at the first of all measurements, using GE Medical System Light Speed Ultra16. Calibration for giving CT-values was made using a pure water standard piece and air. X-ray tube voltage and current were set to 120 kV and 100 mA, respectively. Measurement interval of the helical scan was set to 0.625 mm under the 16 arrays of detectors mode. In this scan mode, it requires about 3 minutes for each 1.5 m section. A CT image of a vertical plane

with 512 x 512 pixels is digitized from a DICOM-formatted file for each core section scan. The ‘detail mode’ was applied for the reconstruction algorithm.

2) Multi-sensor Core Logger (MSCL)

Continuous measurements of non-destructive physical properties were conducted using the Multi-Sensor Core Logger (MSCL) systems of GEOTEK. We have four systems of MSCL onboard: MSCL-W (standard type for whole-round core), MSCL-S (standard type for split-half core), MSCL-I (XYZ type for split-half core) and MSCL-C (XYZ type for split-half core). In this cruise, MSCL-S is excluded from the routine measurement flow in order to increase the core flow rate. MSCL-W and -S systems are designed for logging core sections put sequentially on a track, mounting sensors of core thickness, temperature, gamma-ray attenuation (GRA) density, P-wave velocity (PWV), non-contact electric resistivity (NCR) and magnetic susceptibility (MS). MSCL-W system, in addition, mounts a natural gamma-ray radiation (NGR) sensor. The XYZ-MSCL system is designed for measuring split-half core sections loaded side-by-side with sensors moving above samples. The MSCL-I mounts a digital image scanner and the MSCL-C mounts a spectrophotometric colorimeter (RSC) and a MS sensor. In this cruise, MS data from MSCL-C was not used.

Temperature

Core temperature is equilibrated with the room temperature before the MSCL measurement in order to keep measurement condition stable as much as possible. Confirmation of the temperature equilibration was conducted by means of a thermometer probe inserted into selected core sections from a punctuated hole, where no significant influence is arisen on subsequent measurements. The room temperature, which is regarded as the core temperature, was measured continuously using a standard PRT (platinum resistance thermometer) probe during the logging.

Gamma-rays attenuation (GRA)

Bulk density of sample materials was determined by measuring GRA through the cores. The source of gamma-ray beam is ^{137}Cs with the radiation of 370 Bq and the detector is comprised of a scintillator and integral photo-multiplier tube. Calibration equations for MSCL-W and -S are determined using each standard piece made up of a

stepwise-machined cylindrical aluminum piece, distilled water and a core liner.

Accuracy of GRA data is about 1 % and that of bulk density calculated based on GRA is less than 2 %. The collimator used was 5 mm in diameter. The sampling interval and time were set to 4 cm and 4 seconds, respectively.

P-wave velocity (PWV)

PWV is measured using a pair of the oil filled Acoustic Rolling Contact (ARC) transducers mounted on the MSCL-W and a pair of the piston-type transducer and ARC for the MSCL-S. Calibration was done by using standard pieces made up of a core liner filled with distilled water. The spatial resolution of the sensors is 2 cm. The measurement interval was set to 4 cm.

Core Thickness (Diameter)

Core thickness (diameter) measurement is made by using a pair of displacement transducers (0.01 mm in the resolution) and mechanically coupled to spring loaded P-wave transducers. Core thickness is acquired based on deviation in thickness between a reference piece and each point of a core section; sediment thickness is consequently calculated by subtracting a total liner wall thickness from the core diameter.

Magnetic Susceptibility (MS)

MS measurement for whole-round cores was performed by using the Bartington loop sensor (MS2C) of 8 cm in loop diameter. MS was optionally measured for selected split-half cores by means of the Bartington point sensors (MS2F) mounted on MSCL-S. A spatial resolution of the loop sensor is 20-30 mm, while that of the point sensor is 0.5 cm. The data acquisition intervals for MSCL-W were set to 4 cm, with acquisition time of 1 second. Obtained data were corrected as volume specific magnetic susceptibility.

Non-contact electric resistivity (NCR)

Electric resistivity was measured with a NCR sensor of GEOTEK mounting inductive coil arrays inside. Calibration was performed by using five saltwater standards filled in the short core liner (0, 1.75, 3.5, 17.5, 35 g/l; 0.21-15.48 $\Omega\cdot\text{m}$ @20°C). Zero reset of sensor was automatically done every first section. Special resolution of the sensor is about 2 cm. Sampling interval was set to 4 cm.

Natural gamma-ray radiation (NGR)

NGR measurement was conducted for whole-round core samples, passing through the NGR sensor housing on MSCL-W. Background intensity is about 40 cps, measured under inserting a blank piece filled with distilled water. The spatial resolution for each detector is 15 cm. Measurement interval and time were set to 15 cm and 30 seconds, respectively.

Digital Photo Image

Digital photo images of cores were taken by using MSCL-I from archive-half cores. The GEOSCAN color line scan camera mounted on the MSCL-I system is a 3 CCD device using 3×1024 pixel CCD arrays. White calibration was performed by use of a white tile, Spectraron (Labsphere), with a property causing isotropic scattering of light before scanning. For avoiding white saturation, a color chart, ColorChecker Mini (Gretag-Macbeth AG) put next to the section bottom was scanned together with each section with the camera aperture being adjusted so as not to cause white saturation and a gray correction was made afterwards using an image processing software, Adobe Photoshop. Scanning was 100 pixel/cm in resolution, taking about 5 minutes per section.

Reflectance, Spectrophotometry and Colorimetry (RSC)

RSC data were obtained from archive-half cores with the Konica-Minolta color spectrophotometer mounting on the MSCL-C system, which acquires automatically reflection spectra from the surface of a core. Measured data are expressed by using a CIE (Commission Internationale de Éclairage) three-dimensional color coordinate system with indexes of L^* (lightness), a^* (redness/greenness) and b^* (yellowness/blueness). The accuracy of reflectance data is less than 0.1 % and that of chromaticness is less than 0.04 in a value of ΔE^*_{ab} . The spatial resolution of the spectrophotometer is 0.5 cm. Calibrations were carried out internally by using a white calibration reference spectrum and a zero calibration reference spectrum. The measurement interval was set to 4 cm.

3) Thermal Conductivity System

Thermal conductivity was measured on two whole-round core sections every core using a full-space single-needle probe TeKa (Berlin) TK04 unit. After a hole was drilled in the outer core liner, the measurement was conducted at 3 W/m for 150 seconds with the 2-mm-diameter temperature probe being inserted into the core section. The measurement on each point was repeated three times.

4) Cryogenic Magnetometer

Remanent Magnetization

The measurement of the natural remanent magnetization (NRM) was performed on archive-half sections before and after alternating-field (AF) demagnetization using the pass-through type superconductivity magnetometer, SQUID Magnetometer 760 modified (2G Enterprises). This instrument is equipped with a direct-current superconducting quantum interference device (DC-SQUID) and has an inline AF demagnetizer. Six steps of demagnetization, 2.5, 5, 7.5, 10, 12.5 and 15 mT were applied for C9001C-1H; four steps of demagnetization, 0, 5, 10 and 15 mT were applied for the rest. Measurement intervals were set to 5 cm.

2.3.2. Routine Discrete Sample (Solid and Gas) Measurements

1) GC-NGA

Head Space Gas

Head space gas composition was analyzed by using Gas Chromatograph 6890N FID/TCD (Agilent Technologies) with an auxiliary component for natural gas analyses (Wasson-ECE Instrumentation).

Each sample for head space gas analysis was taken 5 cc in volume from the bottom of section 1 per every core using a syringe tube sampler and was put in a 20 cc glass vial container. Each glass vial was closed with a septum plug and sealed with an aluminum cap. After that, it was heated at 70 °C for 30 min in an oven. Extracted gas of 5 cc in the vial was taken with a gas-tight syringe and was injected to GC-NGA. Measured data are given as intensity calculated from the chromatograph chart, because the quantitative analysis has not been set up as of now.

2) GC-FID

Head Space Gas

Methane and ethane contents in head space gas were analyzed by using Gas Chromatograph 6890N FID (Agilent Technologies Inc.). Sample preparation procedure is as same as that applied for GC-NGA. Measured data, however, is not uploaded to J-CORES.

3) Moisture and Density (MAD)

Wet and dry masses and dry volume of discrete samples were measured to obtain bulk and grain densities and porosity. Sample mass was weighed on an electric balance, Motion Compensated Shipboard Balance System (CDEX). Sample volume was measured by two sets of the Pentapycnometer PPY-15T and PPYC-KU (Quantachrome Instruments).

[Sample preparation and weighing]

Each sample of about 10 cc was taken with a tube syringe sampler from two working-half sections per every core, coded as MAD. The sample was transferred to a glass container of about 6.8 ml and the wet weight was measured with the electric balance system. For the next step, the sample was dried up in a constant temperature windy oven, WFO-451SD (Tokyo Rikakikai) heated at 105 °C oven for 24 hours and then was cooled in a desiccator for one hour. After dry weight being measured with the electric balance, the dry volume was measured by means of the Pentapycnometer. Accuracy of the electric balance is less than 0.1 % in RSD even under rough sea conditions.

[Dry volume measurement]

In measurement with Pentapycnometer, small size cells (10 cc) were used. Calibration was performed using a medium standard sphere (ca 7 cc). The purge time of helium gas was set to 1 min in the flow mode. The measurements for each sample were repeated until the deviation becoming less than 0.01 % or until up to five times. The mean value was adopted to the final data.

4) XRD

Mineralogical analysis by X-ray diffraction was conducted using the CubiX PRO X-ray Diffractometer (PANalytical). Discrete samples of 5 cc were taken with a syringe

tube sampler from two horizons per every split-half core of C9001C and cuttings samples of C9001D were taken from 25 intervals, coded as XRD.

[Sample preparation for bulk sediment measurement]

Sixteen to twenty samples were placed in a plastic desiccator and were freeze-dried for 24-72 hours using a freeze dryer, FZ-4.5CL (Laboconco). After drying, the samples were milled with the Planetary Ball Mill P-5/4 (Fritsch). These dried samples were transferred to 80 cc tungsten carbide containers with 10 mm diameter milling balls and were milled at 200 rpm for 2 minutes. In this connection, the cuttings samples sometimes contain very hard granules to pebbles of several millimeters to 1 cm in diameter (considered to be ice-rafted debris). These hard coarse grains were removed from the samples after milling.

[Sample preparation for clay mineral measurement]

Seven cuttings samples were processed for clay mineral measurement with decomposition of organic matters and size fraction. Each powdered sample of 2 g was mixed with 10 % hydrogen peroxide solution in a 50 cc centrifuge tube for organic matter removal. After being left for about a half day, the mixture were centrifuged at 1000 rpm for 5 minutes for separating the particle fraction less than 2 μm in size using a Tabletop Centrifuge himac CT4D (Hitachi High-Technologies). The centrifuged solution was decanted and spun down again in a new tube at 1500 rpm for 15 minutes to separate suspended clay. After that, the solution was decanted and the remained clay was taken out with distilled water of 40 ml. For removing hydrogen peroxide completely, centrifugation and decantation were repeated 4-5 times as appropriate. An oriented clay mount was prepared by putting 2-3 drops of the solution onto a nonreflective silicon sample holder and drying for 6 hours at the ambient temperature.

[Calibration for semi-quantitative analysis]

Calibration curves for a semi-quantitative analysis on major minerals were obtained by measuring 14 standard powder samples (Nankai-Cascadia-type sediments) provided from Dr. M. Underwood (Univ. of Missouri). For the qualification analysis, a free application software, MacDiff was used. As a result, we got calibration curves of quartz, plagioclase, calcite and clay minerals, where the correlation coefficients are 1.0, 0.99, 0.99 and 0.91, respectively.

[Measurement]

For the bulk XRD measurement, all samples were mounted on the glass holder

(large size) except the sample of 28H-4 for which the small-size glass holder was used. For the clay mineral measurement, each sample was mounted on the nonreflective silicon holder. X-ray tube voltage and current were set to 45 kV and 40 mA, respectively. Scanning was conducted from 2° (2 θ) to 60° (2 θ) with the step size of 0.01° and with the sampling time of 0.1 second per step. Data of quantitative analysis, however, are not uploaded to J-CORES.

5) X-ray Fluorescence Core Logger (XRFCL)

Analysis of bulk chemical composition by an X-ray fluorescence method was conducted using the JSX3600–CA1 XRF core logger/TATSCAN-F2 (JEOL); this machine was applied as an energy dispersive XRF analyzer for discrete samples at this time. 25 cuttings samples from C9001D were measured.

[Sample preparation]

Powdered samples that were prepared for XRD measurement were use for XRF measurement. Two types of sample shape were prepared: pressed pellet and large-size glass holder that is diverted from the XRD measurement. As for making pellets, each powdered sample was mounted in a vinyl chloride ring and pressed with a motorized hydraulic press, 3630 Automated X-Press (SpexCertiprep Group Co.) at 10 ton for 1 minute.

[Measurement]

X-ray tube voltage and current were set to 30 kV and 0.17 mA, respectively. The collimator with 7 mm in diameter was used. Measurement time was set to 300 sec in live time, where dead time was generally 30-40 %. Each sample was placed on the sample table at 10 cm intervals. Qualitative analysis was performed based on the bulk-FP (fundamental parameter) quantification method with bundled software. Measured data, however, are not uploaded to J-CORES.

6) CHNS/O Elemental Analyzer

Total carbon, organic carbon, nitrogen and sulfur contents in sediment samples were measured using two machines of the CHNS/O Elemental Analyzer Flash–EA1112NC (Thermo Electron). Samples were taken from two horizons per every core, coded as CARB.

[Calibration]

Calibration curves were obtained using sulfanilamide standards, of which the mass had been weighed beforehand onshore.

[Sample Preparation]

Samples were freeze-dried for two days using a freeze dryer, FZ-4.5CL (Laboconco) for the beginning. The dried samples were crushed and stored in a desiccator, being put in capped vial containers. Dried samples of 20 mg were weighed by using the Compensated Shipboard Microbalance System (CDEX) and wrapped with tin foil. Furthermore, as to samples for the total organic carbon analysis, several drops of 6 N HCl were added for removing carbonates and the wet samples were dried on an hot plate heated at 80°C. Regarding samples for the sulfur measurement, V₂O₅ of several tens milligram was added as an oxidant.

Accuracy of weighing with the microbalance system onboard was less than 0.2 % in RSD under a calm sea condition.

[Measurement]

No.1 machine was used for measurement of carbon and nitrogen, whereas No.2 machine was dedicated for sulfur measurement, taking difference of retention time (that of sulfur is quite longer than the others) into consideration. The measurement settings for both machines are shown in Table 2.1.

Table 2.1. Measurement settings of CHNS/O Elemental Analyzer

Target	Gas pressure (kPa)		Gas flow rate (ml/min)			Temperature (°C)			GC Column
	O ₂	He	Carrier	Reference	O ₂	Left furnace	Right furnace	Oven	
NC	300	250	130	100	250	1000	840	50	Hayesep
S	300	250	130	100	250	1000	0	90	Porapack

7) Coulometer (Carbonate Analyzer)

Total inorganic carbon content in sediment samples was measured using a carbonate analyzer, UIC CM5012 Model 106 (Nippon Ans Co.). Samples were taken from two horizons per every core, coded as CARB.

[Sample preparation and measurement]

Twenty samples were chosen and were freeze-dried for two days using the freeze dryer, FZ-4.5CL (Laboconco Co.). The dried samples were crushed and weighed on a sheet of aluminum foil using the electric microbalance. Each weighed sample

transferred into the extraction tube with acetone was dried in an oven heated at 80°C. After that, the extraction tube was mounted on the preparation system and 5 cc of 2 N HCl was added to the sample to generate CO₂. Extracted CO₂ was induced to and measured by the coulometer. The calibration curve was created by measuring a calcium carbonate reagent. The standard gas was measured for a drift check after every 5 measurements of unknown sample.

8) Rock Eval

Geochemical parameters indicating types and maturity of organic matters in sediments were measured on an experimental basis using Rock Eval 6 Standard (Vinch Technologies). This instrument is an automated device consisting of two micro-ovens which can be heated up to 850° C. An FID detector measures the H/C gas released during the pyrolysis, while an on-line infrared cell is used to measure the quantity of CO and CO₂ generated during pyrolysis and oxidation of samples.

The samples for the measurement were taken from two horizons per every core, coded as CARB.

[Sample preparation and measurement]

Twenty samples were subsampled from those prepared for the measurement with CHNS/O Elemental Analyzer. Each sample was put in a dedicated crucible, which was baked beforehand in the machine, and was weighed to 100 mg with the electric microbalance. The measurement on Rock Eval was performed by 'Bulk Rock method' on the bundled analytical software. The dedicated standard samples were used for calibration. Major parameters obtained by the Rock Eval measurements, besides TOC and MinC (= inorganic carbon), are listed as follows:

S_1 = the amount of free hydrocarbons (gas and oil) in the sample. S_1 normally increases with depth.

S_2 = the amount of hydrocarbons generated through thermal cracking of nonvolatile organic matter. S_2 is an indication of oil potential. This parameter normally decreases with burial depths >1 km.

S_3 = the amount of CO₂ produced during pyrolysis of kerogen. S_3 is an indication of the amount of oxygen in the kerogen.

HI = hydrogen index ($HI = [100 \times S_2]/TOC$). HI is a parameter used to characterize the origin of organic matter. Marine organisms and algae have

generally a higher ratio of H to C than that of land plants. HI typically ranges from ~100 to 600 in geological samples.

OI = oxygen index ($OI = [100 \times S_3]/TOC$). OI is a parameter that correlates with the ratio of O to C, which is high for polysaccharide-rich remains of land plants and inert organic material encountered as background in marine sediments. OI values range from near 0 to 150.

2.3.3. Interstitial Water Chemistry

Chemical analyses of interstitial water were performed on samples coded MTIW (scientist's sample) and IW (shipboard sample). The samples were initially taken as whole-round core (WRC) from 111 horizons at the QA/QC room according to the shipboard scientists' request after X-ray CT scanning. The sediment samples removed from WRCs were skinned off about 1.5 to 2.5 cm thick to avoid contamination, and subsequently, were squeezed by means of Manheim-type hydraulic squeezers (brought in by the laboratory of Prof. Matsumoto, Univ. of Tokyo, in charge of interstitial water analysis) to extract interstitial water. Squeezed each water sample was retrieved by use of a syringe tube with a chromato-disk of 0.2 μm in pore size and was transferred to a plastic bottle.

Shipboard IW samples were batched off from MTIW samples of 36 horizons and those transferred to 10 ml plastic bottles were stored in a refrigerator cooled at 4°C shielded from light as “stock solution”. Each sample to be measured except that for pH and Alkalinity titration was transferred to a 2 ml microtube through a filter of 0.45 μl in pore size, taken from the stock solutions on the day before the measurement for aliquot; each solution was termed “secondary solution”.

1) pH and Alkalinity Titration

pH and Alkalinity of interstitial water were measured using an automatic titrator, Titrino 794 (Metrohm) immediately after squeezing of the samples. Each test tube where a sample was batched off was soaked in a constant temperature bath heated at 25°C. A sample of 3 ml was taken from the test tube and was set to the titrator kept at the same temperature. Both pH and alkalinity were measured in automatic mode. pH was measured on ahead and then alkalinity was titrated potentiometrically with 0.1 mol

of HCl by the gran plot method within a range from 220 to 240 mV. For the alkalinity titration, we prepared a standard solution of NaHCO_3 of which the alkalinity equals to 50 mM.

2) UV-VIS Spectrophotometer

Ammonium ion concentration of interstitial water was determined using the ultraviolet-visible light spectrophotometer, UV-2550PC (Shimadzu), by measuring absorbance of UV at a certain wavelength according to a calibration curve method.

[Sample preparation]

Each sample of 10 μl was transferred to a 100 ml TPX[®] test tube, taken from the secondary solutions with a digital pipette. The sample solution, to which ultra pure water of 1090 μl was added subsequently, was agitated by use of a vibrator. For the next, the sample solution was agitated again after phenolic alcohol and sodium nitroprusside solutions of 500 μl each and oxidizing agent solution of 1000 μl were added. Then, the sample solution was allowed to stand for 3 hours for coloration.

[Measurement]

After completion of coloration for 3 hours, a sample solution was transferred to a glass cell; the absorbance of the solution at 670 nm in wavelength was measured by means of the UV-VIS spectrophotometer. An experimental repeatability of absorbance determination was 1.6 % in RSD (for a 0.25 mM solution).

3) Ion Exchange Chromatograph

Concentrations of anions, such as sulfate, phosphate, bromine and chlorine, were determined by use of an ion exchange chromatograph, ICS-1500 (Dionex).

[Sample Preparation]

Sample solutions were prepared with three dilution ratios. To begin with, each sample of 100 μl was transferred to a 2 ml microtube, taken from the secondary solution with a digital pipette. Then, the sample solutions were diluted tenfold with ultra pure water of 900 μl . These solutions (Solutions A) were used for sulfate and phosphate measurements. Next, solutions of 100 μl taken from the Solutions A were diluted tenfold again with ultra pure water of 900 μl , after transferred to a 2 ml microtube with a digital pipette. These solutions at hundredfold dilution rate (Solutions

B) were used for bromine measurement. Finally, solutions of 50 μl taken from the Solutions B were diluted twentyfold with ultra pure water of 950 μl , after transferred to a 2 ml microtube with a digital pipette. These solutions at two-thousandfold dilution rate (Solutions C) were used for chlorine measurement.

[Measurement]

Measurement on ICS-1500 was performed by means of the separation column Ion Pac AS12A at 35°C. A mixed solution of 2.7 mM NaCO_3 and 0.3 mM NaHCO_3 were used as the eluate.

4) Chlorine Titration

Chloride concentration was also determined by using an automatic titrator, Titrino 794 (Metrohm), besides the ion exchange chromatograph.

Two methods for titration were examined: mohr's method (manual titration) and potentiometric method (automatic titration). Sample solutions of 0.1 μl , taken from the secondary solutions, were mixed with ultra pure water of 5 ml in 10 ml beakers. For the mohr's method titration, K_2CrO_4 of 0.1 ml was added to the solutions as an indicator reagent. Titration was performed using 0.1 M AgNO_3 solution standardized by IAPSO (chloride concentration = 559 mM). Repeatable accuracies of titration by the mohr's and the potentiometric methods were 0.29 % and 0.19 % in RSD, respectively.

5) ICP-AES

Concentrations of cations, such as calcium, potassium, magnesium, silicon, barium and strontium, and of sulfur were determined by means of an ICP-AES, Ultima2 (HORIBA JOBIN YVON S.A.S.).

[Sample Preparation]

Stock solutions were once transferred to 10 ml polyethylene beakers rinsed out with nitric acid, and then were left to stand in the dark for half a day for being equilibrated with room temperature. Stock solutions of 500 μl , equilibrated with room temperature, were transferred again to 50 ml NALGENE volumetric flasks; indium solution of 1000 $\mu\text{g/ml}$ was added to them as an internal standard substance; and the volumetric flasks were accurately filled with 1 vol% HNO_3 up to 50 ml. Each final

solution was transferred to a plastic sample bottle, filtrated with a syringe filter of 0.2 μm in pore size.

[Measurement]

Each element being set up was measured sequentially with respect to each sample. A blank solution and standard samples were measured after every five unknown samples measurement for verifying instrumental drift. Measurement settings of the instrument for the target elements were optimized by measuring the standard seawater of IAPSO.

6) Refractometer

Salinity was estimated by use of an automatic digital refractometer, RX-5000 α (ATAGO CO.). The calibration curve for this analysis was created based on a relationship between known salinities and measured refraction indexes of several standard solutions made from the diluted standard seawater of IAPSO. The measurement temperature was set to 20 °C.

2.4. Technical Remarks on Measurement Results

Preliminary results of routine instrumental measurement onboard were shown in Appendices. Some items of non-destructive measurement, especially P-wave velocity, electric resistivity and thermal conductivity, were obviously affected by gassy property of the sediments of this hole, varying greatly and/or differing from realistic values (Appendix 3). Moreover, analytical procedures for some items, especially those for interstitial water chemistry, were still under development. Evaluation of each result from a technical viewpoint will be done through further investigation onboard and onshore. We mention here only on noticeable features in some measurement results where data of an item were obtained by means of two different instruments and suggesting a technical problem on coring.

2.4.1. Bulk Density

Bulk density of sediments was obtained from GRA and MAD measurements. Upon comparison of both results, bulk density by MAD demonstrates almost identical

variations in general and tends to be slightly higher than that by GRA (Figure 2.3). Accordingly, measurement with both methods, including those of calibration and sample preparation, can be regarded essentially reliable in case of soft sediment.

2.4.2. Total Organic Carbon and Total Inorganic Carbon

TOC and TIC concentrations were obtained from the CHNS/O Elemental Analyzer and the Coulometer, respectively. Furthermore, measurement with Rock Eval gave also data of these two analytic items. Each analytic item by use of different two instruments provides nearly consentaneous results, as shown in the profiles (Appendix 3); it is indicated that each analysis has acceptable high reliability.

2.4.3. Chloride

Chlorine concentration of interstitial water was determined both by titration and by chromatograph. Results from two instruments are quite different both in trend and in concentration; data by titration shows less variations and high values. Considering the simplicity of the experiment, the data by titration is more reliable. Analytical procedure for chlorine on the ion exchange chromatograph needs to be reexamined and improved.

2.4.4. Paleomagnetic Polarity

The inclination profile shows that the paleomagnetic polarity is essentially normal in the entire hole (Figure 2.4). The following major features are considered to be caused by drilling disturbance: scattered inclinations in the interval of ESCS, apparent reverse

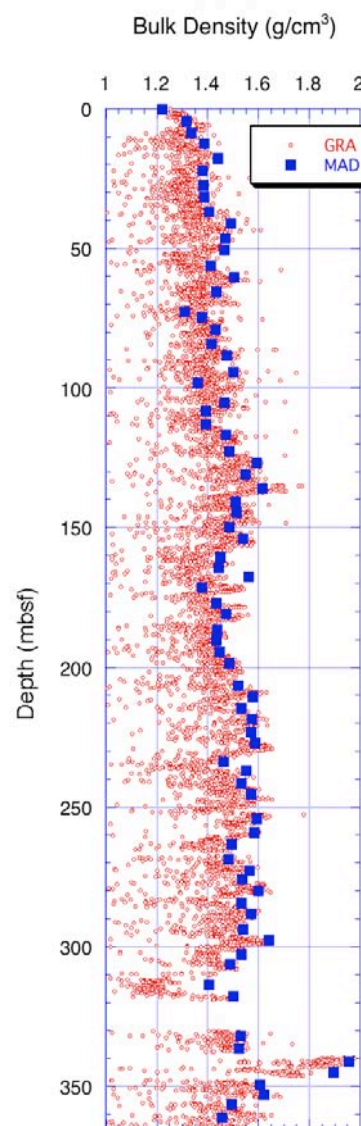


Figure 2.3. Comparison between MAD and GRA bulk density.

polarity of Core 38H consisting of loose sand, and low inclinations in the interval of Core 15H-16H.

As for the declination profiles, downward progressive anti-clockwise rotations within a core are observed in many cores from 6H to 33H: the amount of rotation gets up to 180° (Figure 3.4). This means that these cores are twisted anti-clockwise. Accordingly, it is considered that the core barrel of the HPCS is likely to rotate sometimes during penetration.

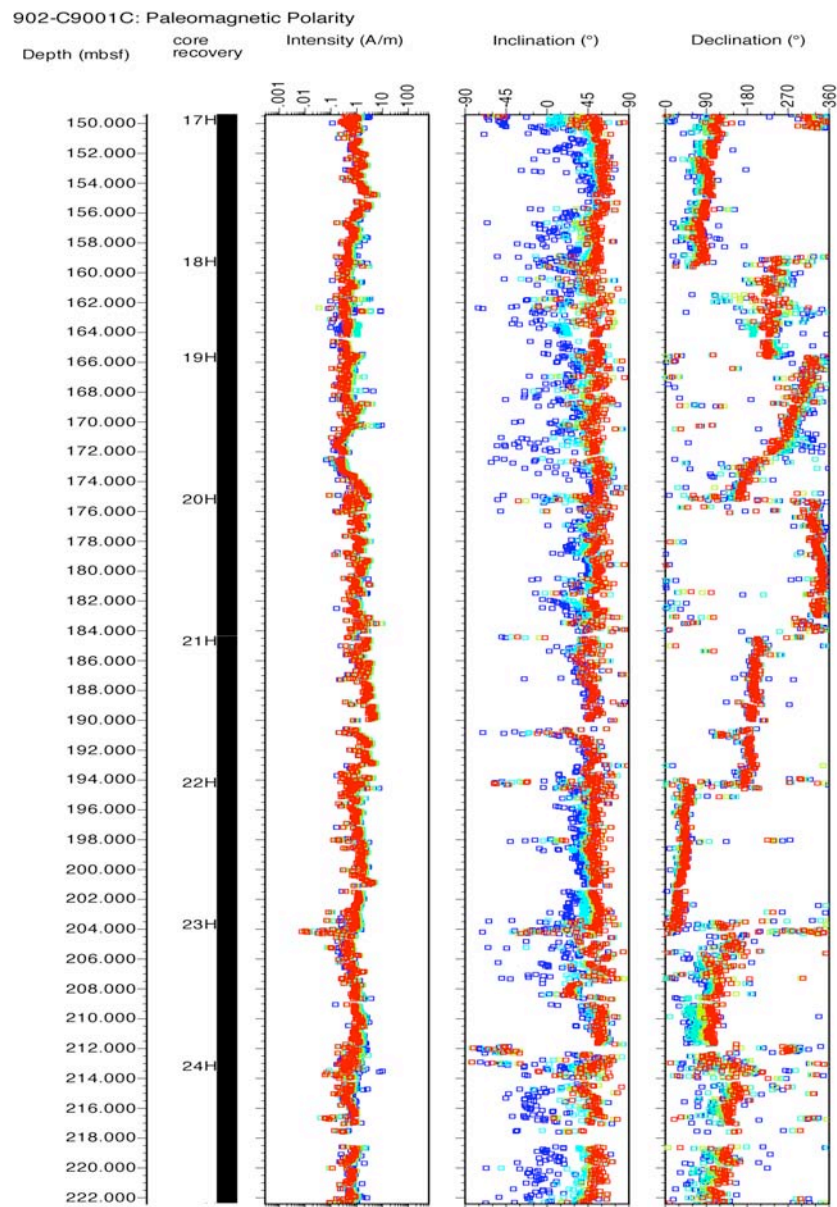


Figure 2.4. Paleomagnetic polarity data profiles from C9001C-17H to 24H.

2.5. Summary of LSIT

All routine measurement items for Hole C9001C cores (14 items) and discrete samples (12 items) were successfully completed. All routine measurement and curatorial data were registered to J-CORES. Live-VCD using tablet PCs was also performed and almost entirely completed onboard. Biostratigraphic sample processing and examination were conducted by invited paleontologists; radiolarian and planktonic foraminiferal ages were preliminarily determined onboard. Cuttings samples were collected at 25 intervals from Hole C9001D and some measurements were carried out (XRD, XRFCL and GCs). Core samples were stored temporarily in Cold Core Storage and in refrigerated core containers until the end of the cruise. After the cruise, they were off-loaded and transferred to the Kochi Core Center.

From routine measurements and basic experiments performed for each instruments, we obtained data and knowledge useful for improving and developing analytical procedures and for modifying laboratory environment. Most of the tools and procedures used during this cruise are primarily for analysis soft sediments, and many issues and tests remain to be carried out for analyses of hard rock samples, such as calibration methods for physical property measurements and chemical processing of discrete samples. Details for each measurement result are described in a separate document.

All lab technicians engaged in every core processing procedure, various instrumental measurements and data processing by rotation. Through these works and various technical suggestions from invited advisors, the lab technicians' knowledge and skills in each area of analysis and handling were significantly increased.

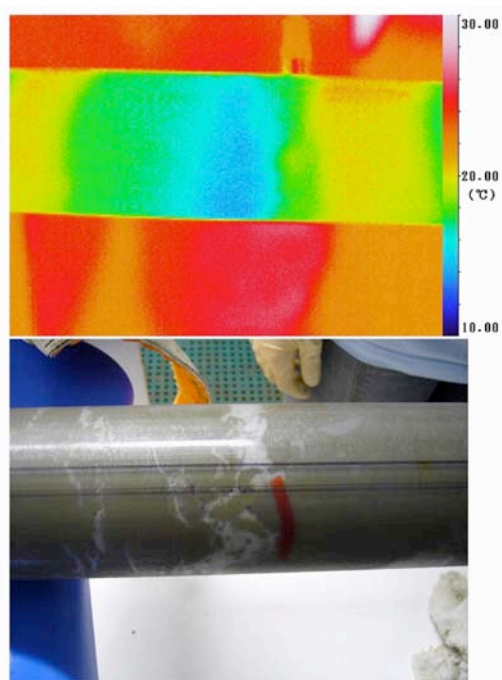
We received many useful suggestions with regard to improvement of laboratory environment, analytical procedures, analytical instruments, curation procedure, data management, so on (totally 151 items) from invited advisory scientists. Their suggestions will be taken into consideration for modifying the laboratory over both the short and long term.

III. Preliminary Scientific Results

Although most core processing and instrumental analyses onboard were primarily conducted for the purposes of technical investigation with the framework of the LSIT, onboard results will be also used as basic data for scientific purposes. We have already acquired several preliminary but interesting scientific findings based on onboard measurement and observation results. Major topics of the findings from Hole C9001C cores and Hole C9001D cuttings are described hereafter.

3.1. Recovery of Methane Hydrates

Layers bearing disseminated, and in some cases thin layers of methane hydrates were found in several horizons in the lower half of Hole C9001C, below 190 mbsf, and were sampled for the first time in the Northeast Japan forearc basin. To recognize the presence of horizons bearing methane hydrates, monitoring with a Thermo-View camera and visual inspection were conducted before partitioning of each core at the Core Cutting Area. We observed several hydrate-bearing horizons where temperatures were significantly decreased by the melting effect of hydrates (Figure 3.1). The



lithology of hydrate-bearing layers was either porous sand or ash. WRCs taken from hydrate-bearing layers were sampled from 12 horizons at the Core Cutting Area and were subjected to subsampling for microbiology and geochemistry in the QA/QC lab. Hydrate samples were stored in liquid nitrogen.

Figure 3.1. A methane hydrate-bearing horizon (bottom) and its thermography image (top). Temperature of the blue part is 5-6°C lower than that of the surrounding horizons. The view is from Hole C9001C Core 21 Section 4, about 190 mbsf.

3.2. Lithostratigraphy

3.2.1. Lithologic Units

Hole C9001C cores are composed mainly of olive black to dark olive gray diatomaceous silty clays bearing microfossils such as siliceous sponge spicules, foraminifera, radiolarians, calcareous nannofossils, and silicoflagellata. Major mineral components are quartz, plagioclase and clay minerals. Flamboyant pyrite and glauconite are characteristically included as subordinate mineral components, found in smear slides. Strong smell of hydrogen sulfide is recognizable in the uppermost two cores, by about 20 mbsf, whereas, it becomes imperceptible below this depth. The main silty clays also contain locally scattered and/or isolated pumices, scattered silt to sand, isolated and/or scattered granules to pebbles that are considered to be ice-rafted debris, and shell fragments. At around 250 mbsf and in some WRC samples, olive crystalline precipitations are observed in small, ~2 cm diameter spaces. XRD analysis indicates that these precipitations are composed of calcite, however the origin of the color is unknown. Tephra and sand layers are intercalated chiefly in the upper and lowermost parts as subordinate lithologic components, and are generally several cm thick. In addition, cuttings samples recovered from 525 to 647 mbsf of Hole C9001D have similar lithology under smear slide and stereomicroscope observation, except slightly higher degree of consolidation. Based on VCD results and physical properties data, Hole C9001C is divided into four lithologic units (Figure 3.2). Depositional age is given for each unit (in parenthesis) based on estimates according to an age model (described later) derived from microfossil analysis.

- 1) Unit A (0 ~ 158 mbsf; 0 ~ 200 ka): diatomaceous silty clay commonly intercalated with tephra and sand layers (~1 tephra/sand layer per core section). Physical properties variation is characterized by generally high magnetic susceptibility; downward increasing NGR and bulk density; and downward decreasing b^* and paleomagnetic intensity.
- 2) Unit B (158 ~ 340 mbsf; 400 ~ 600 ka): diatomaceous silty clay almost devoid of tephra or sand layers. Magnetic susceptibility is relatively low in general.

- 3) Unit C (340 ~ 348 mbsf; 600 ka): composed of thick layers of loose, fine sand
- 4) Unit D (348~365 mbsf; 600 ~ 640 ka): composed mainly of diatomaceous clay intercalated with tephra layers. Magnetic susceptibility level is similar to that of Unit B.

Most of Hole C9001C is occupied by Unit A and B. According to available age data, an accumulation rate in the interval from 60 to 160 mbsf in Unit A is quite slow, less than half, compared to accumulation rates in the rest of the core (assuming that all sedimentary strata were deposited continuously without any distinct hiatuses). It is possible that a sedimentation rate change occurred between Unit A and B, but there is no clear change or gap in lithofacies suggesting such a change of sedimentation rate within Unit A. Clear change in lithofacies and physical properties are recognized only at the boundary between Unit A and B. Since there is neither direct nor indirect evidence in support of such a large sedimentation rate change within Unit A, it is reasonable to assume that an unconformity forms the boundary between Unit A and B. In fact, an unconformity gently inclined from south to north can be recognized in the upper formation in seismic profiles, as mentioned below. The character of the physical boundary between Unit A and B is obscure, but is tentatively interpreted to occur in core 17H, probably between section 17H-8 and 17H-CC, at around 158 mbsf. This interpretation is based on the occurrence of a radiolarian biostratigraphic event identified between 16H-CC and 17H-CC, coupled with a dramatic change in magnetic susceptibility between section 17H-7 (Unit A) and section 17H-8 (Unit B).

When these data and interpretations are overlain on the available seismic profiles, Unit A and B correspond to the upper stratified formation and the upper-middle formation, where reflections are weak and massive (upper) or slightly chaotic (upper-middle), respectively (Figure 3.3). The upper stratified formation onlaps the strata below and this boundary is interpreted as an unconformity that is gently inclined from south to north, with the upper formation gradually getting thicker and higher in amplitude toward the north. This formation probably undergoes a lithofacies change from clay-dominated sediments to coarse sediments such as sand and conglomerate in the north (Figure 3.3A). The unconformity found in the E-W seismic profile can be traced as the boundary between the stratified formation above and the formation showing disturbed reflectance with high amplitude below (Figure 3.3B). However,

lithofacies suggested to correspond to such seismic characteristics (like debris flows or slump deposits) were not noted in the cores taken from the interpreted boundary between Unit A and B.

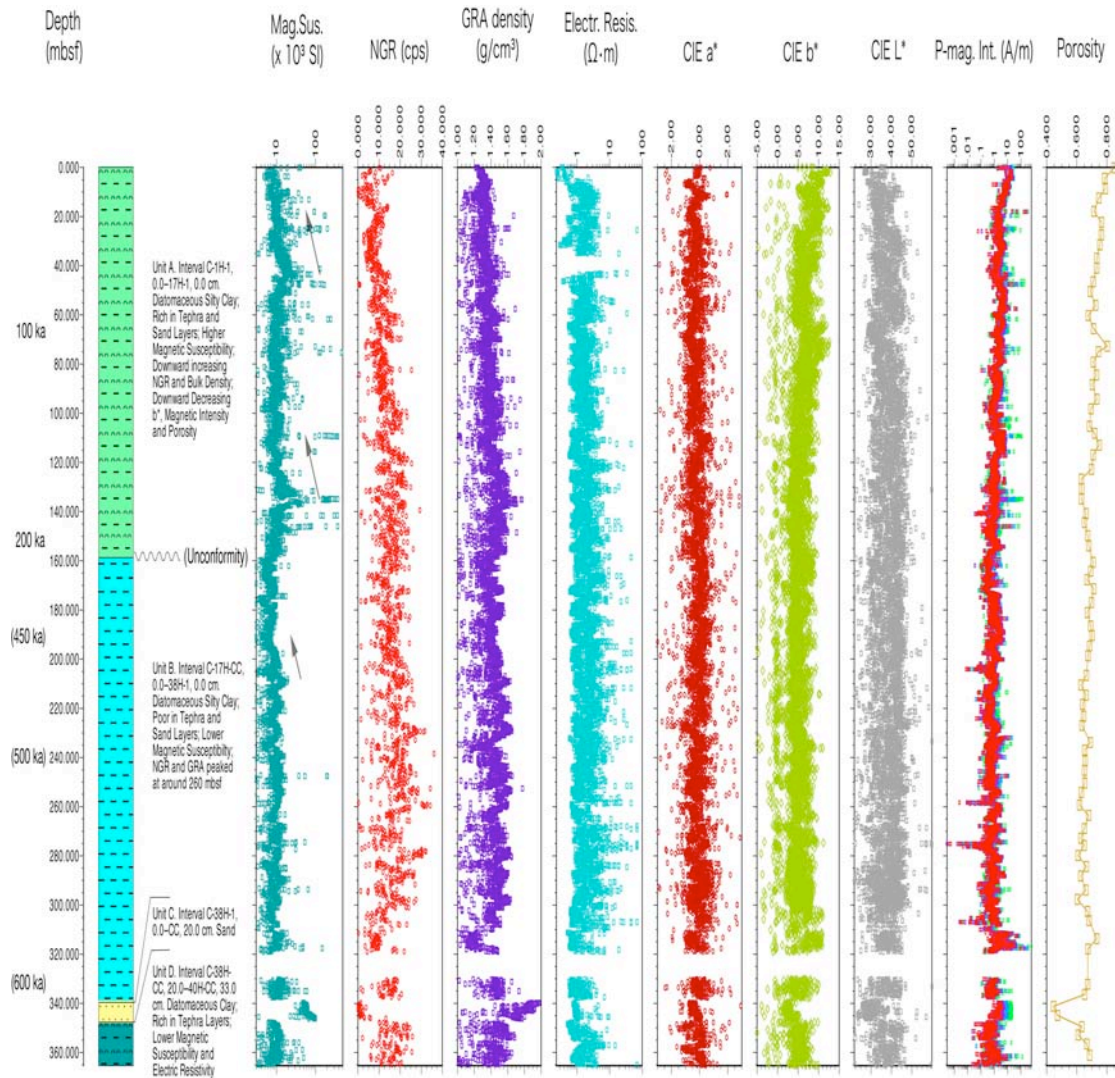


Figure 3.2. Lithologic units and representative physical property profiles from Hole C9001C. Ages indicated beside the depth scale are based on the age model. It is inferred that there is an unconformity between Unit A and B from the age model, accumulation rates calculated from the model, lithology and physical properties, and correlation with seismic data. Gray arrows in the profile of magnetic susceptibility indicate an upward-decreasing trend, probably associated with the early stages of each glacial period.

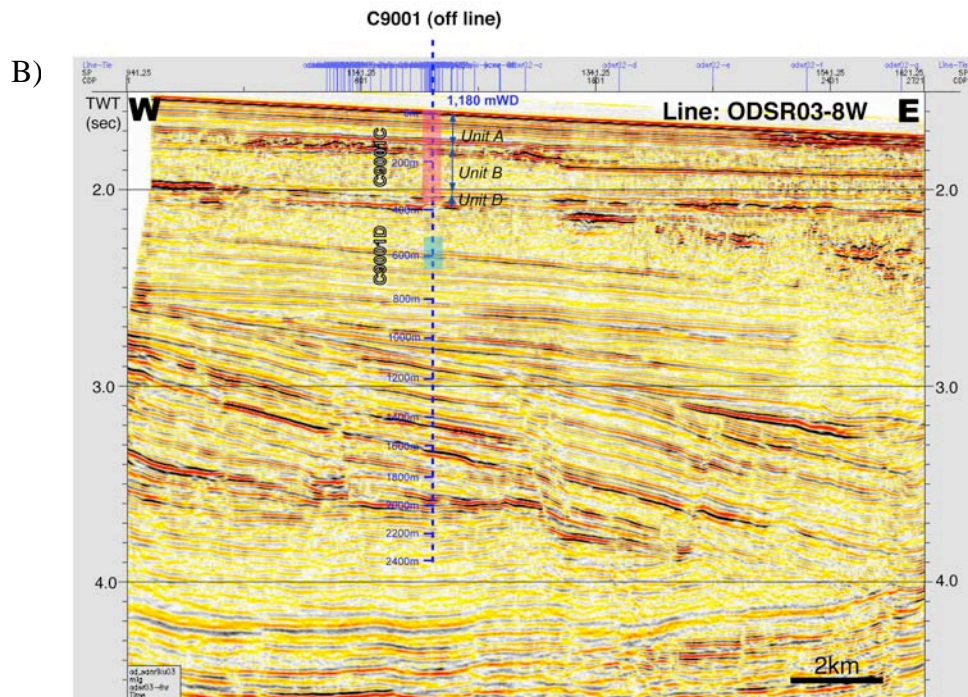
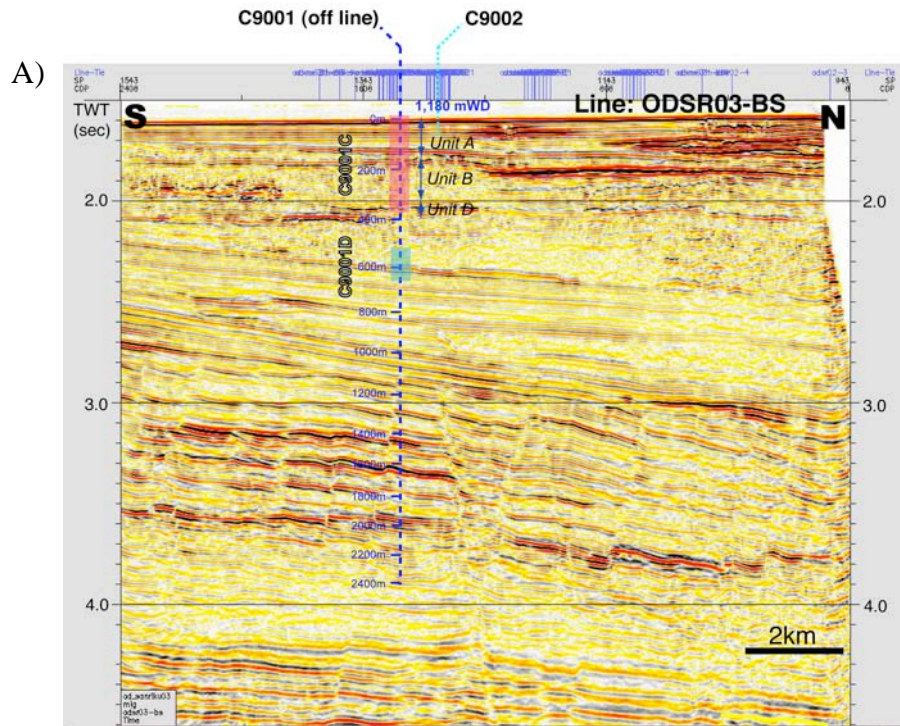


Figure 3.3. A) N-S and B) E-W seismic profiles crossing site C9001 (off line) acquired by during CDEX site survey and a projection of the drilled intervals where cores or cuttings were recovered at Holes C9001C and D. Depth scale is derived from an interval velocity distribution model.

The stratified seismic features of the upper formation are interpreted to reflect the lithofacies of Unit A, characterized by common intercalations of tephra and sand layers. In contrast, the seismic characteristics of the upper-middle formation are generally muted and chaotic, and may reflect the predominantly clay-rich lithofacies of Unit B with few to no intercalations of sand or tephra layers. Unit C (very thin in cores and in seismic section) and Unit D are probably correlated with the top part of the lower stratified formation and are associated with strong reflections, probably due to common intercalations of sand and tephra layers. Another unconformity is also expected to exist at around 600 mbsf in Hole C9001D cutting recovery. This unconformity marks the boundary between Unit D, consisting of chaotic reflections, and the unit below, consisting of thick, well-defined, but relatively weak reflections gently dipping toward the northeast. The lithology of these units is still somewhat uncertain due to lack of core recovery, however, cuttings information reveals lithologies similar to, but more lithified than, the material recovered during coring.

3.2.2. Age model

A preliminary age model was created using shipboard biostratigraphy, tephrochronology and magnetostratigraphy analyses (Figure 3.4 and Figure 3.5). Biostratigraphic examination was conducted as a part of the LSIT by invited micropaleontologists. Three radiolarian and one planktonic foraminiferal datum events, ranging from 50 ka to 600 ka, were determined for cores taken from Hole C9001C. Since samples for micropaleontology were collected from every core catcher, each biochron datum has an intrinsic 9.5 m vertical error. In addition, calcareous nannofossil age was also preliminarily determined onboard only for a cuttings sample from the lowest interval of Hole C9001D; the age is expected to be approximately 1.6 Ma, but additional analysis and investigation are required. More detailed biostratigraphic data will be reported from the micropaleontology team, based on post-cruise shore-based examinations. Tephrochronological data is based on the recovery of two tephra layers that were recovered in Hole C9001C. The same tephra layers were collected from cores in Holes C9001A and C9002B (during the November, 2005 SIT expedition); these tephra have been identified by mineralogical and refractive index investigations. Results of paleomagnetic measurement indicate that the entire interval cored from Hole C9001C is still within the Brunhes epoch of normal polarity, therefore the bottom of the

hole is younger than 780 ka. Identified chronological events are summarized in Table 3.1.

Table 3.1. Stratigraphic events list for C9001C and D, determined onboard.

Event	Hole, Core, Section, Interval (cm)		Depth (mbsf)	Age (ka)	Remarks
	Upper limit	Lower limit			
Spfa-1	C9001C-4H-4, 57-68		30.30 – 30.39	43 ± 1	Tephra
T <i>Lychnocanoma nipponica sakaii</i>	C9001C-4H-CC, 34	C9001C-5H-CC, 36	35.3 - 44.9	50	Rad
Aso-4	C9001C-7H-4, 40-42.5		58.7	87.5 ± 2.5	Tephra
T <i>Stylocentronium aciculatum</i>	C9001C-16-CC, 30	C9001C-17-CC, 30	149.3 - 158.8	400	Rad
T <i>Axoprunum angelinum</i>	C9001C-21H-CC, 34	C9001C-22H-CC, 18	193.9 - 203.3	460 ± 40	Rad
T <i>Neoglobobulimina inflata</i>	C9001C-35X-CC, 13	C9001C-37X-CC	319.2 - 337.8	600 ± 100	Foram
B large <i>Gephyrocapsa</i> spp. ~ B medium <i>Gephyrocapsa</i> spp.	C9001D-25SMW		642 - 647	(1700 - 1480)	Nanno

Note: T = top, B = bottom, Rad = radiolarians, Foram = planktonic foraminifera, and Nanno = calcareous nannofossils. Analyses for identification of two known tephras were done using samples from C9001A and C9002B. Spfa-1 (Shikotsu-daiichi Tephra) is based on analyses at the Kyoto Fission Track Co. Ltd. (CDEX, unpublished) and by Masago (unpublished data). Aso-4 (Aso-daiyon Tephra) was also identified by Masago (unpublished data). Brunhes-Matuyama boundary horizon (780 ka) was not found within Hole C9001C.

The last occurrence of *Stylocentronium aciculatum* (indicating an age of ~400 ka) was identified in C9001C-17H-CC. This biostratigraphic marker fossil was absent from C9001C-16H-CC, indicating a possible biostratigraphic horizon occurred in the interval between cores 16H and 17H. Indeed, a curve extrapolated from biostratigraphic marker fossils found below core 17H falls within the margin of error for this datum, suggesting that the actual biostratigraphic event falls very close the identified horizon at or near 158 mbsf. However, projection of the age curve derived from biostratigraphic markers for the interval above core 17H falls well outside the margin of error for this horizon, indicating either a drastically lowered accumulation rate or an erosional/non-depositional unconformity occurred between the deposition of the lower strata (Unit B) and the upper strata (Unit A). There is an inferred, possibly erosional or

non-depositional unconformity (Unit A (core 16H) lies on Unit B (core 17H)) between these two cores, marked by the change in lithofacies and physical properties, and correlated with significant changes in seismic signature. We infer that the actual biostratigraphic event horizon may have been lost, either due to erosion or non-deposition. The accumulation curve for Unit A above this unconformity is partly tuned (using magnetic susceptibility variation data to calibrate the curve) in order to adjust for changes in sedimentation related to the last two glacial periods. However, even with this tuning, it is clear that there must either be a radical decrease in sedimentation rate, or an erosional event that has eliminated the lower section of Unit A and/or the upper section of Unit B. The actual depositional boundary between these units has been lost.

Sedimentation rates for all of Hole C9001C calculated from the age model vary from 54 cm/ka to 95 cm/ka, both of which are very fast for hemipelagic mud. Although it is quite difficult to create an age model for the interval below 365 mbsf, extrapolation from a single biomarker identified in cuttings retrieved from Hole C9001D suggests that the bottom of the hole is younger than 1.7 Ma.

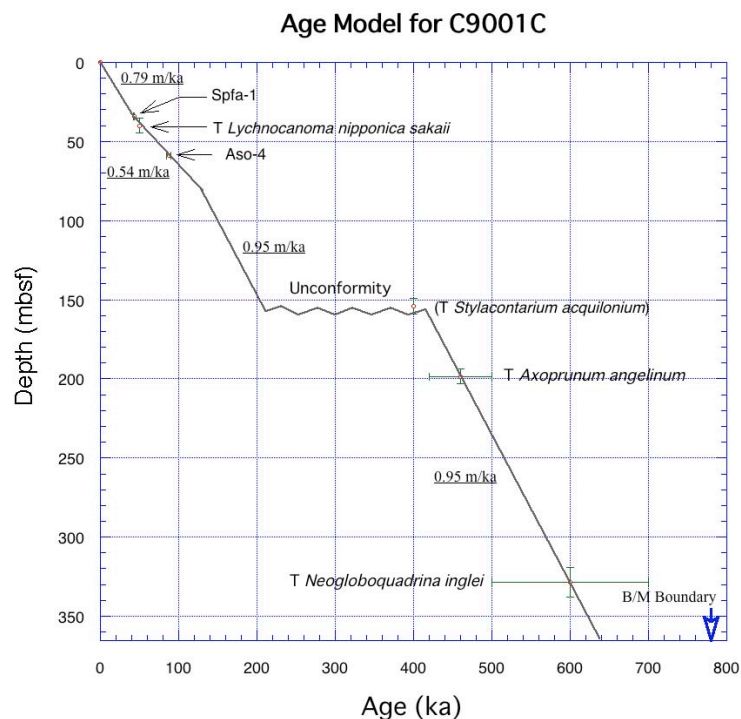


Figure 3.4. Plot of depth versus age for C9001C.

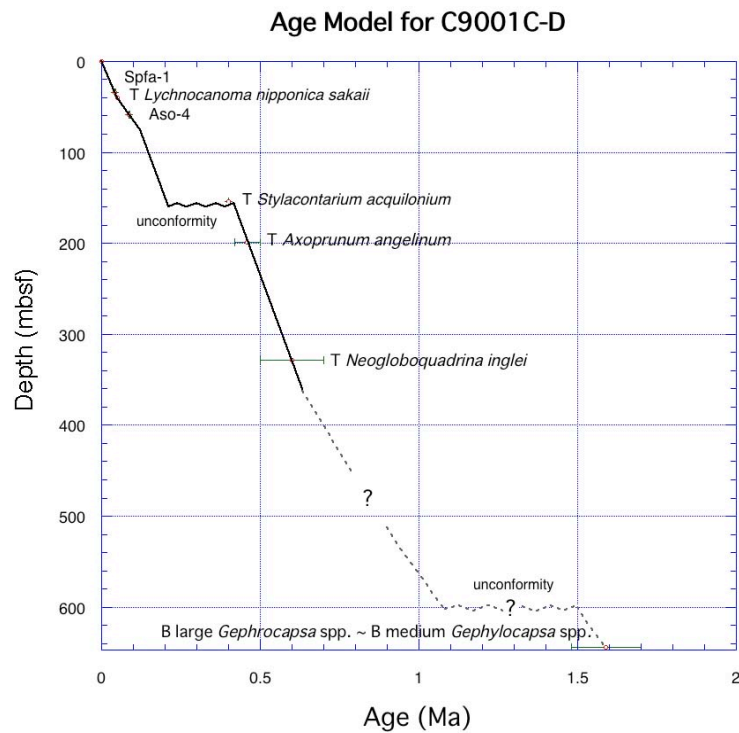


Figure 3.5. Plot of depth versus age for C9001C and D.

3.3. Constraints on Late Quaternary Volcanic Activity in Northeast Japan

Nearly homogeneous hemipelagic mud is the primary lithology of Hole C9001C and this mud is thought to have been accumulating steadily throughout the late Quaternary. The bulk of the cores retrieved fall into two units, A and B, that are divided by an inferred unconformity. The major differences between the two units are 1) the common occurrence of tephra and sand layers in relatively highly magnetic susceptibility hemipelagic mud in Unit A and 2) rare tephra/sand layers in lower magnetic susceptibility hemipelagic mud in Unit B. Tephra, especially andesitic to rhyolitic ones, are generally originate from explosive eruptions of subplinian to plinian types and are distributed over wide areas. The tephra found in Hole C9001C are inferred to be derived mainly from explosive eruptions of volcanoes in northern Northeast Honshu and southern Hokkaido. This region is also thought to be the source area for the terrigenous material found in the cores.

Common tephra layers found in Unit A indicate that volcanic activity in this region was relatively vigorous from about 200 ka to the present. In contrast the paucity of tephra in Unit B suggest that the period from 600 to 400 ka was volcanically relatively calm. In addition to the abundance of tephra layers, of the degree of magnetic susceptibility in hemipelagic mud may also reflect these variations in volcanic activity in the source area for terrigenous material: increased volcanic activity is inferred to provide a larger volume of iron-rich minerals and should lead to increased magnetic susceptibility. Only approximately 20 m of core were retrieved from Unit D, however, in that interval there is again an abundance of tephra layers, suggesting volcanic activity again increased between ~600-640 ka.

The onset of Quaternary volcanic activity in Northeast Japan arc is thought to have begun at around 1.5 Ma (Kimura and Yoshida, 2006), while volcanic activity in Northeast Honshu to southern Hokkaido appears to have started at ~700 ka and become more vigorous since ~300-200 ka (Fig. 2 in Kimura and Yoshida, 2006). More precise determination of temporal variations in volcanic activity for this region have not yet been established, however, a relatively quiescent period from 600 to 400 ka has been identified in cores recovered off Shimokita (e.g. Unit B, discussed above). The hemipelagic mud that comprises the majority of Unit B contain isolated and/or scattered pumices, but very few tephra layers. This is interpreted to indicate that local volcanic activity was relatively calm, while regional volcanic activity may have remained relatively vigorous. A similar period of relative inactivity around 500 ka is recognized in the southern region of Northeast Honshu, in the area around Mt. Bandai (Kimura, 1996). The results from cores collected from Hole C9001C should add constraints to reconstructions of late Quaternary temporal and regional variations in volcanic activity.

3.4. Implications for Late Quaternary Paleoenvironmental Variation of Northeast Japan Forearc Region

3.4.1. Two Major Clays

The lithology and physical properties of the clays comprising cores from Hole C9001C suggest the presence of two dominant clay types, Clay A and Clay B as follows (Figure 3.6):

- 1) Clay A: olive black and relatively rich in diatoms, exhibiting lower magnetic susceptibility, natural gamma radiation and bulk density, and higher electrical resistivity and CIE a* (reddish),
- 2) Clay B: dark olive gray and relatively rich in clastic grains such as quartz and clay minerals, exhibiting higher magnetic susceptibility, natural gamma radiation and bulk density, and lower electric resistivity and CIE a* (greenish).

These two clays alternate every several to tens of meters. The physical properties variations that characterize the two clays are thought to reflect their different sedimentary components. Diatom fossils composed of amorphous silica are porous, hence, sediments rich in diatoms, like Clay A, generally exhibit low bulk density. Porous character in sediments is generally thought to decrease electric resistivity as the pores are commonly filled with interstitial water. In the case of Clay A, however, higher electric resistivity is thought to reflect the presence of a relatively high volume of interstitial gas, rather than water, in the pores. In contrast, the higher magnetic susceptibility and natural gamma radiation in Clay B is thought to reflect high proportions of terrigenous clastic grains, especially magnetic minerals and clay minerals (containing radioactive potassium-40), respectively. Low CIE a* (high greenness) may reflect a high proportion of clay minerals.

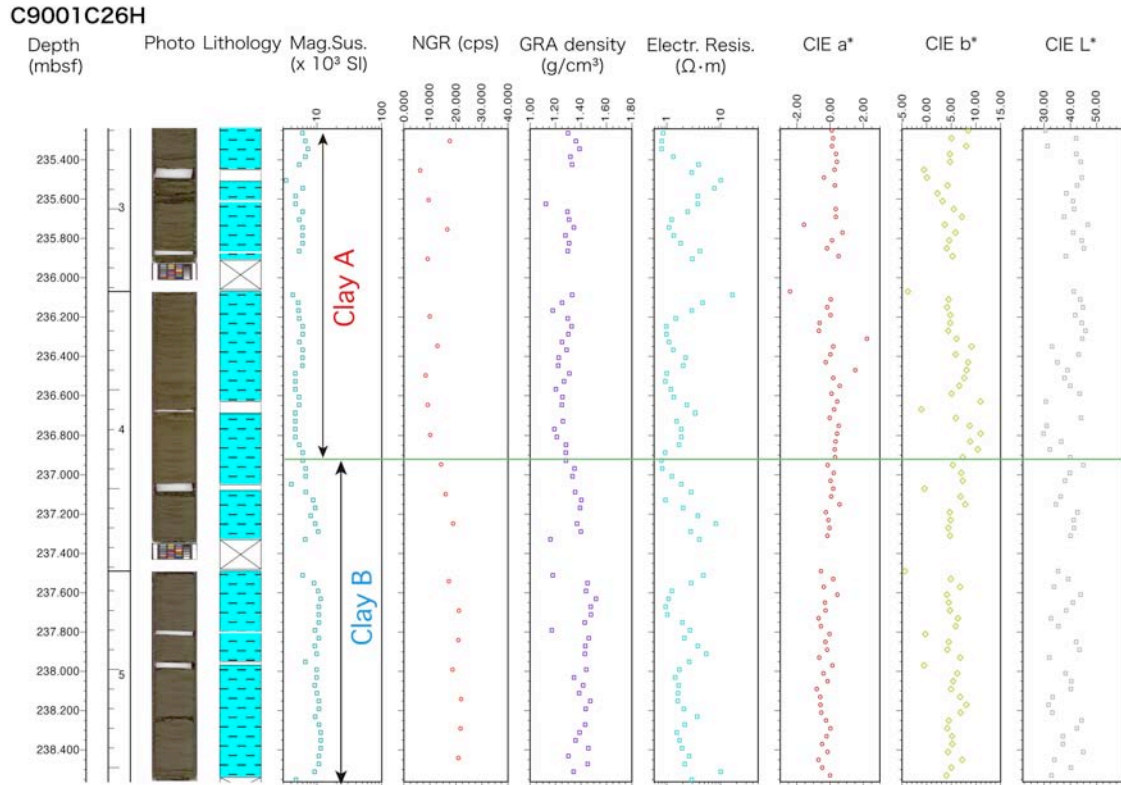


Figure 3.6. Meter-scale lithologic and physical properties variations between the two main clay types in a representative interval chosen from Core C9001C-26H.

3.4.2. Periodic Paleoenvironmental Variations

Paleoenvironment for each unit can be deduced from the characteristics of the clays discussed above. Although it is difficult to estimate absolute clastic flux and sedimentation rate for each interval, Clay A is considered to have deposited during a period with high biological productivity, where clastic grains were diluted relatively by diatoms. On the other hand, Clay B is regarded as having been deposited in a period where terrigenous clastic flux is higher. High biological productivity during periods of Clay A deposition is thought to reflect a relatively warmer climate, whereas high terrigenous clastic flux during periods of Clay B deposition are thought to represent cold climates, and thought to be associated falling sea levels.

The repeated alternation of Clay A and B is most marked from 308 mbsf (about 550 ka) and shallower, and the time intervals of repetition calculated according to the age model are about 40,000 years, 20,000 years, and several thousand years (Figure 3.6). In other words, inferred warm and cold climates repeat at these time intervals,

presumably responding to Milankovitch Forcing (derived from Earth's orbital eccentricity, axial tilt and precession). The 40,000 and 20,000 years cycles observed in these cores seem to directly reflect the Milankovitch Cycles. A robust age model will be established by further shore-based biostratigraphic and stable isotopic investigations, and frequency analyses will be completed on each property profile. These investigations should allow deconvolution of Milankovitch Cycles and other forcing factors affecting the expression of environmental variations in these cores.

Two large peaks in the magnetic susceptibility profile are recognized at depths of 45 mbsf and 135 mbsf, and are associated with Clay B physical and lithological properties (Figure 3.2). This relationship probably indicates enhanced terrigenous clastic flux related to an extreme drop in sea level. These relationships are used to infer that the magnetic susceptibility peaks reflect the impact of the early stages of the last two glacial periods, at ~60 ka and 180 ka, respectively. Using this assumption, the original age model (which is based on chronological events alone) is adjusted so that the two magnetic susceptibility peaks are coincident with these dates (Figure 3.4). Isolated pebbles and other large clasts likely to have originated from ice-rafted debris are unevenly distributed in the intervals thought to correspond to these glacial periods.

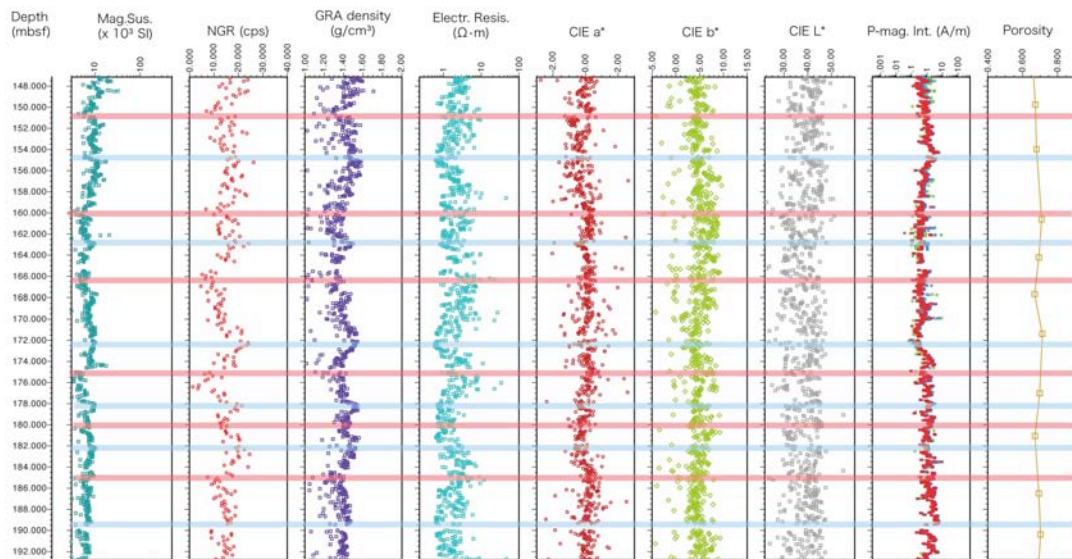


Figure 3.7. Periodic variations of physical properties and lithology. Representative profiles are selected from the interval from 147-193 mbsf. Red line: Clay A indicating warm climate; Blue line: Clay B indicating cold climate.

References

- Seno, T., Sakurai, T. and Stein, S., 1996. Can the Okhotsk plate be discriminated from the North American plate?. *J. Geophys. Res.*, 101, 11305-11315.
- Japan Natural Gas Association and Japan Offshore Petroleum Development Association (Eds.), 1992. Oil and Gas Resources in Japan, Revised Edition. Japan Natural Gas Association and Japan Offshore Petroleum Development Association, 520pp.
- Osawa, M., Nakanishi, S., Tanahashi, M., and Oda, H., 2002. Structure, tectonic evolution and gas exploration potential of offshore Shimokita and Hidaka provinces, Pacific Ocean, off northern Honshu and Hokkaido, Japan. *J. Jap. Assn, Petroleum Tech*, 67: 37-51 (in Japanese with English abstract).
- Kimura, 1996. Near-synchronicity and Periodicity of Back-arc Propagation of Quaternary Explosive Volcanism in the Southern Segment of Northeastern Honshu Arc, Japan: A Study Facilitated by Tephrochronology. *Quaternary International*, 34-36: 99-105.
- Kimura, J. and Yoshida, T., 2006. Contributions of Slab Fluid, Mantle Wedge and Crust to the Origin of Quaternary Lavas in the NE Japan Arc. *J. Petrol.*, 47: 2185-2232.

IV. Curatorial Report

4.1. Summary

Expedition 902 (Shimokita Shakedown Cruise) was focused on System Integration Tests (SIT) of equipment on board Chikyu. The SIT at Site C9001 Hole B was conducted using a drill bit, but without any retrieval of cores. At Hole C, piston coring was done and the 1st core was recovered successfully. However, the piston core assembly had some trouble while drilling for the next core, and the core recovered was without any accurate information about the drilled depth. This core has been recorded as core C9001Z, 1H in J-CORES. Coring was resumed at Hole C after rectification of the problem. In total, 40 cores were collected, and coring was accomplished to a depth of about 365 mbsf. Cores 34 - 37 were collected using ESCS (extended shoe coring system), while all others were collected with HPCS (hydraulic piston coring system). Core handling at the core cutting area was done rather swiftly in order to preserve the material until microbiological sampling could be completed. Each core was scanned with a portable infrared thermal scanner to detect methane hydrate, and some cores did show presence of hydrate particles. Each core was cut into 140 cm long sections, so that total length of each section after expansion did not exceed 150 cm (the limit of section length for measurement on MSCL-W). Head space (HS) and gas (MTGS and MTVG) samples were collected from the bottom of selected sections, and PAL samples were collected from the core catcher at the core cutting area. The top and bottom of each section were clearly marked by permanent ink pen, and blue (for top) and white (for bottom) color end caps were used to close the open ends of each section without using acetone or any other chemical. Large voids in liner were cut out, while soupy and loose sediments were pushed downward from the top of each core before marking the top of each section. Each section was labeled after entering relevant data in the J-CORES database and printing labels for working and archive halves. The sections were scanned with the X-ray CT scanner, and sampled for whole-round cores as per the sampling plan. The sections were then split into working and archive halves, and sampled/described as per the sampling plan. The sections were then put in ESCALTM film bags and vacuum sealed. At Hole D, cuttings samples were collected at the 'shale shaker' at regular

intervals (5 – 10 m) between 527 – 647 mbsf. These samples were washed and sub-sampled for shipboard analysis as well as for sample requests. The samples were dispatched to relevant laboratories for further examination after the end of the cruise, while the core sections and cuttings were brought to the Kochi Core Center for long term storage.

4.2. Core Recovery

Most of the time core recovery was slightly more than 100% (Table 4.1). Most of the cores were gassy, and holes were made on the working half side of the liner to release gas, which sometimes led to loss of sediment through the hole due to positive pressure inside the liner. A number of voids developed inside the liner as sediments moved up and down inside the liner due to the positive pressure. Observations on the condition of individual cores have been recorded in the ‘comments’ column of the J-CORES’ Curation Software.

Table 4.1. Core recovery data

#	type	Core		Liner		# of sections	Time on deck (date, UTC)
		top depth (mbsf)	advance (m)	length (m)	Recovery (%)		
1	H	0.00	6.91	6.92	100.14	5+CC	06.8.18, 06:17
2	H	6.91	9.50	9.75	102.63	7+CC	06.8.19, 08:35
3	H	16.41	9.50	9.88	104.00	7+CC	06.8.19, 10:50
4	H	25.91	9.50	10.17	107.05	7+CC	06.8.19, 12:51
5	H	35.41	9.50	10.17	107.05	7+CC	06.8.19, 13:48
6	H	44.91	9.50	10.22	107.58	7+CC	06.8.19, 15:09
7	H	54.41	9.50	10.15	106.84	7+CC	06.8.19, 17:21
8	H	63.91	9.50	10.20	107.37	7+CC	06.8.19, 19:32
9	H	73.41	9.50	10.27	108.11	7+CC	06.8.19, 20:35
10	H	82.91	9.50	10.51	110.63	7+CC	06.8.19, 21:37
11	H	92.41	9.50	10.23	107.68	7+CC	06.8.19, 23:59
12	H	101.91	9.50	10.18	107.16	7+CC	06.8.20, 01:10
13	H	111.41	9.50	10.21	107.47	7+CC	06.8.20, 02:07
14	H	120.91	9.50	10.15	106.84	7+CC	06.8.20, 03:21

Table 1 (continued). Core recovery data

#	type	Core		Liner	Recovery	# of	Time on deck
		top depth	advance	length		sections	
		(mbsf)	(m)	(m)	(%)		(date, UTC)
15	H	130.41	9.50	10.72	112.84	9+CC	06.8.20, 04:54
16	H	139.91	9.50	10.33	108.74	8+CC	06.8.20, 06:05
17	H	149.41	9.50	10.39	109.37	8+CC	06.8.20, 06:43
18	H	158.91	6.50	7.24	109.54	5+CC	06.8.20, 08:55
19	H	165.41	9.50	10.10	106.32	7+CC	06.8.20, 11:15
20	H	174.91	9.50	10.09	106.21	8+CC	06.8.20, 12:20
21	H	184.41	9.50	10.40	109.47	7+CC	06.8.20, 13:36
22	H	193.91	9.50	10.53	110.84	8+CC	06.8.20, 14:32
23	H	203.41	9.50	10.57	111.26	7+CC	06.8.20, 16:22
24	H	212.91	9.50	10.37	109.16	7+CC	06.8.20, 17:11
25	H	222.41	9.50	10.84	114.11	8+CC	06.8.20, 17:57
26	H	231.91	7.12	8.01	112.50	6+CC	06.8.20, 19:12
27	H	239.03	9.50	9.97	104.95	8+CC	06.8.21, 01:26
28	H	248.53	9.50	10.30	108.42	7+CC	06.8.21, 02:45
29	H	258.03	9.50	8.47	89.16	6+CC	06.8.21, 04:18
30	H	267.53	6.83	8.08	118.30	6+CC	06.8.21, 05:46
31	H	274.36	8.30	10.14	122.17	7+CC	06.8.21, 07:26
32	H	282.66	9.50	10.33	108.74	8+CC	06.8.22, 10:45
33	H	292.16	9.50	10.38	109.26	8+CC	06.8.22, 11:48
34	X	301.66	9.50	9.85	103.68	8+CC	06.8.22, 13:33
35	X	311.16	9.50	8.08	85.05	7+CC	06.8.22, 19:12
36	X	320.66	9.50	--	0.00	No recovery.	
37	X	330.16	9.50	7.70	81.05	6+CC	06.8.22, 21:48
38	H	339.66	7.97	9.35	117.56	7+CC	06.8.22, 23:11
39	H	347.63	8.20	7.51	91.59	13+CC	06.8.23, 00:51
40	H	355.83	9.50	9.95	104.74	14+CC	06.8.23, 04:32

Abbreviations: H, hydraulic piston coring system
X, extended shoe coring system
CC, core catcher
mbsf, meter below sea floor

4.3. Sample Requests

Fifteen sample requests were submitted to CDEX for this expedition. All sample requests were approved, except one (90211A), which is under revision at present (Table

4.2). Sample requests 90213A to 90215A are for technical purpose in order to prepare better laboratory procedures for use in future expeditions of *D/V Chikyu*. These 3 sample requests are not subject to moratorium related issues. Sample codes were assigned a prefix ‘902’ in order to distinguish them from routine sample codes and codes used in previous expeditions.

4.4. Samples

The grand total for all core sediment samples taken on board is 1458 (Tables 4.3, 4.4a and 4.4b). This total includes 576 samples for shipboard analysis of parameters such as dissolved gas, pore water and biostratigraphic age determination. Due to the ephemeral nature of properties required to effectively investigate organic material, pore water, and microbiology, sampling for these analyses was performed on board. Some samples showed signs of methane hydrates at a depth of about 190 m and below. Layers of tephra and the existence of some fossilized shells were also observed. Cuttings samples (total 149 in number) were also collected at regular interval at the shale shaker on board. An archive of 25 cuttings samples (~500 g each) has also been prepared for sampling and storage at the Kochi Core Center.

Table 4.2. Summary of sample requests

Request #	Requester	Organization	Sample code	Research objective
90201A	Kitazato H. Tsuchiya M.	IFREE	none	Extraction of ancient eukaryotic DNA from anoxic sediment
90202A	Sakamoto T. Iijima K. Saito S.	IFREE	none	Mineralogy, elemental chemistry, IRD counting, high resolution sedimentology, core-logging
90203A	Nunoura T.	XBR	902NUNOW 902NUNOD	Microbial DNA analysis
90204A 90205A	Takai K. Inagaki F.	XBR XBR	902KEN 902INAWF 902INAWD 902INAD	Cultivation of microbes Cell counting, microbe detection, gene function analysis
90206A	Masui N.	XBR	902MAS10 902MAS50	Microbial contamination in drill mud
90207A	Takami H.	XBR	902TKM	Meta-genome analysis

Table 4.2. (continued) Summary of sample requests

90208A	Matsumoto R. Ogihara S.	University of Tokyo	902MTGS 902MTIW 902MTIWS 902MTMH 902MTVG 902MTWC	Gas and methane hydrate analysis
90209A	Masago H.	CDEX	902MSCR 902MSCT	Heavy mineral composition
90210A	Lin W.	JAMSTEC	902LIN	Anelastic strain recovery of rock core
90211A	Uchida M.	IORGC	902UCD	Reconstruction of glacial-interglacial cycle
90212A	Yoshioka H.	AIST	902YSW	Methane production by microbes
90213A	Underwood M.	U. Missouri	902MUB 902MUC	Interlaboratory calibration of XRD
90214A	Sugiyama K.	MWJ	902MWJ	On board instrument calibration and training
90215A	Saffer D.	Penn. State U.	902SAF	Interlaboratory QA/QC for PP

Table 4.3. Number of samples taken on board ship as per sample request

# of samples	J-CORES code	Sample type, volume	Sample requester
1	902INAD	Whole	Inagaki F.
11	902INADMH	Sediments, 50 cc	Inagaki F.
8	902INAWD	Whole round, 10 cm	Inagaki F.
84	902INAWF	Whole round, 10 cm	Inagaki F.
31	902KEN	Sediments, 100 cc	Takai K.
11	902KENMH	Sediments, 50 cc	Takai K.
76	902MTGS	Sediments, 5 cc	Matsumoto R.
234	902MTIW	Pore water 50 cc	Matsumoto R.
215	902MTIWS	Squeeze cake	Matsumoto R.
12	902MTMH	Whole round, 10 cm	Matsumoto R.
9	902MTVG	Void gas, 5 cc	Matsumoto R.
76	902MTWC	Sediments, 5 cc	Matsumoto R.
10	902MUB	Sediments, 15-50 cc	Underwood M.
5	902MUC	Sediments, 50 cc	Underwood M.
39	902MWJ	Sediments, 100 cc	Sugiyama K.
44	902NUNOW	Whole round, 10 cm	Nunoura T.
2	902SAF	Sediments, 900 cc	Saffer D.
7	902TKM	Whole round, 20 cm	Takami H.
7	902YSW	Whole round, 20 cm	Yoshioka H.
882	; total # of samples		

Table 4.4a. Samples taken for shipboard analyses (core samples).

# of samples	J-CORES code	Sample type, volume
78	CARB	Sediments, 5 cc
38	HS	Sediments, 5 cc
78	ICP	Sediments, 10 cc
36	IW	Pore water, 10 cc
39	PAL	Whole round, 10 cm
3	PMAG	Sediments, 7 cc
80	PP	Sediments, 5 cc
139	SS	Sediments, 0.1 cc
85	XRD	Sediments, 5 cc
576 ; total # of samples		

Table 4.4b. Samples taken for shipboard analyses (cuttings samples).

# of samples	J-CORES	Weight (g)
6	CARB	250
6	HS	300
12	PAL	300
25	PMAG	100
25	PP	100
25	SS	0.1
25	XRD	100
25	XRF	100
149; total # of samples		

4.5. Inventory

Core sections packed in ESCAL™ film were placed into D-tubes before transportation to the KCC. Since the length of some sections was quite short, 2 or 3 of them were placed into a single D-tube. The total number of these D-tubes is 540. As shown in Table 4a, there are 139 smear slide samples and 25 cuttings samples (for archive). All of these samples will be transported to the KCC and stored there for future sampling party, examination, analyses etc. Smear slides are with Kan Aoike, CDEX for the time being.

4.6. Shipments

There are 6 box palettes containing Archive and Working halves of the all cores. All palettes have been sent to the Kochi Core Center.

- 1) PAL samples were shipped to Prof. M. Oda, Tohoku University. Sub-samples for examination of foraminifera, coccolithophore, radiolaria, diatom and silicoflagellate will be redistributed to other scientists.
- 2) Residue of PP and XRD samples to be shipped to Dr. T. Sakamoto, IFREE/JAMSTEC.
- 3) 902MUB and 902MUC samples to be sent to Prof. Mike Underwood, University of Missouri, USA.
- 4) 902SAF samples to be shipped to Prof. Demian Saffer, Penn. State University, USA.
- 5) Samples taken for microbiological research by the XBR research group have been taken along by the group as its members disembarked the ship.

4.7. Residue Distribution

Most residues from Expeditions 902 were forwarded to shipboard scientists to allow completion of the required shipboard science and descriptions. The remainder will be sent to the Kochi Core Center. The residues from Expedition 902 are as follows (number inside brackets is the request number):

Table 5. Residue distribution

Sample code	Destination
PMAG	KCC
PP	Tatsuhiko Sakamoto, JAMSTEC (90202A)
PAL	A consortium of paleo-scientists
IW	KCC
XRD	Tatsuhiko Sakamoto, JAMSTEC (90202A)
CARB	Chikyu

4.8. Action Items for Curator and Superintendents

- 1) Some color-dot seals of 5-mm in diameter were put on the end cap of D-tube to indicate the following situations. Note that usage of the colors are different from the ODP standard:

Red = Archive half

Yellow = the section was temporarily stored in a D-tube without ESCAL film, because the film was in short supply on board. Instead, it was wrapped 2-layers of cooking film (Saran wrap) and stored in a D-tube until the supply of new ESCAL film from shore. Yellow dot with black-marker check means that the section was re-wrapped properly in the ESCAL film during the cruise. The yellow-dotted sections are as follows: 26H-6A/CCA to 40H-14A/CCA, 31H-1W to 40H-14W/CCW.

Green = Archive half, which was demagnetized up to 25 mT. A routine core process of the demagnetization during this cruise is up to 10 mT. However, the SAC decided that they would conduct the over-demagnetization on some cores to identify the critical horizon of Brunhes / Matuyama Boundary in the Shimokita cores. The green-dotted sections are as follows: 33H-2A to 5A, 40H-2A to 5A, 8A to 10A, and 12A to 13A.

- 2) Update the J-CORES for the curated length and location and width of voids.
- 3) Correction of J-CORES data for the sample interval
- 4) Expedition 902 Post-cruise sample party - The sample party at the KCC will be held within FY2006.

4.9. Problems Encountered

4.9.1. *Partial Loss of Sample*

Since the sediments in Shimokita area are gassy, small holes were drilled on the working half side of the core to relieve the pressure inside the liner (Figure 4.1). Some amount of sediments was lost through these holes. The degassing took 1 – 2 minutes to complete, following that core was cut into appropriate number of sections. The gas continued to expand inside the sections and small pieces of regular liner were patched at the lower end of many sections to contain the protruding sediments, and loss of

sediments was minimized.

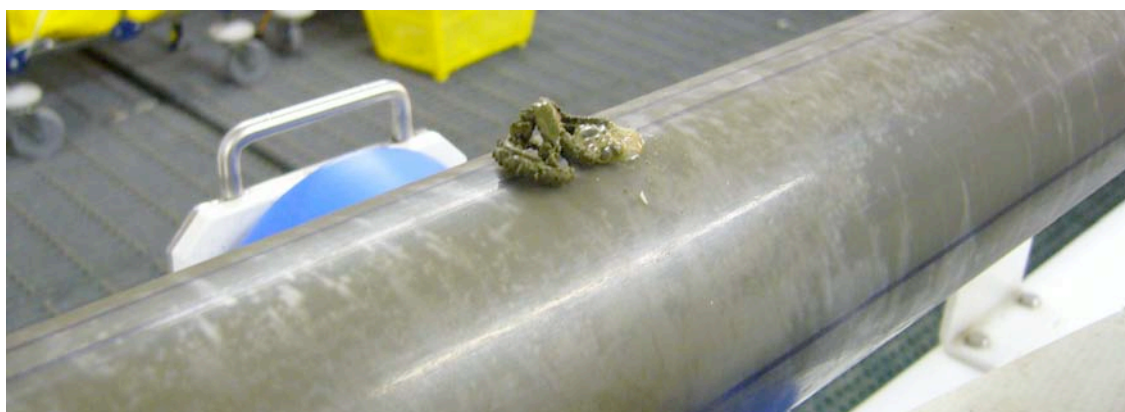


Figure 4.1. Sediment noodle oozing out of small hole drilled on the liner to release gas pressure of sediments inside the liner.

In the case of core 18, about 2.5 m long piece of liner from the top side was cut on the core cutting area, because this piece of liner contained soupy sediments originating from ‘washing’ of the drill string. The washing was conducted by the driller without any prior information to curator about this operation, and it was told afterwards that such washing is a common process in the drilling activity. The remaining length of the liner was curated as in the case of other cores.

While collecting core 39, the core barrel was shot without a liner inside the barrel due to some mistake. The mistake was realized only when core barrel was brought up on deck. The sediments were removed from the barrel and packed in small pieces of newly cut liner on the core cutting area.

4.9.2. Bent Core Liner

Due to expanding gases, the liner of core 32 could not be pulled out of the core barrel in the usual way. In stead it had to be pulled out of the barrel by using a chain hoist. This led to a bend in the lowermost part of the liner (Figure 4.2). Sediments in this part of the liner were badly disturbed and were put into a separate section.



Figure 4.2. Core liner (core # 32) bent in the process of being pulled out of core barrel.

4.9.3. Twisted and Broken Liner

In another case (core 40) of core liner remaining stuck inside the core barrel, the liner was twisted while being pulled out of core barrel by the driller (Figure 4.3). Due to over twisting, the liner got shattered and sediments were badly disturbed throughout the core.



Figure 4.3 Twisted and shattered liner of core # 40.

After pulling out the broken liner, the remaining piece of liner was pulled out by the driller by inserting a metal rod (ca. 1.5 cm in diameter) into the core from bottom side, and then pulling the liner out of core barrel (Figure 4.4). This led to serious

damage in the sediments. Liner was cut into pieces smaller than 140 cm to remove the rod safely. Removal of the rod from the sediments at the core cutting area left a long hole (void) in the sediments (Figure 4.5), especially in the section # 10 and 12.



Figure 4.4. A metal rod stuck in sediments of core # 40.



Figure 4.5. A columnar void space was created by the metal rod which was pulled out of sediments.

4.9.4. Handling of Carbonate Nodule

A round cobble was present in core # 28, section 4, 30 - 37 cm (Figure 4.6a). It was impossible to split by the strings, so that we first recorded the orientation of the nodule, picked it up from the section, and split by a core cutter in sampling room, then returned them to each Archive and Working half section (Figure 4.6b). The mineral content of the nodule was determined by the observation of a smear slide.



Figure 4.6a Carbonate nodule in core # 28, section 4.



Figure 4.6b. Split carbonate nodule in core # 28, section 4.

4.9.5. Pebble

A hard subrounded siltstone in pebble size was found at the top of core # 40, section 1, 0-10 cm (Figure 4.7). It was also impossible to split by the strings, so we split it by the same way of the carbonate nodule handling described above. This pebble is not a so-called dropstone, because small dots of blue paint adhered on the surface. Accordingly, it is considered that this stone was caught occasionally in the core barrel during the coring operation at the drill floor.



Figure 4.7. A pebble at the top of core # 40, section 1.

4.10. Other Problems

- 1) Residue of 902KEN, 12H-5, is missing.
- 2) An interval of 902MTIWS from 902-C9001C-38H-6 seems to be wrong. According to J-CORES data, it was taken at 110-130 cm, however the section is intact at 110-119 cm. In addition, the curatorial length of the section is 139 cm. Therefore, it was concluded that the WR sample of 902MTIWS was taken not from the interval of 110-130 cm but of 119-139 cm, and the data on J-CORES were corrected properly. An action is required on this problem, that is to inform the correction to the sample requester.
- 3) Some interval data of SS samples as entered in the J-CORES are obviously wrong. Although we could spend sometime to confirm all of them during this shakedown cruise because we had no cores, it is difficult to confirm one by one during a regular cruise.
- 4) Shortage of supplies, from basic stationary goods to sampling tools.
- 5) Lack of communication among LMs and curator. In many cases, most of the decisions on core handling were made without consulting the curator.
- 6) We have no equipment to seal WR samples by WAX as processed during ODP era.
- 7) Relocation of fully loaded Box Palette from Cold Core Storage is almost impossible. This problem is a pending matter.

- 8) A problem related to core handling: sometimes power cable of the Tablet PC, used for VCD, scratches on surface of Archive Half on Description Table. Proper handling of cables is required while conducting the VCD.
- 9) Problems related to the specification of J-CORES:
- i. Requirement of a function to produce Site/Core/Section/Sample summaries on J-CORES. Information of all Comment fields should be included in the summary.
 - ii. Requirement of additional columns for recording 2nd (or more) curated lengths (original data should not be deleted from database).
 - iii. Requirement of search/sort function by a comment field for tracking shipped sample residues and publication activities by each sample request number.
 - iv. 'Role' definition: Although we need to give a role of 'curator' to onboard scientists to input 'sample' data, it seems to be dangerous because all people onboard can edit original data of cores, sections, and samples. We need a discussion.

To solve the problem of mistype in J-CORES, check the entered values twice, and again at the end of the day. If there is any value different from that in sample request, then write an explanation in the comment column as to why sample has been taken from a different location. Any unusual location value discovered later will be modified to usual value by the curator.

Appendix:

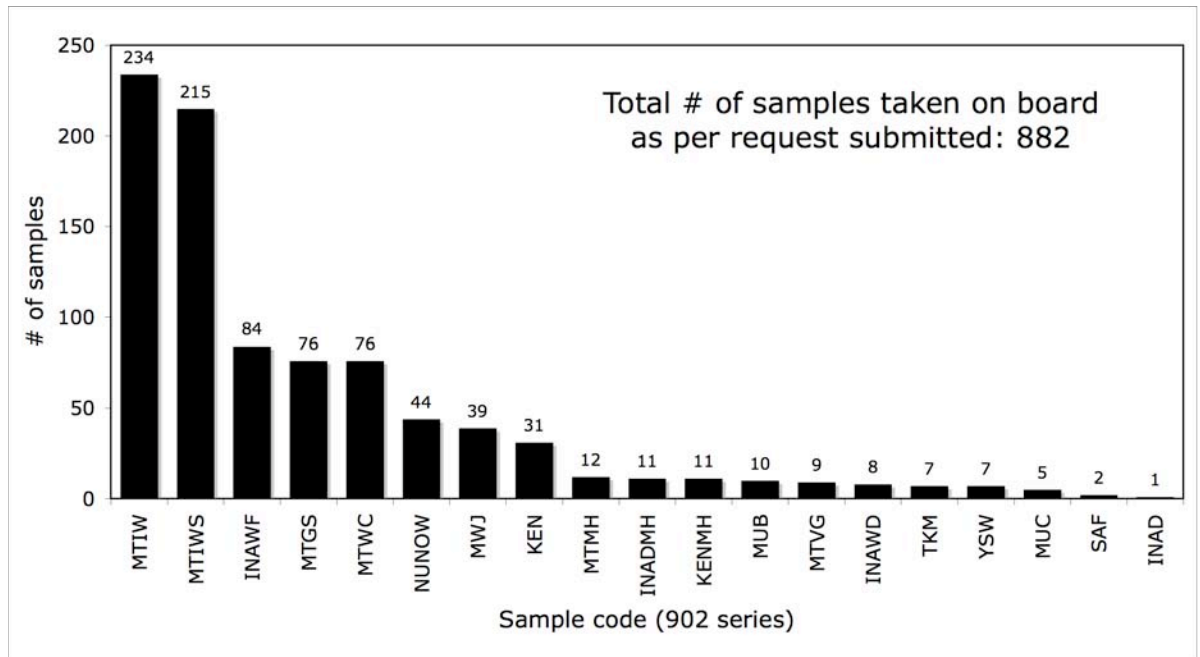


Figure 4A-1. Number of core samples taken on board as per sample requests.

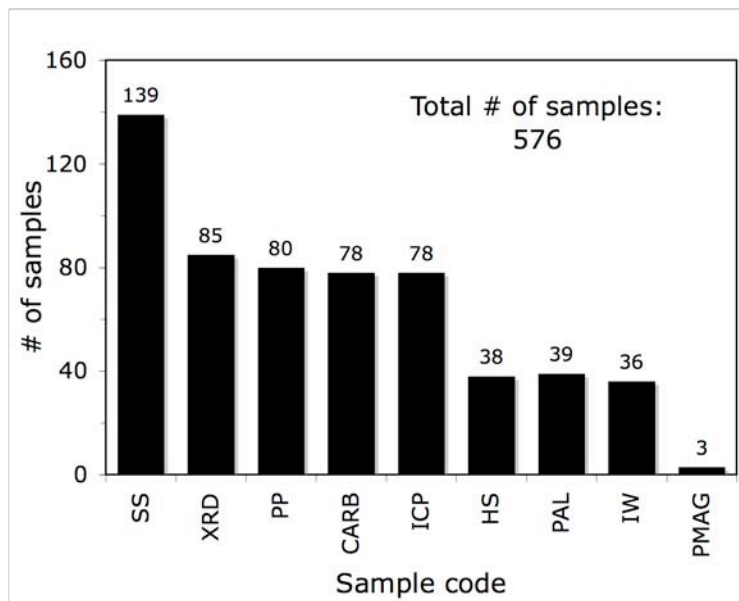


Figure 4A-2. Number of core samples taken for shipboard analysis.

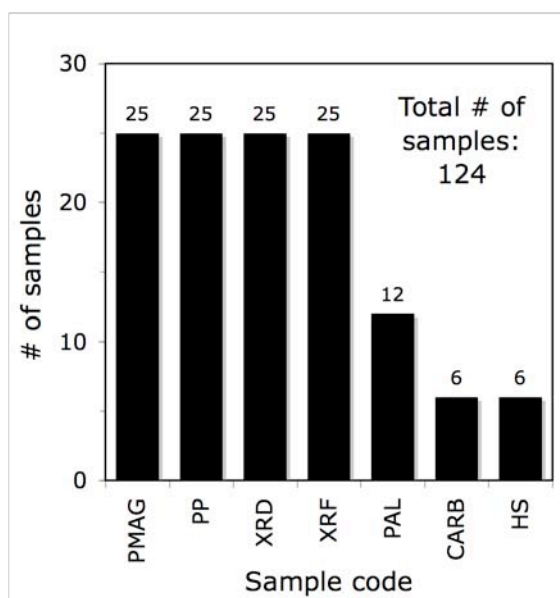


Figure 4A-3. Number of cuttings samples taken for shipboard analysis.

V. Laboratory Data Management Report

5.1. Goals

The data management goals during CK06-06 cruise were as follows:

1. Collect the data produced in the laboratory
2. Distribute the scientific data to scientists onboard
3. Store and back-up the scientific data
4. Perform on-the-job-training for Arakawa to be onboard system manager in laboratory

5.2. Targets and Methods

5.2.1. J-CORES System

Oracle relational database server and Apache http server were configured on a Sun Microsystems computer in order to provide J-CORES services. On client PCs/Macs J-CORES applications behaved as human-interfaces accessing the host server. Via http, the server provided application configurations, some scripts (to be explained detail later), application user manuals and so on.

Automated backup of the database was configured to take database dump on 11:00 and 23:00 JST (hereafter, all the time-zone are so in this document) every day. The dump files were written onto SDLT tape. The dump taken on 2006-10-21 11:00 was the final one and would be migrated to the shore database.

On 2006-09-19 a HDD in the RAID system connected to the J-CORES server was broken and potential risk to lose the data consequentially increased (to be described detail later). After that, all database files were backed up by writing to SDLT tape from 17:00 to 19:00 every day. While this backup work the Oracle service was down.

5.2.2. Web Directory to Collect Raw Data

Raw data file outputs from the laboratory instruments were stored into the RAID system connected to the J-CORES server. The Apache program on the server provided the WebDAV remote sharing directory service.

After the RAID trouble on 2006-09-19, the raw data were backed up using SDLT tape, similar to the method followed for the Oracle database files from 17:00 to 19:00 every day. The final set was written on 2006-10-21 13:00 and was moved to shore.

5.2.3. Material Registration

Curators, laboratory technicians and some scientists registered sections, core cuttings, and samples using J-CORES Applications “Operation,” “Curation,” and “Sample.”

Prior to the cruise, two label printers were prepared in the Core Registration Room on Lab Roof Deck and QA/QC Laboratory on Core Processing Deck in order to register sections and whole-round microbiology samples. After Hole C9001C coring, in the printer in the Core Registration Room was moved to the sampling table in Core Laboratory on Core Processing Deck in order to register samples from section halves. Several barcode readers were prepared in various laboratories.

5.2.4. Visual Core Description

Scientists described cores visually using J-CORES Application “VCD” without any intermediate medium such as paper barrel sheets: They called this procedure ‘Live VCD’ and finished an instruction document titled ‘Live J-CORES VCD実践マニュアル’ (in Japanese) meaning ‘Practical instruction of live VCD’). To use Application VCD, two Tablet PCs with stylus pen devices were employed.

5.2.5. Biostratigraphy

Paleontologists observed microfossils and found some biostratigraphic horizons. These data were entered into J-CORES by using Application “Stratigraphy.”

5.2.6. Provisional Archiving System of X-ray CT Scanning Image

We prepared a provisional archiving system for X-ray CT scanning images for this cruise. Two NAS system TeraStation hard disks provided Windows shared directory services and these directories were mounted over the network on the second console of the GE X-ray CT scan system in the Data Integration Center on the Lab Management Deck. X-ray CT scanning images were retrieved by the first console in CT Scan Laboratory on Core Processing Deck and transferred automatically to the provisional

archive system.

After the measurement campaign, the images stored in the TeraStations were sorted by sections, compressed and written to two SDLT tapes. These tapes were shipped to the shore.

5.2.7. The Other Instrumental Measurements in the Laboratory

Laboratory technicians stored the measurement results by laboratory instruments into JCORES database by using Application “Uploader.” Before loading the data, most needed to be converted from original formats to J-CORES' formats using several scripts prepared before the cruise or by hand (Table 5.1). The original data files were collected into the web directory.

Table 5.1. Laboratory instruments and methods to load their data into J-CORES database.

Instrument	Load method
Gas Chromatography NGA	Upload original files to J-CORES
Whole Core MSCL	Convert another format by a script
Thermal Conductivity	Upload original files to J-CORES
SQUID Magnetometer (section halves)	Convert another format by a script
Kappabridge	Upload original files to J-CORES
Image Line Scan MSCL	Convert another format by a script
CHNS/O Element Analyzer	Create J-CORES CSV by hand
Magnetic Susceptibility (core cuttings)	Create J-CORES CSV by hand
Colorimetry MSCL	Convert another format by a script
Moisture and Density	Hand-enter by J-CORES interface
Rock Eval	Create J-CORES CSV by hand
Interstitial Water Analysis	Create J-CORES CSV by hand
XRD	Upload original files to J-CORES

5.2.8. Wireline Logging Data

From a logging engineer, casing collar locator (CCL) data was provided in the LAS ascii format. The data were converted into J-CORES CSV format and loaded into the J-CORES database.

5.2.9. Mud Logging Data

Mud gas data (including total gas and C1 values) provided by well-site geologists, were converted into J-CORES CSV format and loaded onto the J-CORES database.

5.2.10. Drilling Parameters

Rate of penetration (ROP) values were also provided by well-site geologists. The data were converted into J-CORES CSV format and loaded onto the J-CORES database.

5.3. Results

5.3.1. Data Quantities

The laboratory personnel collected scientific data and the J-CORES system stored them (Table 5.2).

Table 5.2. Data quantities collected during the cruise. * Data items not collected during the last year cruise CK05-04 Leg 2.

Item	Quantity
Section	28 sections
*Core Cuttings	5 core cuttings
Sample	1607 samples
Gas Chromatography NGA	38 samples measured
X-ray CT scan	276 sections measured
Whole Core MSCL	294 sections measured
*Thermal Conductivity	79 horizons measured
SQUID Magnetometer (section halves)	26017 measurements done
*Kappabridge	2 samples measured
Image Line Scan MSCL	327 sections measured
Colorimetry MSCL	326 sections measured
Visual Core Description	488 lithology distributions, 1099 structures 561 drilling 64 microscope slides described
*Micropaleontology	39 samples observed; 14 planktonic foraminifers species 44 radiolarians species identified
*Biostratigraphy	5 biostratigraphic horizons found

Table 5.2. (continued)

Item	Quantity
Moisture and Density	77 samples measured
*Carbonate Analyzer	20 samples measured
CHNS/O Element Analyzer	78 samples measured
*Interstitial Water Analysis	86 samples measured
*XRD	86 samples measured
*Logging CCL	5688 horizons
*Mad Gas	126 horizons
*ROP	126 horizons

In comparison with last year's cruise (CK05-04 Leg 2), data counts and total data length were roughly two or three time larger and 11 data items out of 22 were treated for the first time during this cruise.

5.3.2. *Server hardware troubles*

On 2006-09-19 a HDD in the RAID system of the J-CORES server was broken. Fortunately, no serious losses occurred before 2006-10-23. The system will be repaired by replacing the broken HDD on 2006-10-27 during the port call at Hachinohe Port.

During the cruise the J-CORES server dropped under the following circumstances: (a) It was hotter than approx. 33°C in Computer Server Room, (b) Several hundreds of large (around 600 to 700 MB) files were written onto a remote SDLT tape by using rsh. No errors were recorded into the system log files.

5.3.3. *J-CORES software issues*

The following issues were raised during the cruise.

- 1) Difficult to distinguish archive and working halves on section label printed by Application "Curation"
- 2) Application "CompositeLogViewer" outputs curatorial data poorly. JCORES' identifier values of sections, miscellaneous materials and samples were hidden.
- 3) CompositeLogViewer does not output depth values in site/hole/core/section/interval form when exporting numerical data
- 4) CompositeLogViewer does not show graphs of water content
- 5) Poor human-interface to enter horizons of litho-boundaries and so on in

Application “VCD”

- 6) Adjacent tiny buttons ‘reload’ and ‘Save’ caused frequent data lost trouble in Application “VCD”
- 7) No GUI implementation to recognize stratigraphic horizons

5.3.4. Limitation of the provisional archiving system of X-ray CT scanning image

The provisional archiving system of X-ray CT scanning image required approx. 20 minutes for typical section with 1.5 m length to complete transportation from the first console to the second console, while the actual measurement took only approx. 10 minutes. Consequently, the file transfer queue became quite long and reduced the performance of the first console. The first console worked slowly after approx. 12 hours continuous work, and rebooting was recommended once every 12 hours.

5.4. Summary

The laboratory data management system during the cruise mainly consisted of the J-CORES system, the web directory to store raw data, and the provisional archiving system of X-ray CT scanning image and all they worked well. Data collected during the cruise are significantly larger than those during the last year cruise CK05-04 Leg 2.

There are however some issues remaining, and there is significant need to conduct investigations to solve them before the coming IODP expedition.

VI. Shipboard Scientific Party Report

Fumio Inagaki (XBR/KCC/JAMSTEC)

6.1. Routine Sampling

All WRC samplings have been carried out at QA/QC lab after scanning XCT images. Since the pore-water chemistry in shallow sediments might be strongly affected by microbial activities, such as sulfate reduction, methanogenesis, and anaerobic oxidation of methane, we collected WRCs from all sections of cores 1 to 4. From the cores below 40mbsf (Core 4), two WRCs for microbiology were routinely sampled from section horizons that headspace gas sample was collected at the catwalk deck while WRCs for porewater chemistry were sampled from all section ends. 3cc and 5cc of headspace sediments were collected routinely from the sections 1 and 4 at the catwalk deck for analyses of gas chemistry and water content, respectively. See sample log sheet provided by the curator.

6.2. Methane-hydrate Sampling

The presence of methane hydrates was all monitored by Thermo-View camera and visual inspection on the catwalk deck. We observed several hydrate-bearing horizons that temperatures were significantly decreased by melting effect of hydrates. The lithology of hydrates observed were composed of either sand or ash layers. The WRCs of hydrate horizons have been specifically sampled as WRC at Core Cutting Area and were subjected to subsampling for microbiology and geochemistry at QA/QC lab.

6.3. Sample Preparations

Pore water was squeezed by three 20t-press squeezers at QA/QC lab and stored at 4°C. We provided approximately 30ml porewaters from all section 4 to MWJ for the assessment of lab equipments. The residues of squeezed sediment core were stored at 4°C for shore-based organic geochemistry analysis. From core 1 and core 3, we collected 20cm WRCs for activity measurements and metagenomic analyses. The WRC

samples for activity measurements were immediately transferred to the anaerobic globe box, put into oxygen-penetration resistant vinyl bags, and then stored at 4°C. To evaluate cell population in sediments, 10cc sediments were collected from innermost part of core by 3cc tip-cut sterilized syringe and stored at 4°C. The cell abundance will be evaluated by staining DNA according to the SYBER-II protocol. To visualize some specific cells that contain RNA, we perform the catalyzed-reporter deposition fluorescence in situ hybridization analysis (CARD-FISH). For the CARD-FISH analysis, cells in 1cc sediments collected by 3cc tip-cut syringe were suspended with 9ml phosphate buffer saline (PBS) with 2% paraformaldehyde and fixed at 4°C for 6 hours. After the fixation, the sediment was washed with PBS twice by centrifuging at 4000rpm for 10 min, re-suspended with 10ml PBS-ethanol (1:1), and stored at -20°C. For cultivation analysis, we prepared anaerobic slurry samples of innermost core sediments with and without reducing reagents (0.05% v/v Na₂S, pH7.2). All subsampling procedures using tip-cut syringes and slurry preparations have been done in the lamina-flow clean bench to avoid potential contamination from surrounding dust and air. Other WRC samples for molecular (DNA/RNA) analyses including for metagenome analysis were stored at either -80°C or -100°C immediately after split works at QA/QC lab.

6.4. pH and Alkalinity Measurement

After processing all WRC samples and porewater squeezing, we measured pH and alkalinity in porewaters of selected horizons using a Titrator at geochemistry lab. Temperature of samples was kept at 25°C with water bath. Capitulation of pH and alkalinity with standard solutions were carried out every 10 measurements.

Appendix

- 1. Core Photo Images**
- 2. X-ray CT Images**
- 3. Onboard Measurement Results**
- 4. Visual Core Description**

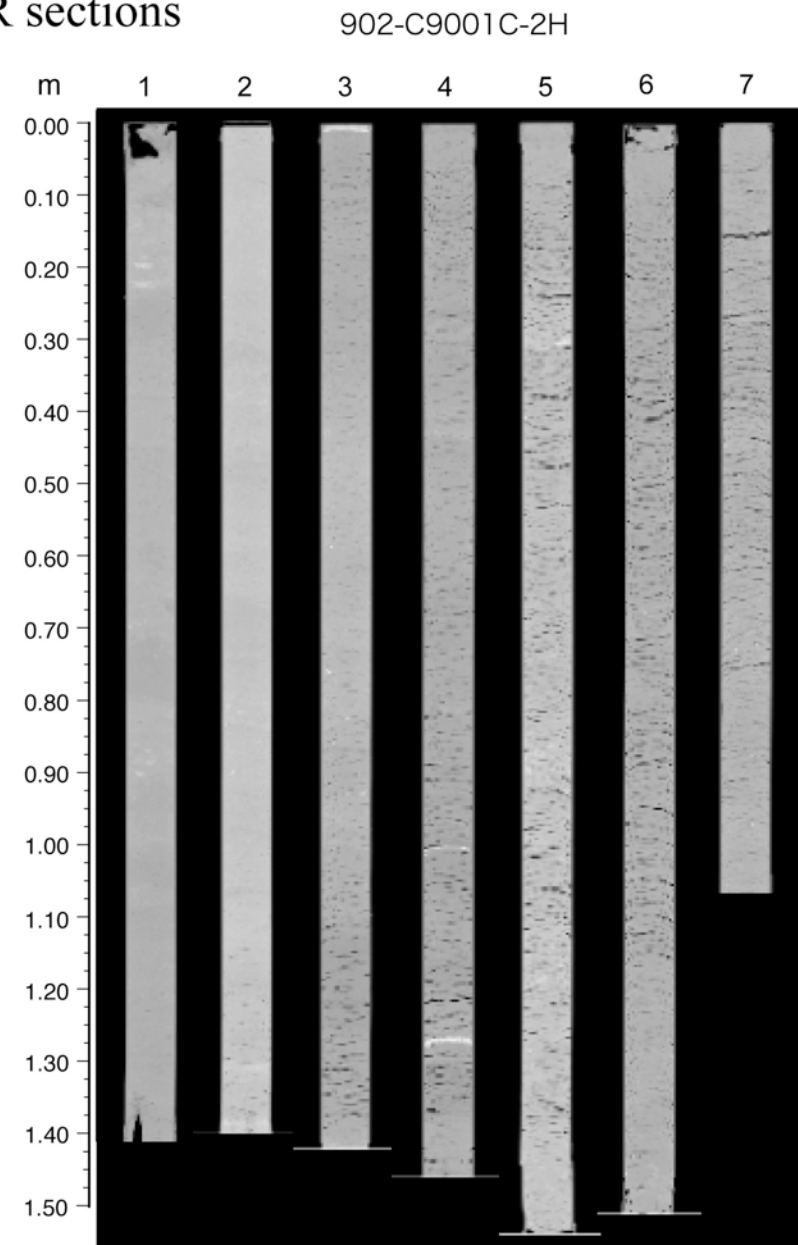
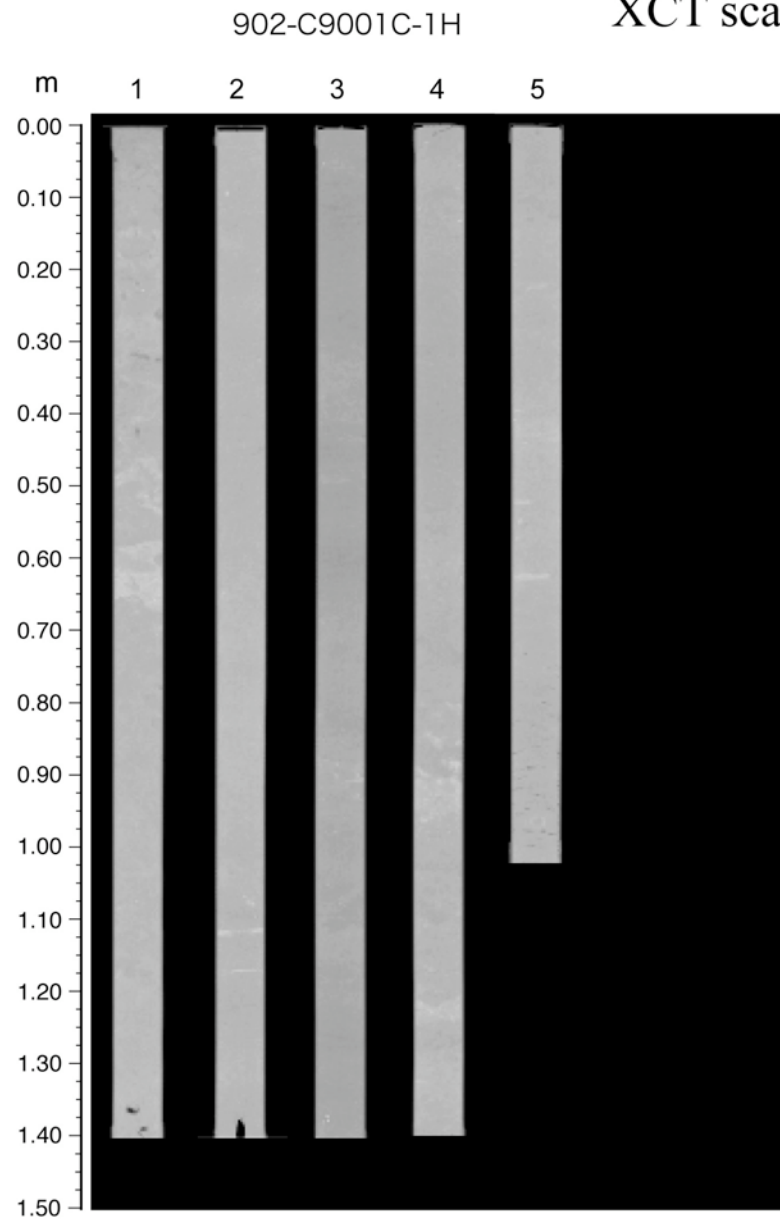
Appendix 1

C9001C

X-ray CT Images

Note: Brightness and contrast of the CT images are not adjusted to a certain reference CT value. Therefore, apparent brightness changes section by section do not necessarily reflect actual density variations

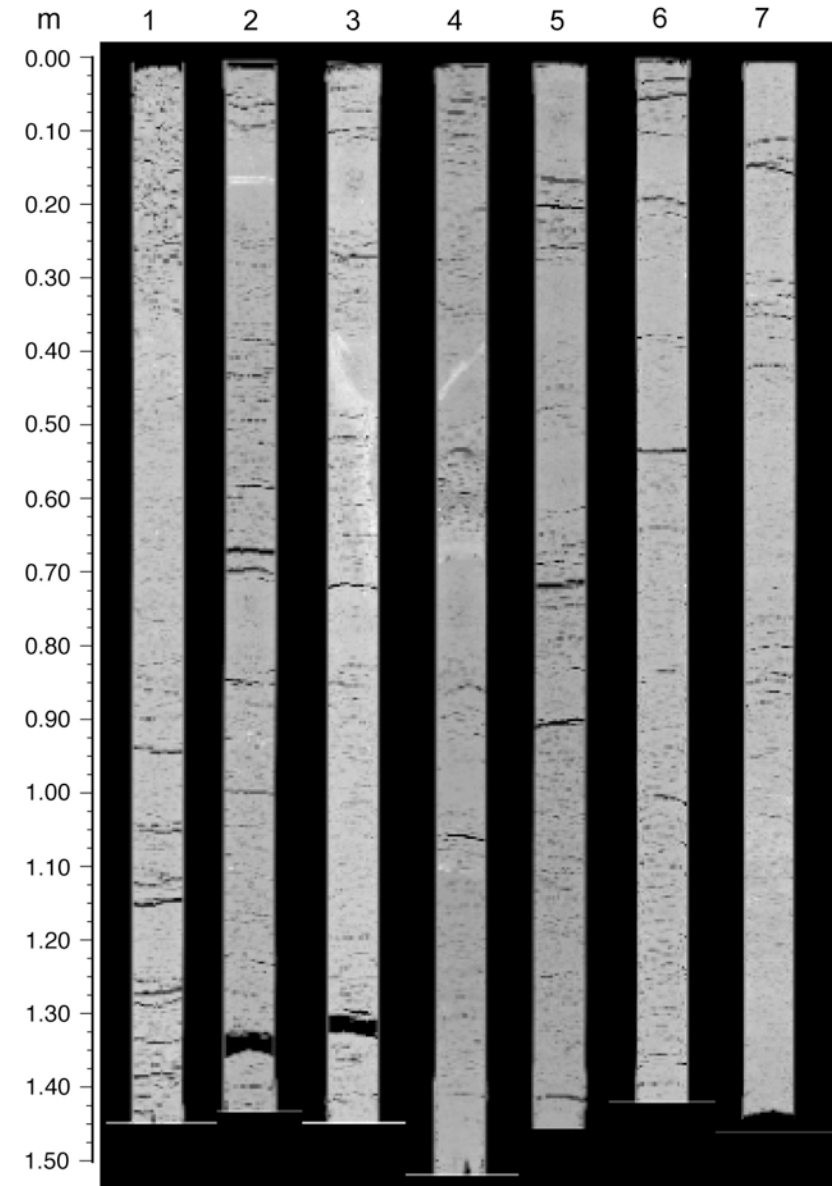
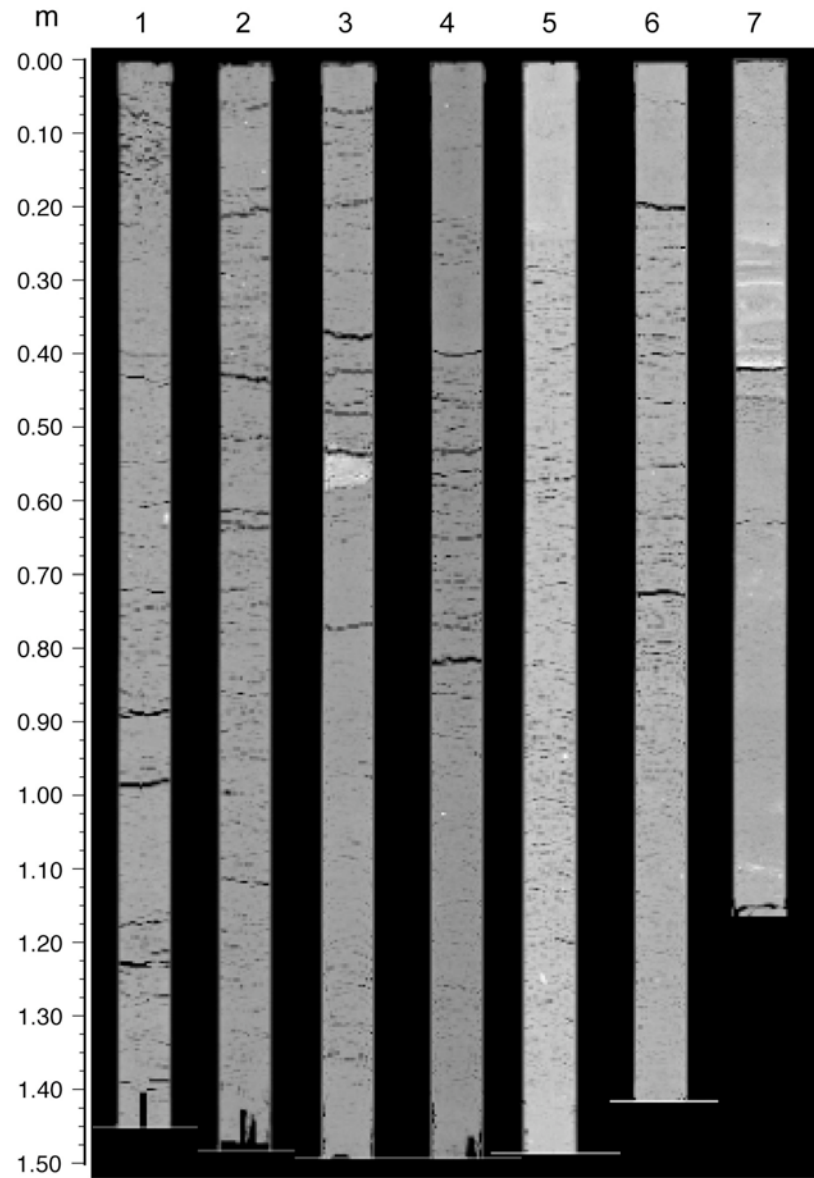
XCT scans of WR sections



902-C9001C-3H

XCT scans of WR sections

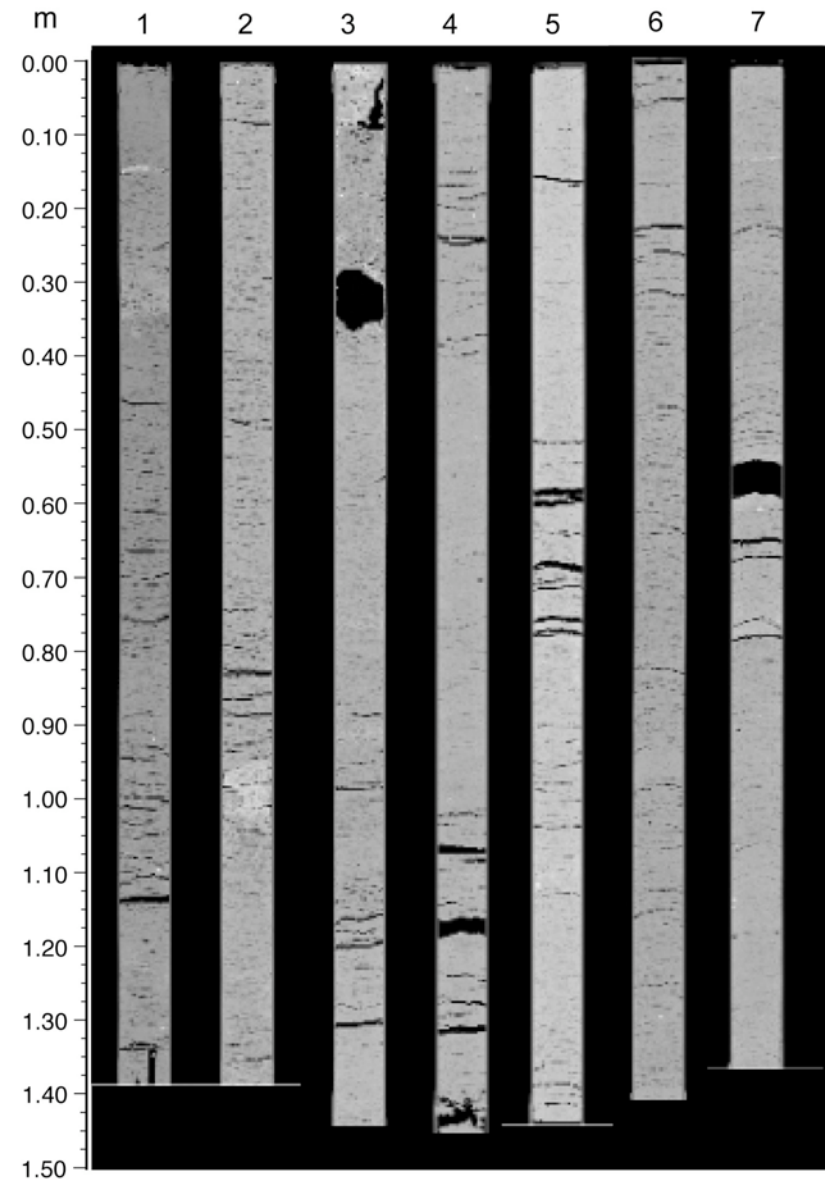
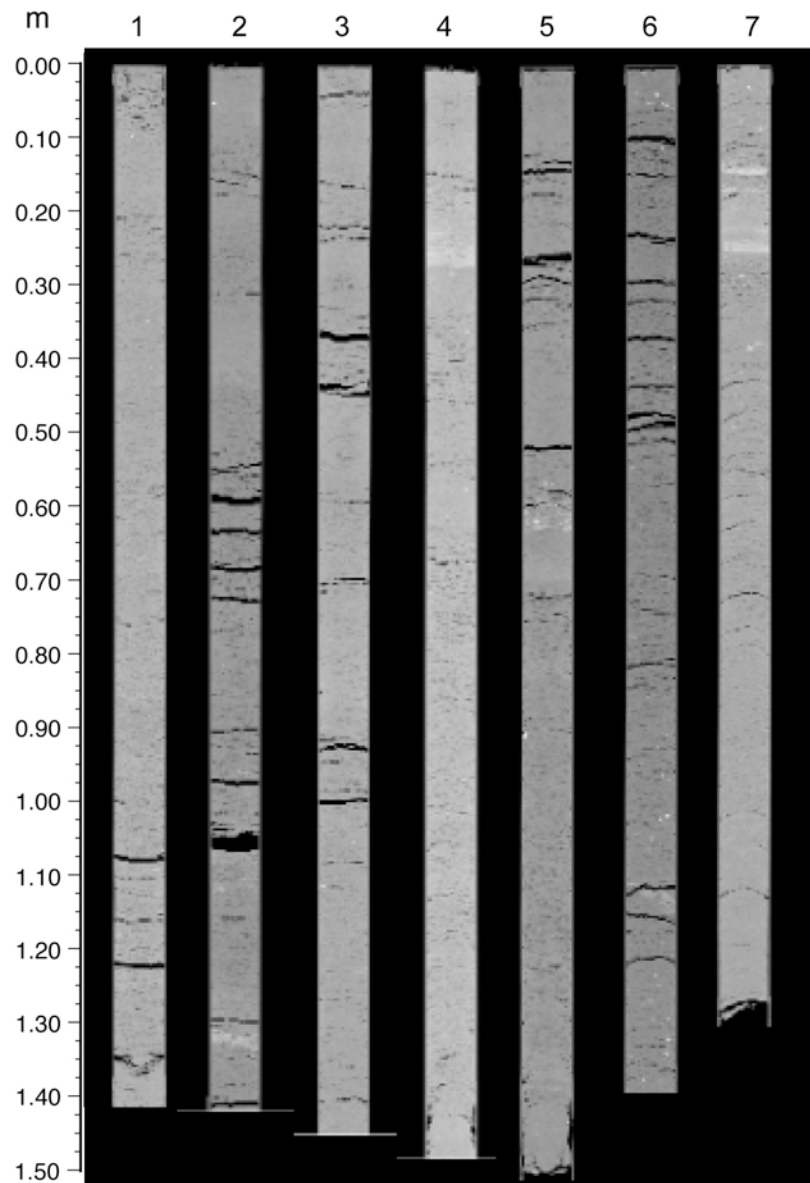
902-C9001C-4H



902-C9001C-5H

XCT scans of WR sections

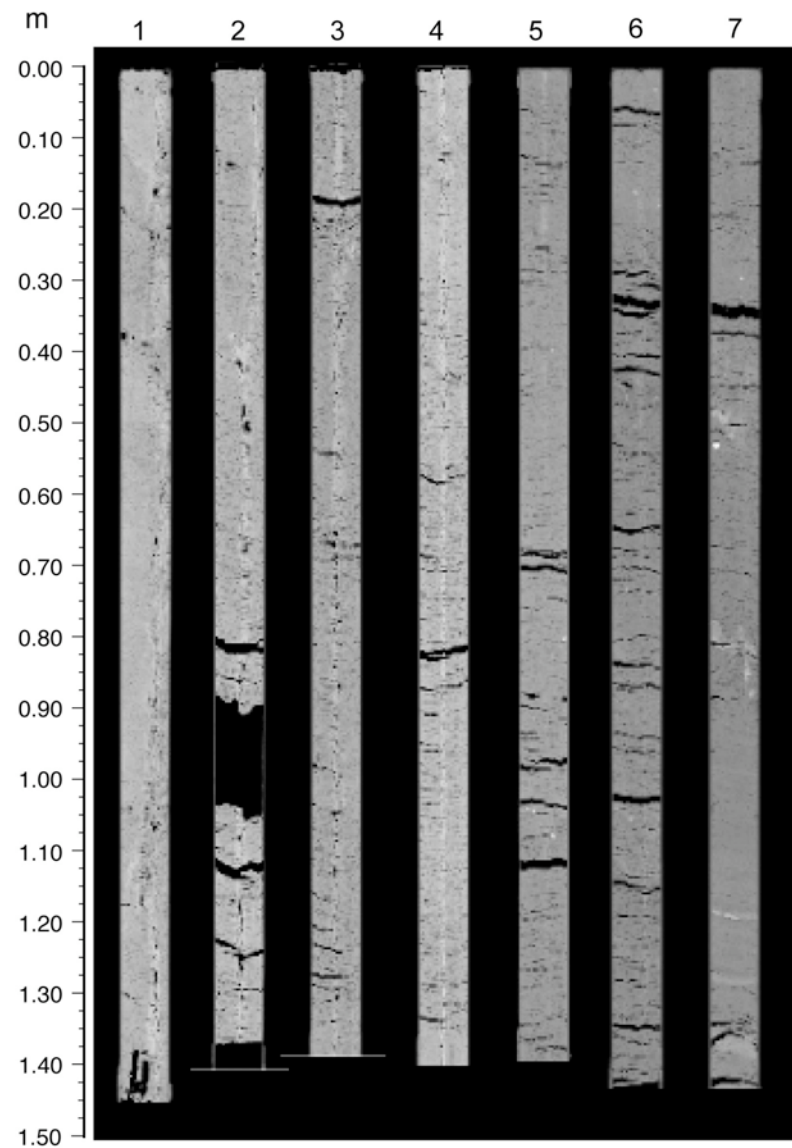
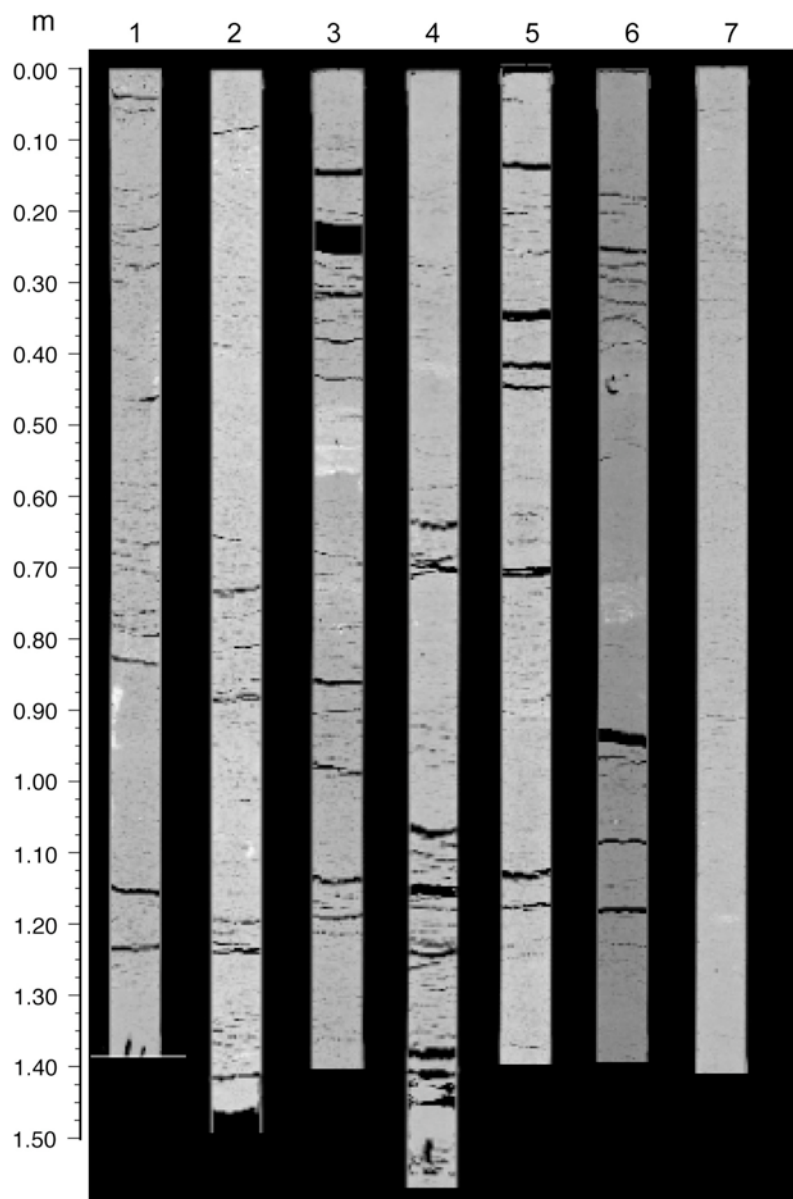
902-C9001C-6H



XCT scans of WR sections

902-C9001C-7H

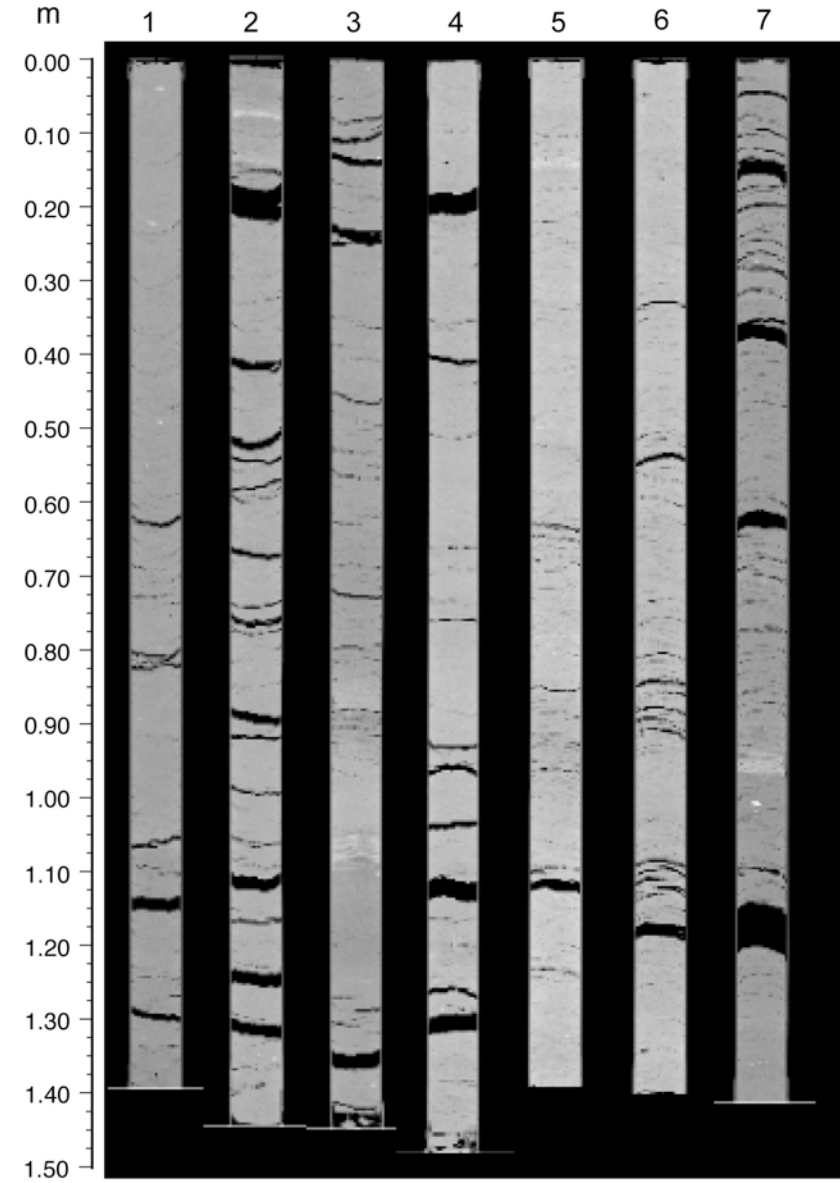
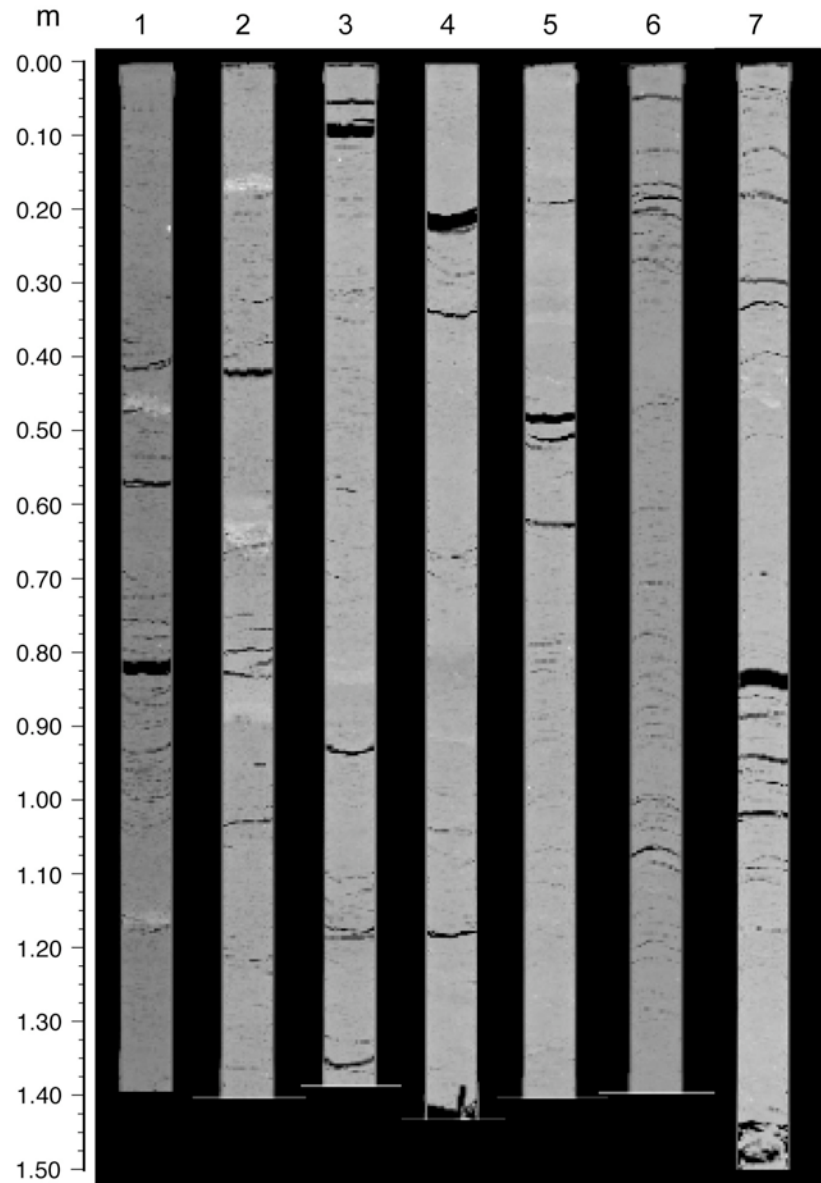
902-C9001C-8H



902-C9001C-9H

XCT scans of WR sections

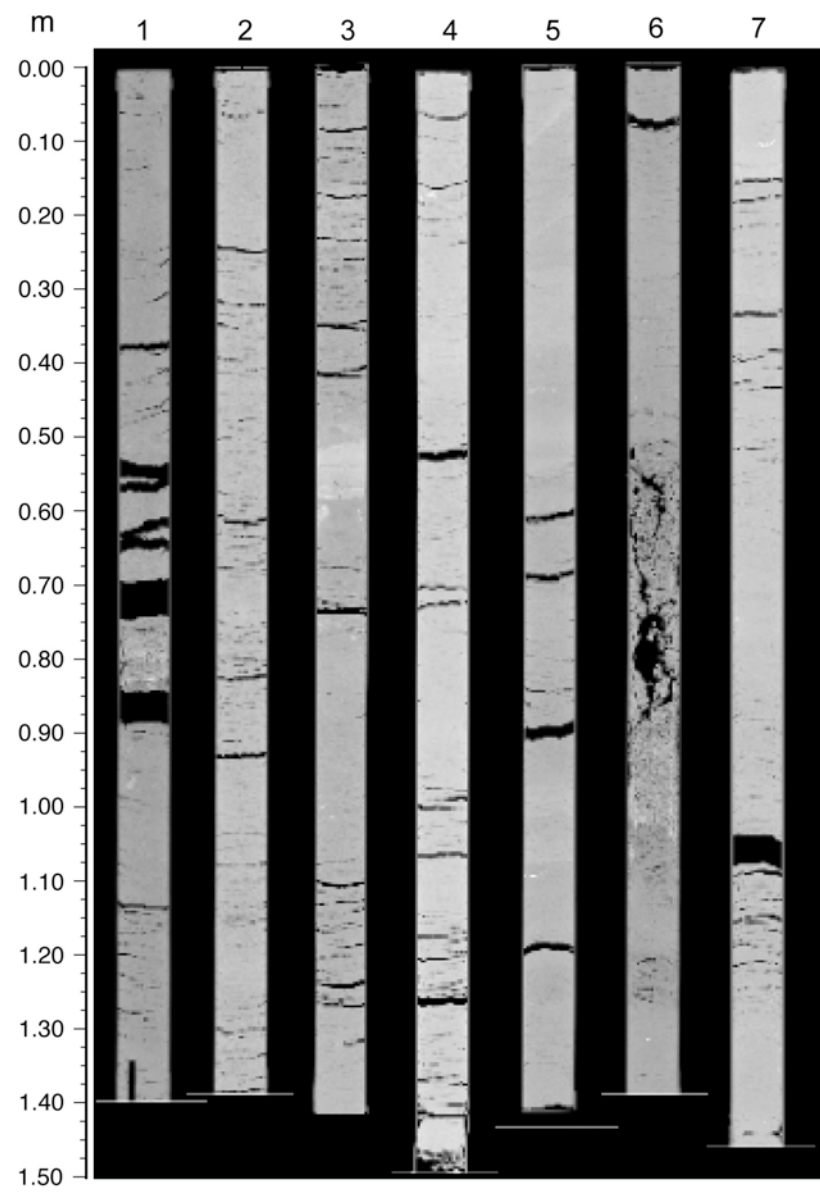
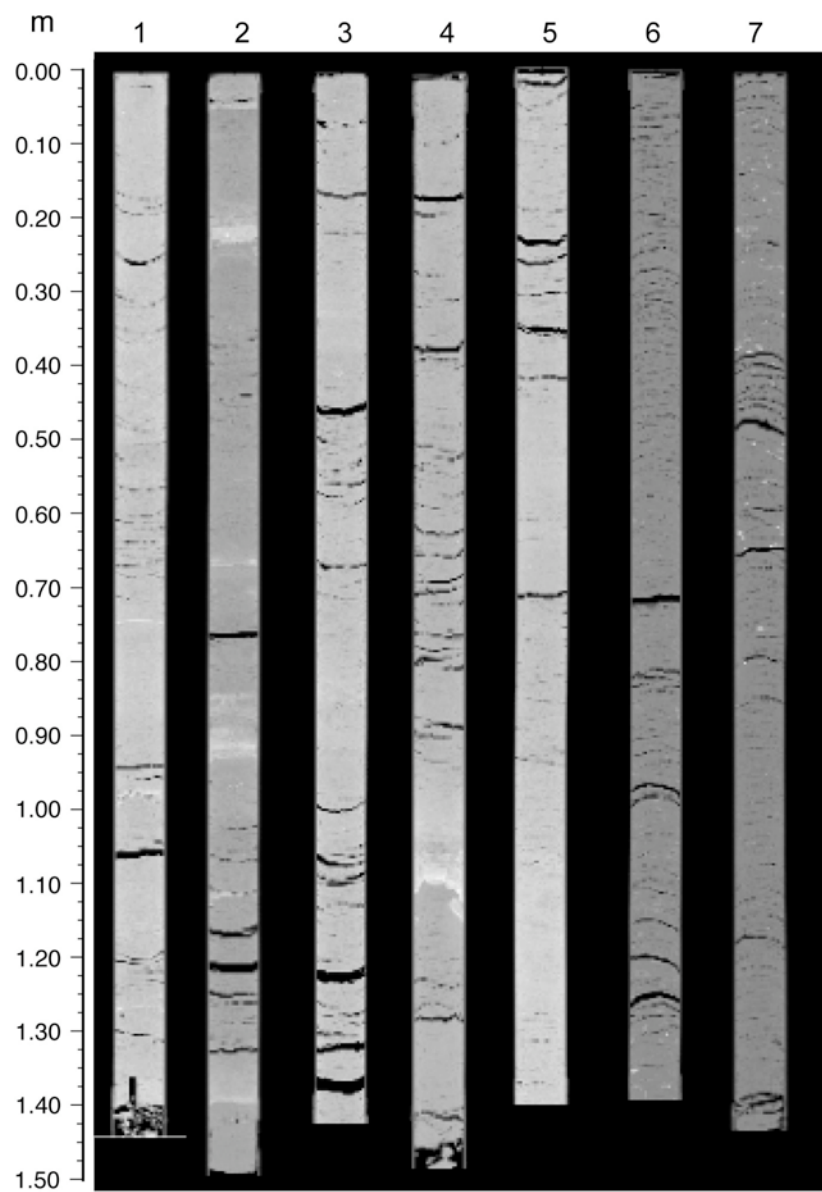
902-C9001C-10H



902-C9001C-11H

XCT scans of WR sections

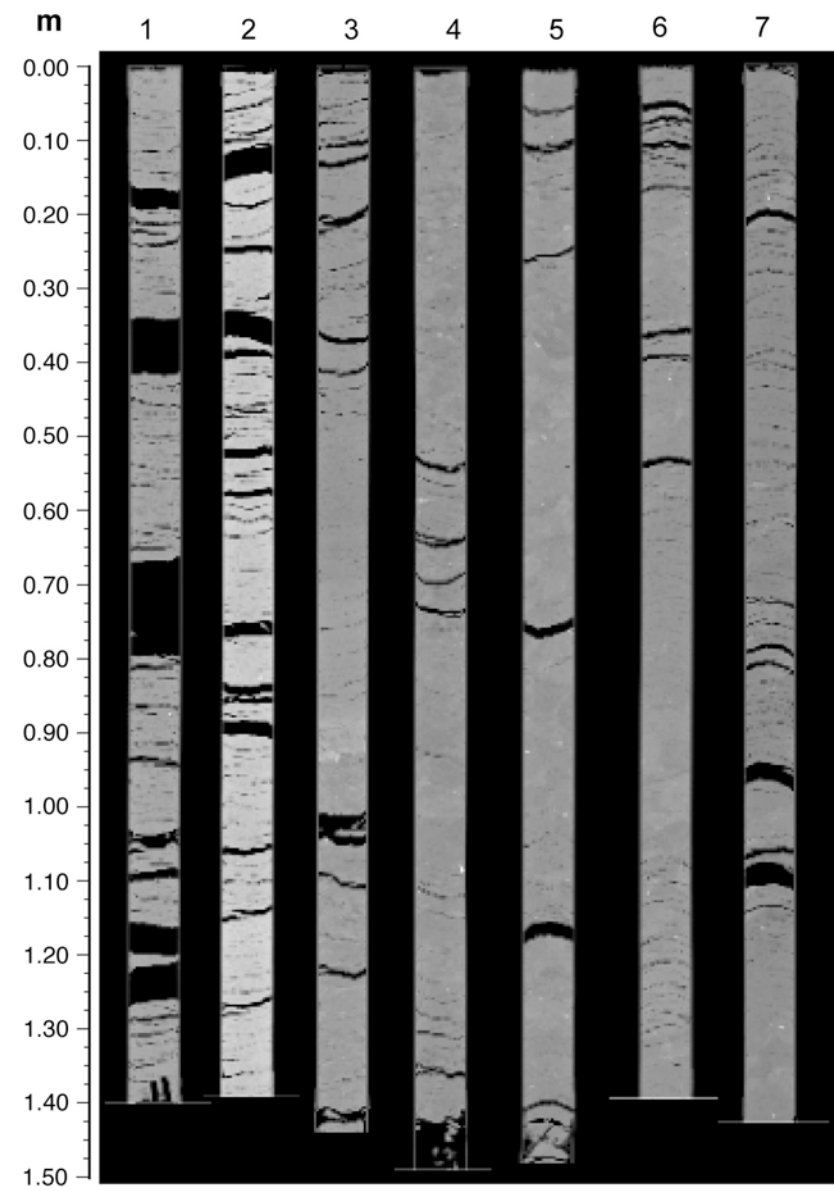
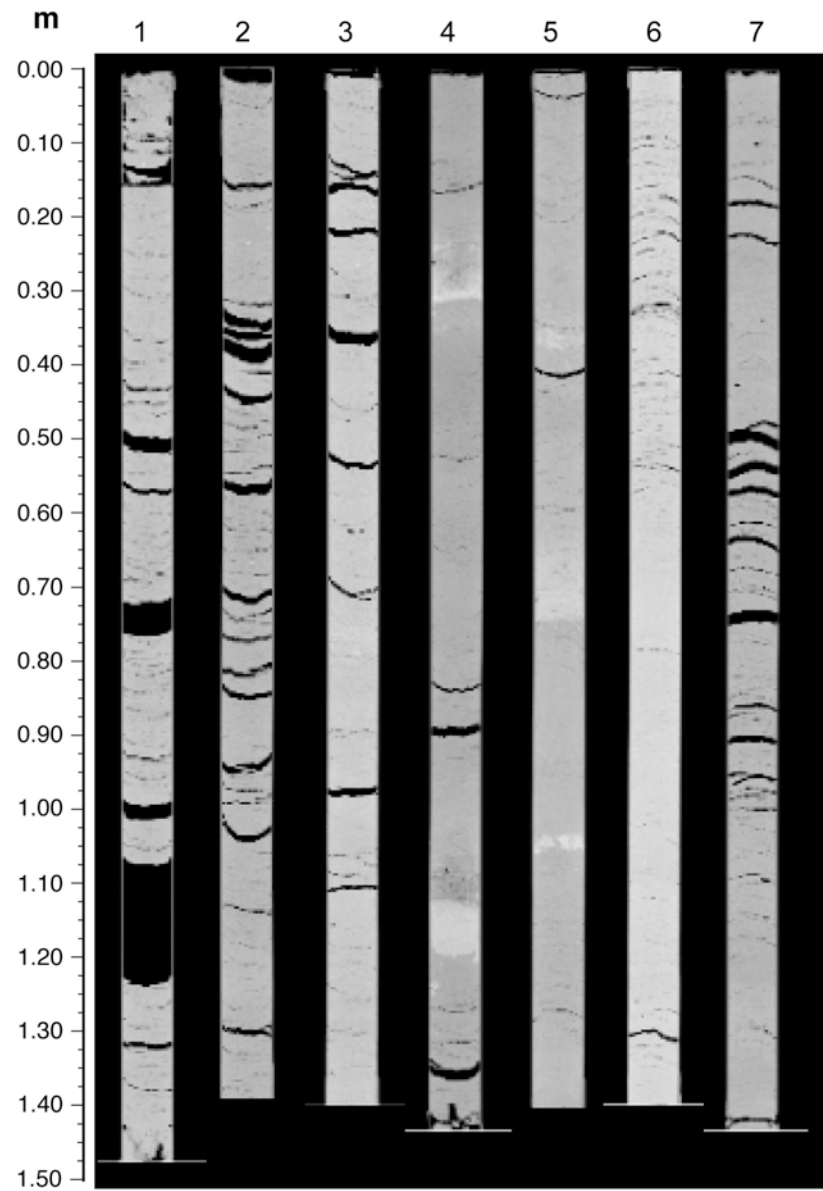
902-C9001C-12H



902-C9001C-13H

XCT scans of WR sections

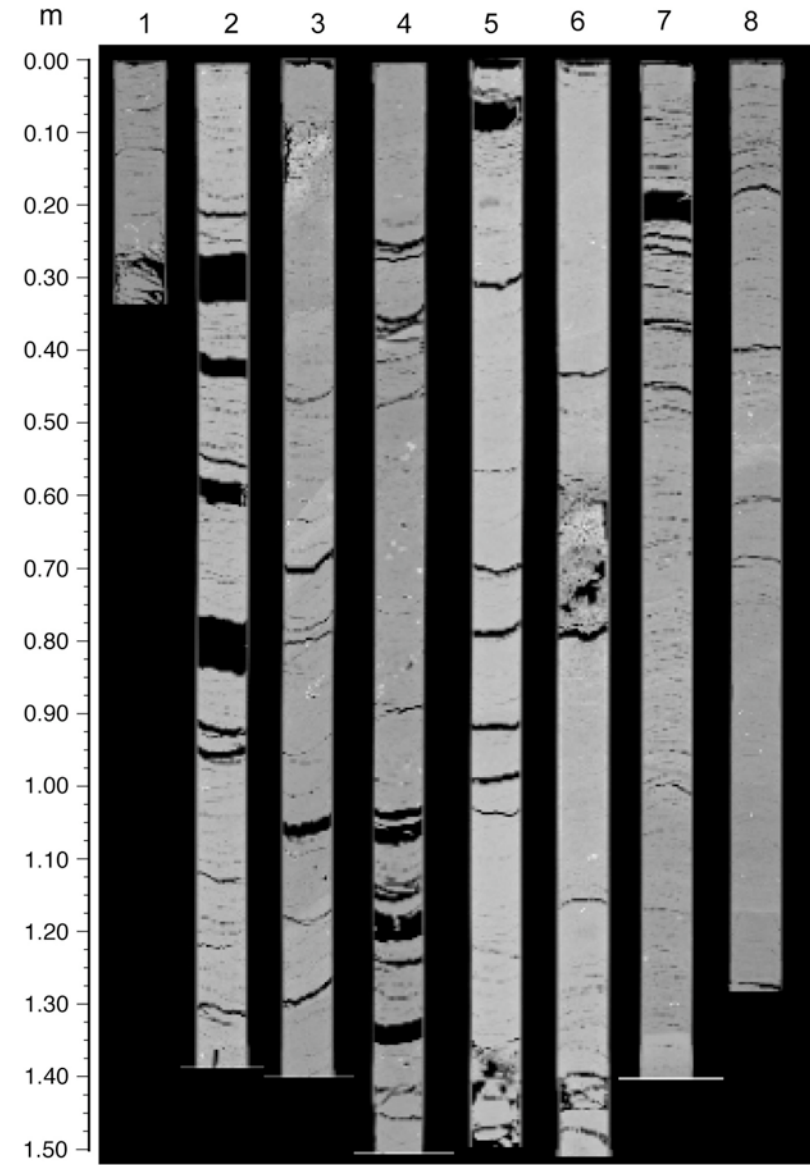
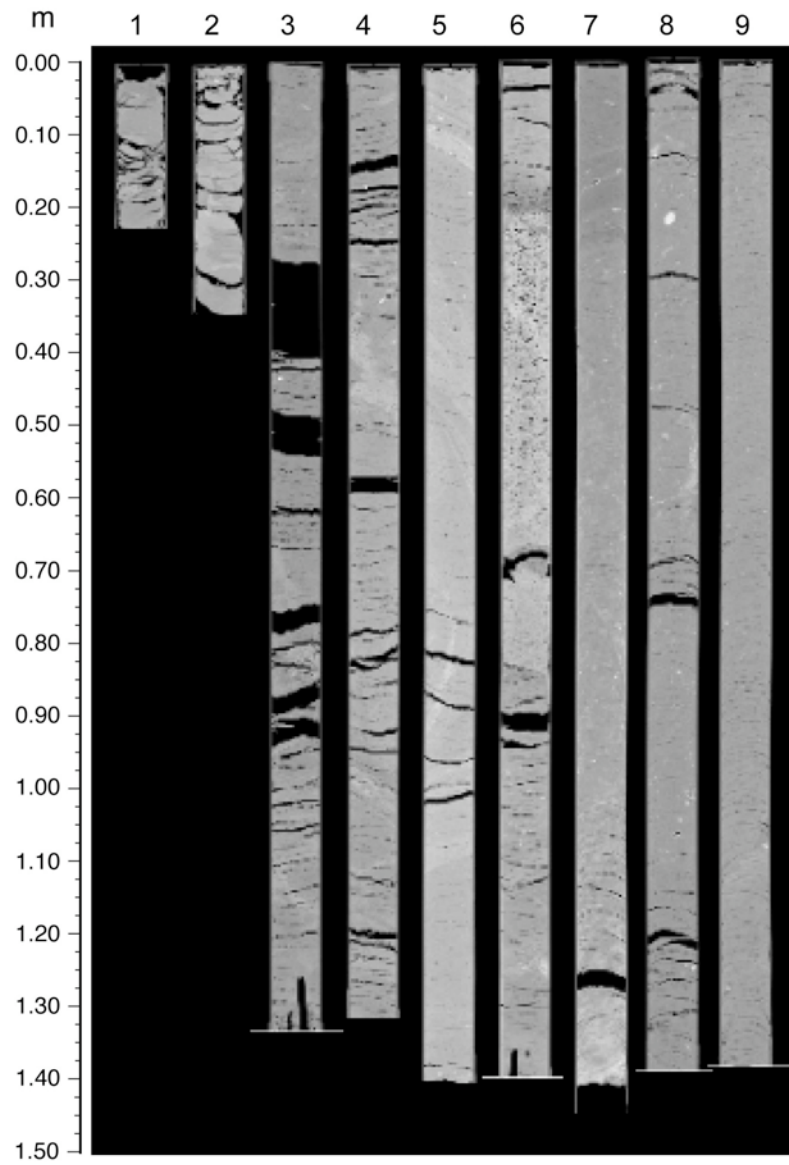
902-C9001C-14H



902-C9001C-15H

XCT scans of WR sections

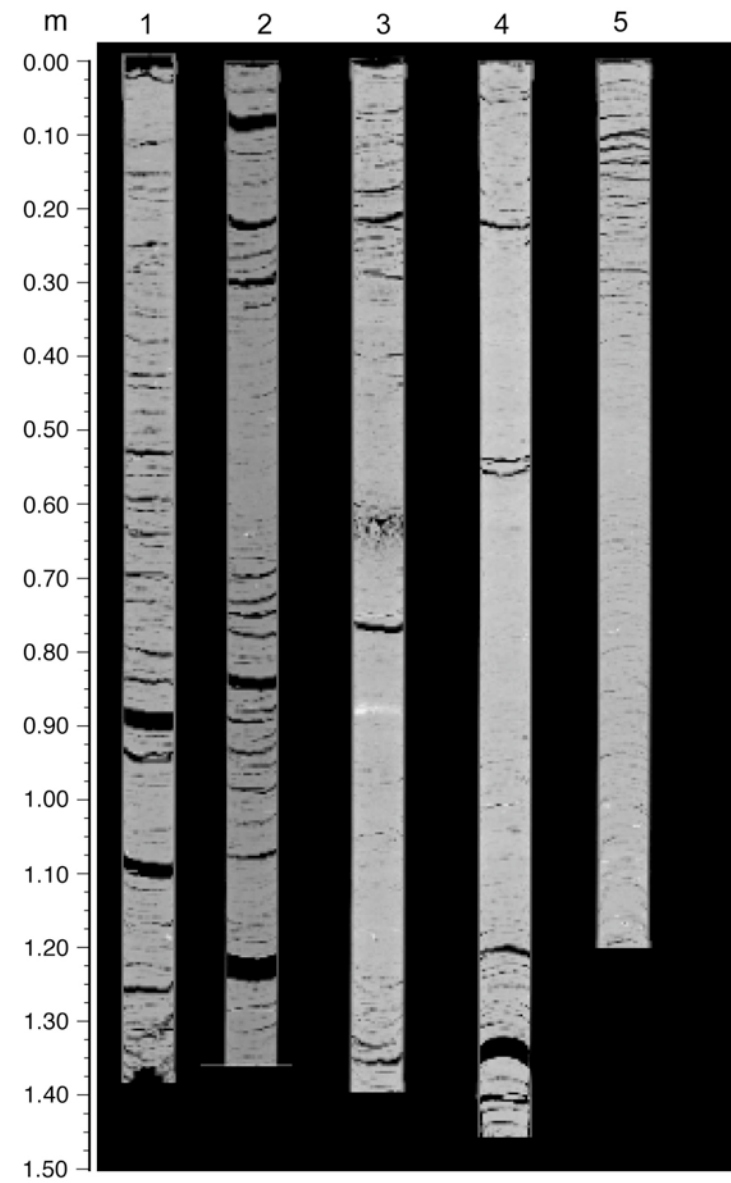
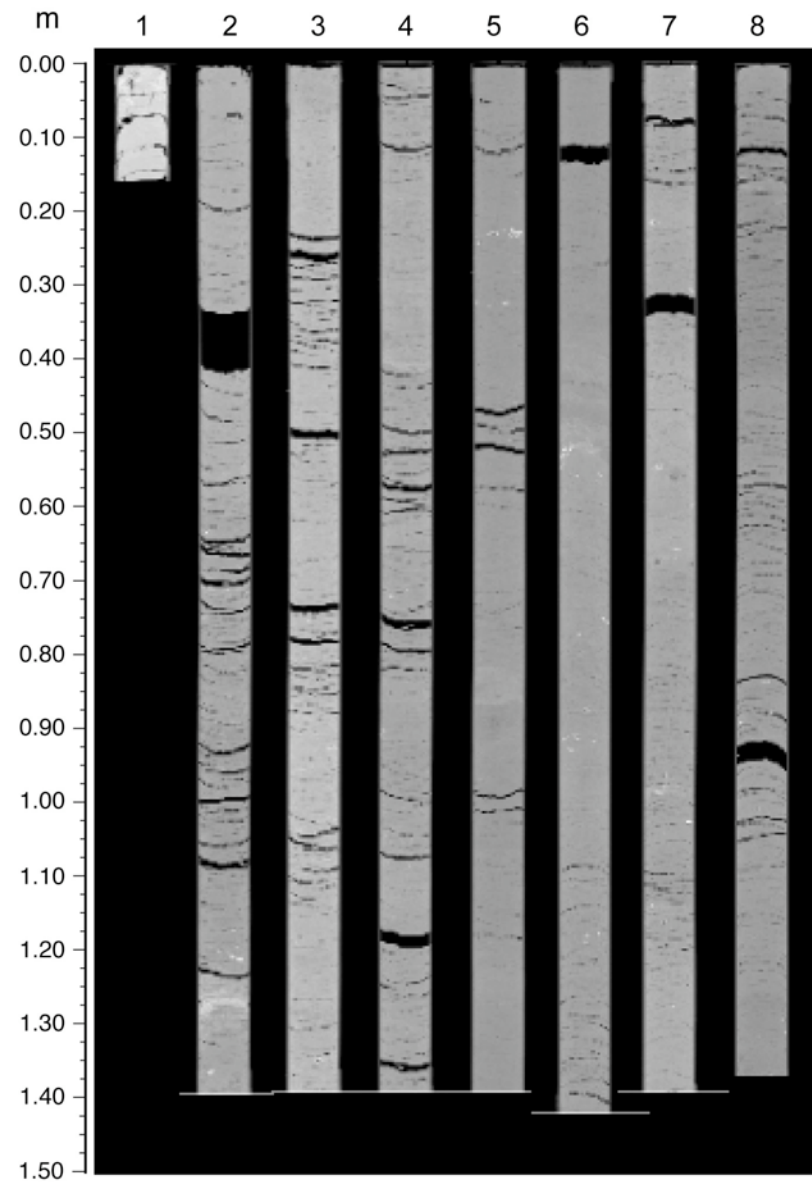
902-C9001C-16H



902-C9001C-17H

XCT scans of WR sections

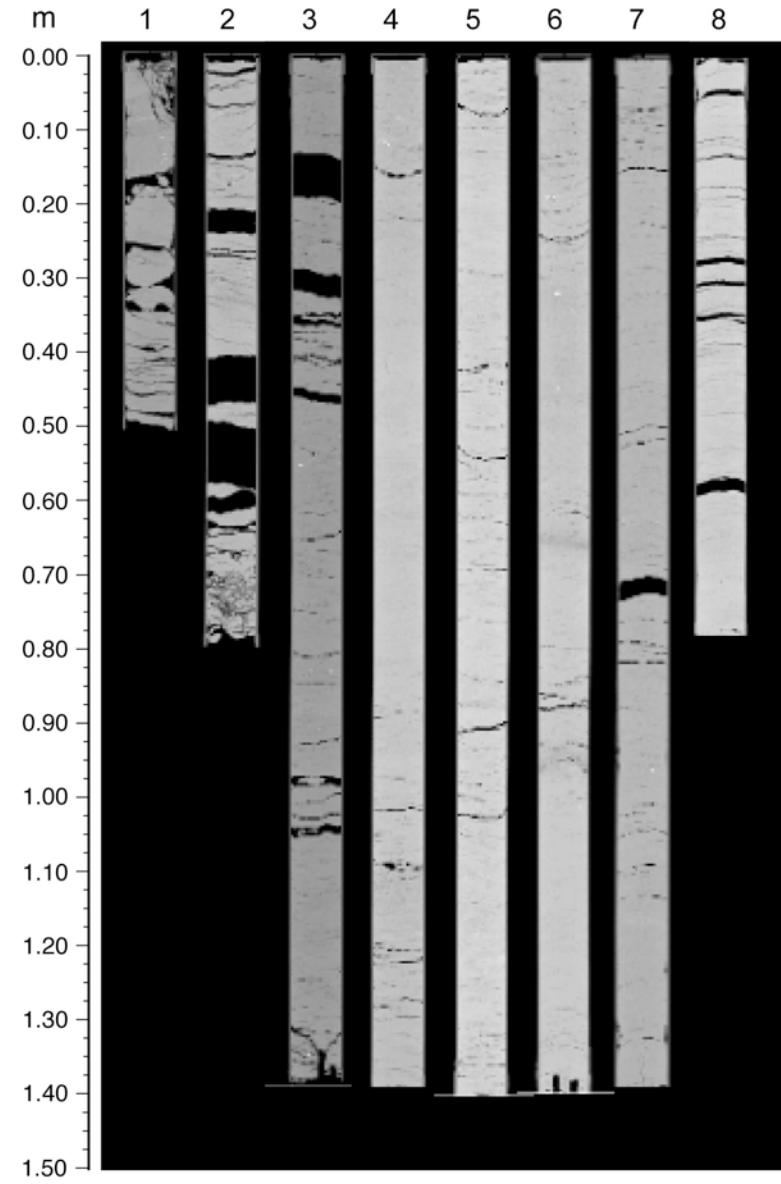
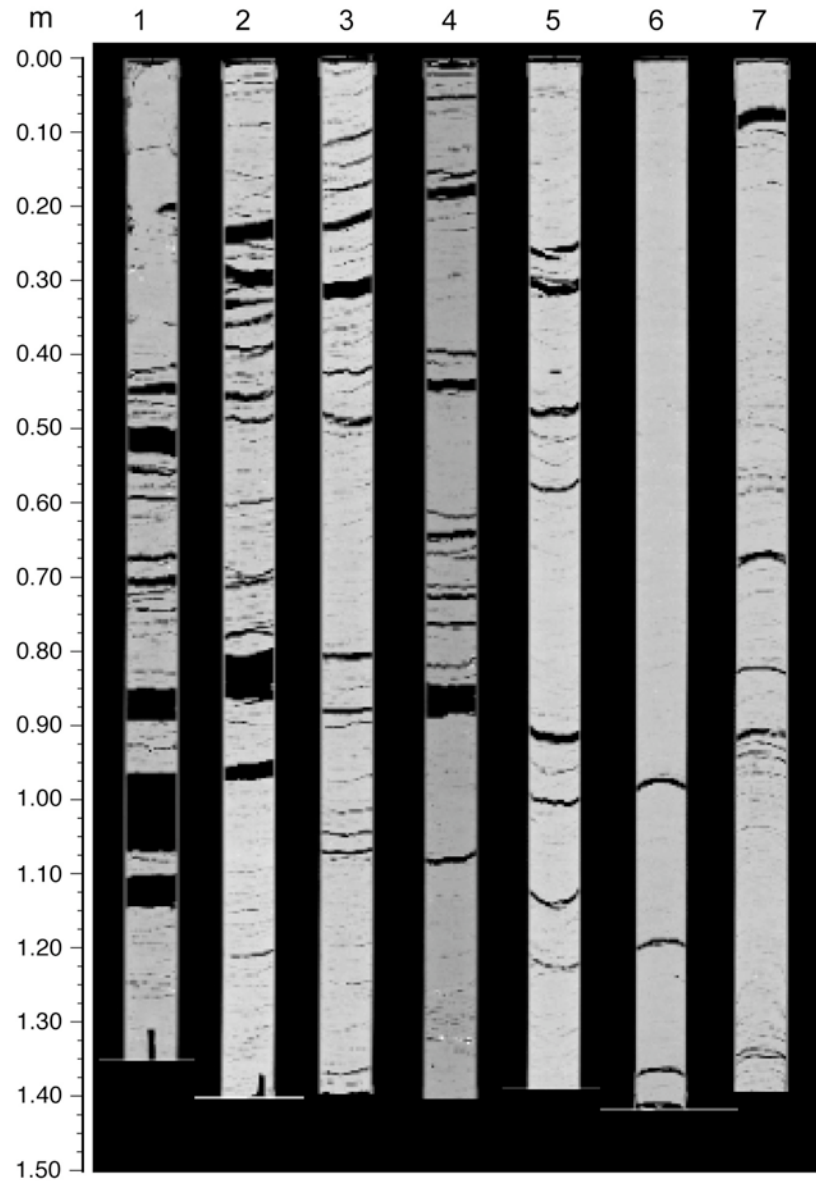
902-C9001C-18H



902-C9001C-19H

XCT scans of WR sections

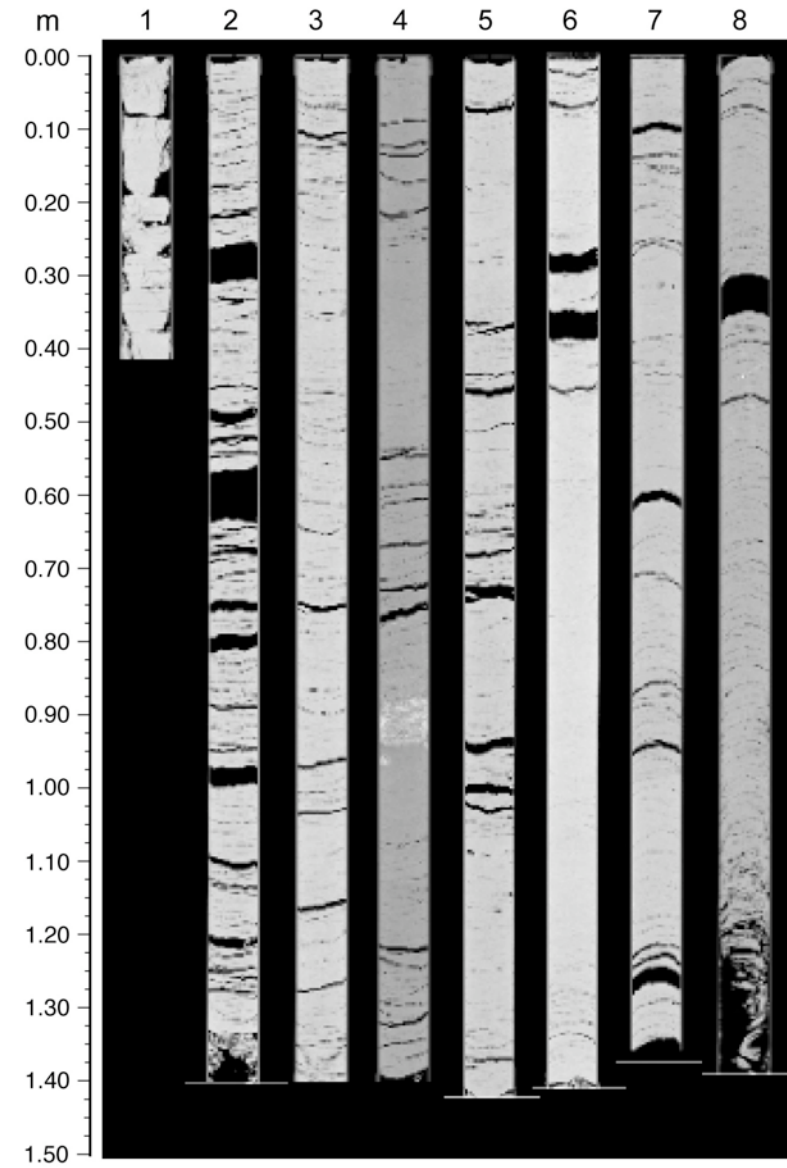
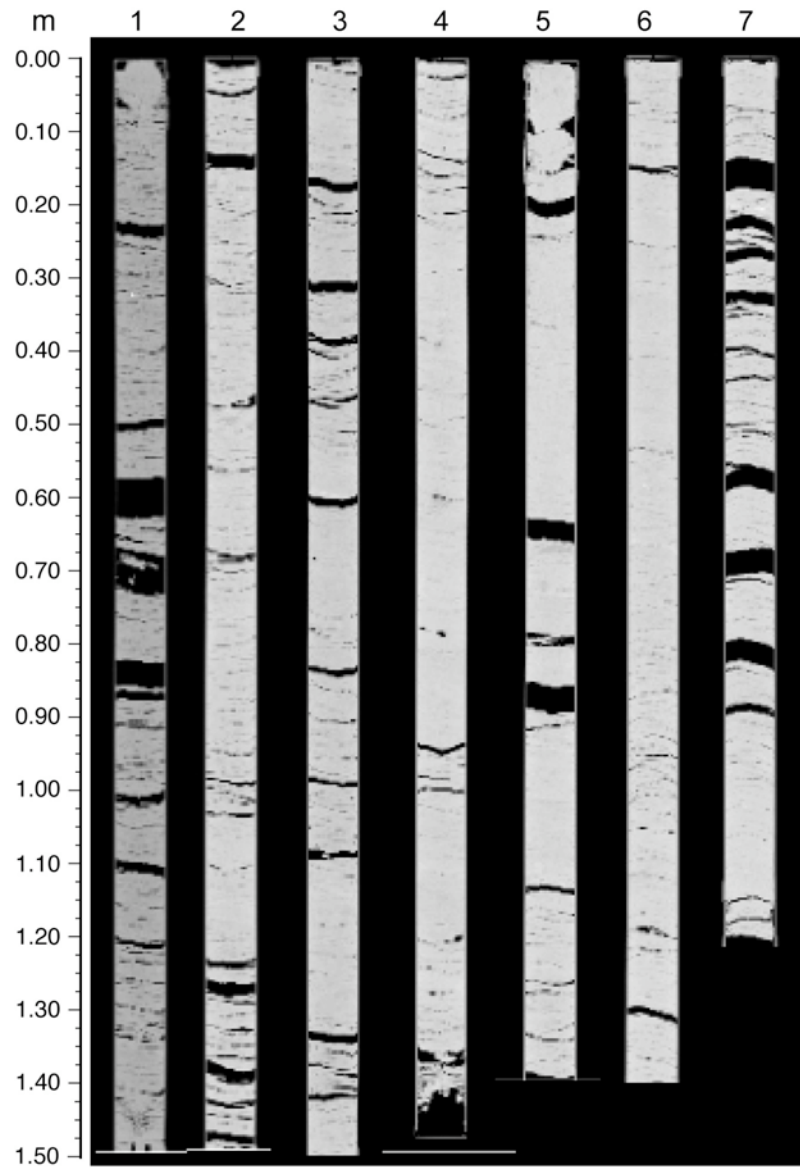
902-C9001C-20H



902-C9001C-21H

XCT scans of WR sections

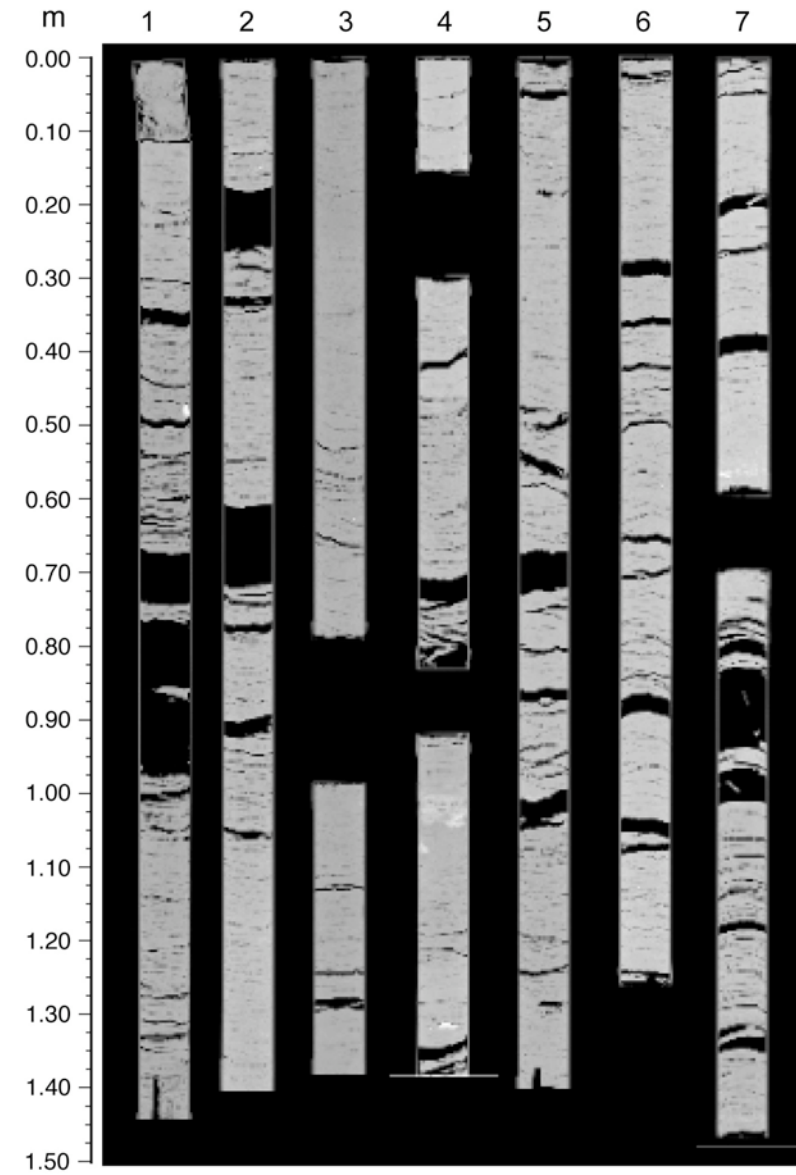
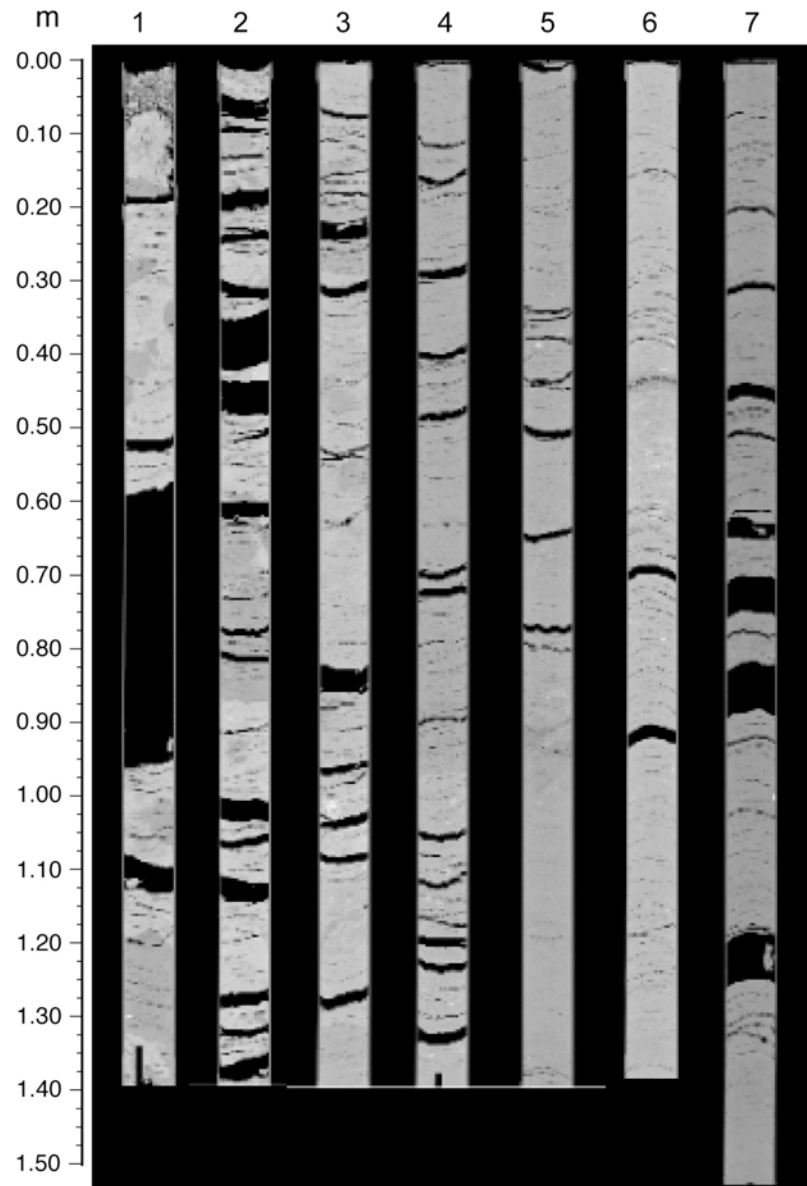
902-C9001C-22H



902-C9001C-23H

XCT scans of WR sections

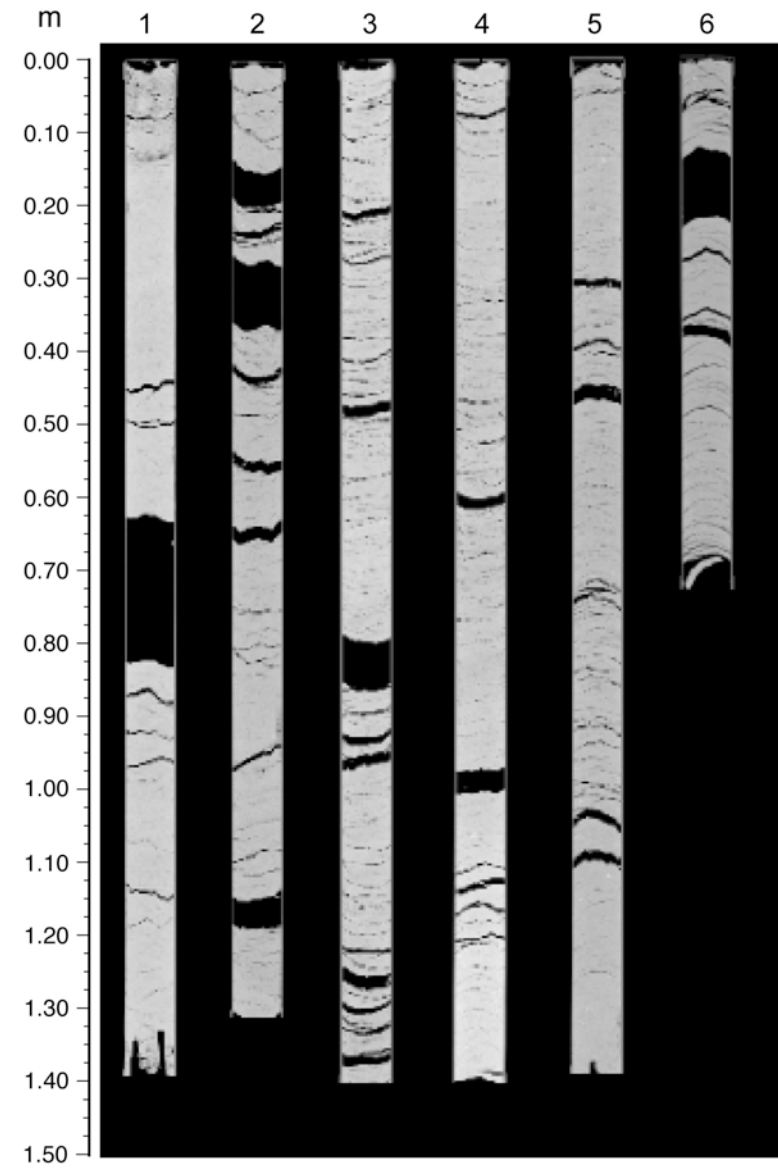
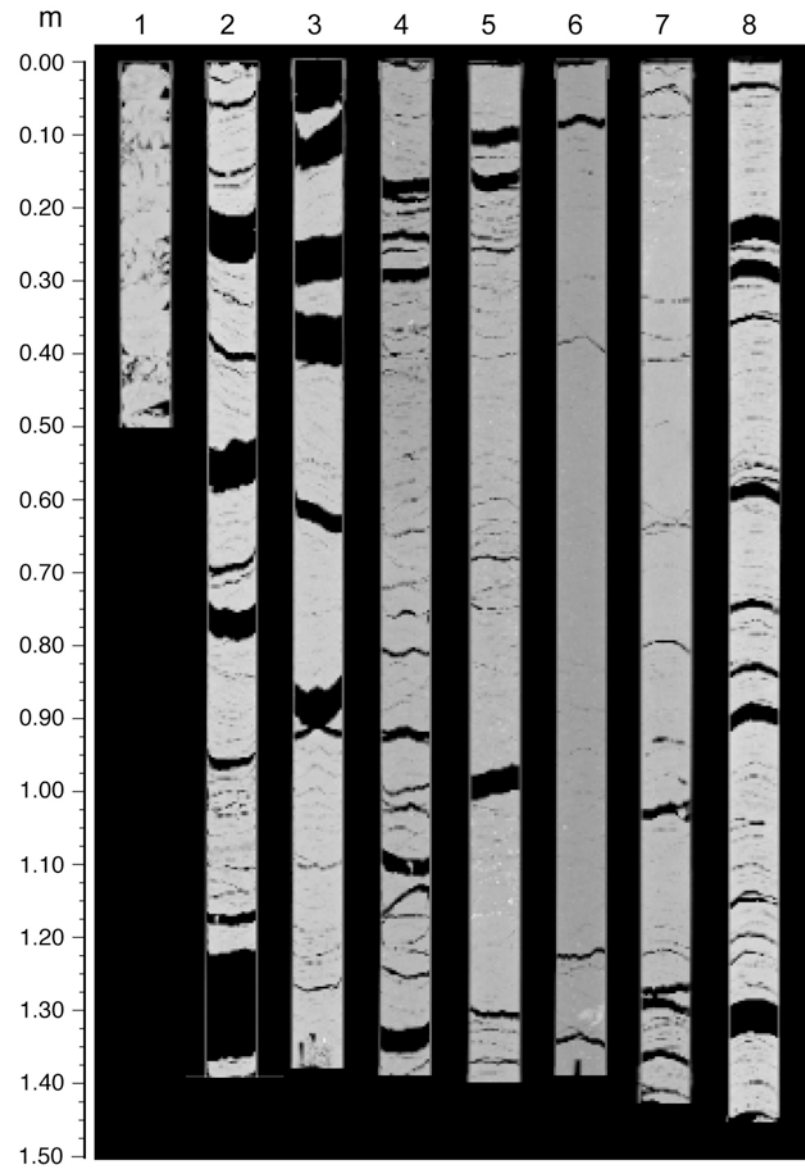
902-C9001C-24H



902-C9001C-25H

XCT scans of WR sections

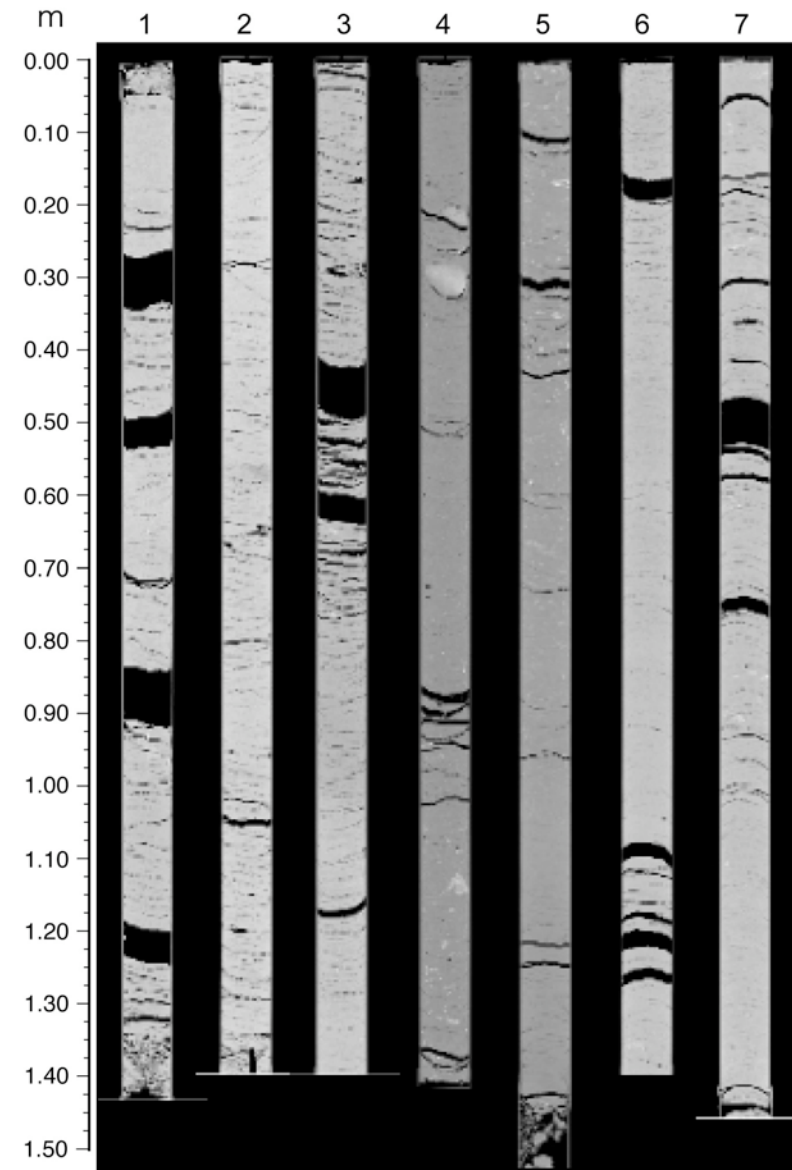
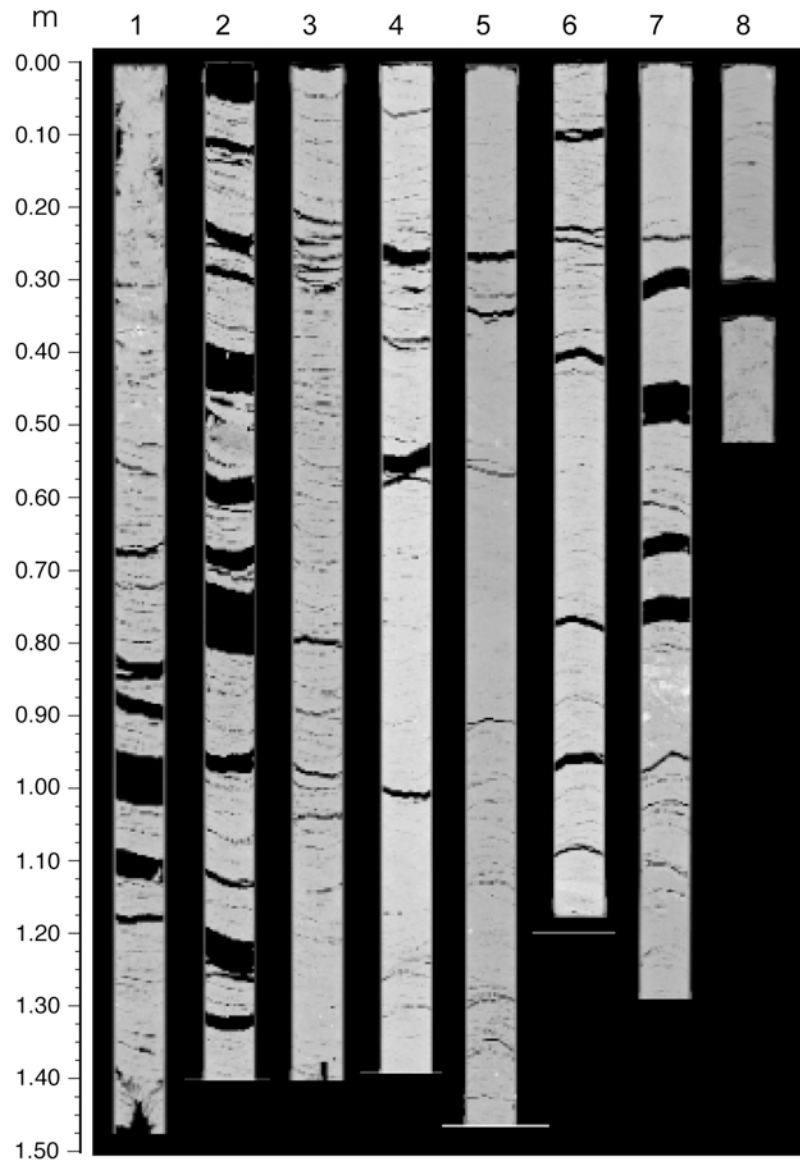
902-C9001C-26H



902-C9001C-27H

XCT scans of WR sections

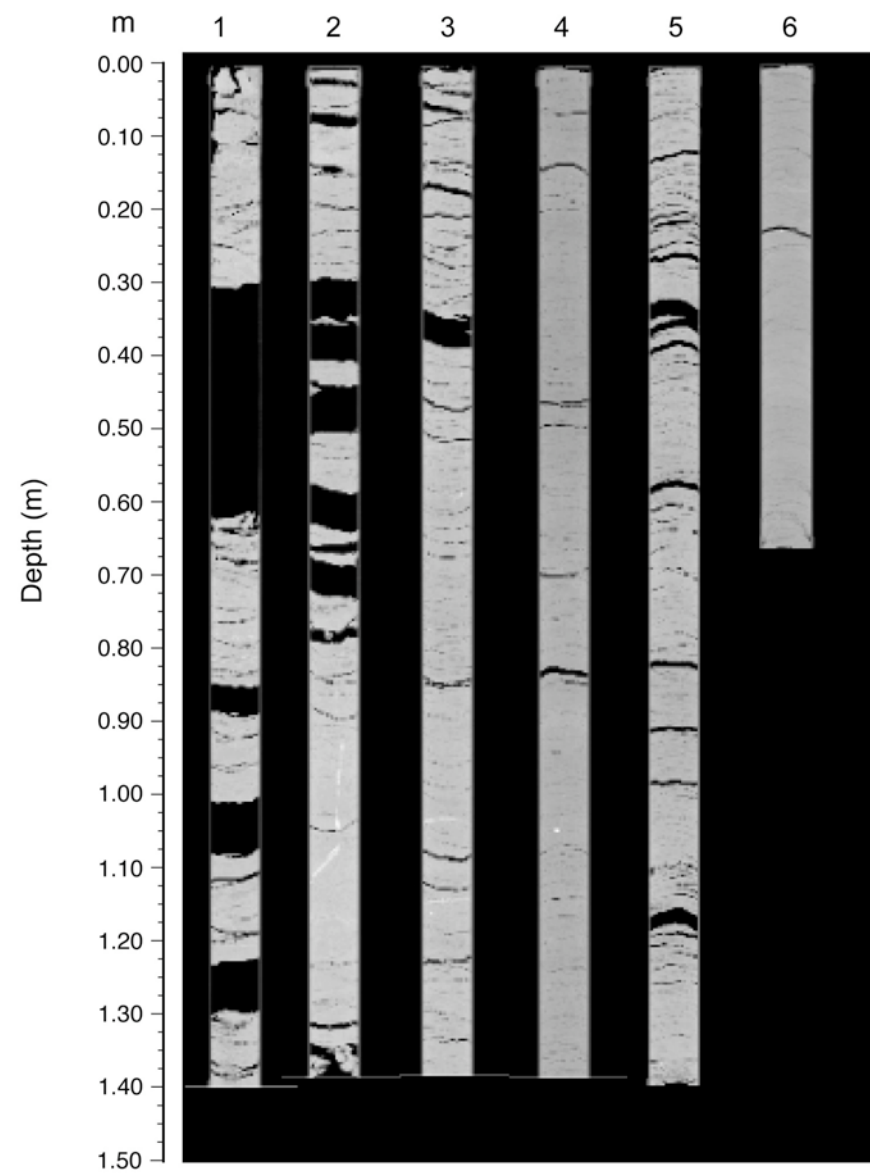
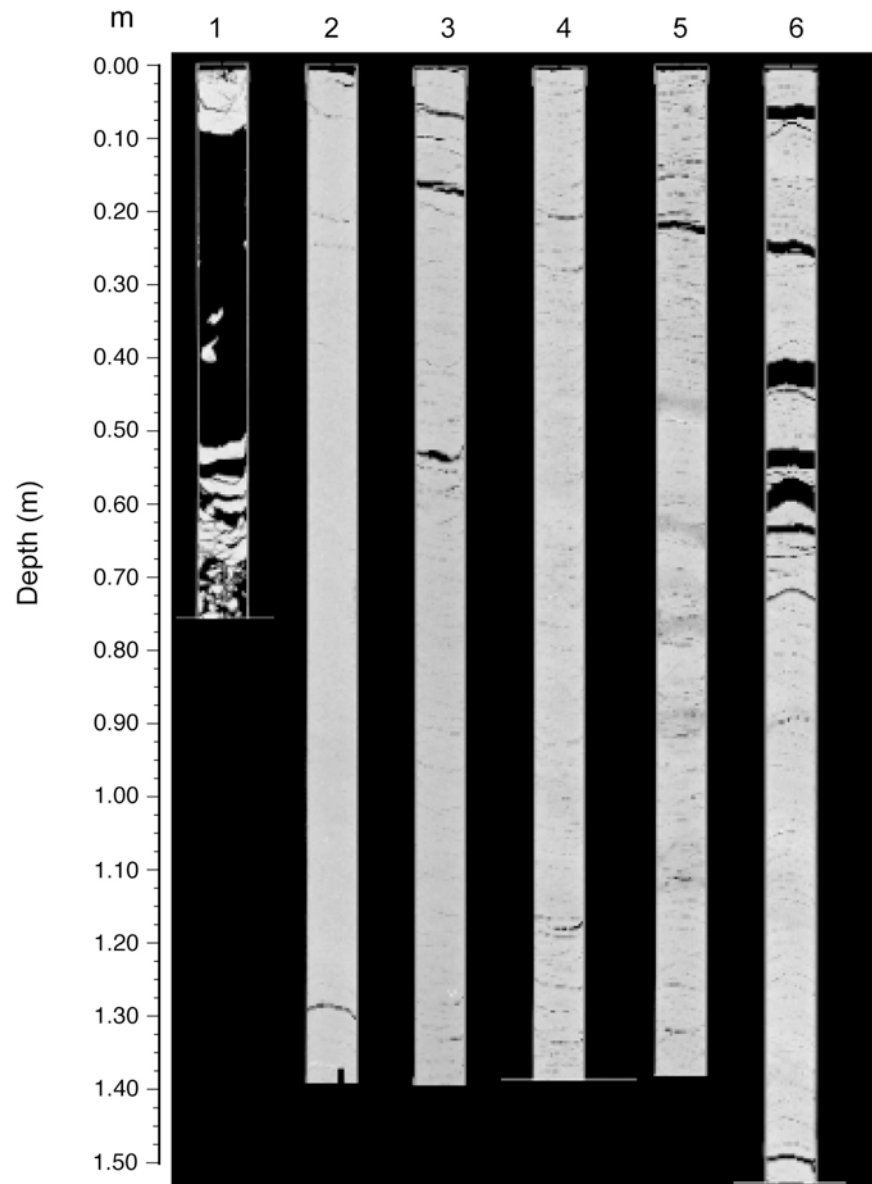
902-C9001C-28H



902-C9001C-29H

XCT scans of WR sections

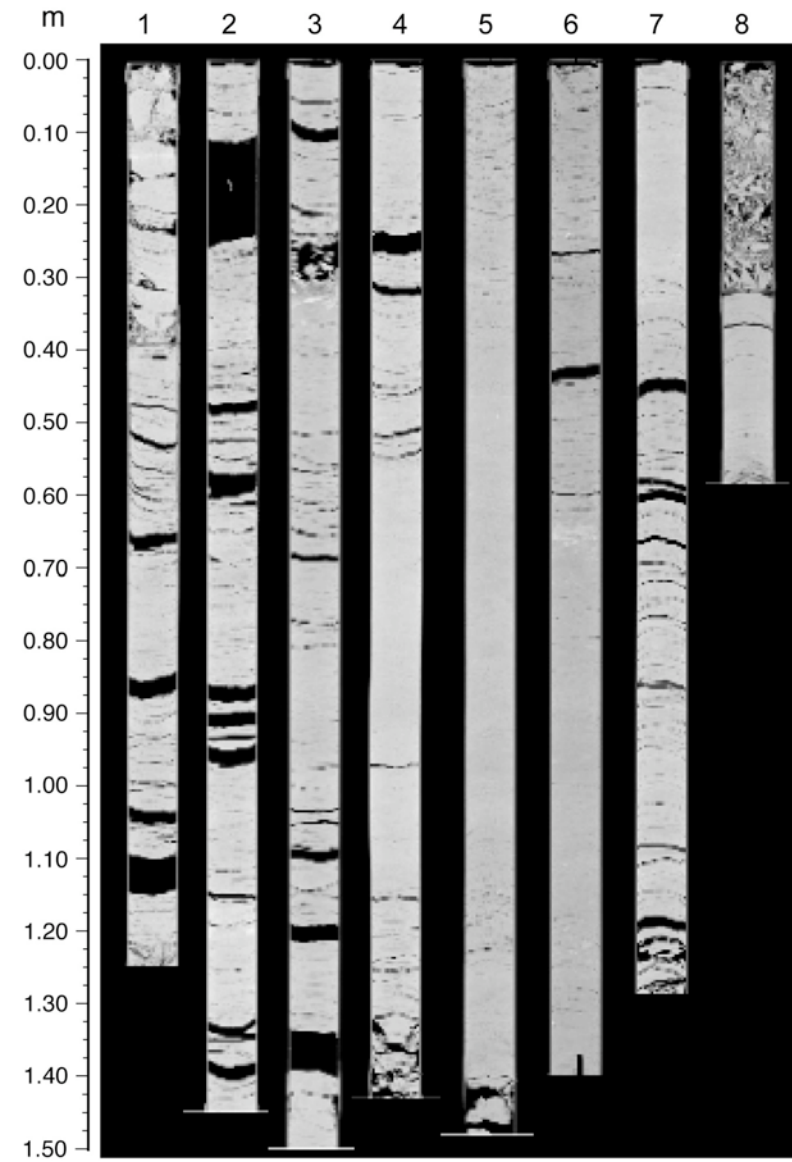
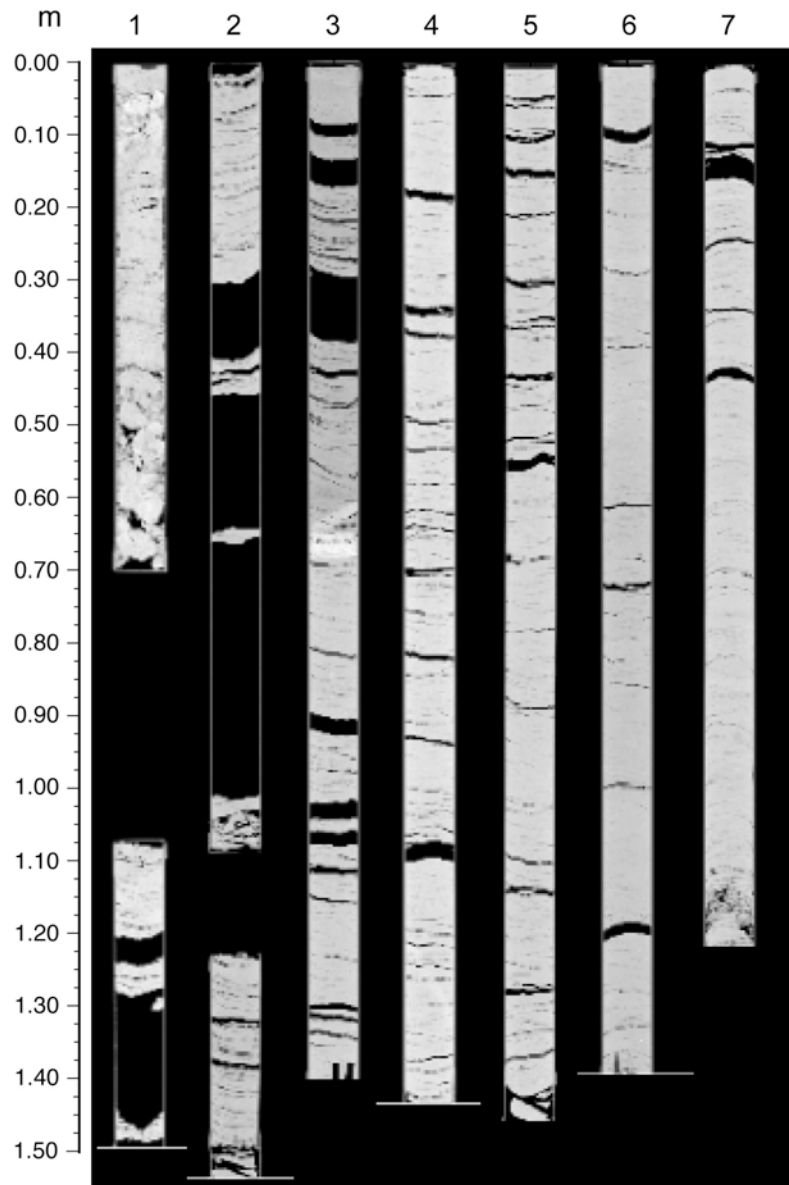
902-C9001C-30H



902-C9001C-31H

XCT scans of WR sections

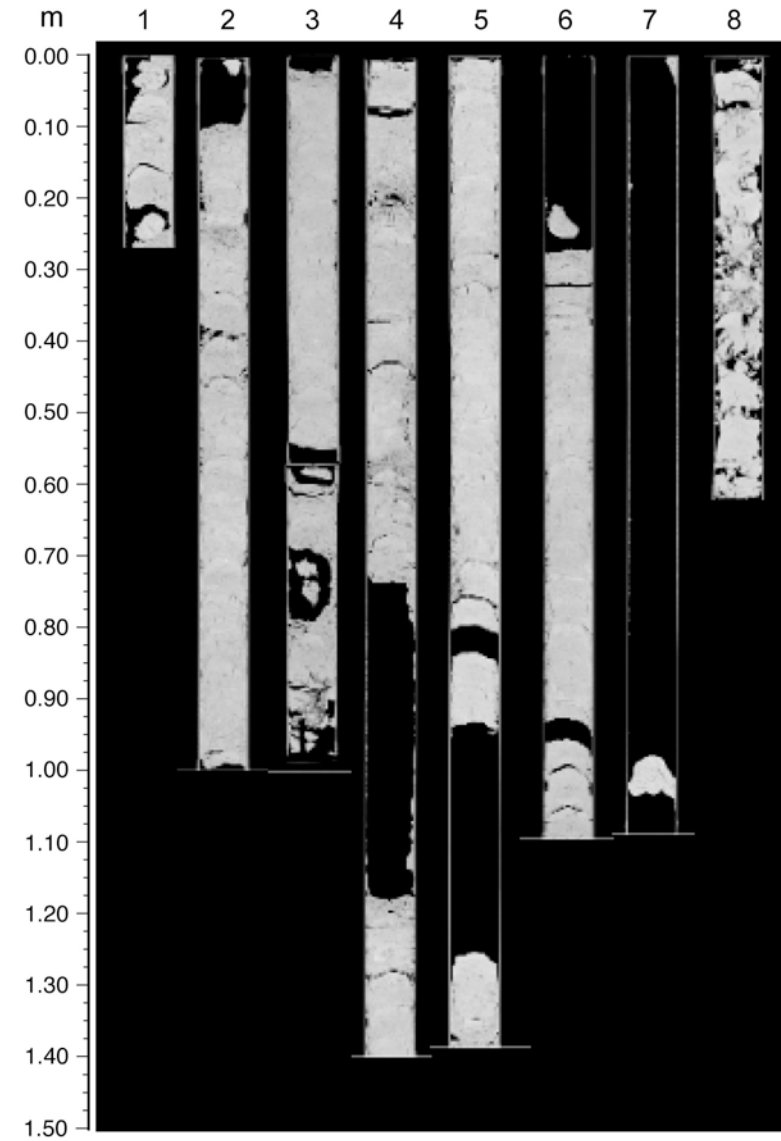
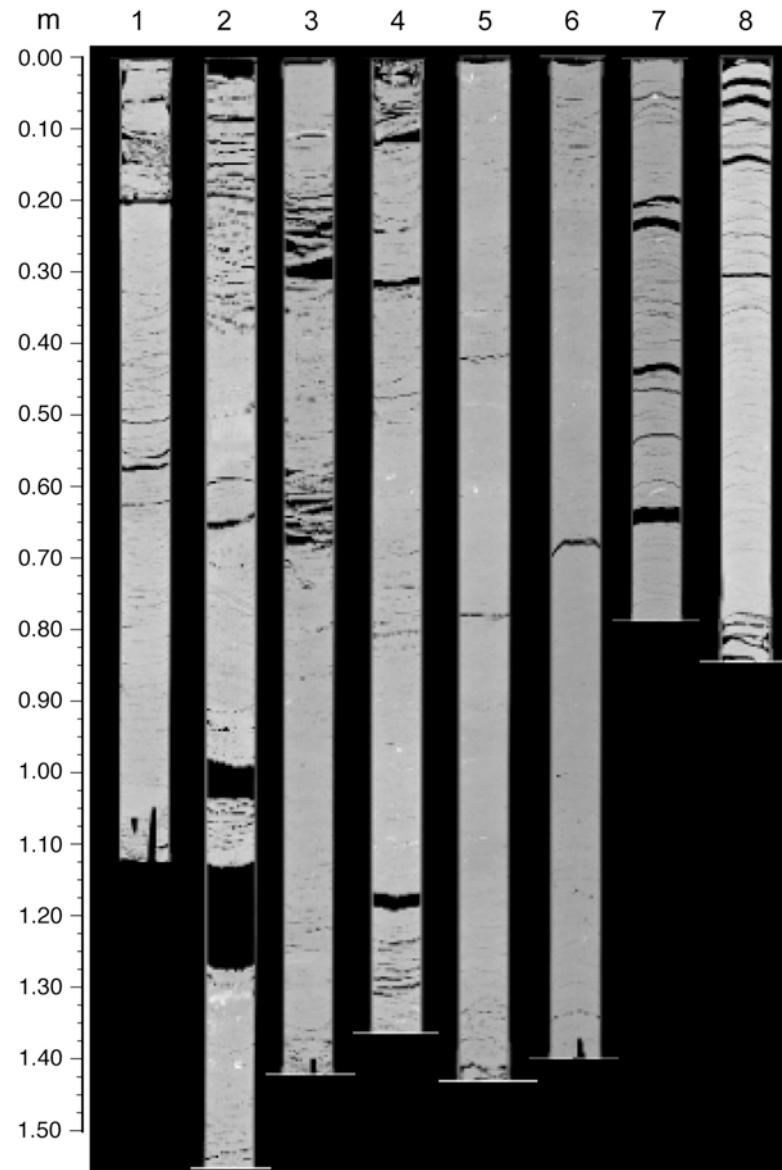
902-C9001C-32H



902-C9001C-33H

XCT scans of WR sections

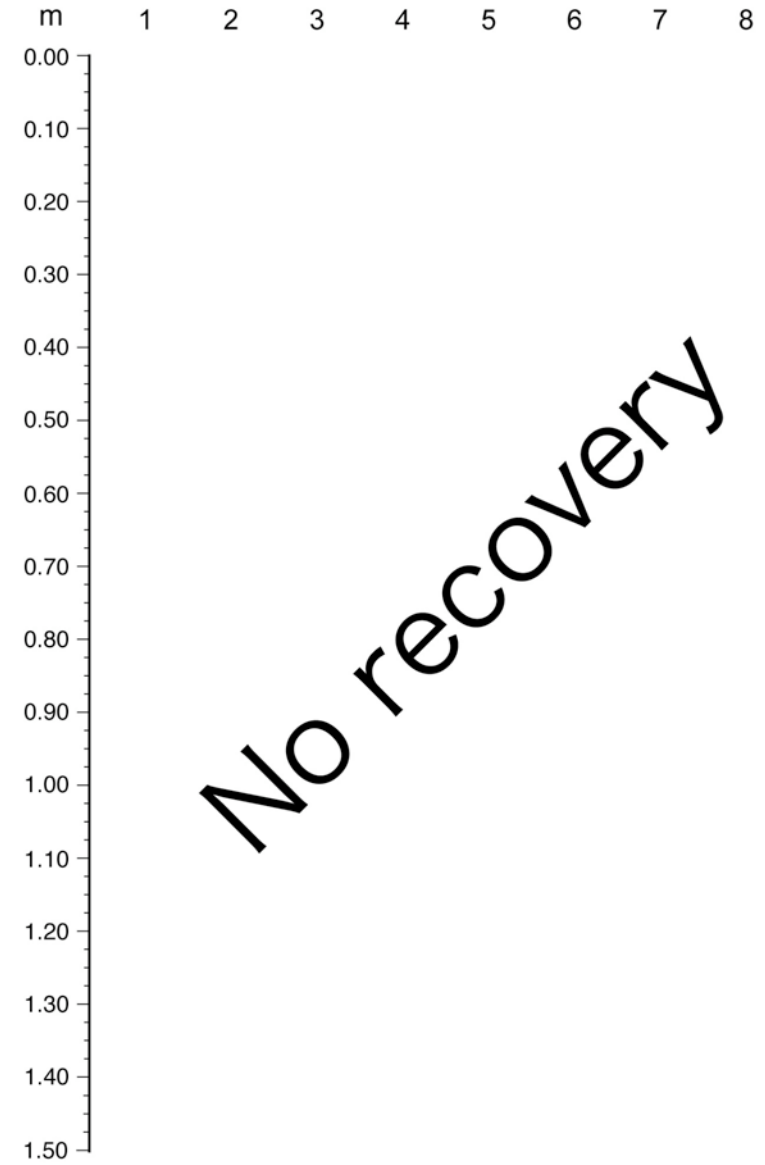
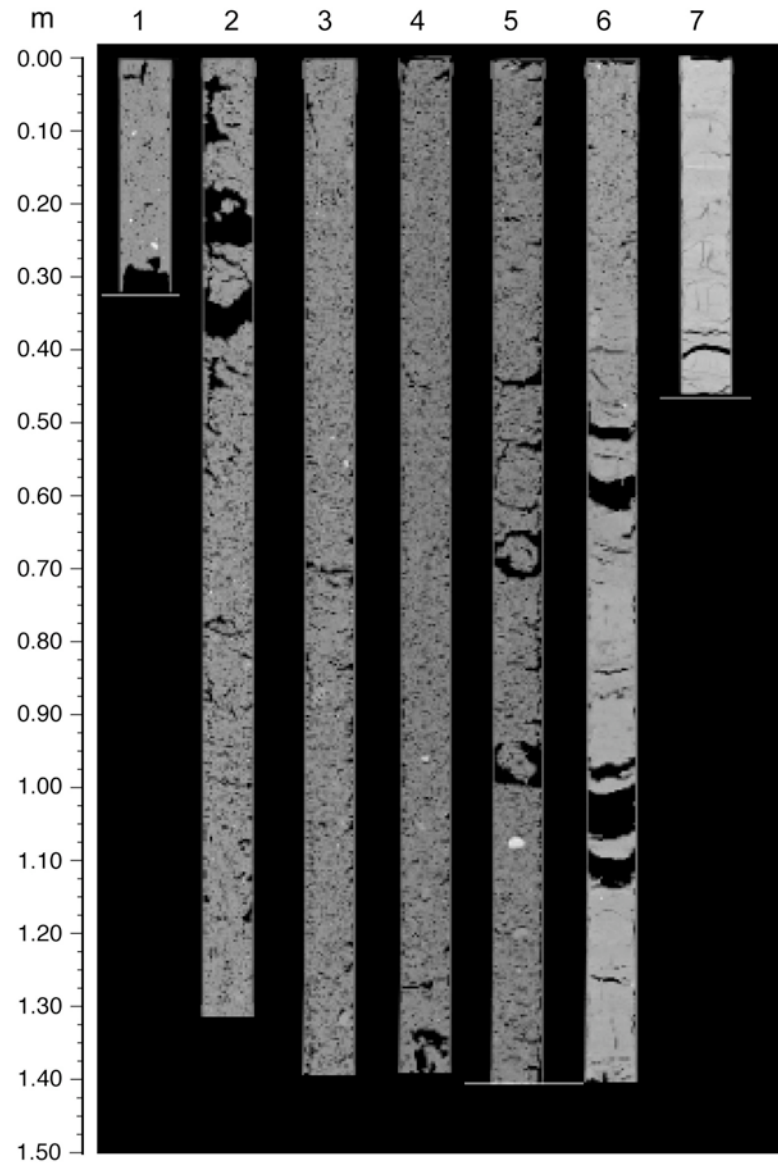
902-C9001C-34X



902-C9001C-35X

XCT scans of WR sections

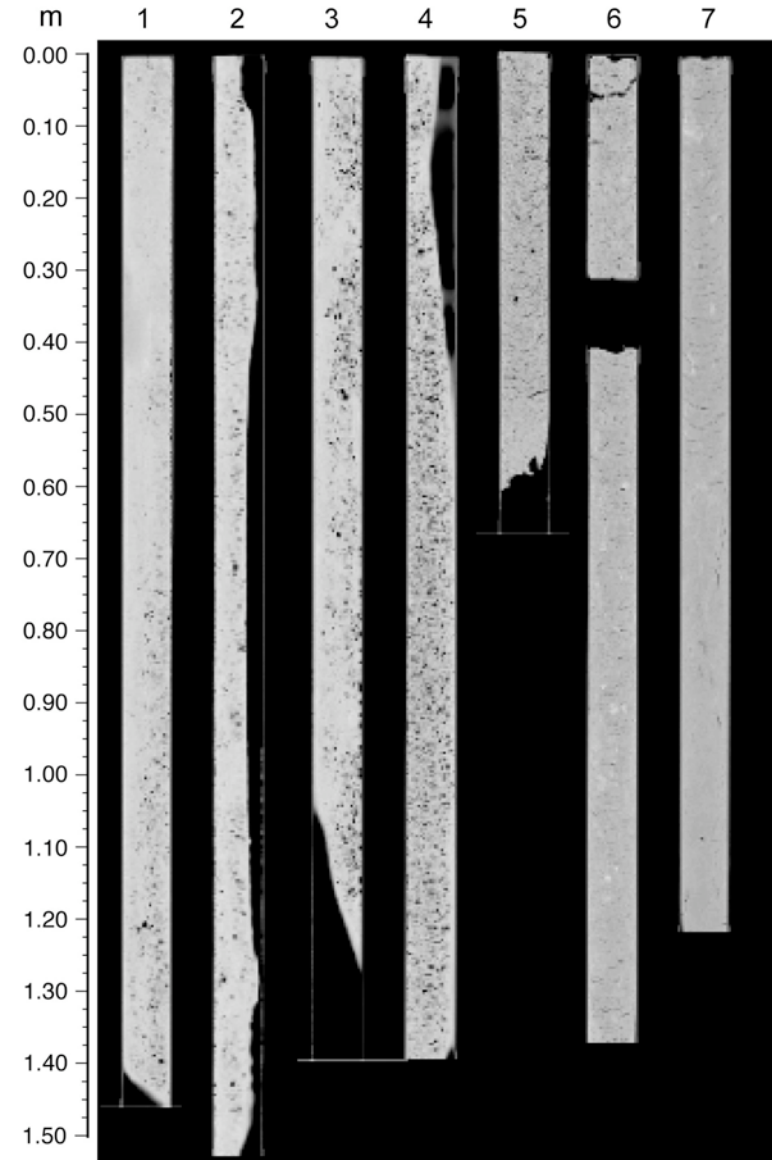
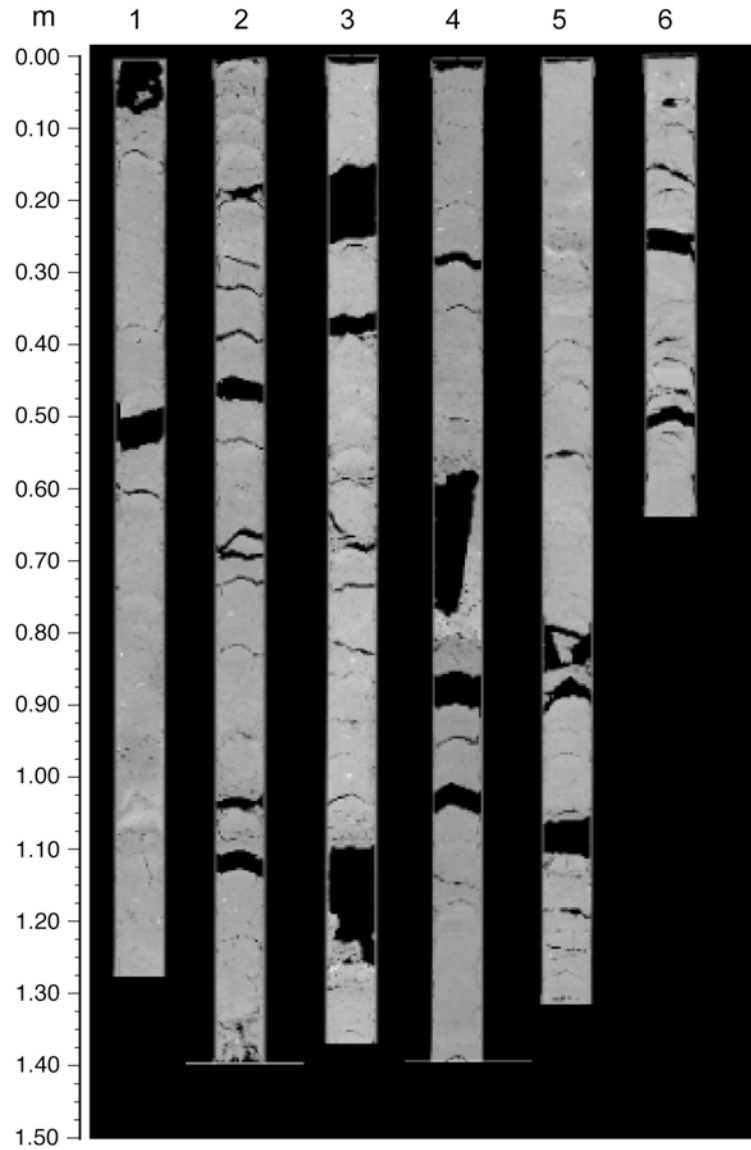
902-C9001C-36X

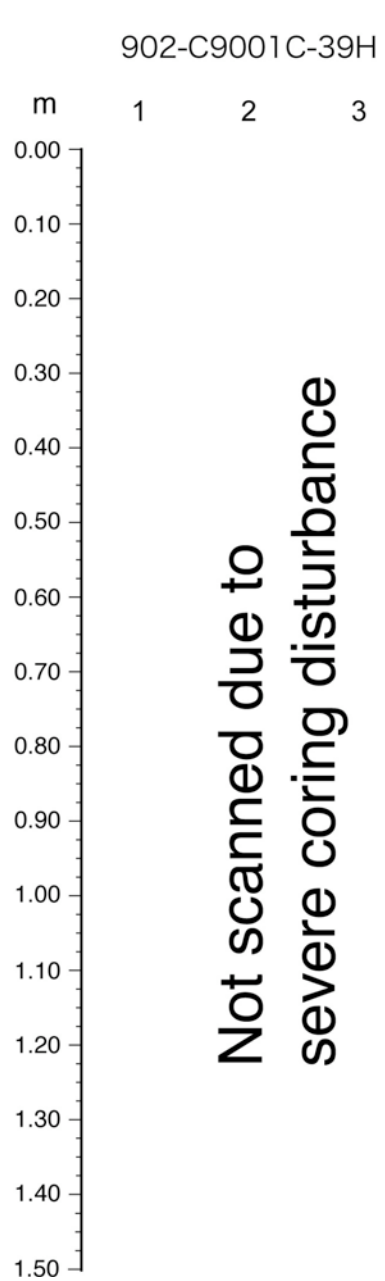


902-C9001C-37X

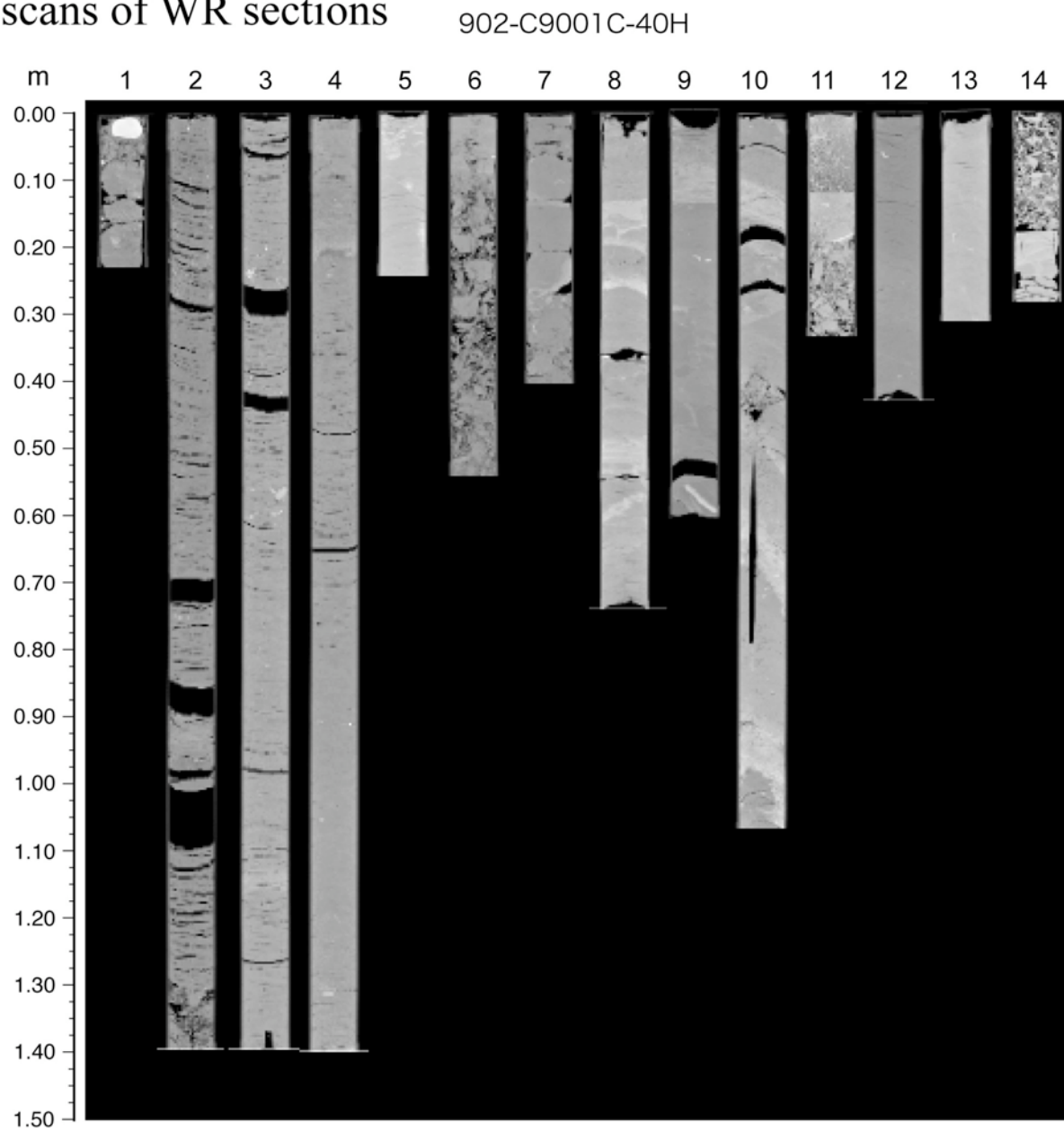
XCT scans of WR sections

902-C9001C-38H





XCT scans of WR sections



Appendix 2

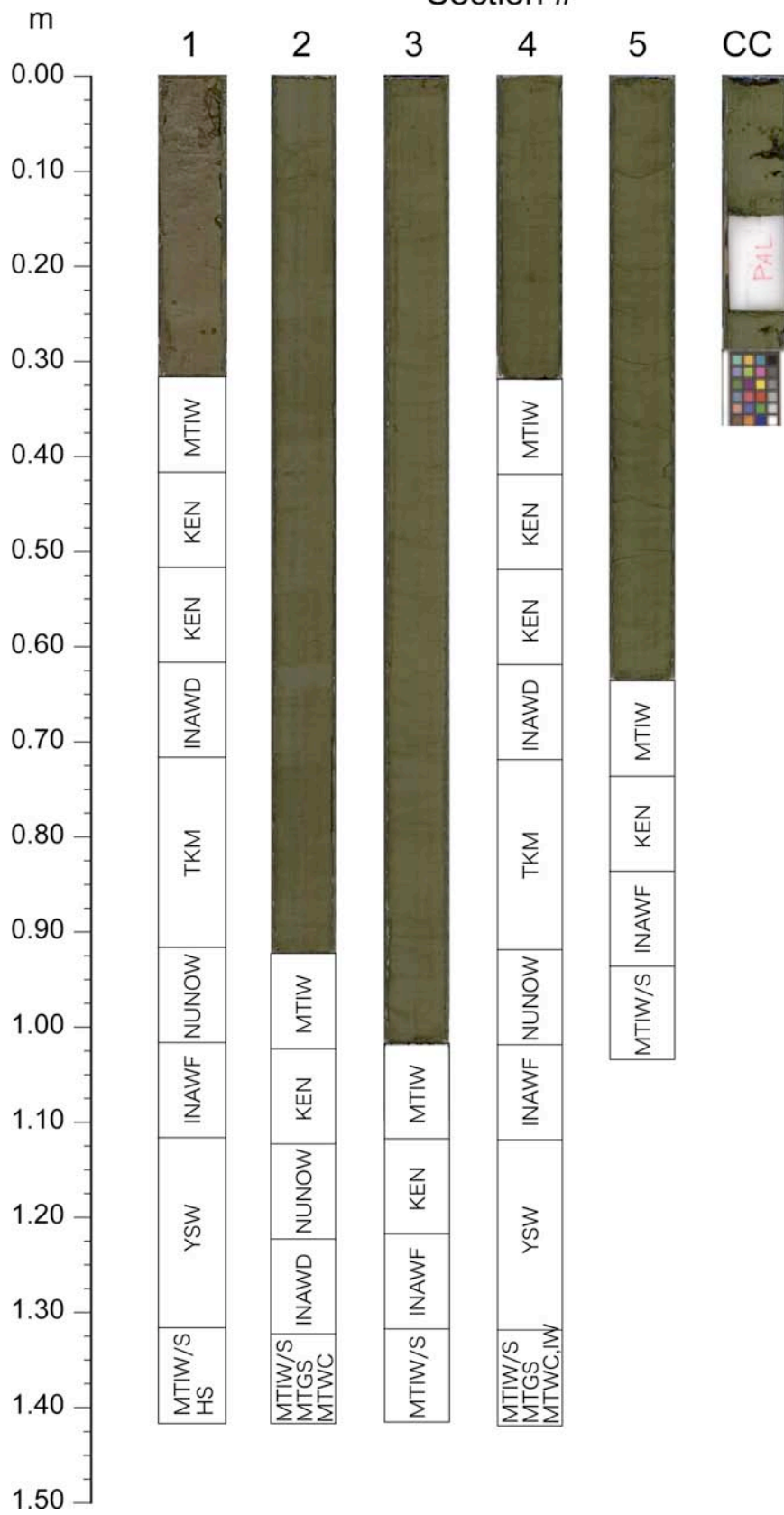
C9001C

Core Photo Images

Note: Open boxes with sample codes such as MTIW indicate intervals where whole-round cores samples are taken for the purposes of microbiology or interstitial water chemistry analyses. Lightness correction of the digital core images was tried to make as a part of LSIT in this cruise, however, it does not produce appropriate results. The procedure is still under development. Therefore, apparent color changes core by core and/or section by section do not necessarily reflect actual sediment color variations.

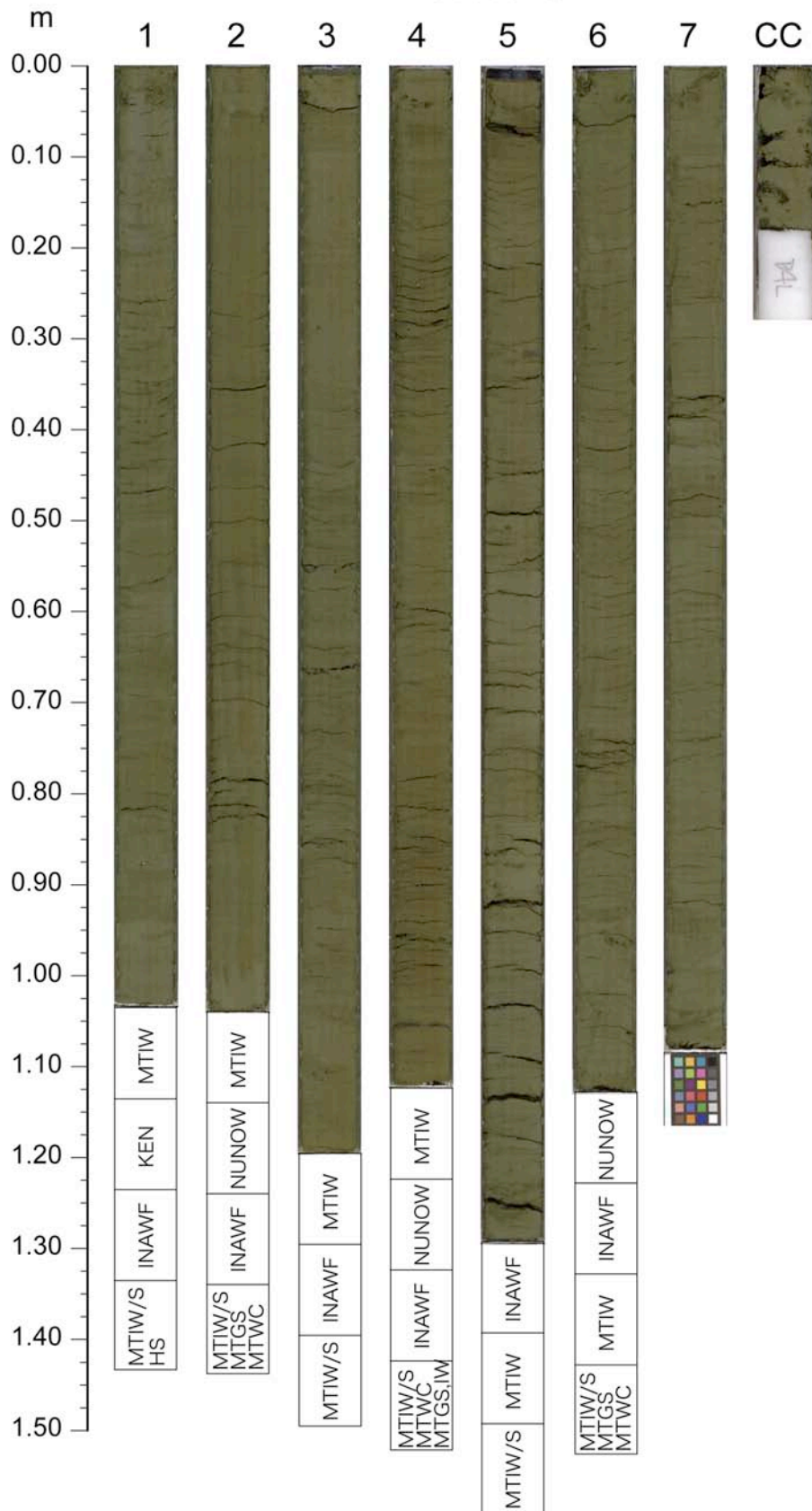
Core 902-C9001C-1H

Section



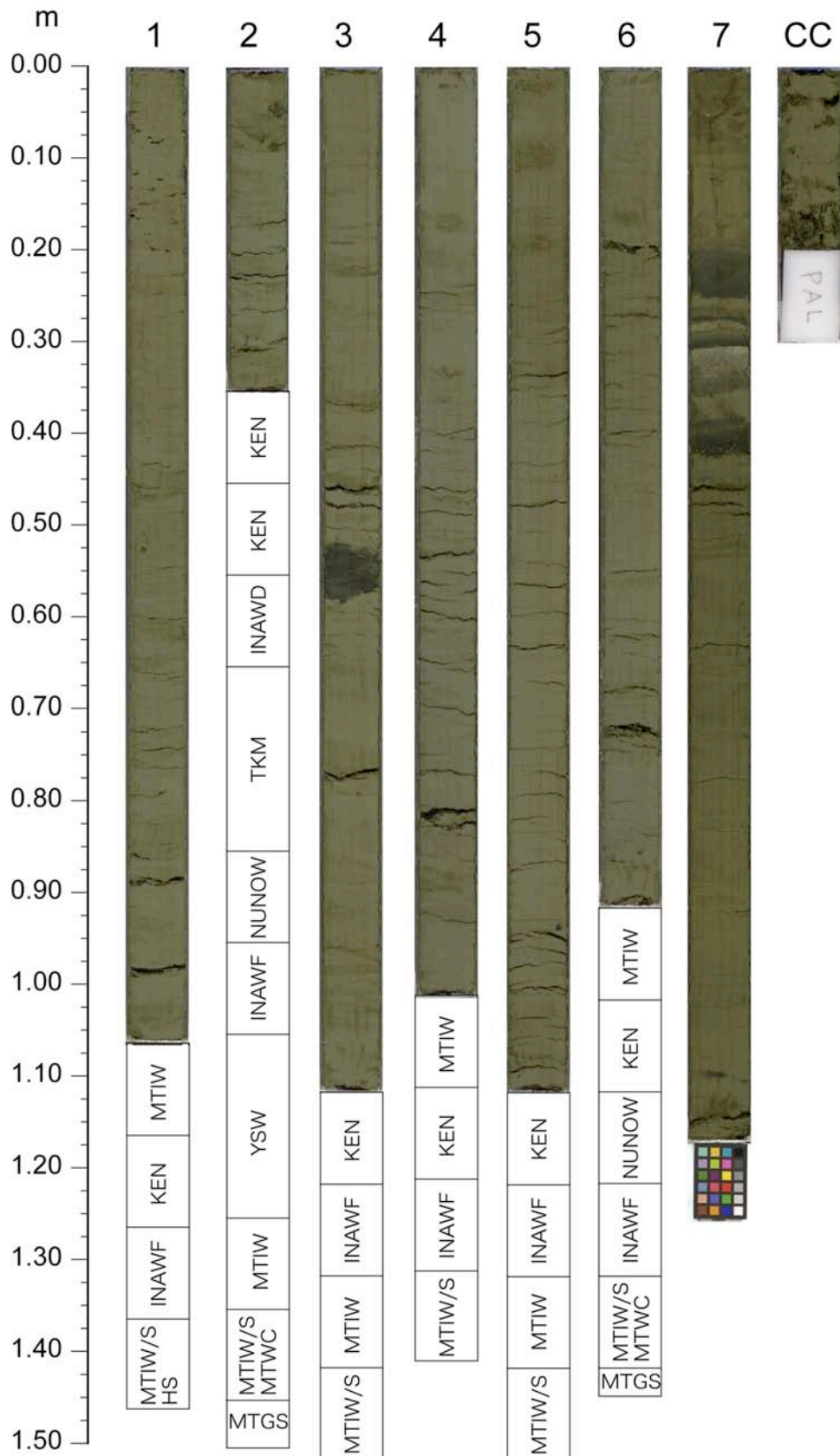
Core 902-C9001C-2H

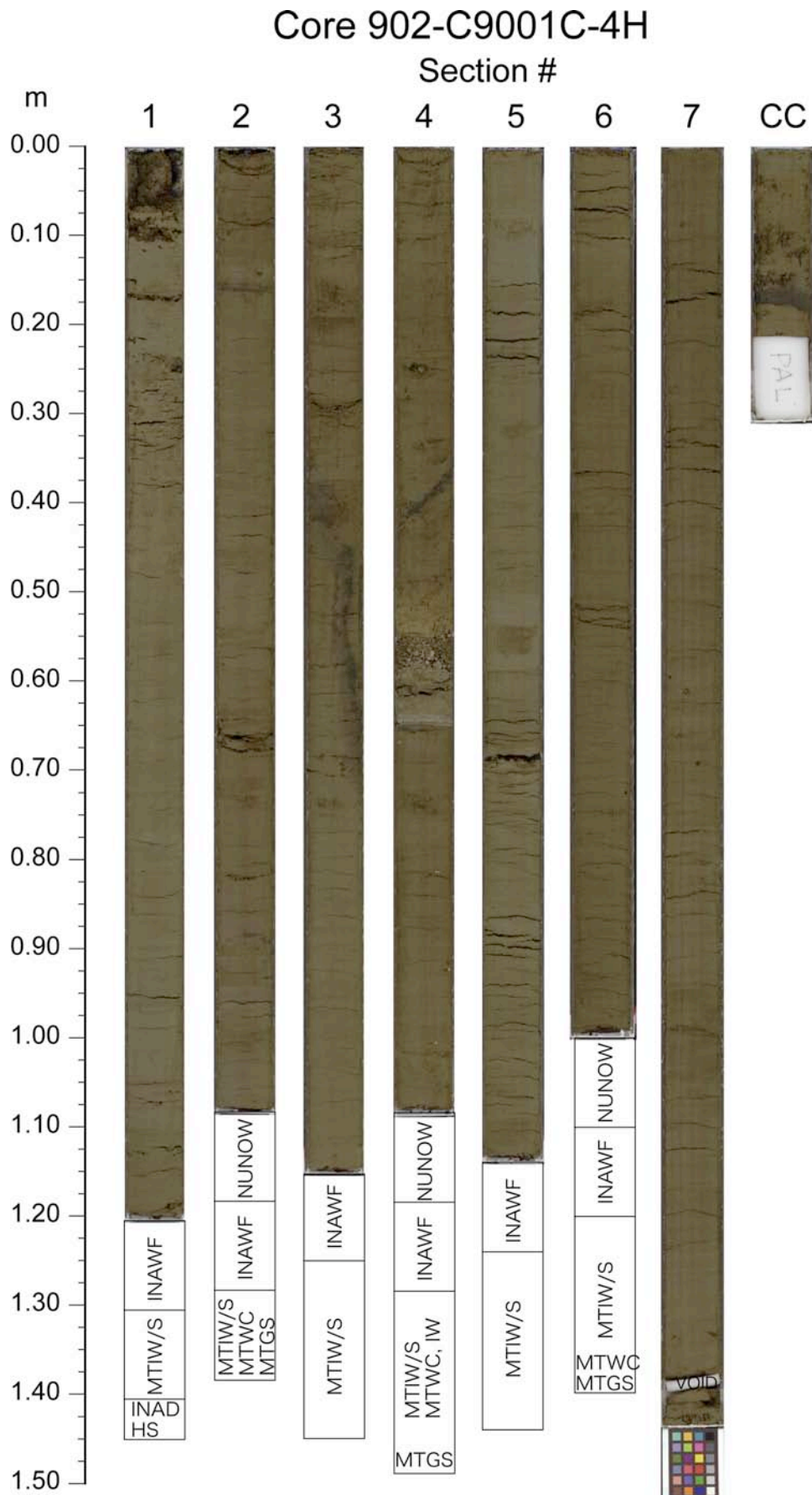
Section #



Core 902-C9001C-3H

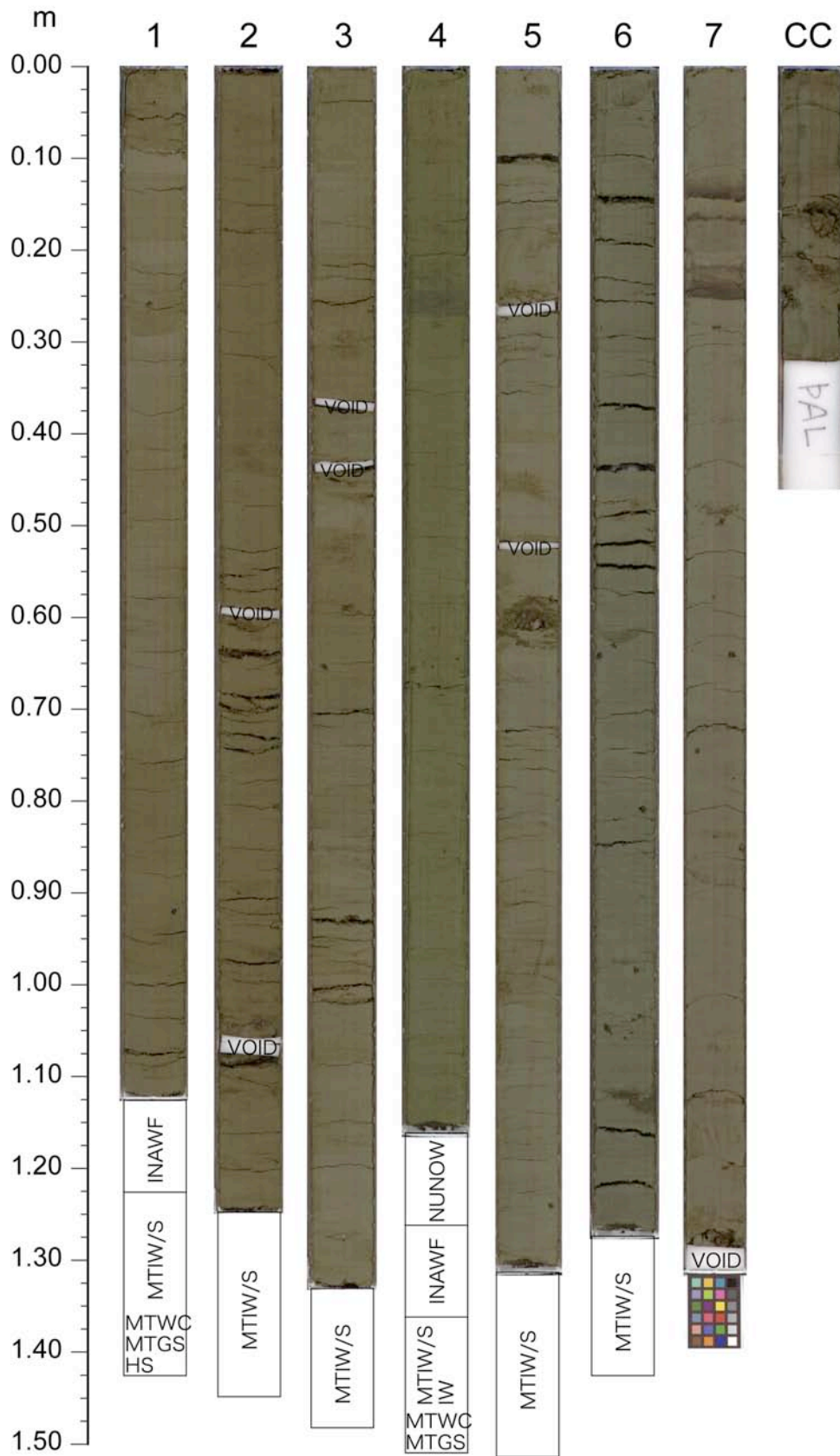
Section #





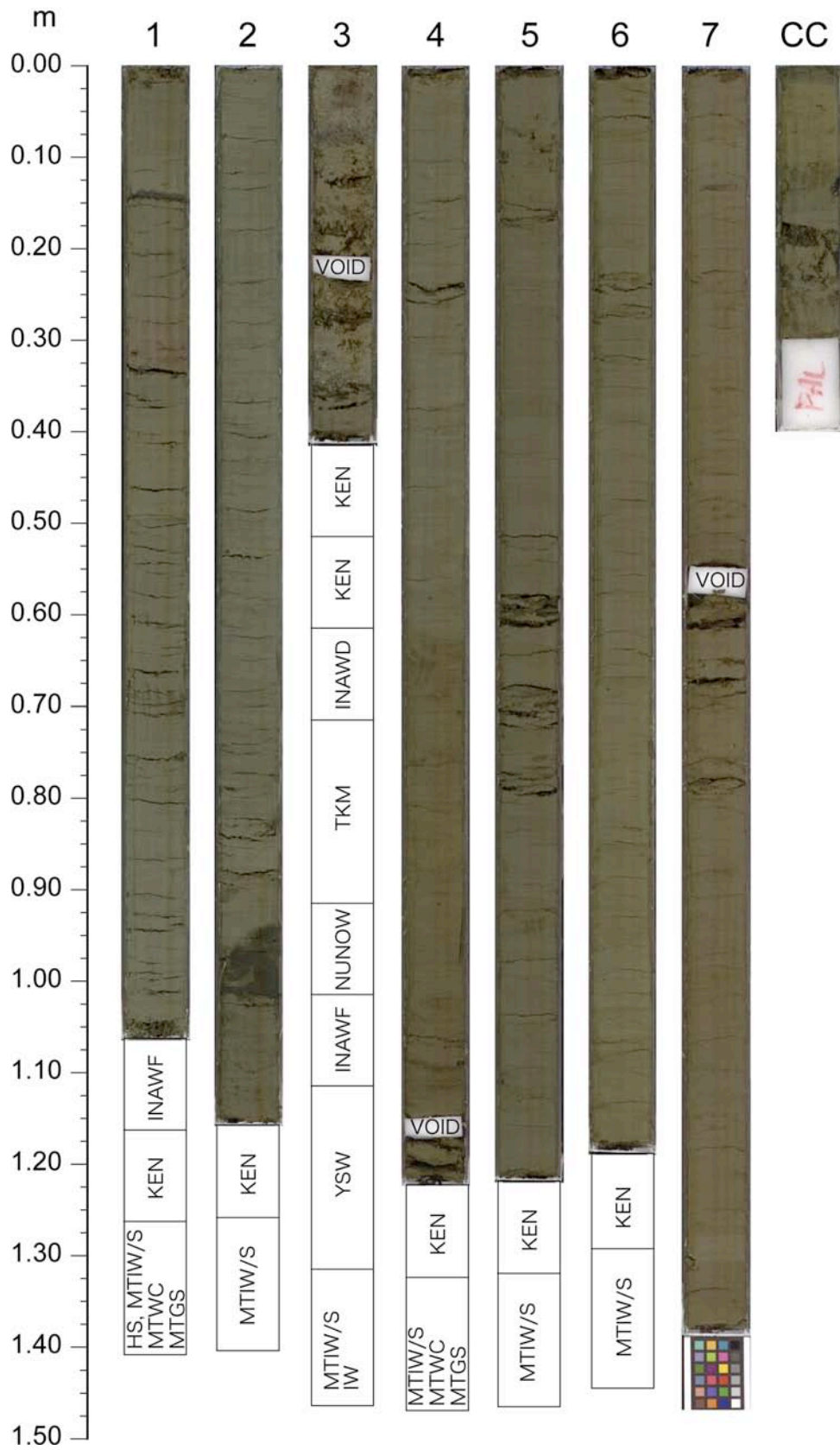
Core 902-C9001C-5H

Section #



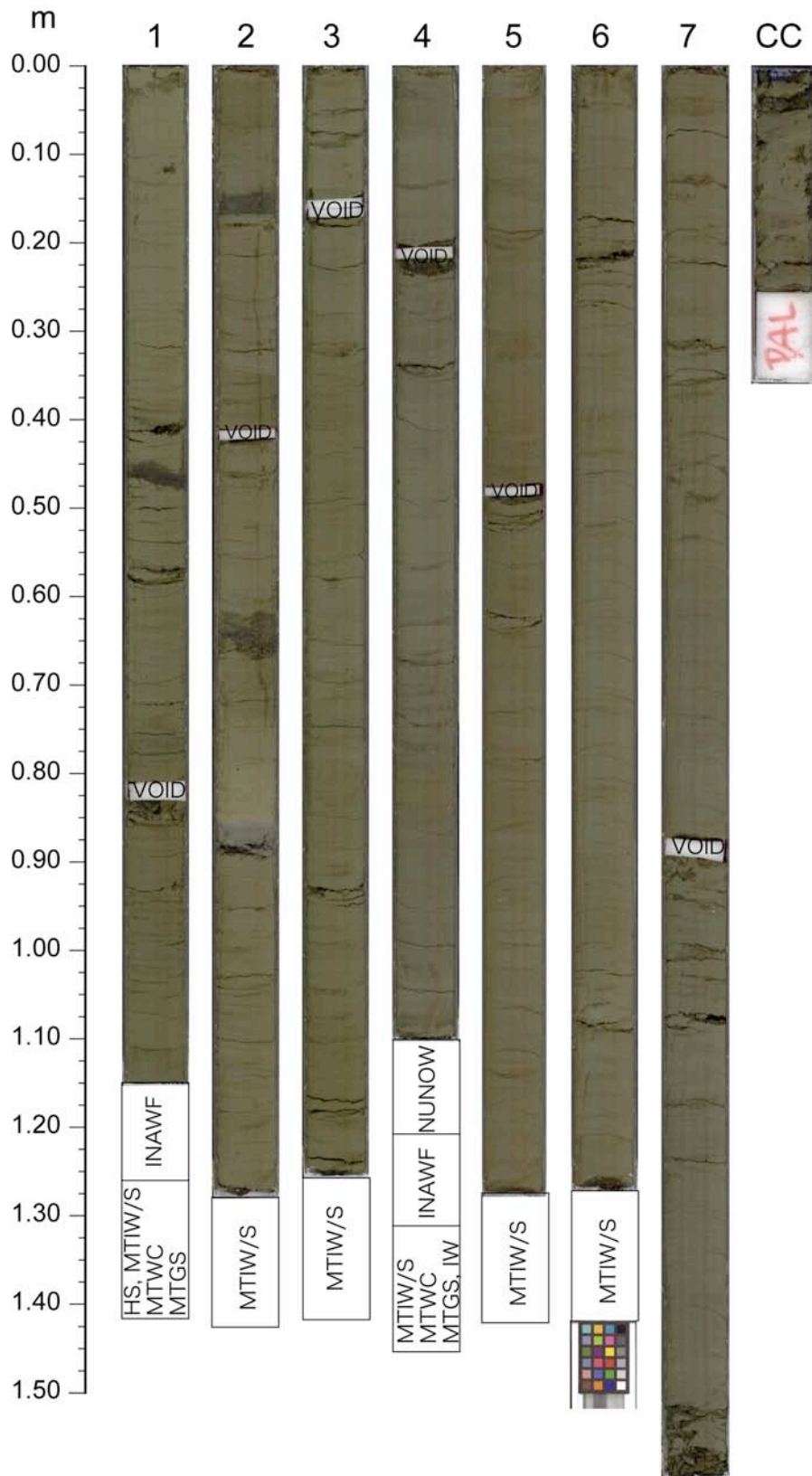
Core 902-C9001C-6H

Section #

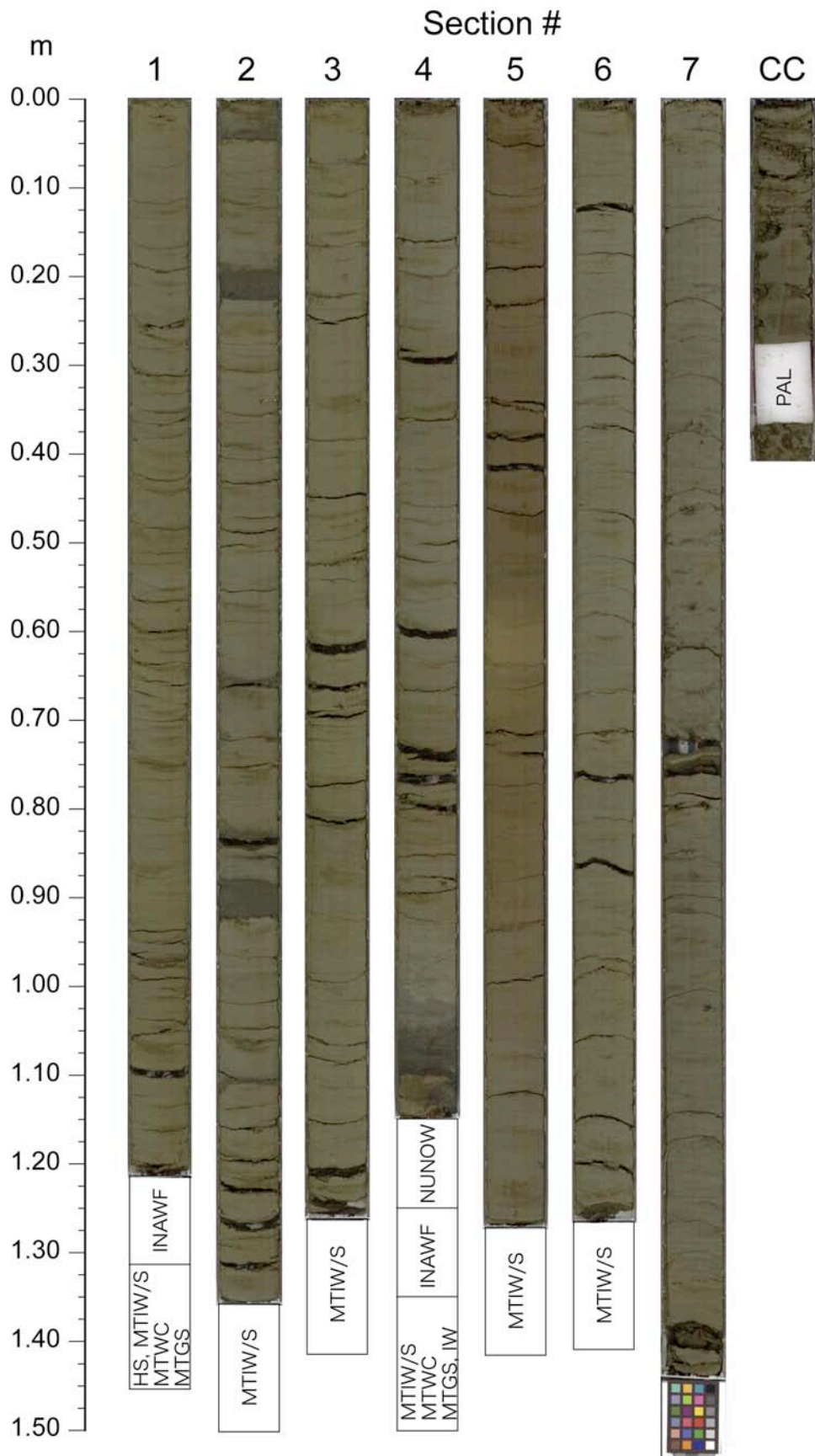


Core 902-C9001C-9H

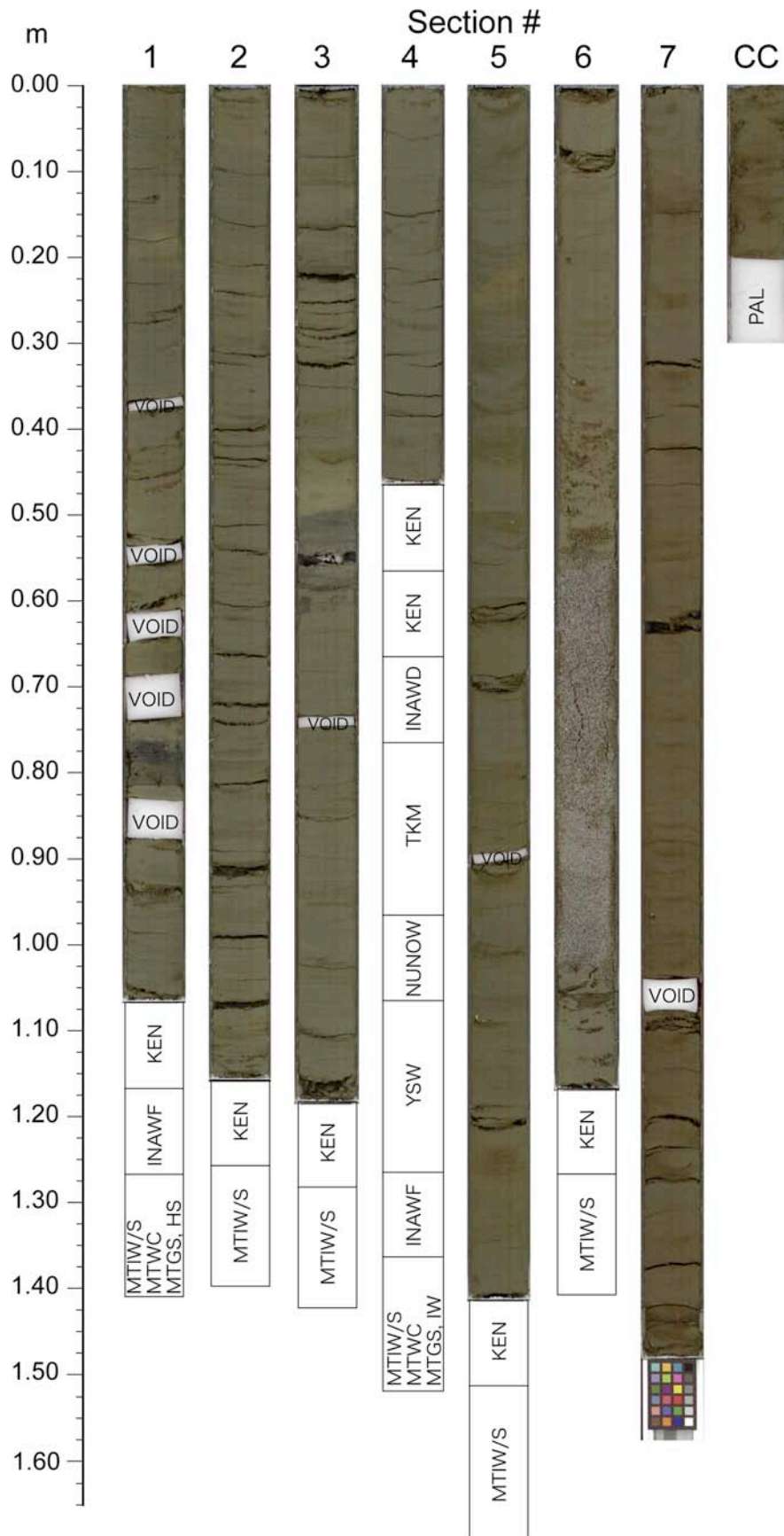
Section #



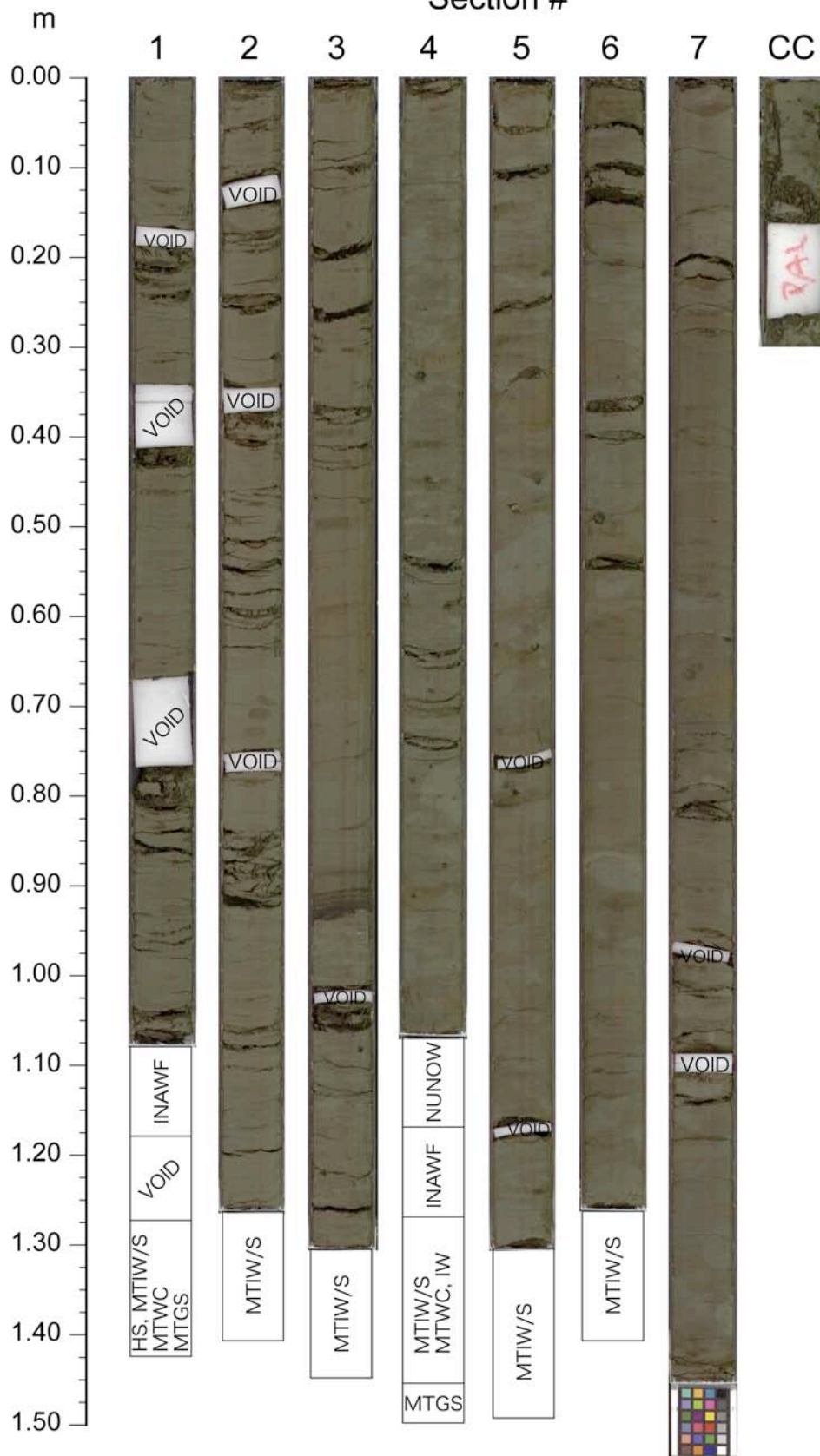
Core 902-C9001C-11H



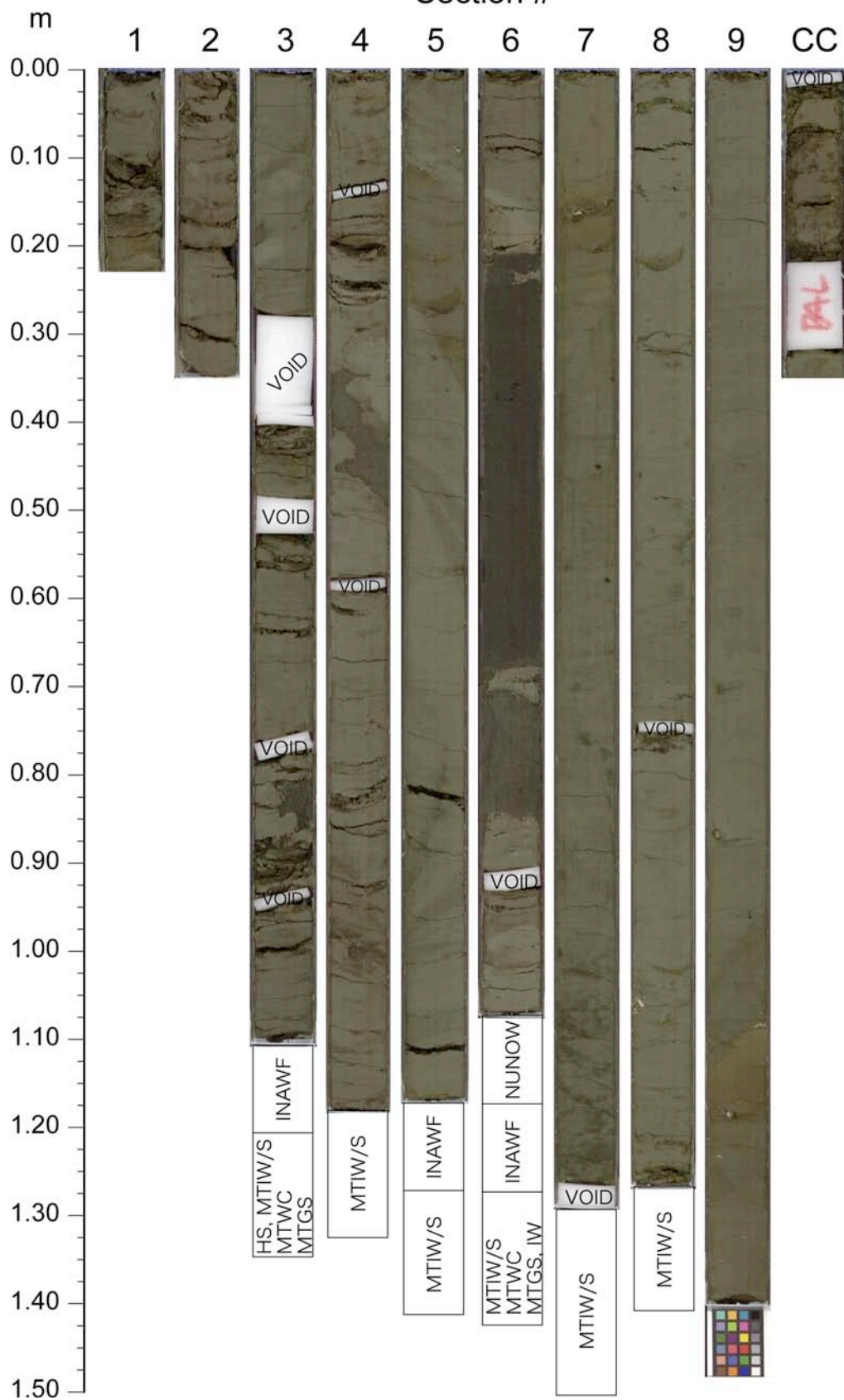
Core 902-C9001C-12H



Section

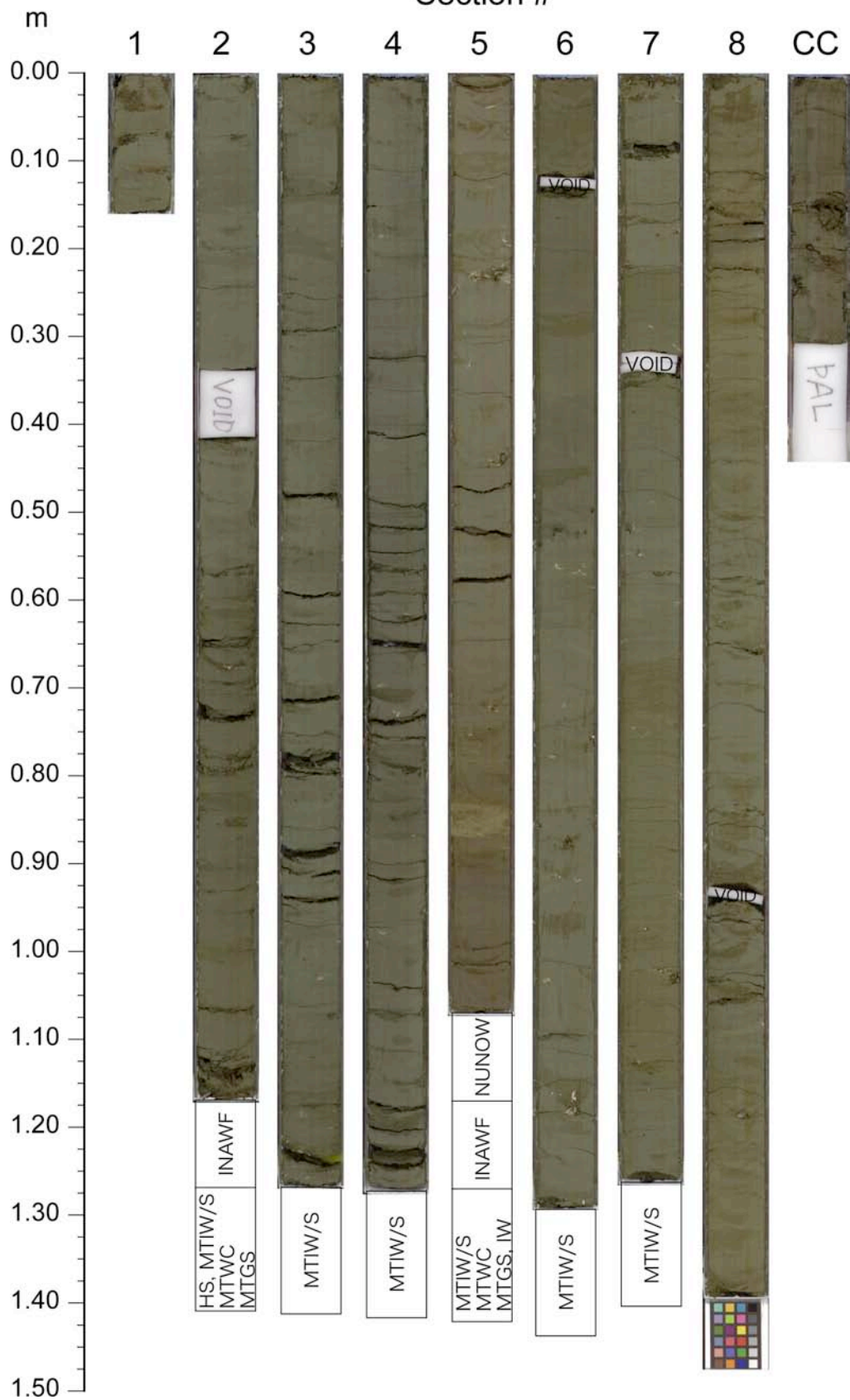


Section

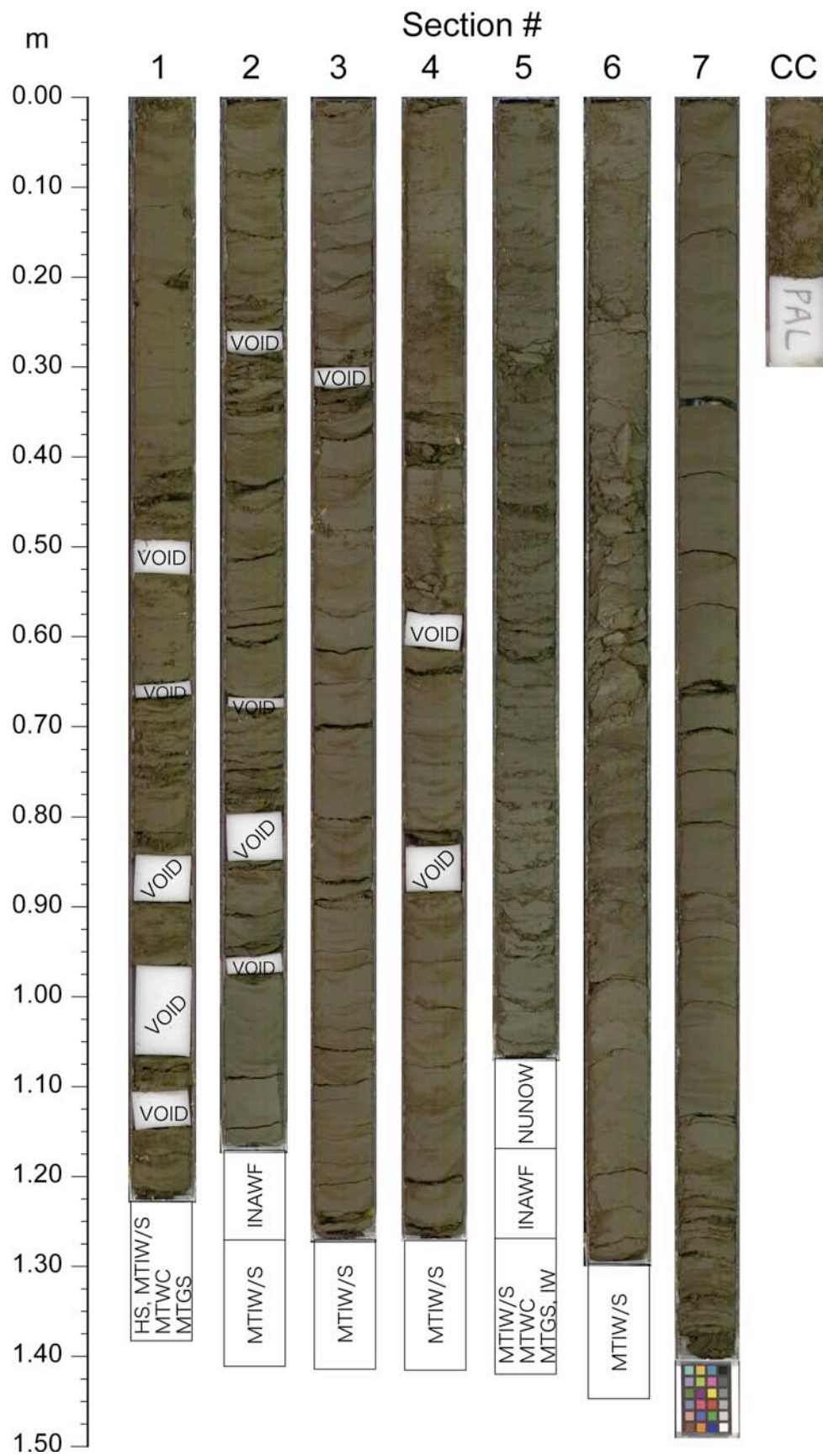


Core 902-C9001C-17H

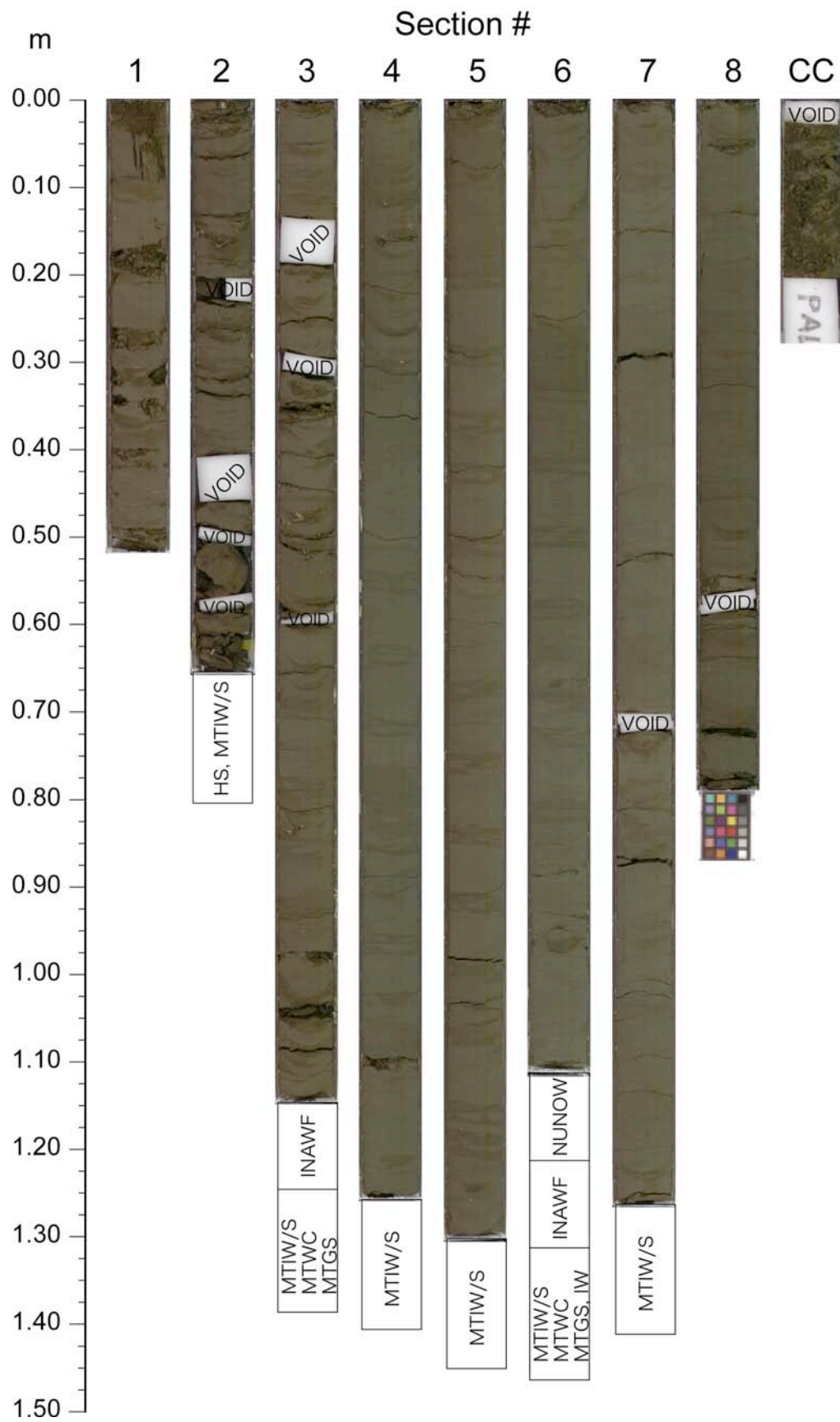
Section #



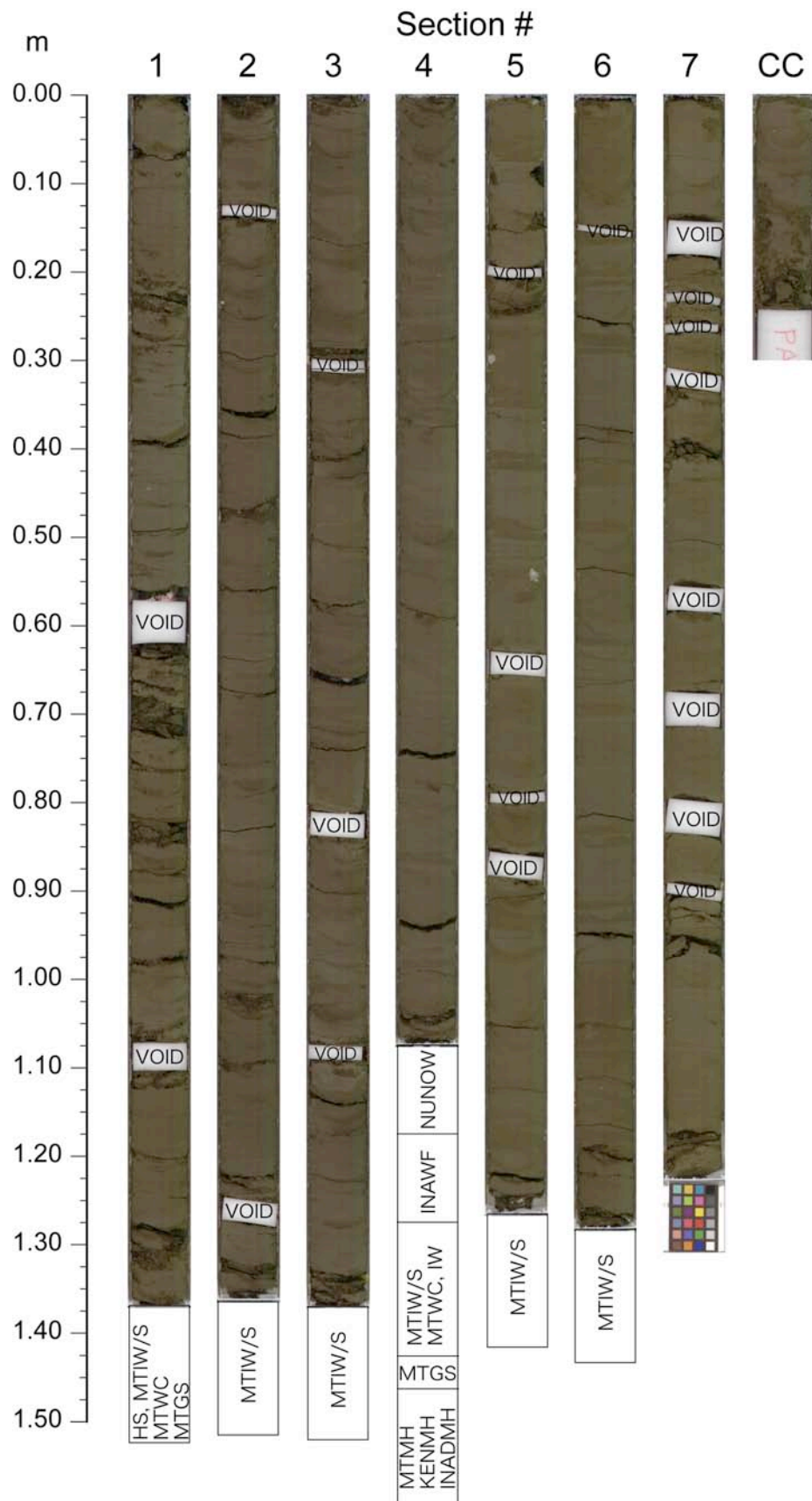
Core 902-C9001C-19H



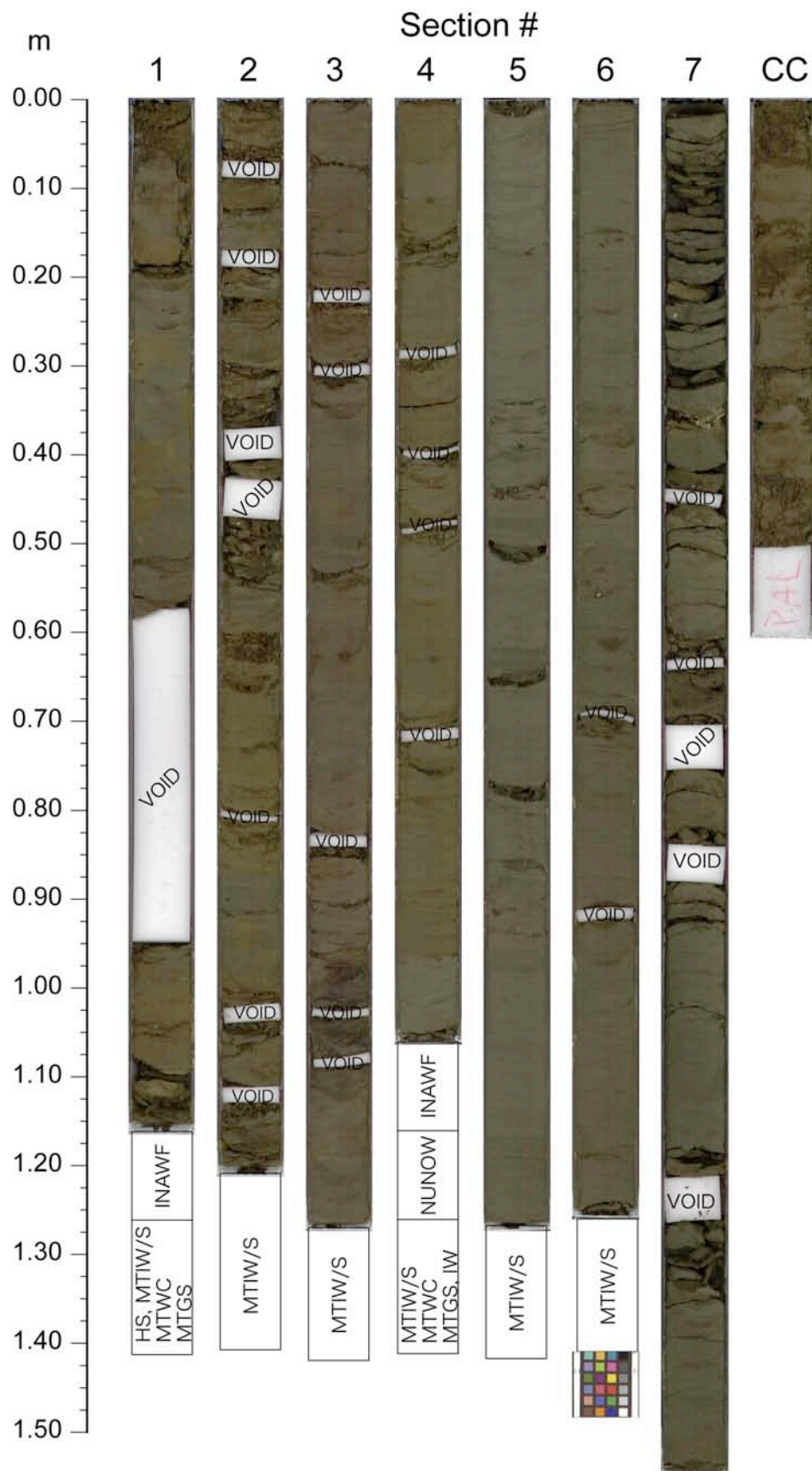
Core 902-C9001C-20H



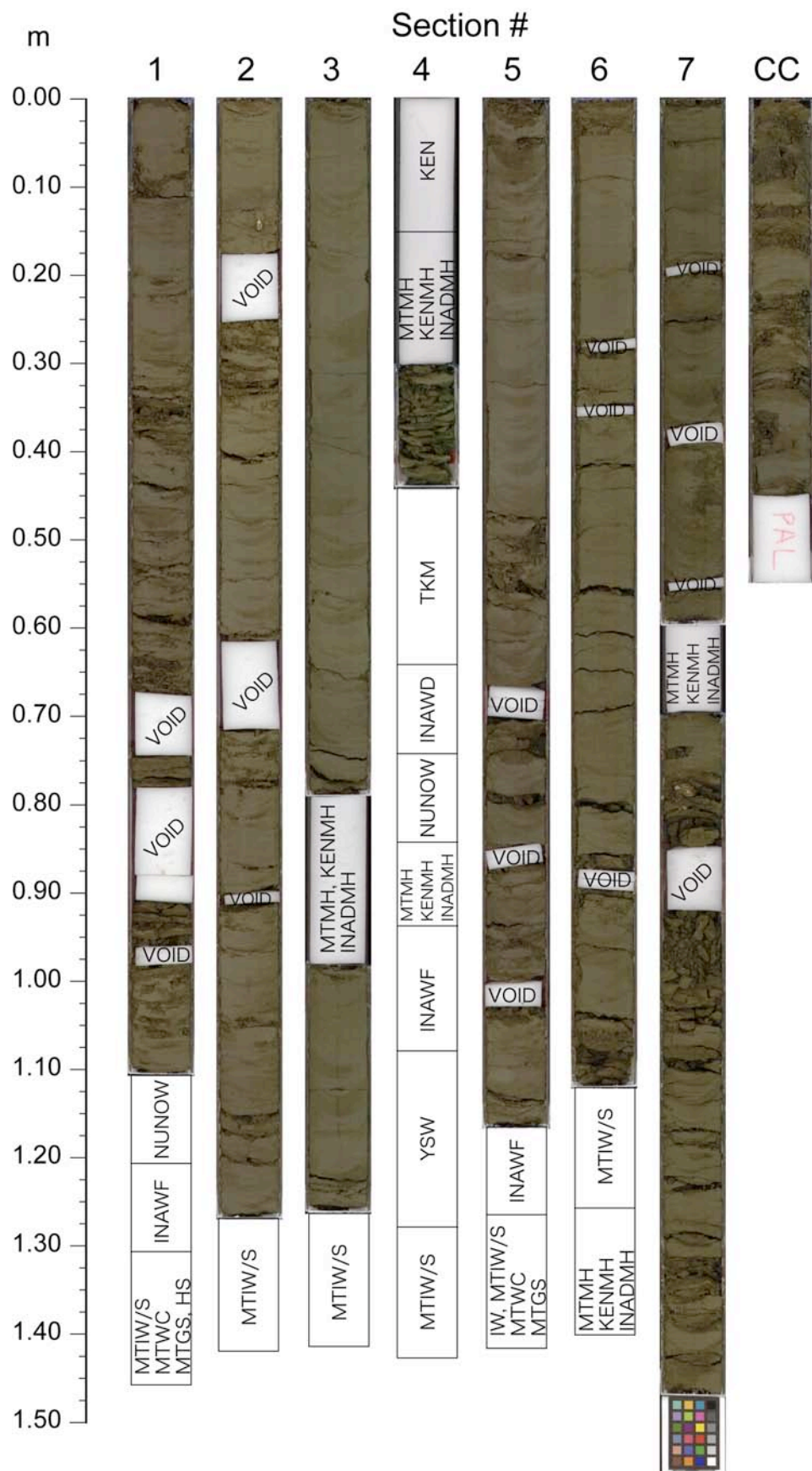
Core 902-C9001C-21H



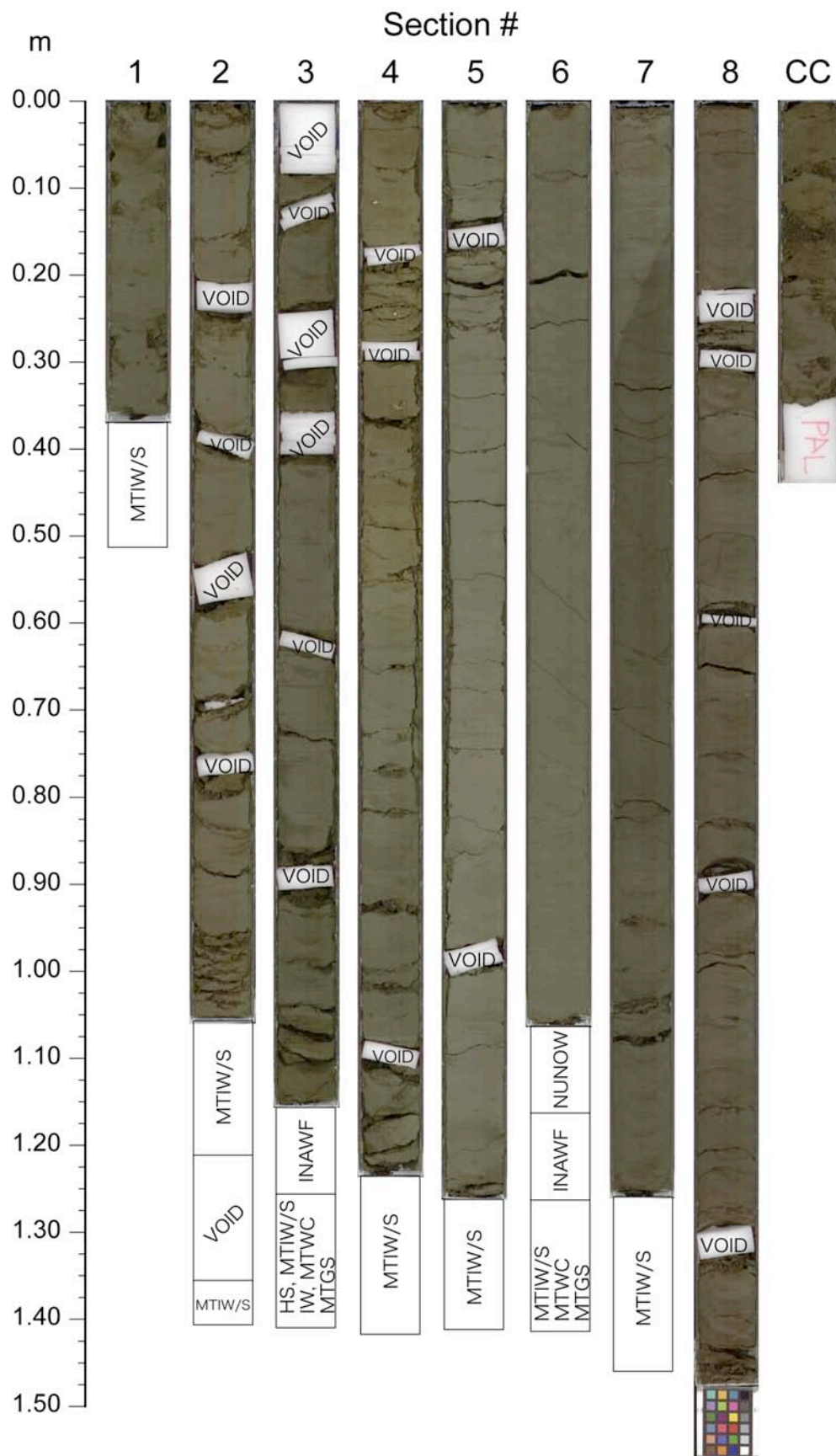
Core 902-C9001C-23H



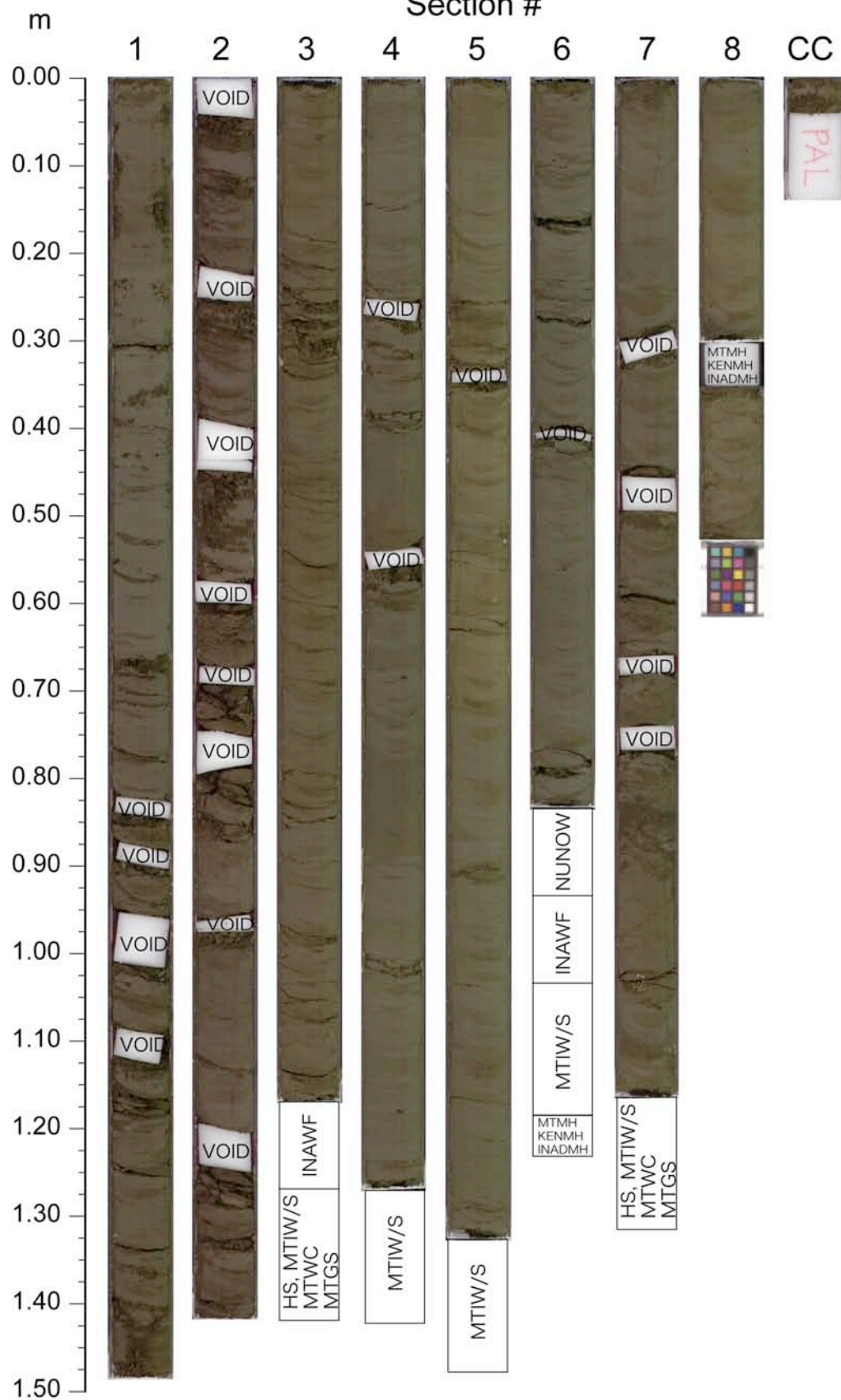
Core 902-C9001C-24H



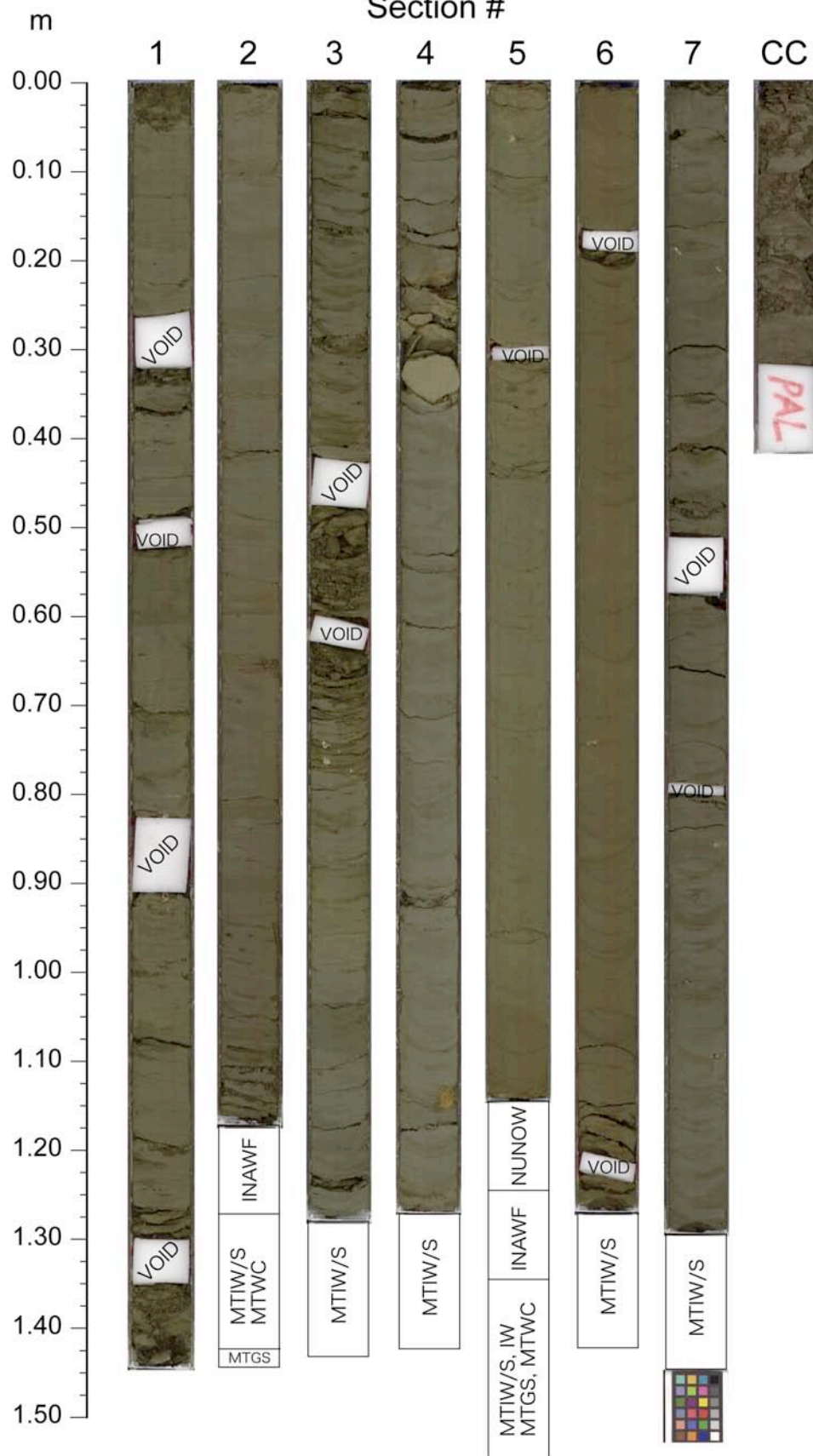
Core 902-C9001C-25H



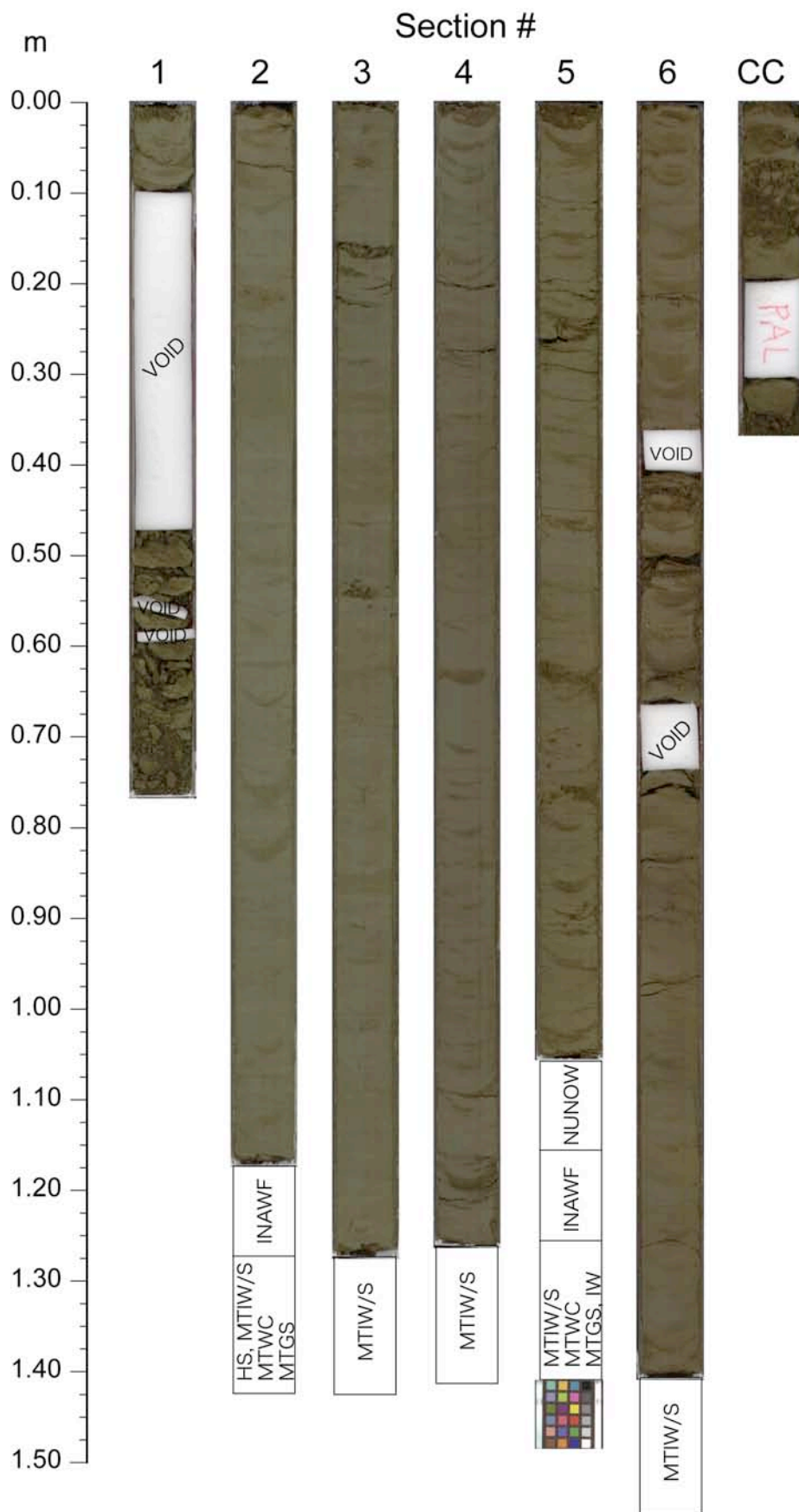
Section



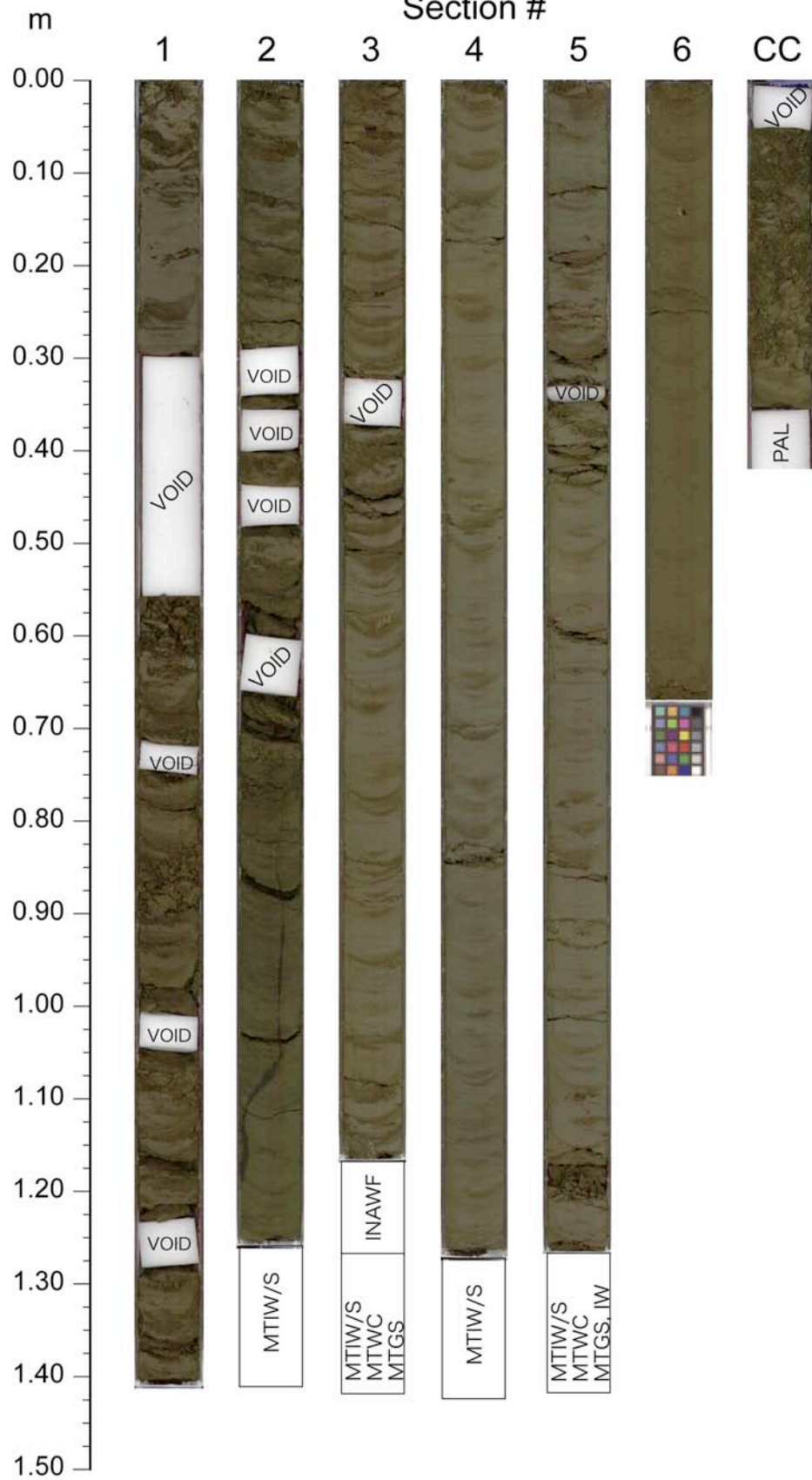
Section



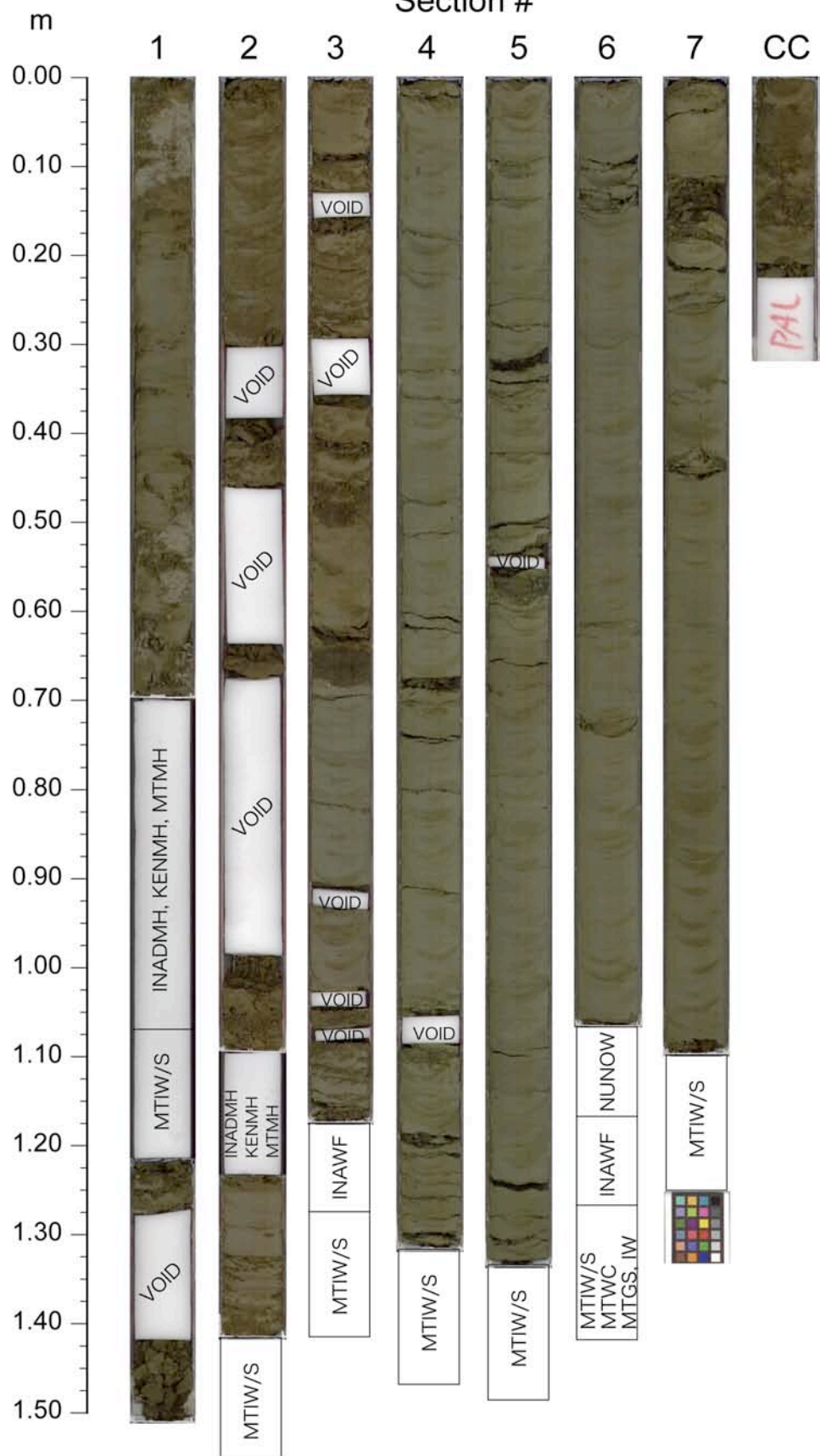
Core 902-C9001C-29H



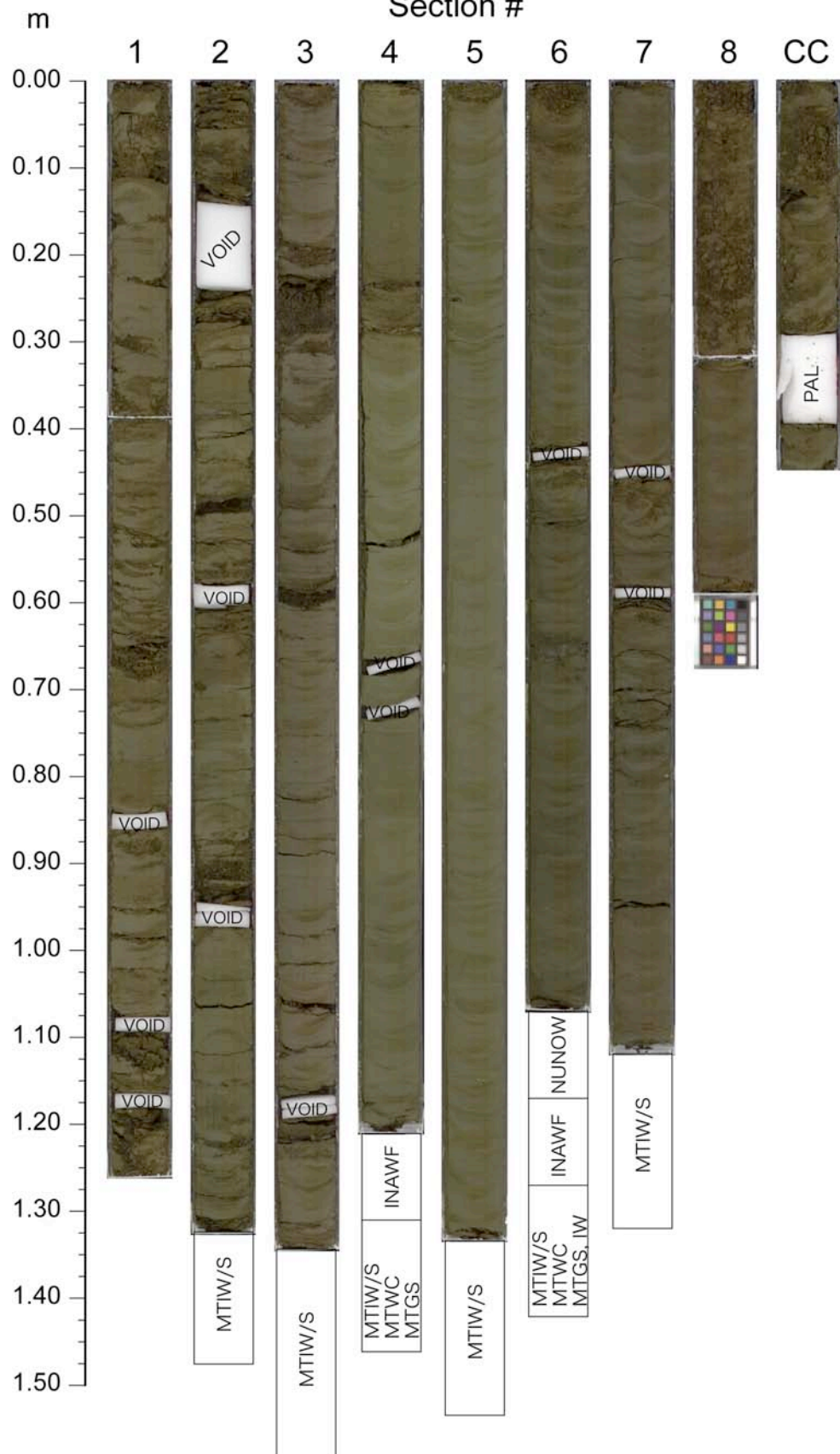
Section



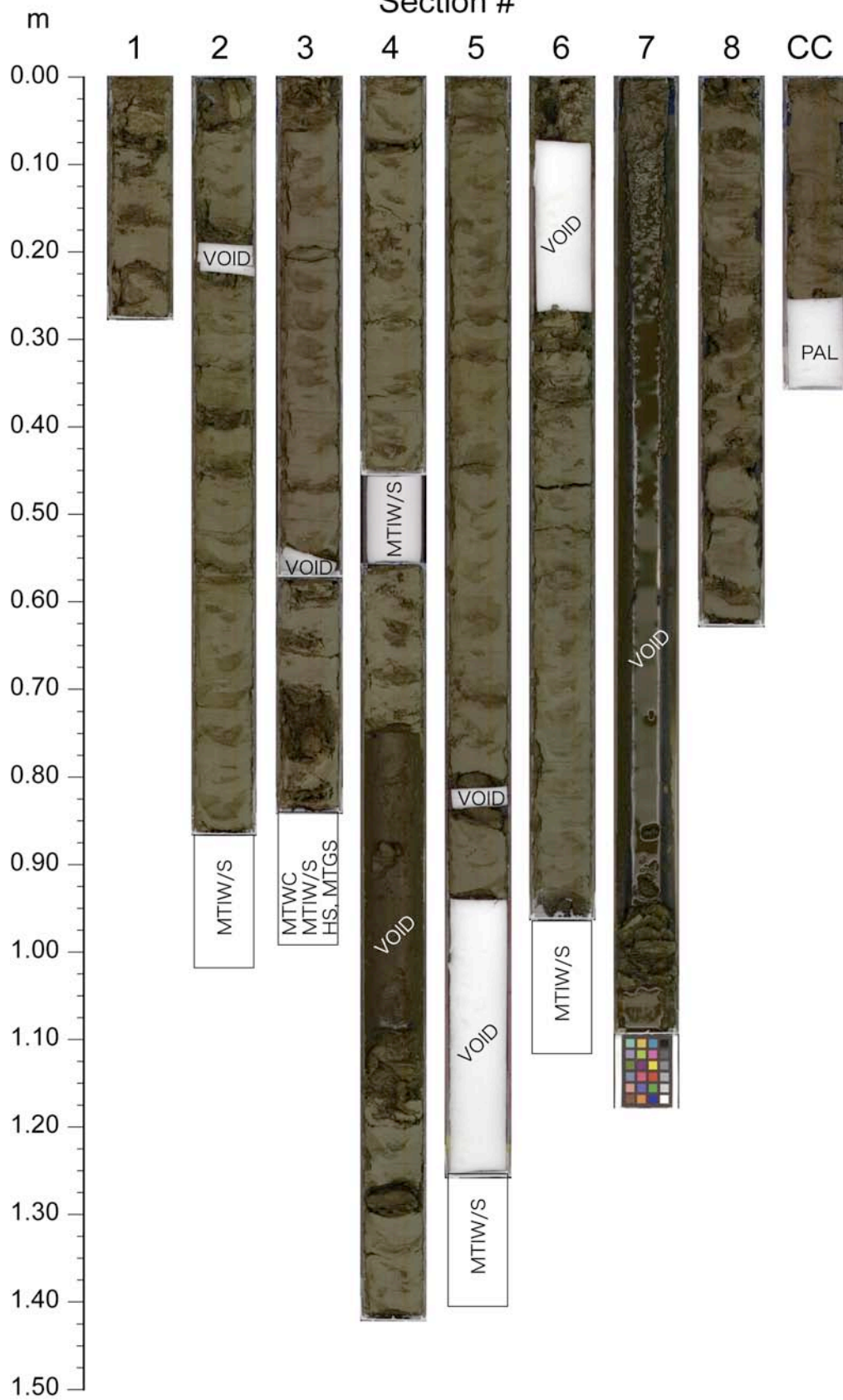
Section

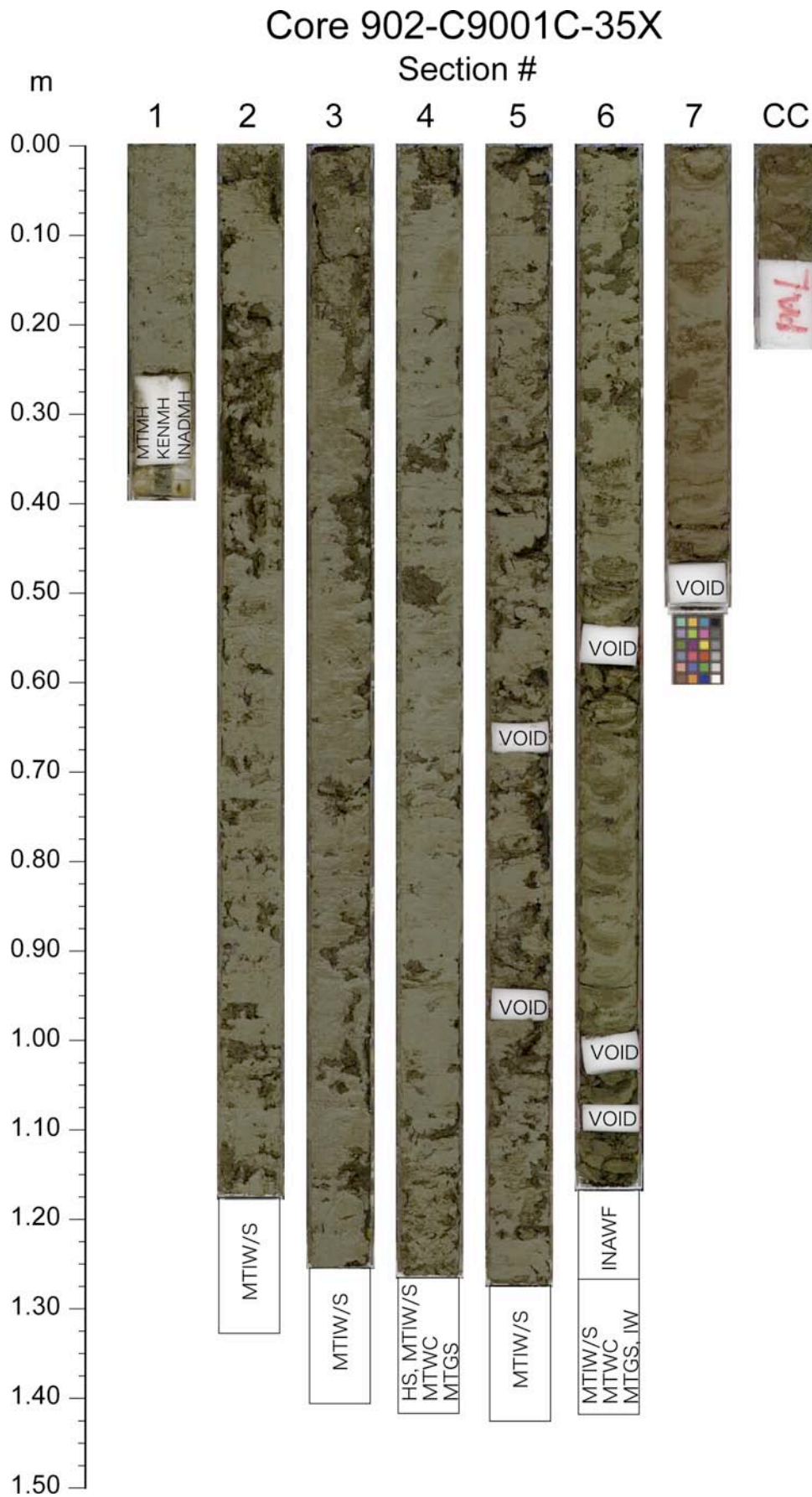


Section



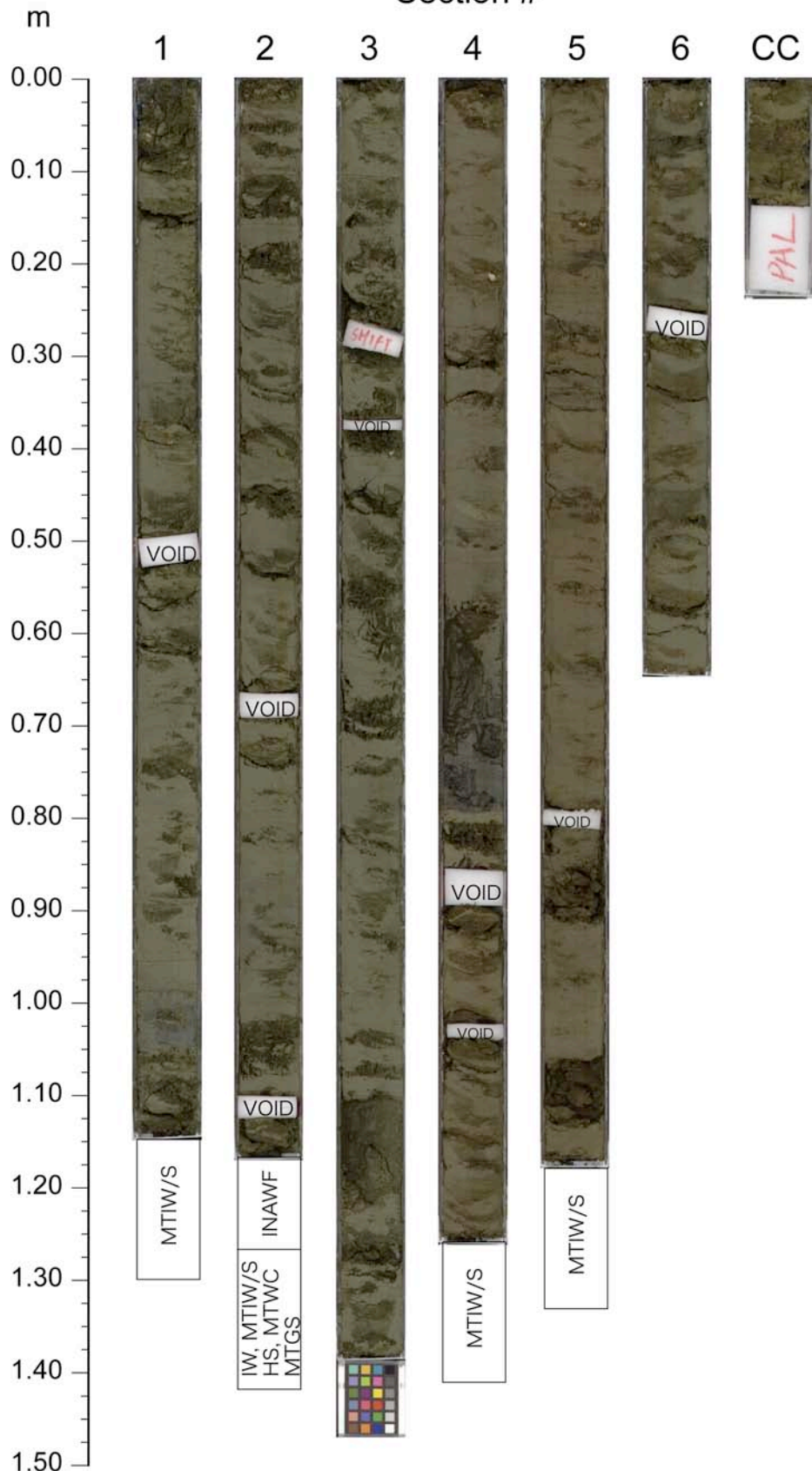
Section





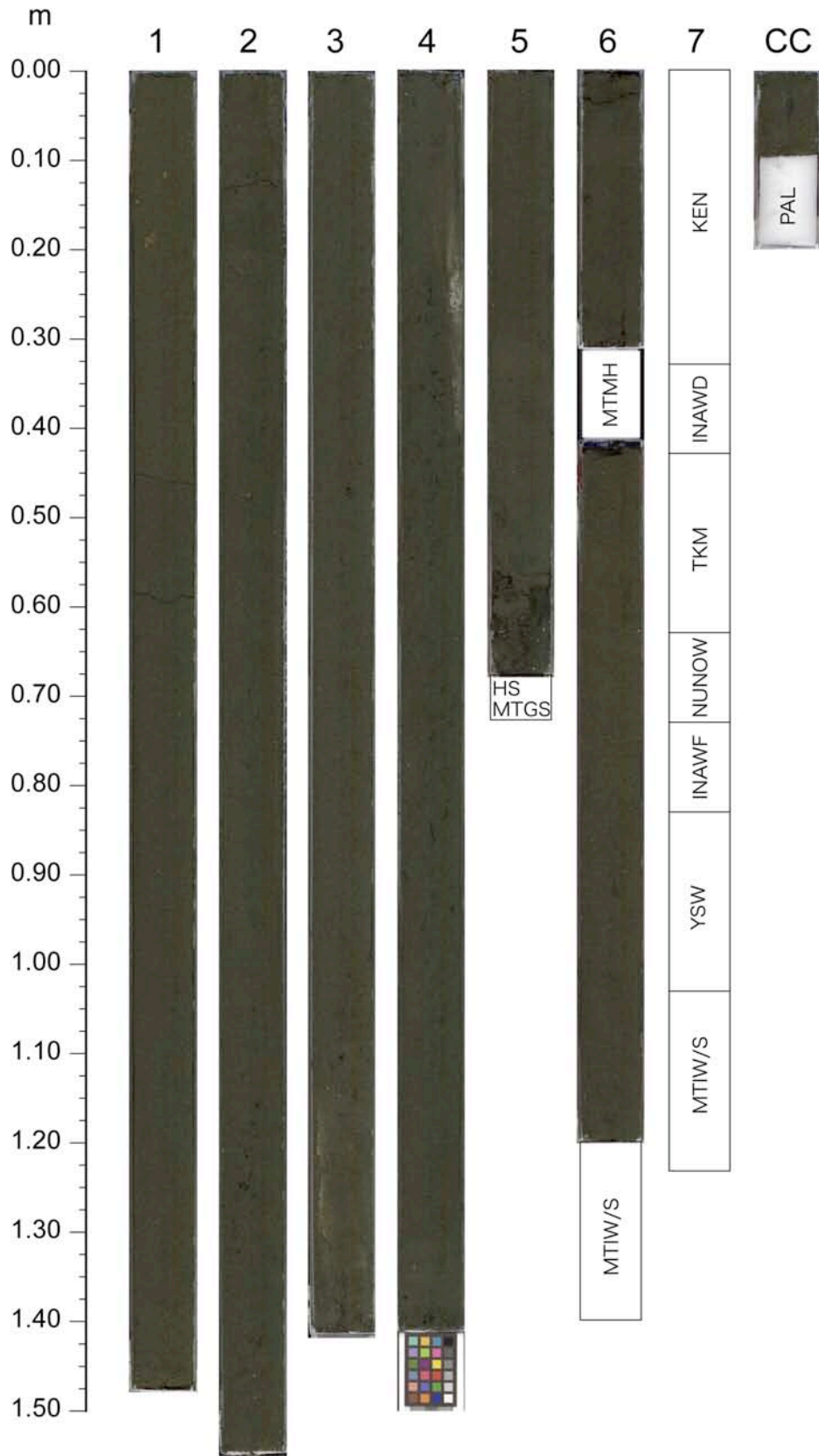
Core 902-C9001C-37X

Section #



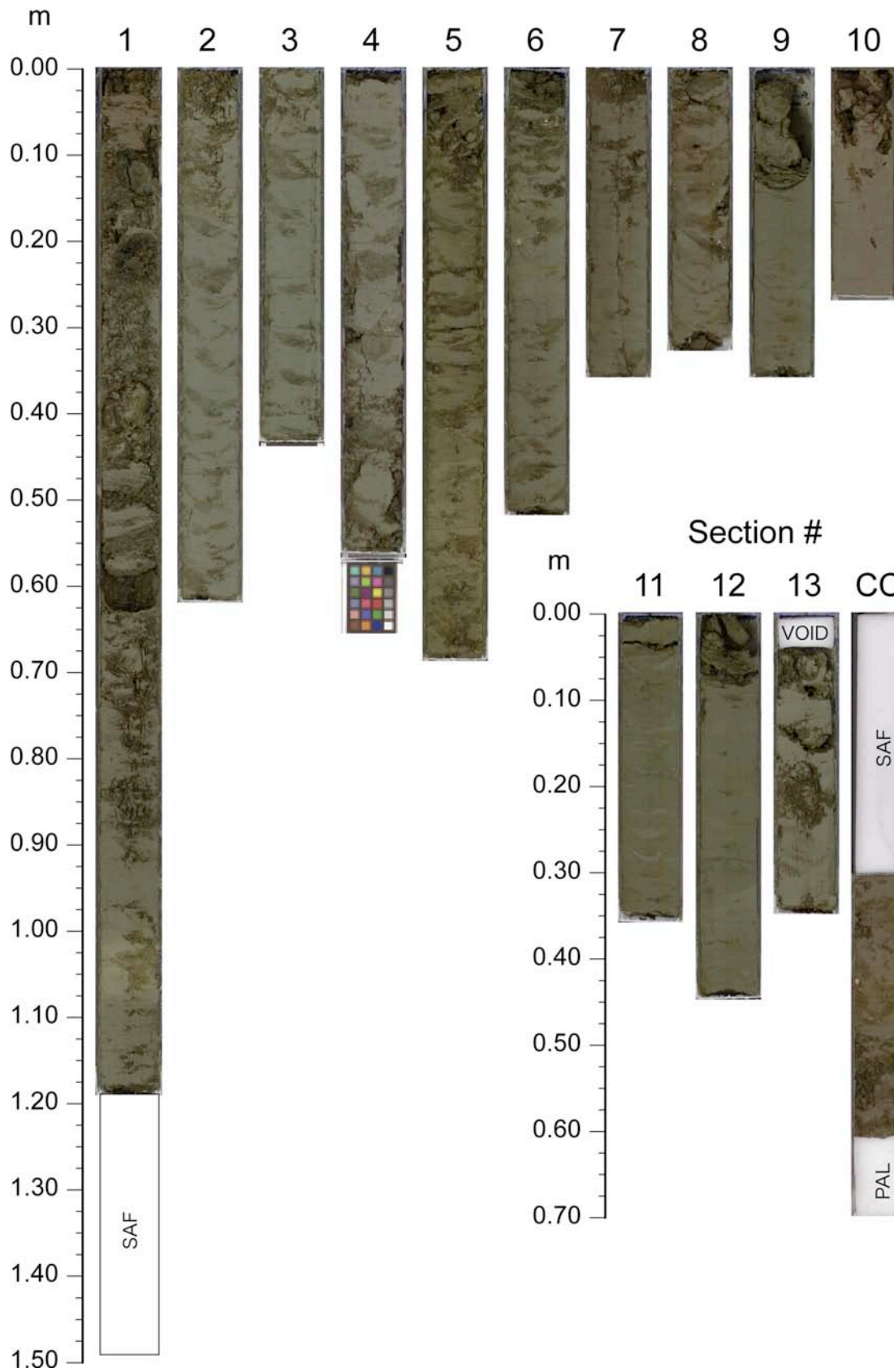
Core 902-C9001C-38H

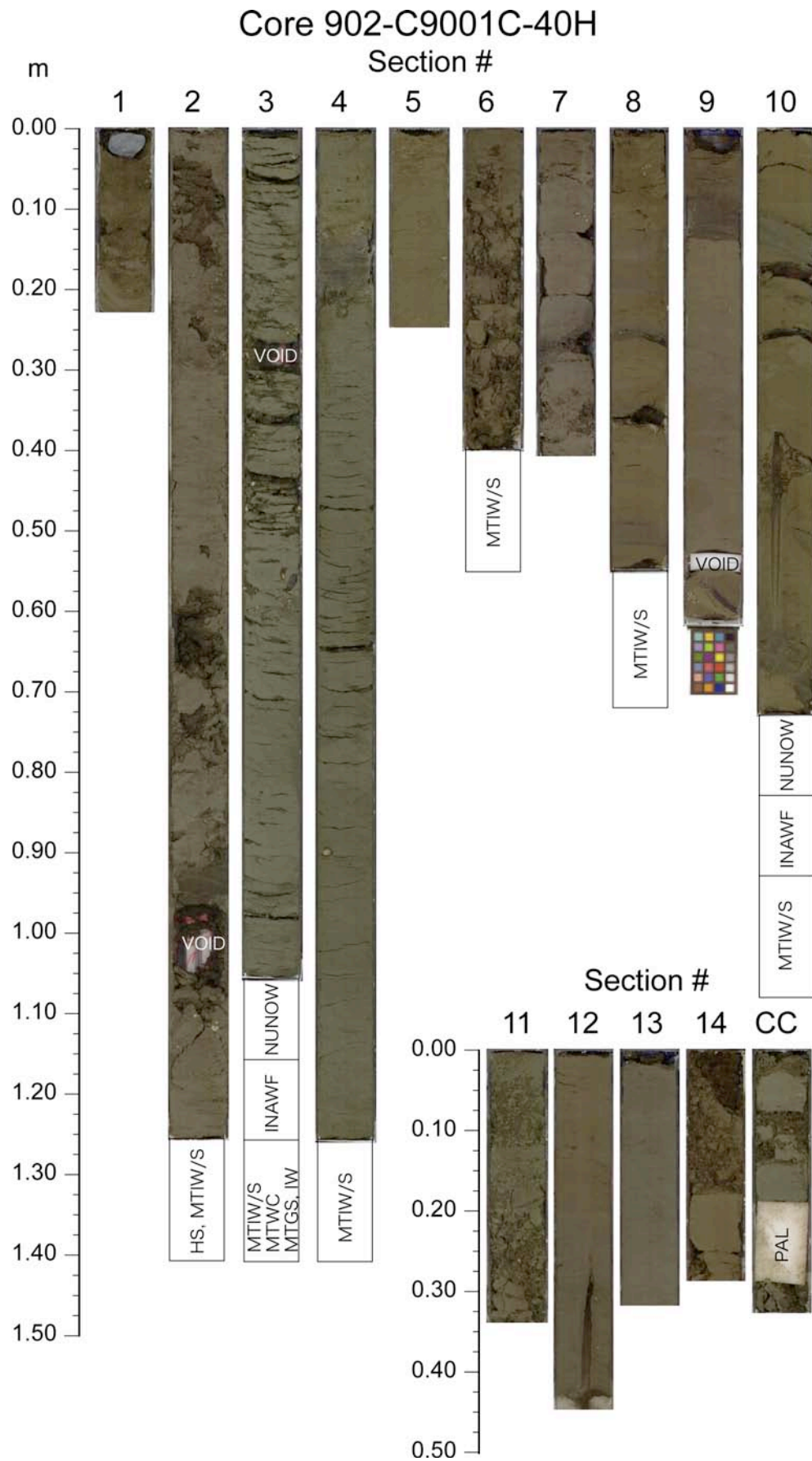
Section #



Core 902-C9001C-39H

Section #





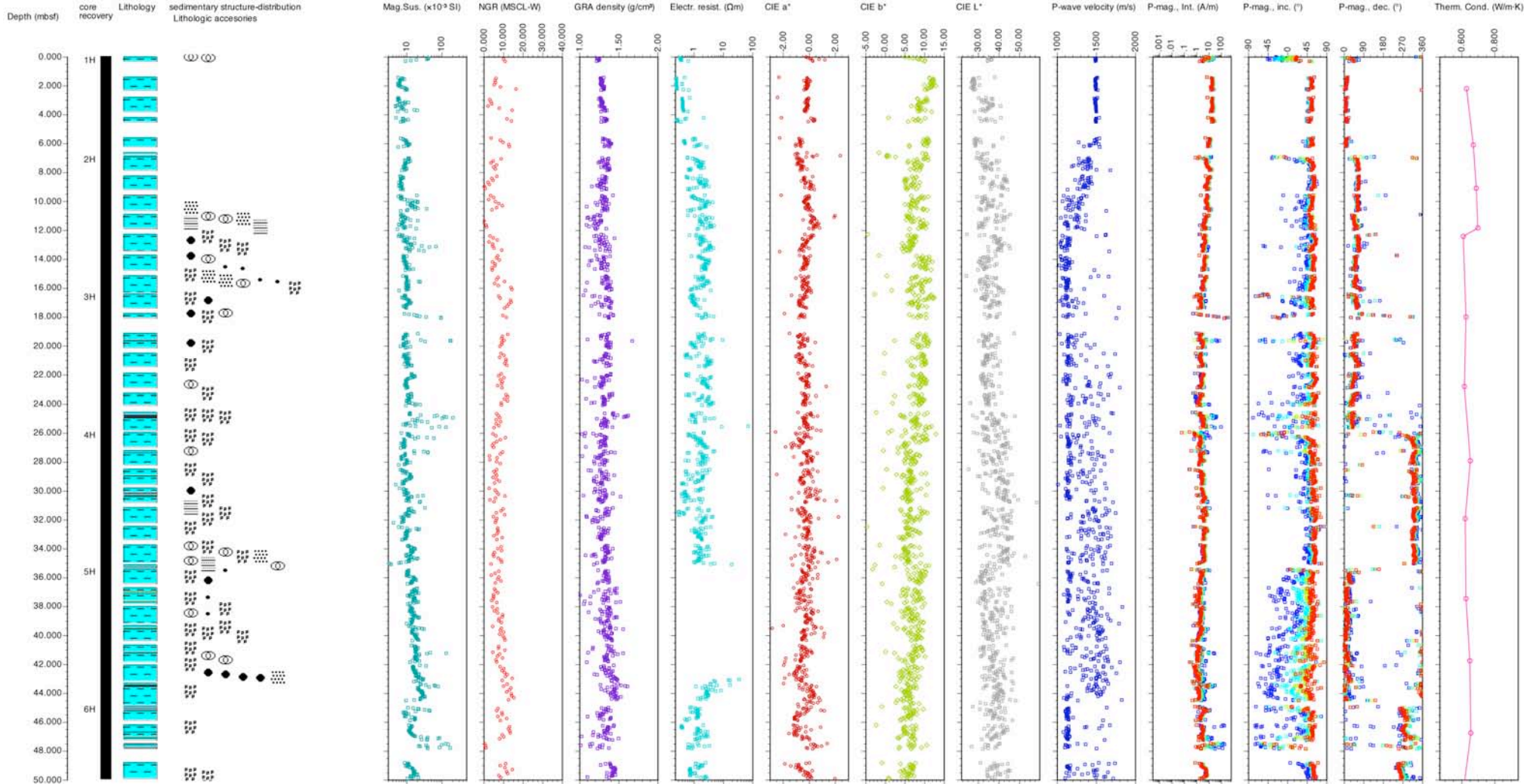
Appendix 3

C9001C

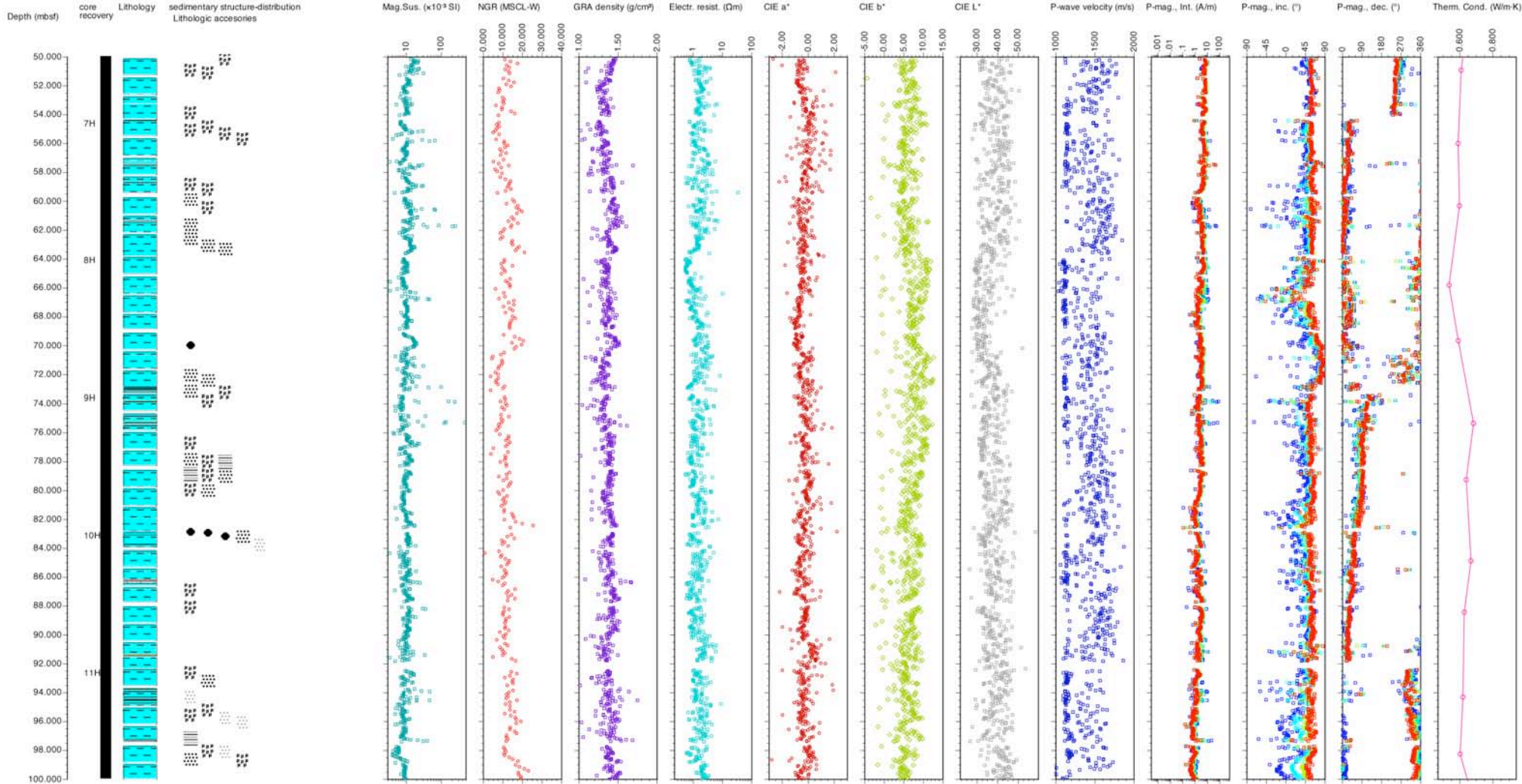
Onboard Measurement Results

Note: Data shown hereinafter are preliminary results of onboard measurements that were conducted as part of LSIT, including those of which the analytical method is still under development.

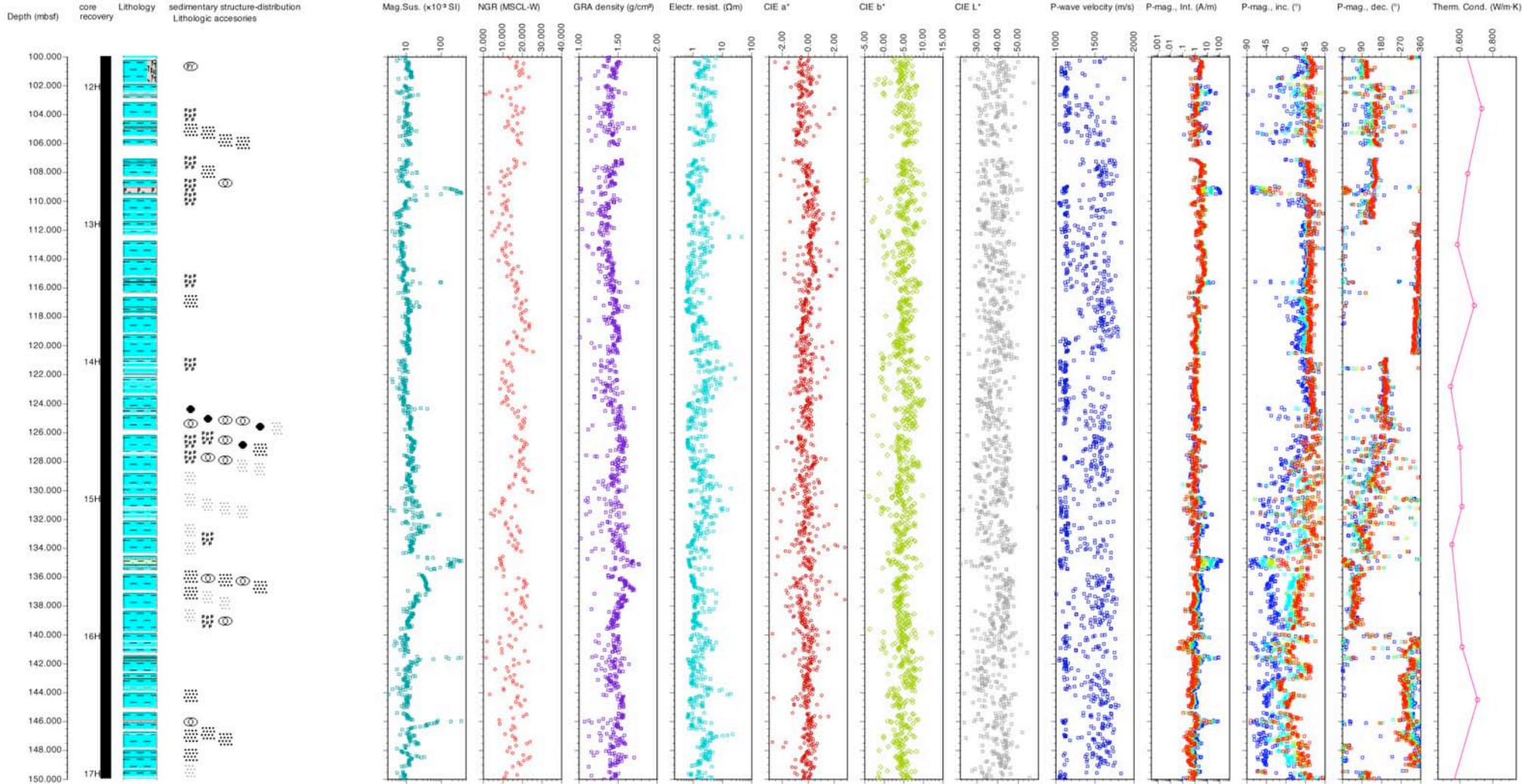
902-C9001C (0 ~ 50 mbsf)



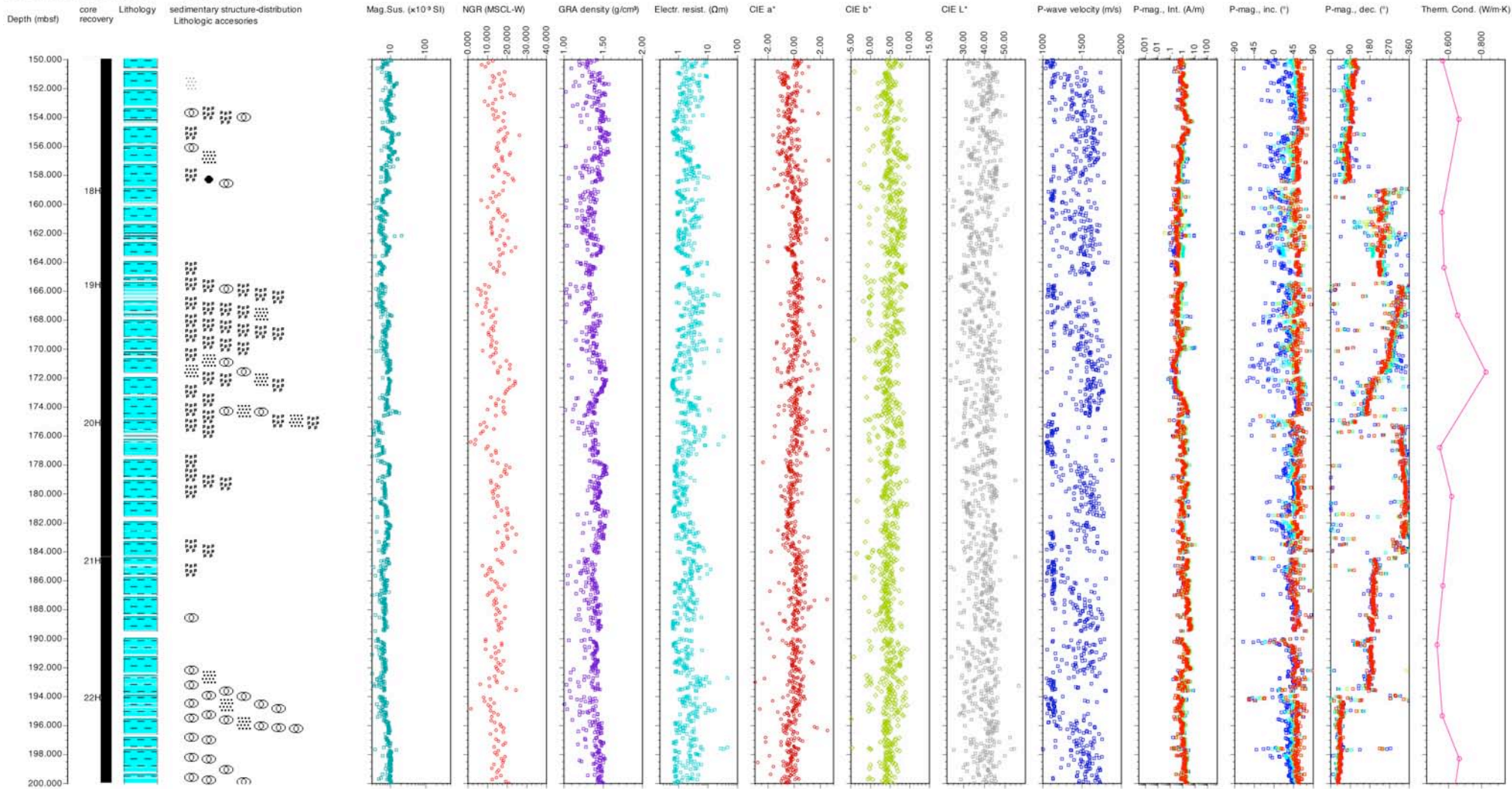
902-C9001C (50 ~ 100 mbsf)



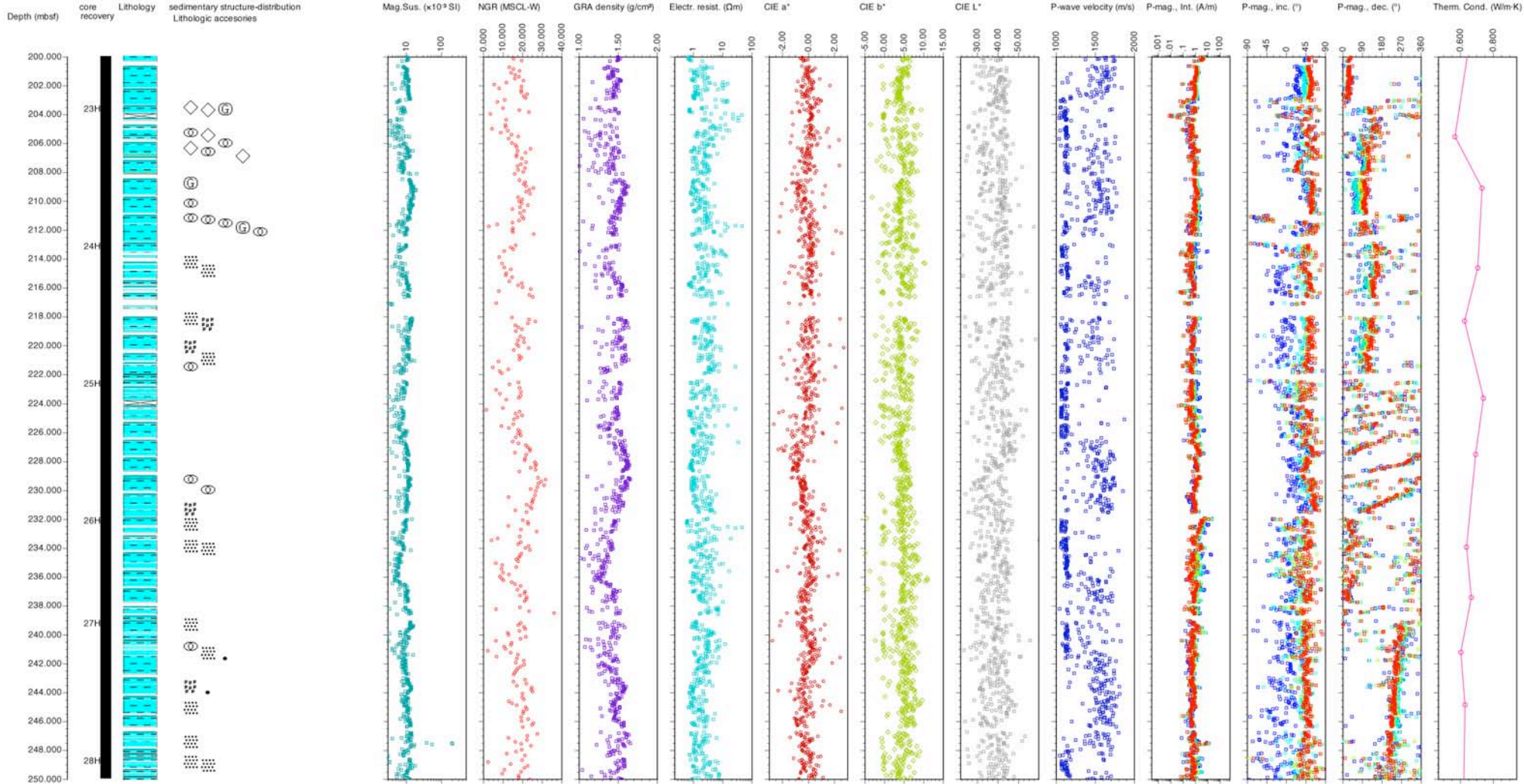
902-C9001C (100 ~ 150 mbsf)



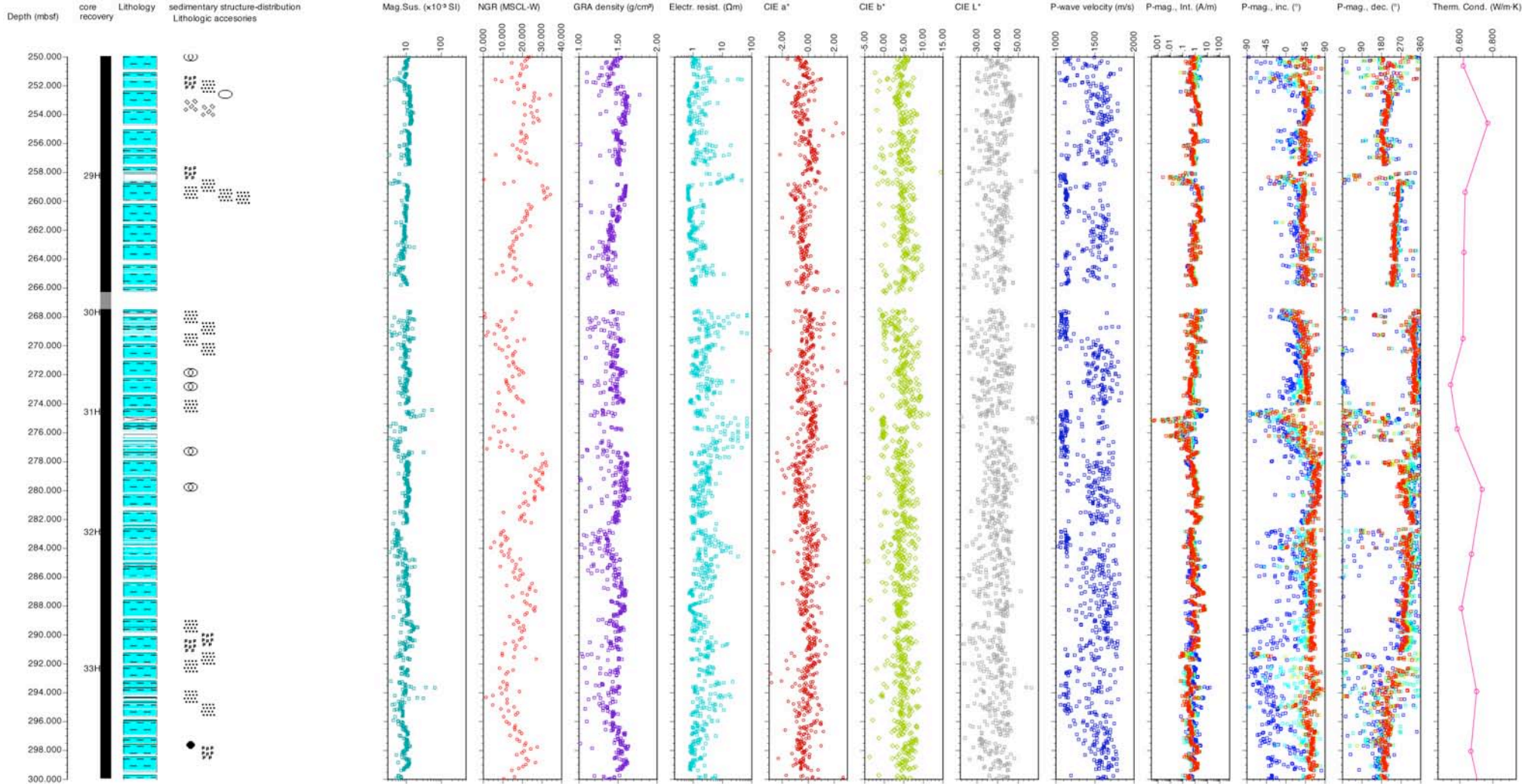
902-C9001C (150 ~ 200 mbst)



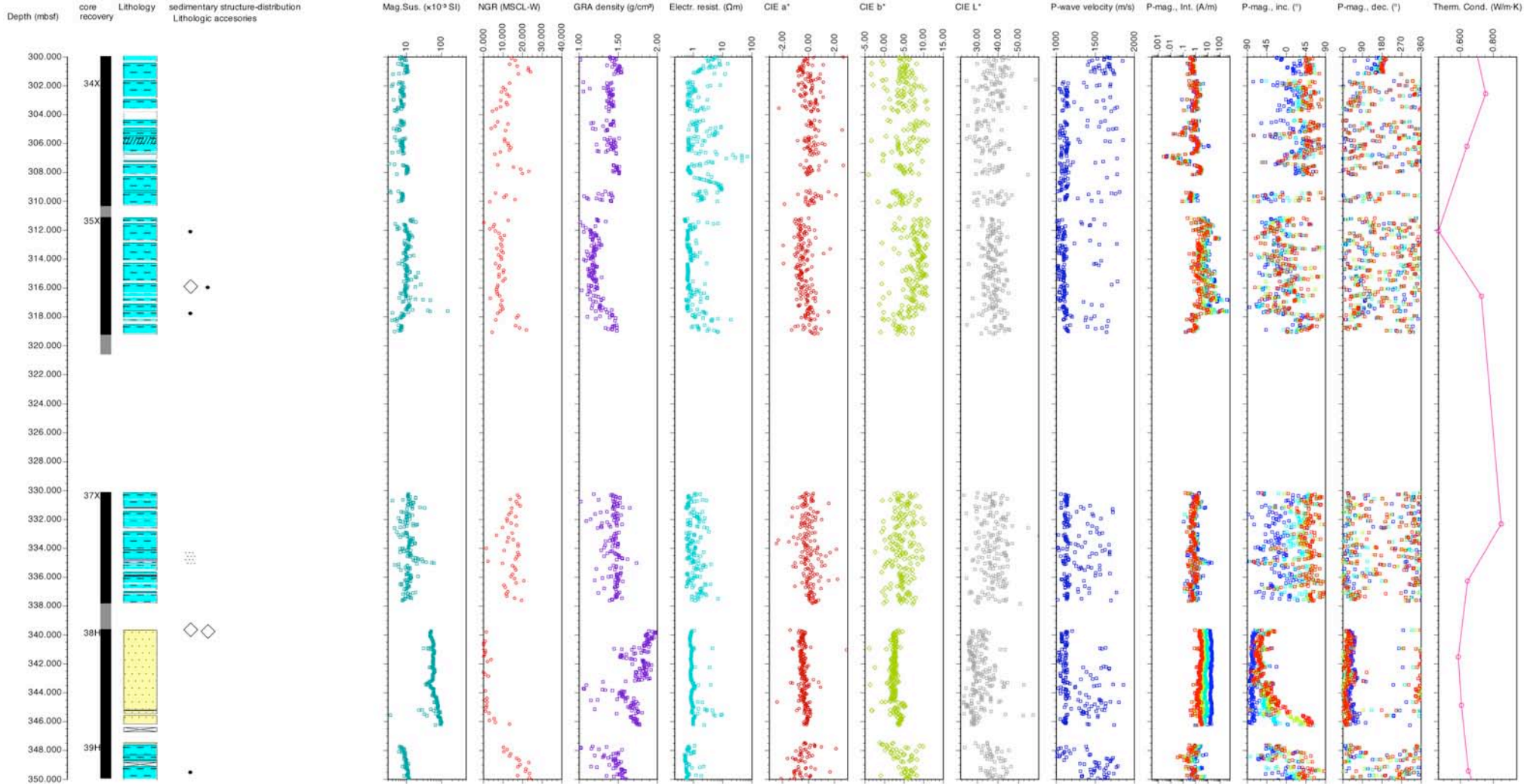
902-C9001C (200 ~ 250 mbsf)



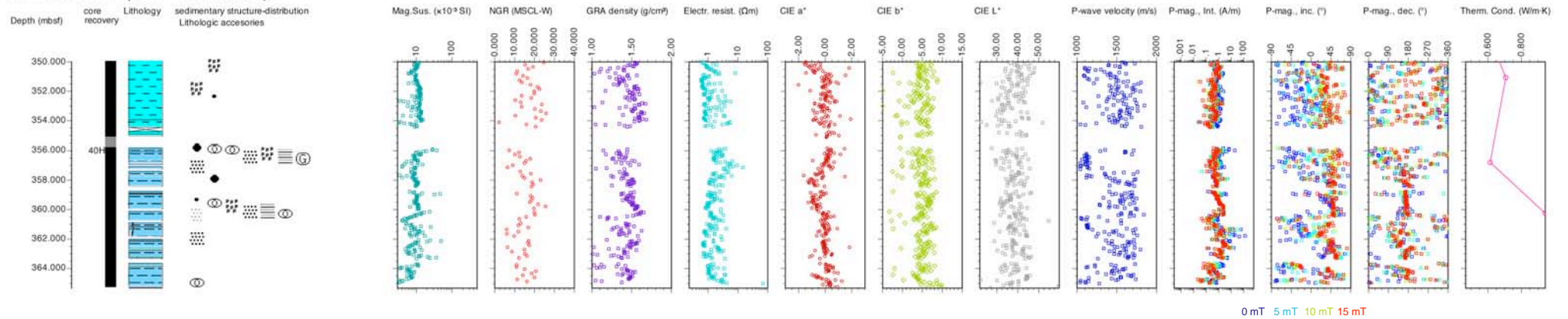
902-C9001C (250 ~ 300 mbsf)



902-C9001C (300 ~ 350 mbsf)



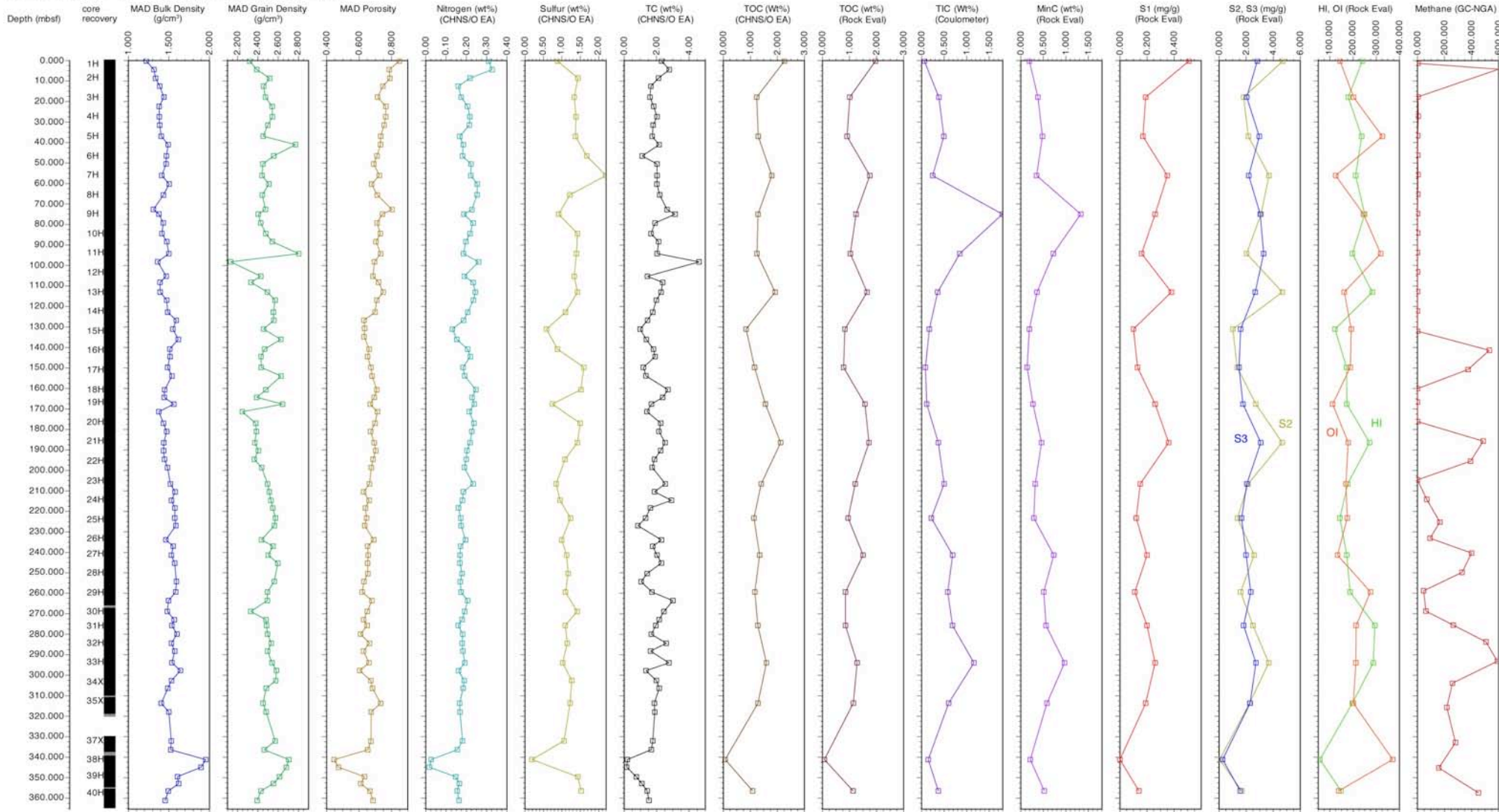
902-C9001C (350 ~ 365 mbsf)



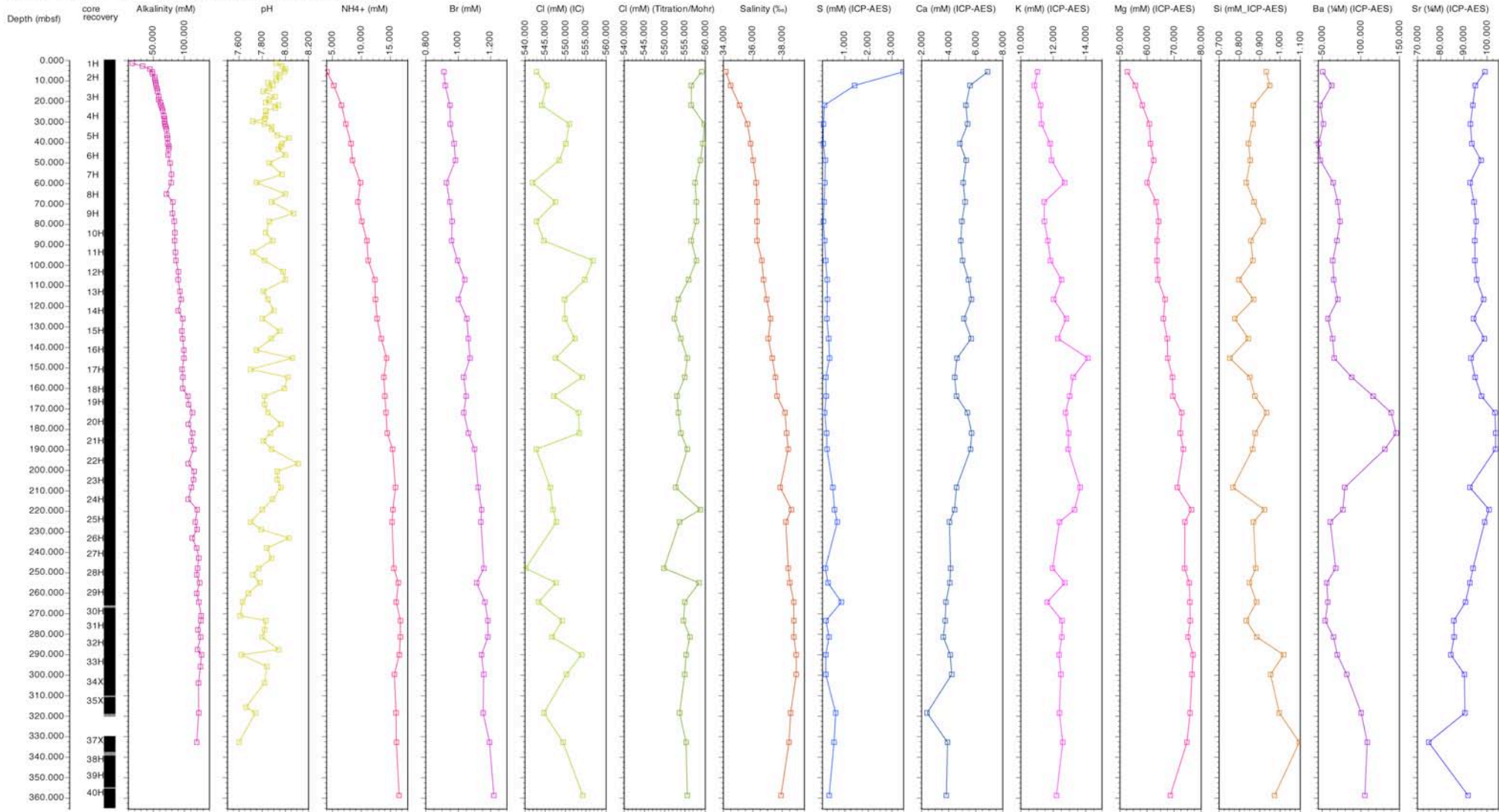
Legend

- | | |
|------------------------|-----------------------------------|
| Sand | Lithoclast |
| Silty | General nodule / concretion |
| Sandy Silt | Pyrite nodule / Pyrite concretion |
| Silty Clay | Gravel |
| Clay | Pumice |
| Ash | Sand scattering |
| Metalliferous (Pyrite) | Color banding |
| | Pumice scattering |
| | Isolated pebble |
| | Isolated granule |
| | Silt scattering |
| | Crystalline precipitation |

902-C9001C (0 ~ 365 mbst) Solid & Gas



902-C9001C (0 ~ 365 mbsf) Interstitial Water



Appendix 4




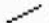
C9001C

Visual Core Description

Note: VCD data input was performed on VCD/J-CORES by means of tablet PCs at the core description and the microscope tables without use of hand-writing barrel sheets.

Legend






Boundary

-  sharp contact
-  gradual contact
-  wavy contact
-  inclined


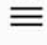
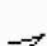
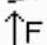
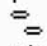

Lithology

- granular sediment
- siliciclastic sediment
 -  sand
 -  silt
 -  sandy silt
 -  clayey silt
 -  clay
 -  sandy clay
 -  silty clay
- volcaniclastic sediment
 -  ash
 -  felsic ash
 -  mafic ash
 -  pumice
- chemical sediment
- metalliferous sediment
 -  pyrite

Drilling Disturbance

-  Slightly Disturbed
-  Moderately Disturbed
-  Highly Disturbed
-  Soupy
-  Flow inn

Sedimentary structures

-  Graded bedding (normal)
-  Planar lamination/
mm-scale color banding/Laminae
-  Flaser bedding/Flaserlike bedding
-  Fining-Upward Sequence
-  Patch
-  Tube structure

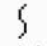

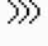
Lithologic accessories

-  General nodule/concretion
-  isolated pebble
-  Lithoclast
-  Pyrite nodule/Pyrite concretion
-  Gravel
-  Pumice
-  sand scattering
-  color-banding
-  pumice scattering
-  isolated granule
-  silt scattering
-  Crystalline precipitation

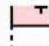
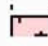
Fossils



-  Shell fragments
-  Wood Fragments
-  Bivalve
-  Foraminifer
-  organic material

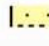
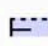
Bioturbation

-  Slight bioturbation
-  Moderate bioturbation
-  Heavy bioturbation

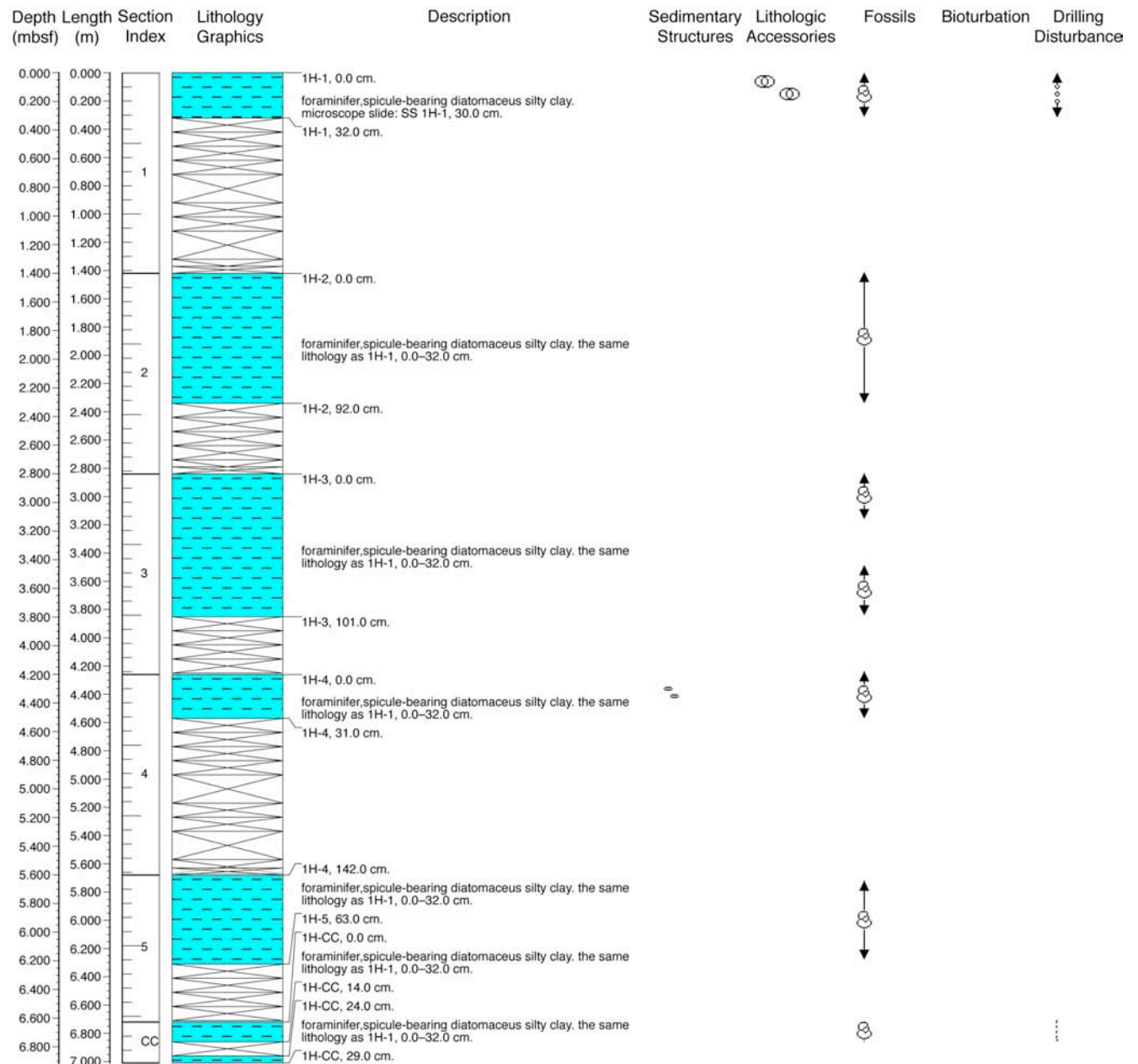
-  core gap
- 

-  void / exotic material
- 

-  whole-round sampling
- 

-  split boundary through depth processing
- 

902-C9001C-1H (0–6.91 mbsf)



902-C9001C-2H (6.91–16.41 mbsf)

Depth (mbsf)	Length (m)	Section Index	Lithology Graphics	Description	Sedimentary Structures	Lithologic Accessories	Fossils	Bioturbation	Drilling Disturbance
7.000	0.000			2H-1, 0.0 cm.					
7.200	0.200								
7.400	0.400			foram,rads,spicule-bearing diatomaceous silty clay. microscope slide: SS 2H-1, 50.0 cm.					
7.600	0.600								
7.800	0.800	1							
8.000	1.000			2H-1, 101.0 cm.					
8.200	1.200								
8.400	1.400			2H-2, 0.0 cm.					
8.600	1.600								
8.800	1.800			foram,rads,spicule-bearing diatomaceous silty clay. the same lithology as 2H-1, 0.0–101.0 cm.					
9.000	2.000	2							
9.200	2.200			2H-2, 101.0 cm.					
9.400	2.400								
9.600	2.600			2H-3, 0.0 cm.					
9.800	2.800			silt-bearing ash. microscope slide: SS 2H-3, 0.5 cm.					
10.000	3.000			2H-3, 1.0 cm.					
10.200	3.200			foram,rads,spicule-bearing diatomaceous silty clay. the same lithology as 2H-1, 0.0–101.0 cm.					
10.400	3.400	3							
10.600	3.600								
10.800	3.800			2H-3, 114.0 cm.					
11.000	4.000								
11.200	4.200			2H-4, 0.0 cm.					
11.400	4.400								
11.600	4.600			foram,rads,spicule-bearing diatomaceous silty clay. the same lithology as 2H-1, 0.0–101.0 cm.					
11.800	4.800	4							
12.000	5.000			2H-4, 104.5 cm.					
12.200	5.200			silt. microscope slide: SS 2H-4, 105.0 cm.					
12.400	5.400			2H-4, 105.5 cm.					
12.600	5.600			foram,rads,spicule-bearing diatomaceous silty clay. the same lithology as 2H-1, 0.0–101.0 cm.					
12.800	5.800			2H-4, 107.0 cm.					
13.000	6.000			2H-5, 0.0 cm.					
13.200	6.200			foram,rads,spicule-bearing diatomaceous silty clay. the same lithology as 2H-1, 0.0–101.0 cm.					
13.400	6.400	5							
13.600	6.600								
13.800	6.800			2H-5, 124.0 cm.					
14.000	7.000								
14.200	7.200			2H-6, 0.0 cm.					
14.400	7.400								
14.600	7.600			foram,rads,spicule-bearing diatomaceous silty clay. the same lithology as 2H-1, 0.0–101.0 cm.					
14.800	7.800	6							
15.000	8.000								
15.200	8.200			2H-6, 111.0 cm.					
15.400	8.400								
15.600	8.600			2H-7, 0.0 cm.					
15.800	8.800								
16.000	9.000	7		foram,rads,spicule-bearing diatomaceous silty clay. the same lithology as 2H-1, 0.0–101.0 cm.					
16.200	9.200								
16.400	9.400								
	9.600								
	9.800								
	10.000								
	10.200	CC		2H-CC, 18.0 cm.					

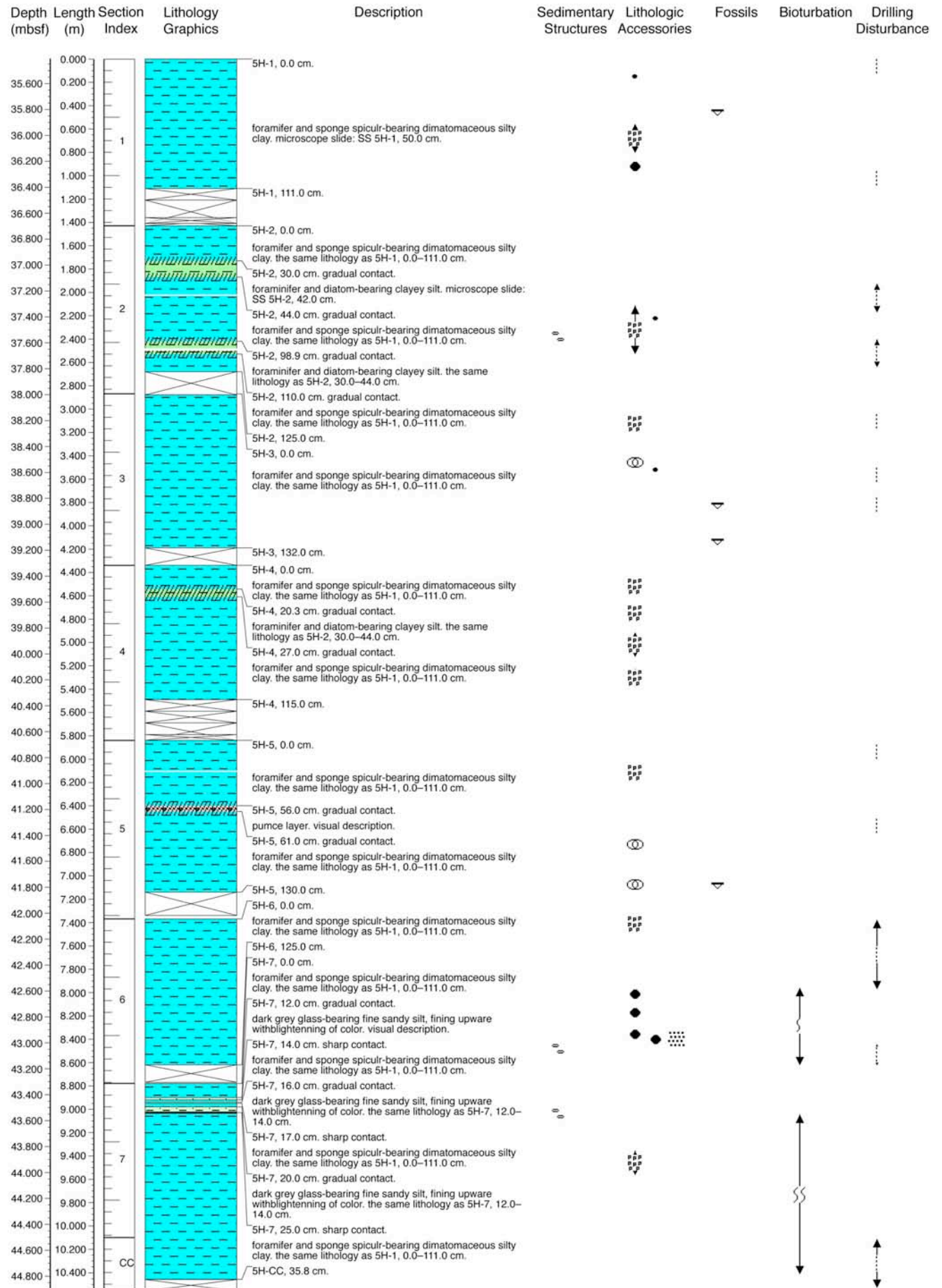
902-C9001C-3H (16.41–25.91 mbsf)

Depth (mbsf)	Length (m)	Section Index	Lithology Graphics	Description	Sedimentary Structures	Lithologic Accessories	Fossils	Bioturbation	Drilling Disturbance
0.000				3H-1, 0.0 cm.					
16.600	0.200								
16.800	0.400								
17.000	0.600			Silty clay. microscope slide: SS 3H-1, 50.0 cm.					
17.200	0.800	1							
17.400	1.000			3H-1, 105.9 cm.					
17.600	1.200								
17.800	1.400			3H-2, 0.0 cm.					
18.000	1.600			Silty clay. the same lithology as 3H-1, 0.0–105.9 cm.					
18.200	1.800			3H-2, 36.0 cm.					
18.400	2.000	2							
18.600	2.200								
18.800	2.400								
19.000	2.600								
19.200	2.800			3H-3, 0.0 cm.					
19.400	3.000			Silty clay. the same lithology as 3H-1, 0.0–105.9 cm.					
19.600	3.200			3H-3, 52.0 cm.					
19.800	3.400	3		vitric ash. microscope slide: SS 3H-3, 55.0 cm.					
20.000	3.600			3H-3, 58.0 cm.					
20.200	3.800			Silty clay. the same lithology as 3H-1, 0.0–105.9 cm.					
20.400	4.000			3H-3, 111.0 cm.					
20.600	4.200								
20.800	4.400			3H-4, 0.0 cm.					
21.000	4.600			Silty clay. the same lithology as 3H-1, 0.0–105.9 cm.					
21.200	4.800	4							
21.400	5.000			3H-4, 101.0 cm.					
21.600	5.200								
21.800	5.400								
22.000	5.600			3H-5, 0.0 cm.					
22.200	5.800								
22.400	6.000			Silty clay. the same lithology as 3H-1, 0.0–105.9 cm.					
22.600	6.200	5							
22.800	6.400			3H-5, 111.0 cm.					
23.000	6.600			3H-6, 0.0 cm.					
23.200	6.800			Silty clay. the same lithology as 3H-1, 0.0–105.9 cm.					
23.400	7.000			3H-6, 91.0 cm.					
23.600	7.200			3H-7, 0.0 cm.					
23.800	7.400			Silty clay. the same lithology as 3H-1, 0.0–105.9 cm.					
24.000	7.600			3H-7, 18.8 cm. gradual contact.					
24.200	7.800			dark gray vitric ash. visual description.					
24.400	8.000			3H-7, 25.2 cm. wavy contact.					
24.600	8.200	6		Silty clay. the same lithology as 3H-1, 0.0–105.9 cm.					
24.800	8.400			3H-7, 27.5 cm. wavy contact.					
25.000	8.600			dark gray vitric ash with light gray coarse pumice and gray coarse pumice layer in the middle of layer. visual description.					
25.200	8.800			3H-7, 31.0 cm.					
25.400	9.000			light gray vitric ash with pumiceous bottom layer. visual description. bottom 8s garish and coarse pumice grain rich					
25.600	9.200			3H-7, 35.6 cm. wavy contact.					
25.800	9.400			Silty clay. the same lithology as 3H-1, 0.0–105.9 cm.					
26.000	9.600			3H-7, 38.4 cm. gradual contact.					
26.200	9.800	7		dark gray ash lay. visual description. 41-42cm, bottom; coarse pumice, glass. 40-41cm; fine vitric ash. 39.5-40cm; mixture of ash and silty clay. 38.5-39.5 gray vitric very fine ash.					
26.400	10.000			3H-7, 42.3 cm. wavy contact.					
26.600	10.200			Silty clay. the same lithology as 3H-1, 0.0–105.9 cm.					
26.800	10.400			3H-CC, 20.0 cm.					

902-C9001C-4H (25.91–35.41 mbsf)

Depth (mbsf)	Length (m)	Section Index	Lithology Graphics	Description	Sedimentary Structures	Lithologic Accessories	Fossils	Bioturbation	Drilling Disturbance
26.000	0.000			4H-1, 5.0 cm.					
26.200	0.200								
26.400	0.400								
26.600	0.600			foraminifer-bearing diatomaceous silty clay. microscope slide: SS 4H-1, 60.0 cm.					
26.800	0.800	1							
27.000	1.000			4H-1, 117.6 cm.					
27.200	1.200			4H-2, 0.0 cm.					
27.400	1.400			foraminifer-bearing diatomaceous silty clay. microscope slide: SS 4H-2, 60.0 cm.					
27.600	1.600			4H-2, 16.0 cm.					
27.800	1.800			lithic grain rich sandy silt. microscope slide: SS 4H-2, 16.5 cm.					
28.000	2.000	2		4H-2, 17.0 cm.					
28.200	2.200			foraminifer-bearing diatomaceous silty clay. the same lithology as 4H-2, 0.0–16.0 cm.					
28.400	2.400			4H-2, 112.0 cm.					
28.600	2.600			4H-3, 0.0 cm.					
28.800	2.800			foraminifer-bearing diatomaceous silty clay. the same lithology as 4H-2, 0.0–16.0 cm.					
29.000	3.000	3		4H-3, 49.7 cm.					
29.200	3.200			glauconite-bearing pumiceous sandy sily. microscope slide: SS 4H-3, 50.0 cm.					
29.400	3.400			4H-3, 52.7 cm. original layer might be disturbed by gas expansion during drill-hole on cat walk					
29.600	3.600			foraminifer-bearing diatomaceous silty clay. the same lithology as 4H-2, 0.0–16.0 cm.					
29.800	3.800			4H-3, 118.9 cm.					
30.000	4.000			4H-4, 0.0 cm.					
30.200	4.200			foraminifer-bearing diatomaceous silty clay. the same lithology as 4H-2, 0.0–16.0 cm.					
30.400	4.400	4		4H-4, 38.0 cm.					
30.600	4.600			dark gray sandy-silt-bearing pumiceous ash, inclined. visual description.					
30.800	4.800			4H-4, 43.0 cm.					
31.000	5.000			foraminifer-bearing diatomaceous silty clay. the same lithology as 4H-2, 0.0–16.0 cm.					
31.200	5.200			4H-4, 57.0 cm. sharp contact.					
31.400	5.400			light gray granule to pebble sized pumice. visual description.					
31.600	5.600			4H-4, 61.0 cm. gradual contact.					
31.800	5.800			light gray very fine to silt vitric ash. microscope slide: SS 4H-4, 66.0 cm.					
32.000	6.000	5		4H-4, 68.0 cm. wavy contact.					
32.200	6.200			foraminifer-bearing diatomaceous silty clay. the same lithology as 4H-2, 0.0–16.0 cm.					
32.400	6.400			4H-4, 112.4 cm.					
32.600	6.600	6		4H-5, 0.0 cm.					
32.800	6.800			foraminifer-bearing diatomaceous silty clay. the same lithology as 4H-2, 0.0–16.0 cm.					
33.000	7.000			4H-5, 116.7 cm.					
33.200	7.200			4H-6, 0.0 cm.					
33.400	7.400			foraminifer-bearing diatomaceous silty clay. the same lithology as 4H-2, 0.0–16.0 cm.					
33.600	7.600			4H-6, 102.0 cm.					
33.800	7.800			4H-7, 0.0 cm.					
34.000	8.000	7		foraminifer-bearing diatomaceous silty clay. the same lithology as 4H-2, 0.0–16.0 cm.					
34.200	8.200			4H-7, 143.1 cm.					
34.400	8.400			4H-7, 154.6 cm.					
34.600	8.600			foraminifer-bearing diatomaceous silty clay. the same lithology as 4H-2, 0.0–16.0 cm.					
34.800	8.800			4H-CC, 16.0 cm.					
35.000	9.000			dark gray silty ash. visual description.					
35.200	9.200			4H-CC, 18.3 cm. wavy contact.					
35.400	9.400			foraminifer-bearing diatomaceous silty clay. the same lithology as 4H-2, 0.0–16.0 cm.					
35.600	9.600			4H-CC, 24.0 cm.					
35.800	9.800								
36.000	10.000								
36.200	10.200								
36.400	10.400								
36.600	10.600								

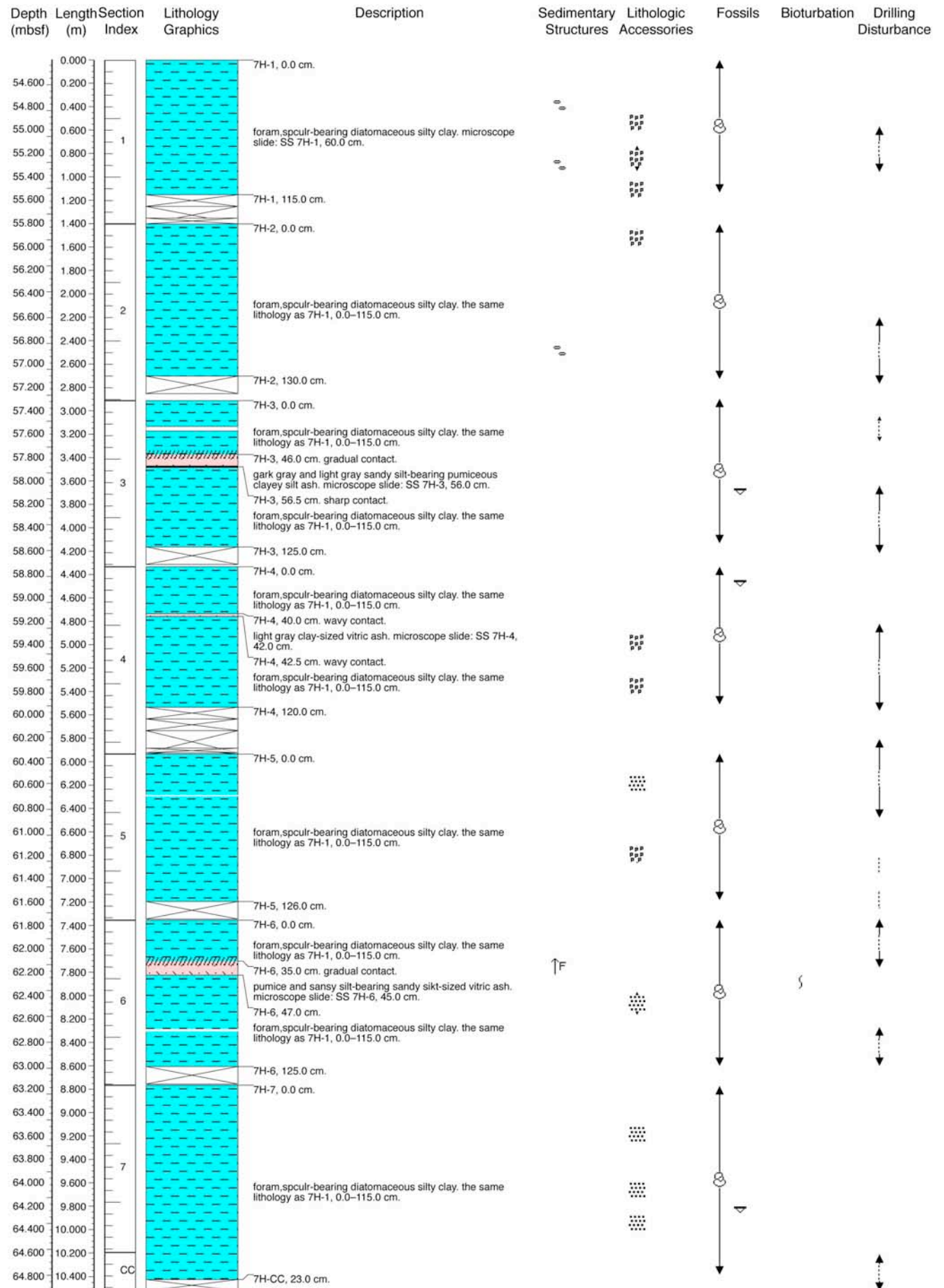
902-C9001C-5H (35.41–44.91 mbsf)



902-C9001C-6H (44.91–54.41 mbsf)

Depth (mbsf)	Length (m)	Section Index	Lithology Graphics	Description	Sedimentary Structures	Lithologic Accessories	Fossils	Bioturbation	Drilling Disturbance
45.000	0.000			6H-1, 0.0 cm.					
45.200	0.200			foram, nanno, calcareous spicule-bearing diatomaceous silty clay. microscope slide: SS 6H-1, 60.0 cm.					
45.400	0.400			6H-1, 13.5 cm.					
45.600	0.600			glass, pumice, scoria-bearing silt. microscope slide: SS 6H-1, 14.0 cm.					
45.800	0.800	1		6H-1, 14.5 cm.					
46.000	1.000			foram, nanno, calcareous spicule-bearing diatomaceous silty clay. the same lithology as 6H-1, 0.0–13.5 cm.					
46.200	1.200			6H-1, 24.0 cm. gradual contact.					
46.400	1.400			foram, diatom, spicule, and framboidal pyrite-bearing clay-sized volcanic ash. microscope slide: SS 6H-1, 31.0 cm.					
46.600	1.600			6H-1, 33.0 cm.					
46.800	1.800			foram, nanno, calcareous spicule-bearing diatomaceous silty clay. microscope slide: SS 6H-1, 60.0 cm.					
47.000	2.000	2		6H-1, 105.0 cm.					
47.200	2.200			6H-2, 0.0 cm.					
47.400	2.400			foram, nanno, calcareous spicule-bearing diatomaceous silty clay. the same lithology as 6H-1, 33.0–105.0 cm.					
47.600	2.600			6H-2, 52.0 cm. gradual contact.					
47.800	2.800			glass-bearing calcareous silty clay. microscope slide: SS 6H-2, 53.0 cm.					
48.000	3.000			6H-2, 54.0 cm. gradual contact.					
48.200	3.200			foram, nanno, calcareous spicule-bearing diatomaceous silty clay. the same lithology as 6H-1, 33.0–105.0 cm.					
48.400	3.400			6H-2, 94.0 cm. wavy contact.					
48.600	3.600			bioturbated dark grey silty sand. visual description.					
48.800	3.800			6H-2, 101.1 cm. wavy contact.					
49.000	4.000	3		foram, nanno, calcareous spicule-bearing diatomaceous silty clay. the same lithology as 6H-1, 33.0–105.0 cm.					
49.200	4.200			6H-2, 115.0 cm.					
49.400	4.400			6H-2, 139.8 cm.					
49.600	4.600			gray coarse pumice. visual description.					
49.800	4.800			6H-3, 9.0 cm. wavy contact.					
50.000	5.000			foram, nanno, calcareous spicule-bearing diatomaceous silty clay. the same lithology as 6H-1, 33.0–105.0 cm.					
50.200	5.200			6H-3, 30.0 cm. wavy contact.					
50.400	5.400			gray coarse pumice. the same lithology as 6H-2, 139.8–6H-3, 9.0 cm.					
50.600	5.600			6H-3, 36.0 cm. wavy contact.					
50.800	5.800			foram, nanno, calcareous spicule-bearing diatomaceous silty clay. the same lithology as 6H-1, 33.0–105.0 cm.					
51.000	6.000	4		6H-3, 39.8 cm.					
51.200	6.200			6H-4, 0.0 cm.					
51.400	6.400			rich foram-bearing diatomaceous silty clay. microscope slide: SS 6H-4, 58.0 cm.					
51.600	6.600			6H-4, 121.0 cm.					
51.800	6.800			6H-5, 0.0 cm.					
52.000	7.000			rich foram-bearing diatomaceous silty clay. the same lithology as 6H-4, 0.0–121.0 cm.					
52.200	7.200			6H-5, 121.0 cm.					
52.400	7.400			6H-6, 0.0 cm.					
52.600	7.600			rich foram-bearing diatomaceous silty clay. the same lithology as 6H-4, 0.0–121.0 cm.					
52.800	7.800	6		6H-6, 118.1 cm.					
53.000	8.000			6H-7, 0.0 cm.					
53.200	8.200			rich foram-bearing diatomaceous silty clay. the same lithology as 6H-4, 0.0–121.0 cm.					
53.400	8.400			6H-CC, 30.0 cm.					
53.600	8.600			6H-CC, 33.7 cm.					
53.800	8.800			ash. visual description. ash were recovered in pALS sample in CC					
54.000	9.000	7		6H-CC, 36.0 cm.					
54.200	9.200								
54.400	9.400	CC							

902-C9001C-7H (54.41–63.91 mbsf)



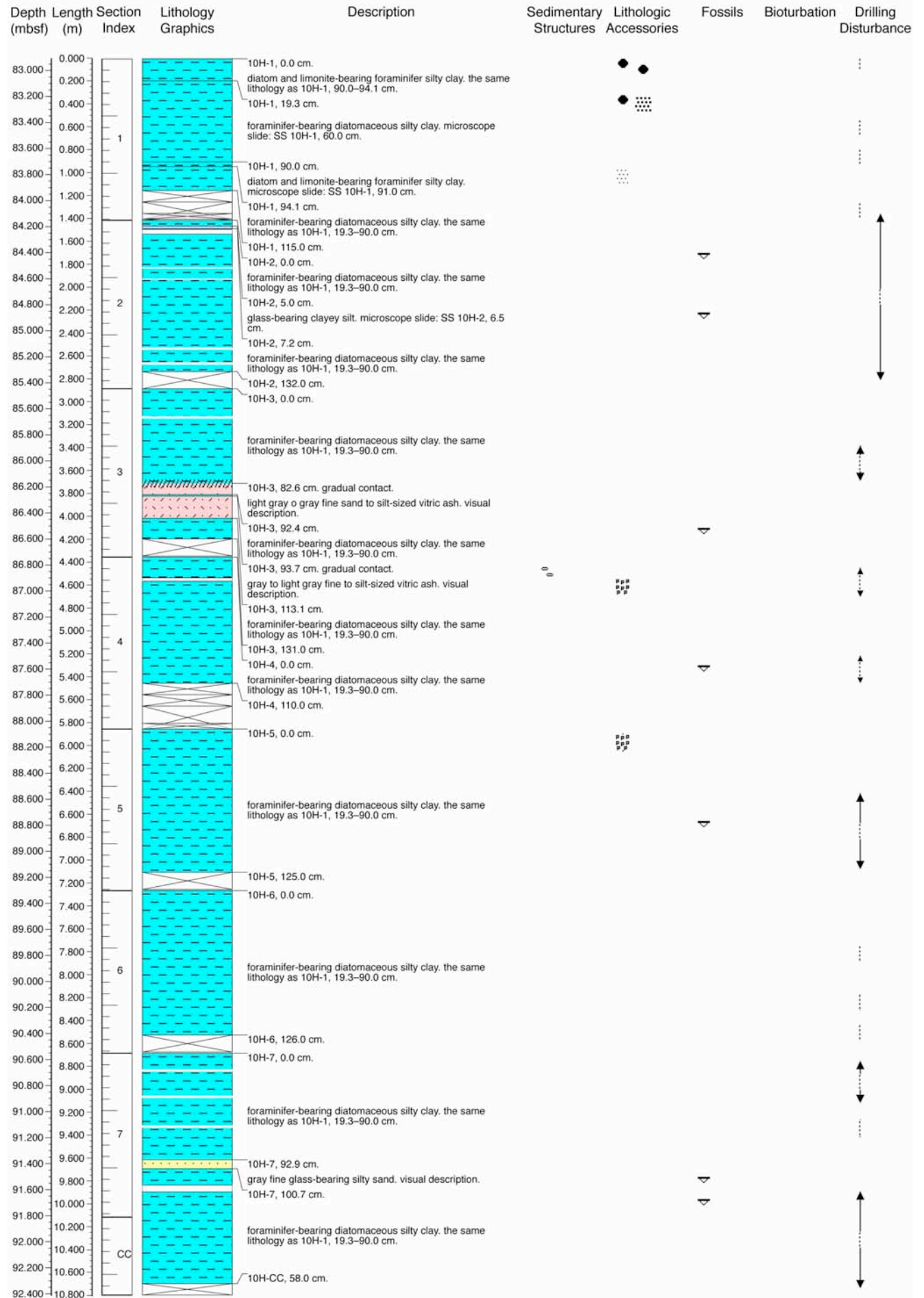
902-C9001C-8H (63.91–73.41 mbsf)

Depth (mbsf)	Length (m)	Section Index	Lithology Graphics	Description	Sedimentary Structures	Lithologic Accessories	Fossils	Bioturbation	Drilling Disturbance
64.000	0.000			8H-1, 0.0 cm.					
64.200	0.200								
64.400	0.400								
64.600	0.600			foram, spculr-bearing diatomaceous silty clay. the same lithology as 7H-1, 0.0–115.0 cm.					
64.800	0.800	1							
65.000	1.000								
65.200	1.200			8H-1, 121.0 cm.					
65.400	1.400			8H-2, 0.0 cm.					
65.600	1.600								
65.800	1.800								
66.000	2.000	2		foram, spculr-bearing diatomaceous silty clay. the same lithology as 7H-1, 0.0–115.0 cm.					
66.200	2.200								
66.400	2.400								
66.600	2.600			8H-2, 128.0 cm.					
66.800	2.800			8H-3, 0.0 cm.					
67.000	3.000								
67.200	3.200								
67.400	3.400	3		foram, spculr-bearing diatomaceous silty clay. the same lithology as 7H-1, 0.0–115.0 cm.					
67.600	3.600								
67.800	3.800								
68.000	4.000			8H-3, 126.0 cm.					
68.200	4.200			8H-4, 0.0 cm.					
68.400	4.400								
68.600	4.600								
68.800	4.800	4		foram, spculr-bearing diatomaceous silty clay. the same lithology as 7H-1, 0.0–115.0 cm.					
69.000	5.000								
69.200	5.200								
69.400	5.400			8H-4, 106.0 cm.					
69.600	5.600								
69.800	5.800			8H-5, 0.0 cm.					
70.000	6.000								
70.200	6.200	5		foram, spculr-bearing diatomaceous silty clay. the same lithology as 7H-1, 0.0–115.0 cm.					
70.400	6.400								
70.600	6.600			8H-5, 125.0 cm.					
70.800	6.800			8H-6, 0.0 cm.					
71.000	7.000			foram, spculr-bearing diatomaceous silty clay. the same lithology as 7H-1, 0.0–115.0 cm.					
71.200	7.200			8H-6, 129.0 cm.					
71.400	7.400			8H-7, 0.0 cm.					
71.600	7.600			foram, spculr-bearing diatomaceous silty clay. the same lithology as 7H-1, 0.0–115.0 cm.					
71.800	7.800	6		8H-7, 118.0 cm.					
72.000	8.000			dark grey and light gray coarse pimiceous sand. visual description.					
72.200	8.200			8H-7, 120.0 cm.					
72.400	8.400			foram, spculr-bearing diatomaceous silty clay. the same lithology as 7H-1, 0.0–115.0 cm.					
72.600	8.600			8H-7, 127.0 cm. gradual contact.					
72.800	8.800			dark gray silt. visual description.					
73.000	9.000			8H-7, 129.0 cm.					
73.200	9.200			foram, spculr-bearing diatomaceous silty clay. the same lithology as 7H-1, 0.0–115.0 cm.					
73.400	9.400	7		8H-7, 135.0 cm. gradual contact.					
73.600	9.600			dark olive gray silty clay-sized vitric ash. visual description.					
73.800	9.800			8H-7, 138.0 cm. gradual contact.					
74.000	10.000			foram, spculr-bearing diatomaceous silty clay. the same lithology as 7H-1, 0.0–115.0 cm.					
74.200	10.200			8H-CC, 0.0 cm.					
74.400	10.400			light gray sil-sized vitric ash. visual description.					
74.600	10.600			8H-CC, 11.0 cm.					
74.800	10.800			foram, spculr-bearing diatomaceous silty clay. the same lithology as 7H-1, 0.0–115.0 cm.					
75.000	11.000	CC		8H-CC, 24.0 cm.					

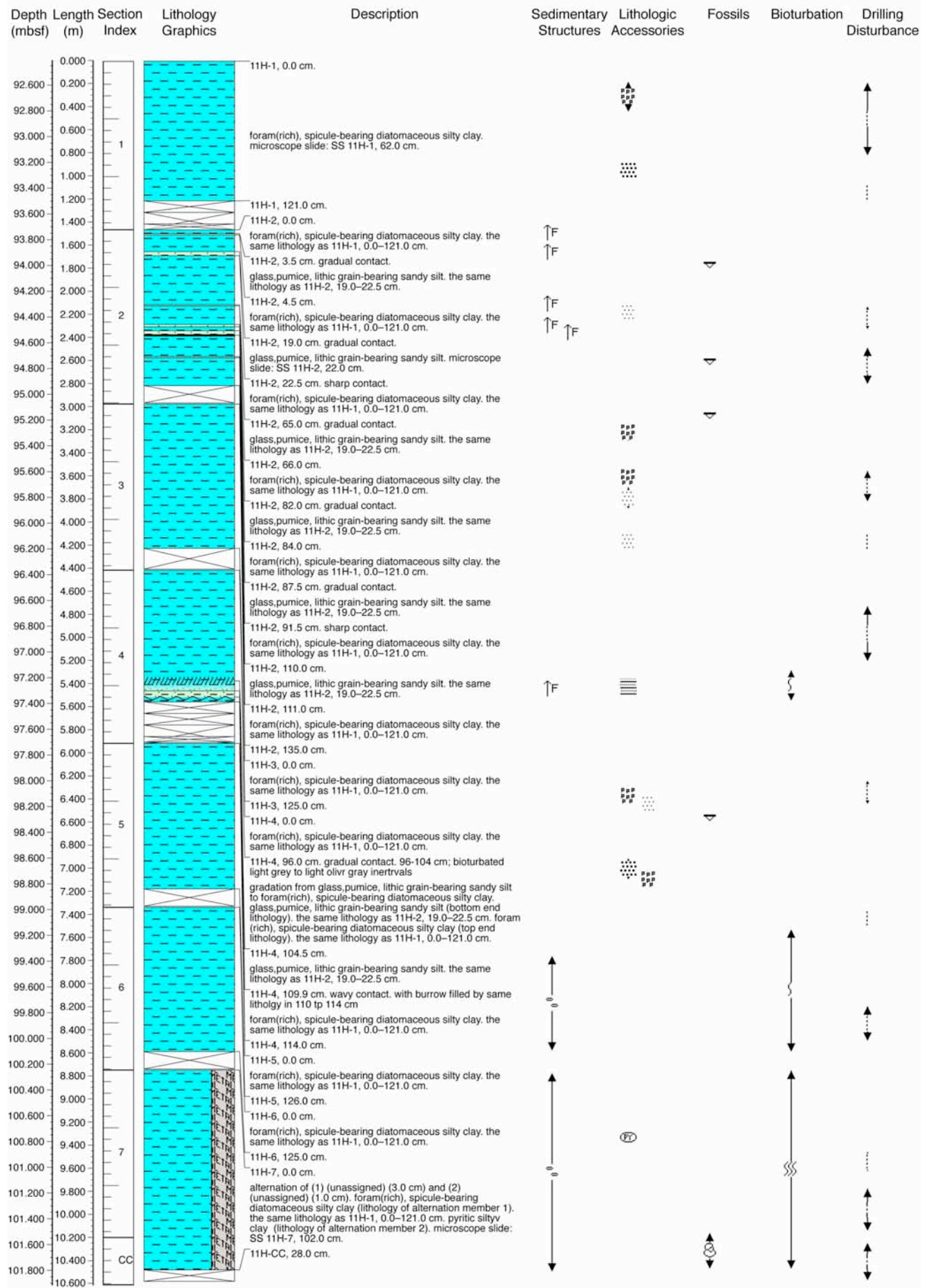
902-C9001C-9H (73.41–82.91 mbsf)

Depth (mbsf)	Length (m)	Section Index	Lithology Graphics	Description	Sedimentary Structures	Lithologic Accessories	Fossils	Bioturbation	Drilling Disturbance
0.000				9H-1, 0.0 cm.					
73.600	0.200			foram, nanno, spicule -bearing diatomaceous silty clay. microscope slide: SS 9H-1, 60.0 cm.					
73.800	0.400			9H-1, 44.4 cm. gradual contact.	↑F	PPP			
74.000	0.600			glass-bearing silty sand. microscope slide: SS 9H-1, 46.0 cm.					
74.200	0.800	1		9H-1, 47.6 cm.					
74.400	1.000			foram, nanno, spicule -bearing diatomaceous silty clay. the same lithology as 9H-1, 0.0–44.4 cm.					
74.600	1.200			9H-1, 115.0 cm.					
74.800	1.400			9H-2, 0.0 cm.					
75.000	1.600			foram, nanno, spicule -bearing diatomaceous silty clay. the same lithology as 9H-1, 0.0–44.4 cm.					
75.200	1.800			9H-2, 14.0 cm.	↑F				
75.400	2.000	2		glassand pumice-bearing silt. microscope slide: SS 9H-2, 16.0 cm.					
75.600	2.200			9H-2, 17.0 cm.	↑F				
75.800	2.400			foram, nanno, spicule -bearing diatomaceous silty clay. the same lithology as 9H-1, 0.0–44.4 cm.					
76.000	2.600			9H-2, 61.5 cm. wavy contact.					
76.200	2.800			glass-bearing silty sand. microscope slide: SS 9H-2, 64.5 cm.					
76.400	3.000			9H-2, 67.5 cm. wavy contact.					
76.600	3.200			foram, nanno, spicule -bearing diatomaceous silty clay. the same lithology as 9H-1, 0.0–44.4 cm.					
76.800	3.400			9H-2, 85.0 cm. sharp contact.					
77.000	3.600	3		silt-bearing silt-sized pumiceous ash. microscope slide: SS 9H-2, 86.0 cm.					
77.200	3.800			9H-2, 89.0 cm. sharp contact.					
77.400	4.000			foram, nanno, spicule -bearing diatomaceous silty clay. the same lithology as 9H-1, 0.0–44.4 cm.					
77.600	4.200			9H-3, 0.0 cm.					
77.800	4.400			foram, nanno, spicule -bearing diatomaceous silty clay. the same lithology as 9H-1, 0.0–44.4 cm.					
78.000	4.600			9H-3, 125.0 cm.					
78.200	4.800			9H-4, 0.0 cm.					
78.400	5.000	4		foram, nanno, spicule -bearing diatomaceous silty clay. the same lithology as 9H-1, 0.0–44.4 cm.					
78.600	5.200			9H-4, 109.0 cm.					
78.800	5.400			9H-5, 0.0 cm.					
79.000	5.600								
79.200	5.800								
79.400	6.000	5		foram, nanno, spicule -bearing diatomaceous silty clay. the same lithology as 9H-1, 0.0–44.4 cm.					
79.600	6.200								
79.800	6.400								
80.000	6.600			9H-5, 126.0 cm.					
80.200	6.800			9H-6, 0.0 cm.					
80.400	7.000								
80.600	7.200	6		foram, nanno, spicule -bearing diatomaceous silty clay. the same lithology as 9H-1, 0.0–44.4 cm.					
80.800	7.400								
81.000	7.600								
81.200	7.800			9H-6, 126.0 cm.					
81.400	8.000			9H-7, 0.0 cm.					
81.600	8.200	7							
81.800	8.400								
82.000	8.600			foram, nanno, spicule -bearing diatomaceous silty clay. the same lithology as 9H-1, 0.0–44.4 cm.					
82.200	8.800								
82.400	9.000								
82.600	9.200								
82.800	9.400								
83.000	9.600								
83.200	9.800								
83.400	10.000								
83.600	10.200	CC		9H-CC, 26.0 cm.					
83.800	10.400								

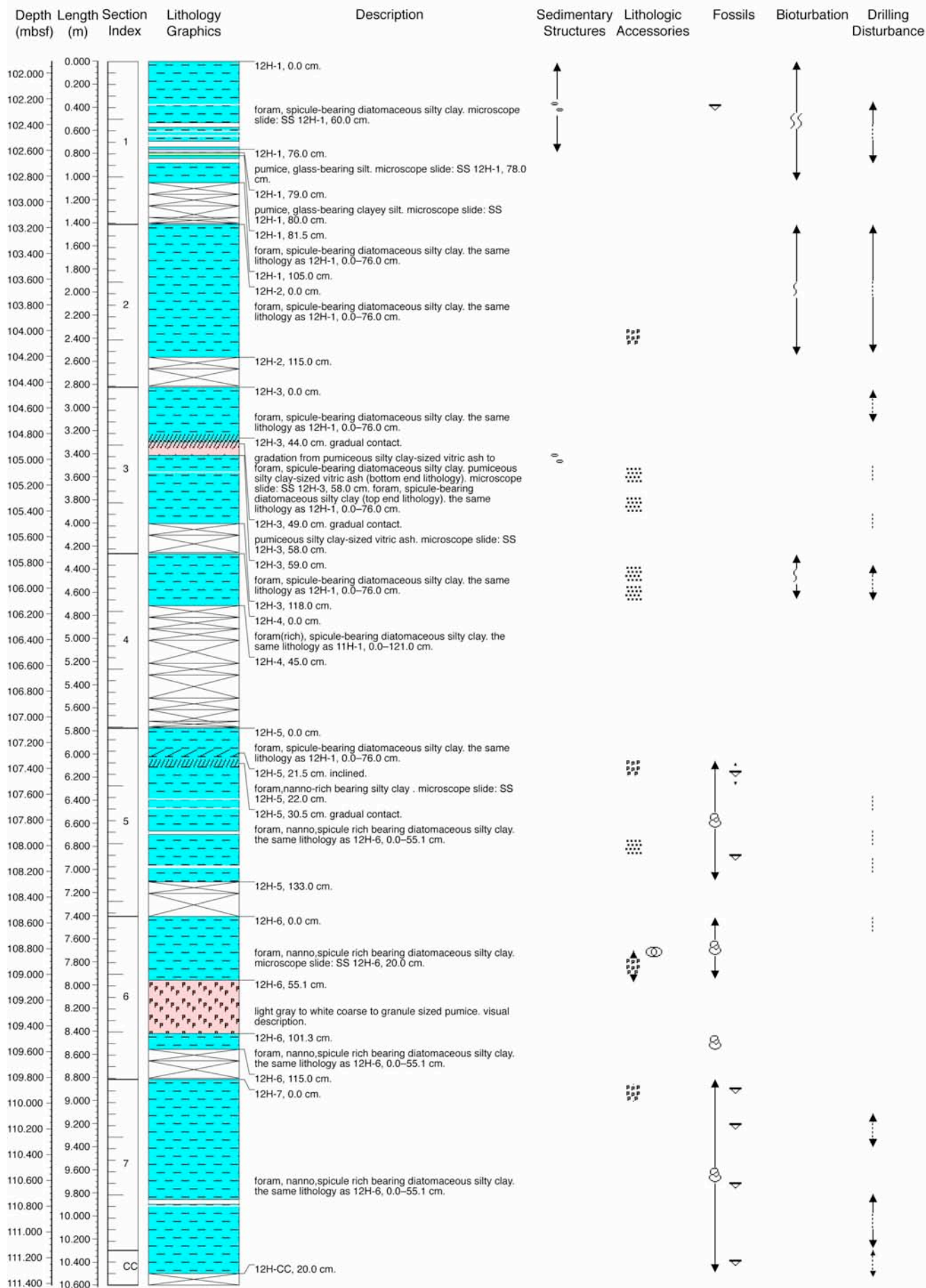
902-C9001C-10H (82.91–92.41 mbsf)



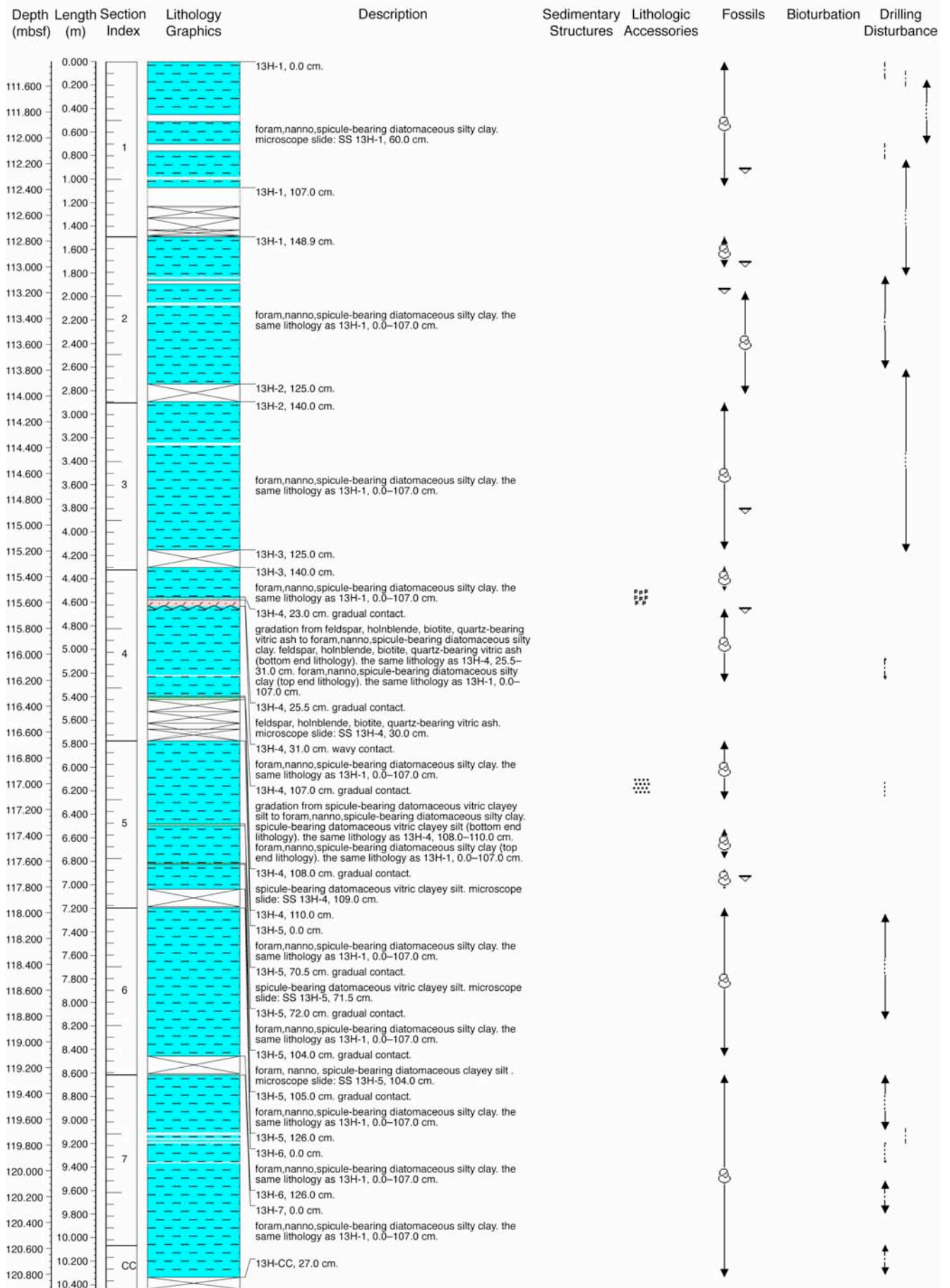
902-C9001C-11H (92.41–101.91 mbsf)



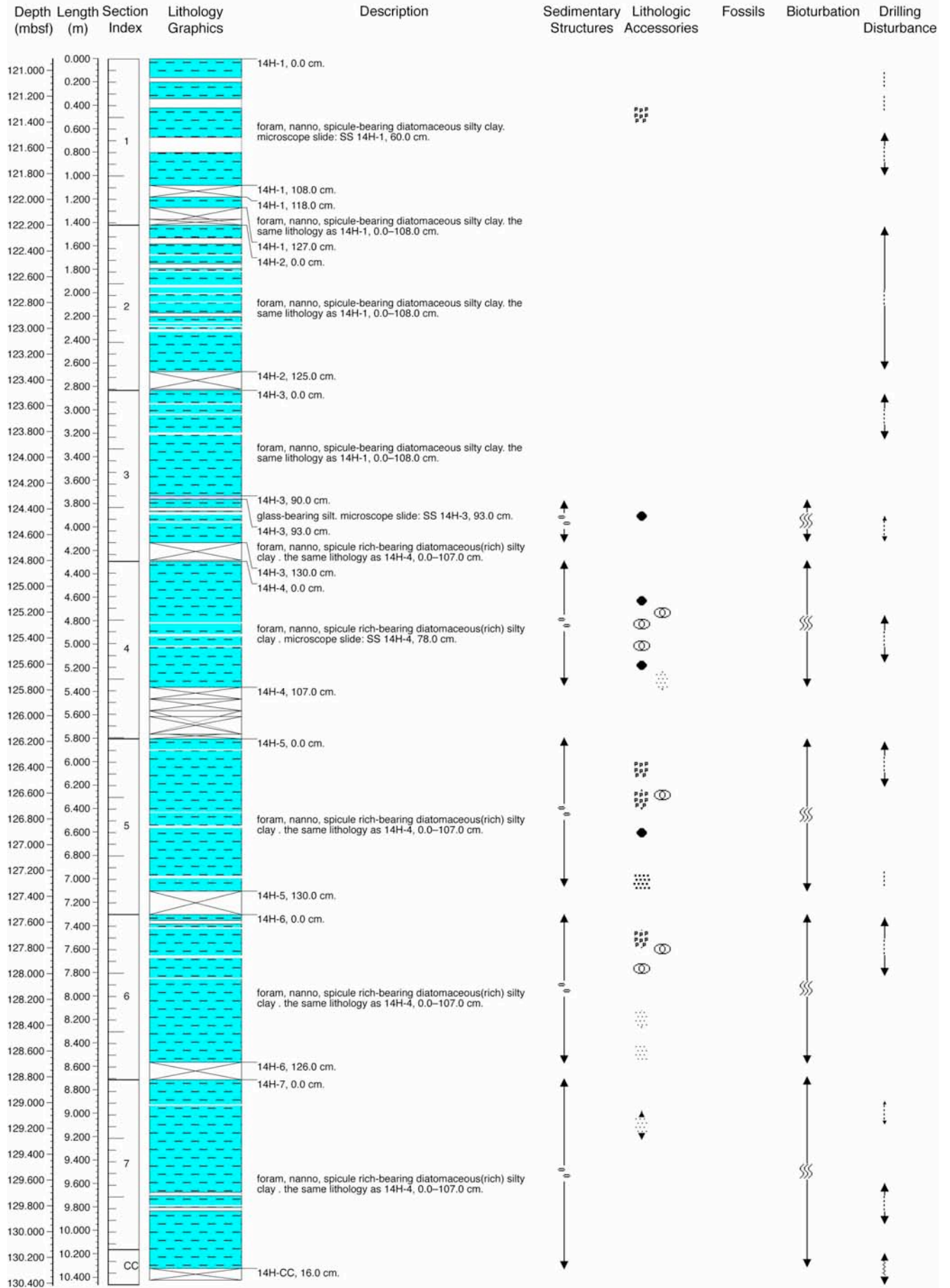
902-C9001C-12H (101.91–111.41 mbsf)



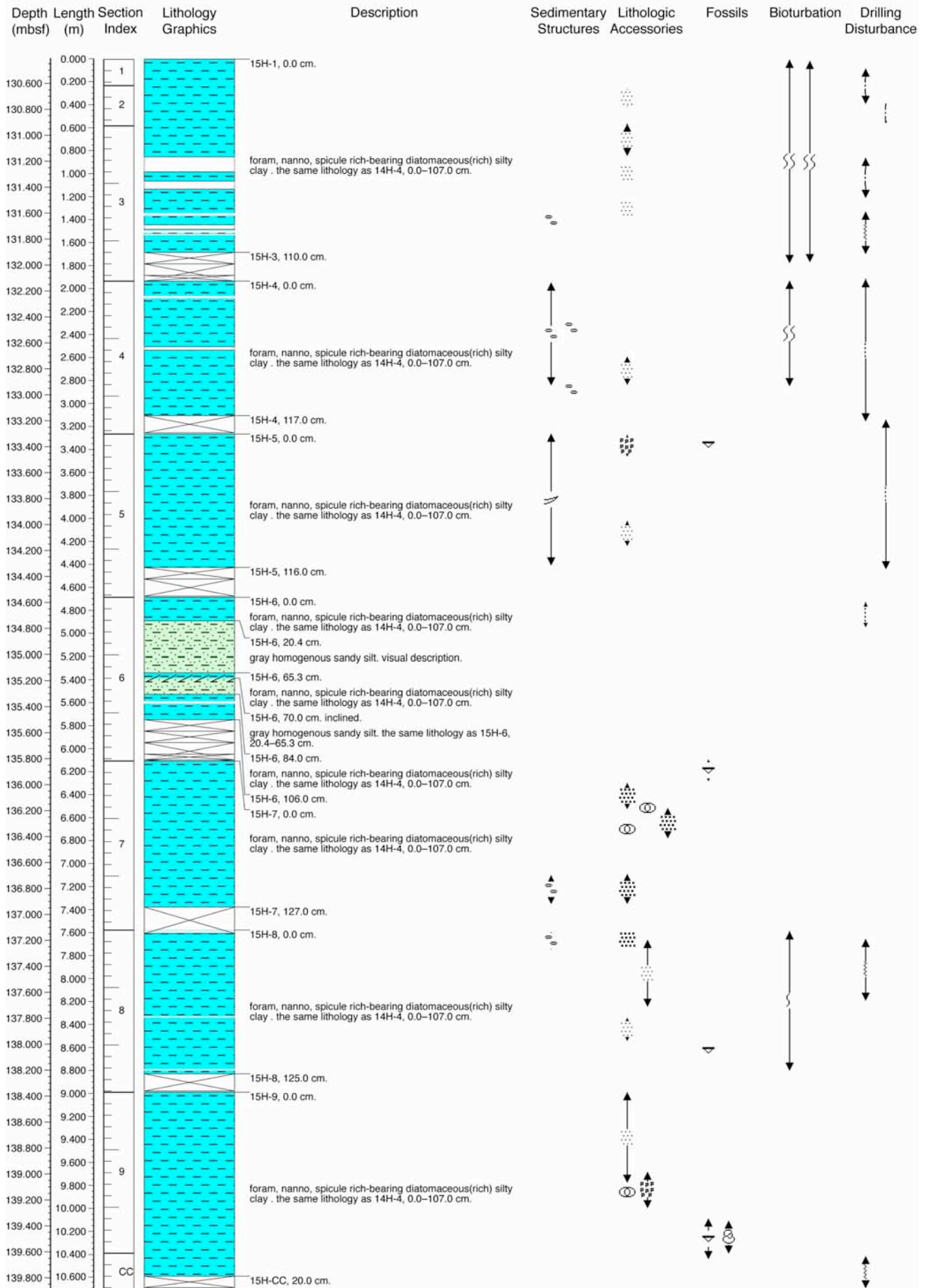
902-C9001C-13H (111.41–120.91 mbsf)



902-C9001C-14H (120.91–130.41 mbsf)



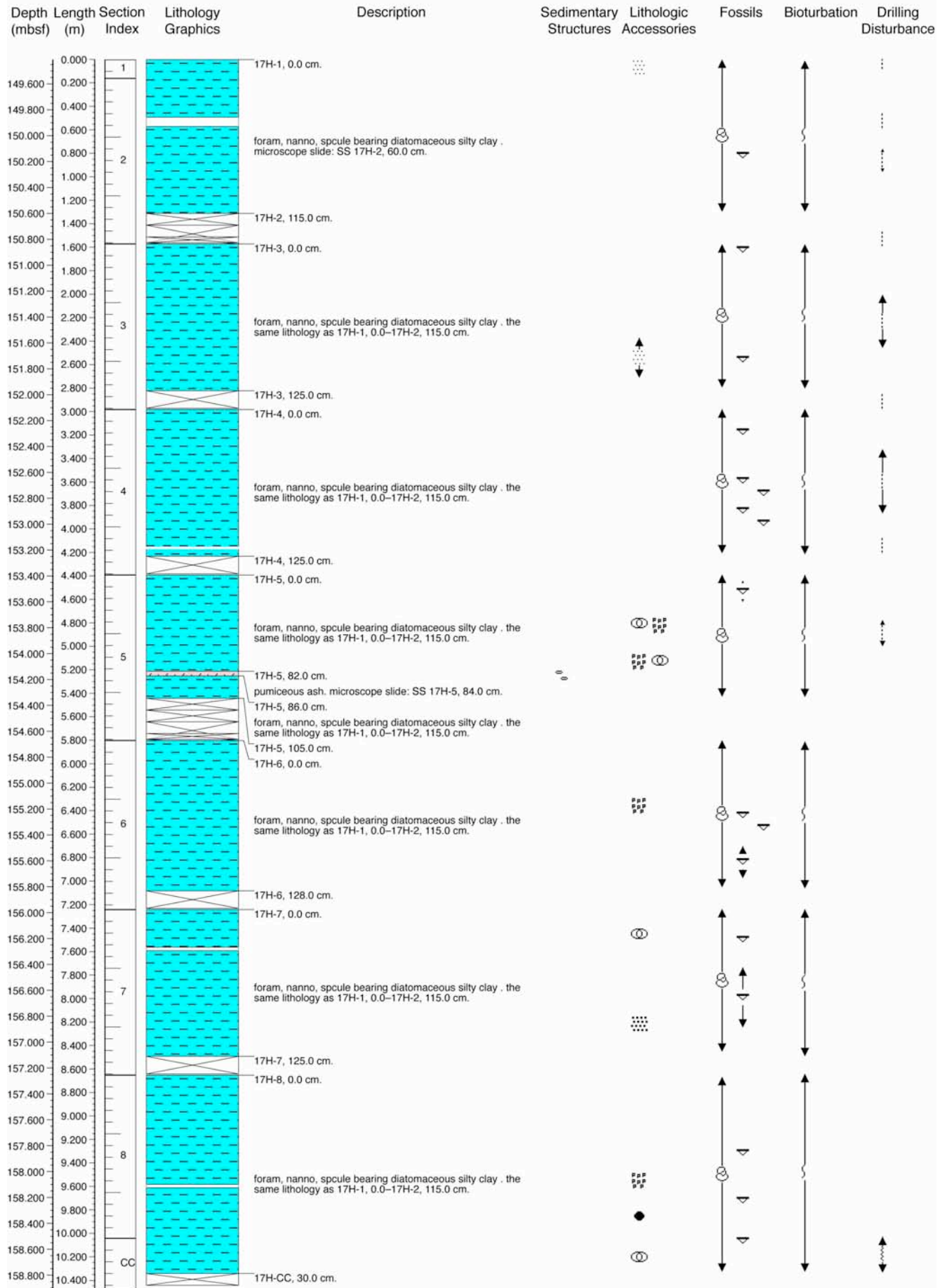
902-C9001C-15H (130.41–139.91 mbsf)



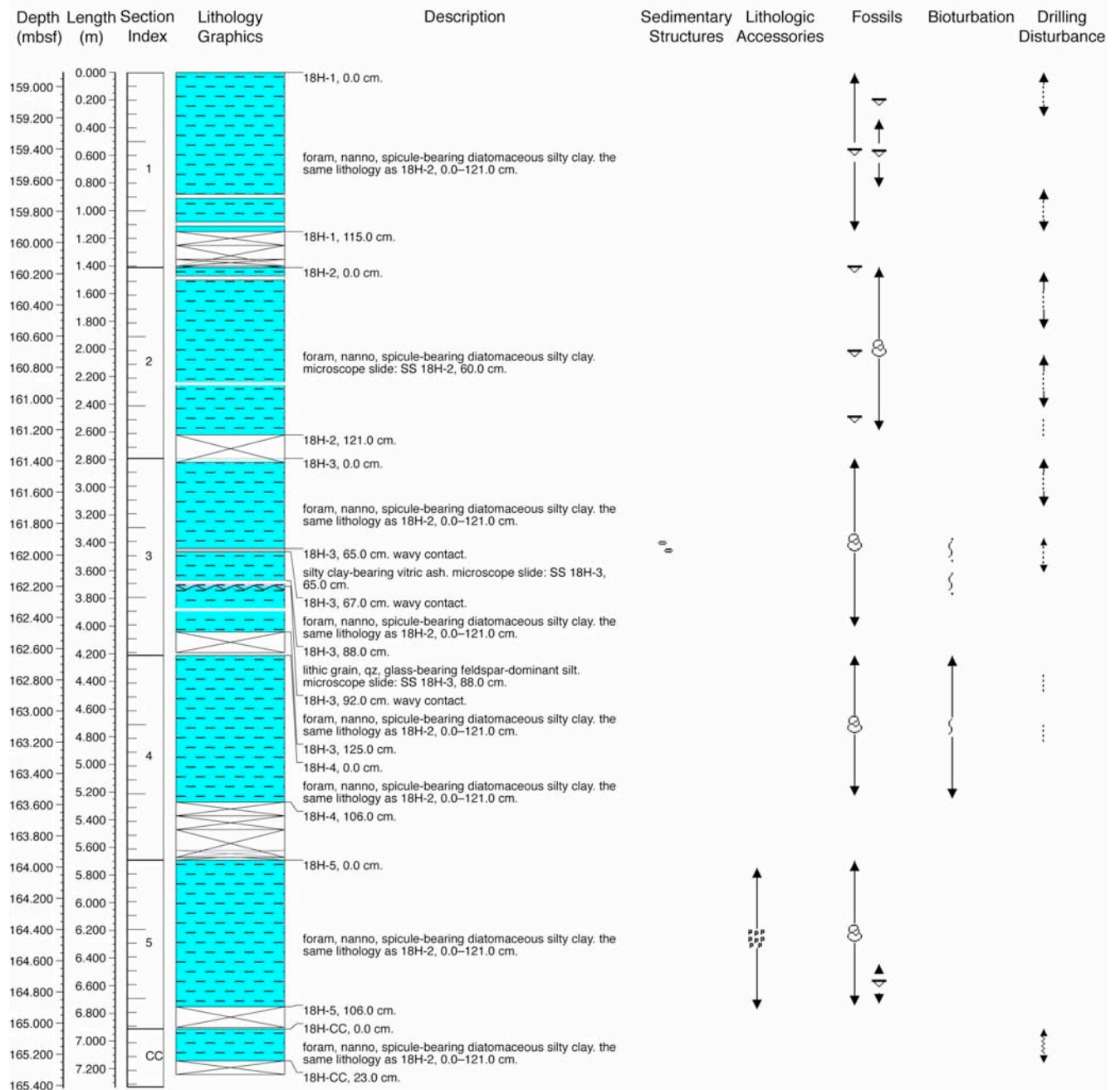
902-C9001C-16H (139.91–149.41 mbsf)

Depth (mbsf)	Length (m)	Section Index	Lithology Graphics	Description	Sedimentary Structures	Lithologic Accessories	Fossils	Bioturbation	Drilling Disturbance
140.000	0.000	1		16H-1, 0.0 cm.					
140.200	0.200								
140.400	0.400								
140.600	0.600								
140.800	0.800	2		nanno, foram, spicule-bearing diatomaceous silty clay. microscope slide: SS 16H-2, 65.0 cm.					
141.000	1.000								
141.200	1.200								
141.400	1.400								
141.600	1.600	3		16H-2, 115.0 cm.					
141.800	1.800			16H-2, 140.0 cm.					
142.000	2.000			nanno, foram, spicule-bearing diatomaceous silty clay, the same lithology as 16H-1, 0.0–16H-2, 115.0 cm.					
142.200	2.200			16H-3, 9.0 cm. gradual contact.					
142.400	2.400	4		feldspar, hornblende, rock fragment bearing vitric ash. microscope slide: SS 16H-3, 13.0 cm.					
142.600	2.600			16H-3, 15.0 cm. wavy contact.					
142.800	2.800			gradation from nanno, foram, spicule-bearing diatomaceous silty clay to feldspar, hornblende, rock fragment bearing vitric ash. nanno, foram, spicule-bearing diatomaceous silty clay (bottom end lithology), the same lithology as 16H-1, 0.0–16H-2, 115.0 cm. feldspar, hornblende, rock fragment bearing vitric ash (top end lithology), the same lithology as 16H-3, 9.0–15.0 cm.					
143.000	3.000			16H-3, 20.0 cm. gradual contact.					
143.200	3.200	5		nanno, foram, spicule-bearing diatomaceous silty clay, the same lithology as 16H-1, 0.0–16H-2, 115.0 cm.					
143.400	3.400			16H-3, 33.7 cm.					
143.600	3.600			foram, nanno, spicule, glass-bearing diatomaceous clayey silt. microscope slide: SS 16H-3, 36.0 cm.					
143.800	3.800			16H-3, 41.0 cm. gradual contact.					
144.000	4.000	6		foram, nanno, spicule-bearing diatomaceous silty clay. microscope slide: SS 16H-3, 58.0 cm.					
144.200	4.200			16H-3, 126.0 cm.					
144.400	4.400			16H-3, 140.6 cm.					
144.600	4.600			foram, nanno, spicule-bearing diatomaceous silty clay, the same lithology as 16H-3, 41.0–126.0 cm.					
144.800	4.800	7		16H-4, 35.0 cm.					
145.000	5.000			diatom-rich foram, nanno, spicule-bearing vitric clayey silt. microscope slide: SS 16H-4, 36.5 cm.					
145.200	5.200			16H-4, 38.0 cm.					
145.400	5.400			foram, nanno, spicule-bearing diatomaceous silty clay, the same lithology as 16H-3, 41.0–126.0 cm.					
145.600	5.600	8		16H-4, 135.0 cm.					
145.800	5.800			16H-5, 0.0 cm.					
146.000	6.000			foram, nanno, spicule-bearing diatomaceous silty clay, the same lithology as 16H-3, 41.0–126.0 cm.					
146.200	6.200			16H-5, 115.0 cm.					
146.400	6.400	9		16H-6, 0.0 cm.					
146.600	6.600			nanno, foram, spicule-bearing diatomaceous silty clay, the same lithology as 16H-1, 0.0–16H-2, 115.0 cm.					
146.800	6.800			16H-6, 60.0 cm. wavy contact.					
147.000	7.000			feldspar, hornblende, vitric. microscope slide: SS 16H-6, 68.0 cm.					
147.200	7.200	10		16H-6, 76.0 cm. gradual contact.					
147.400	7.400			nanno, foram, spicule-bearing diatomaceous silty clay, the same lithology as 16H-1, 0.0–16H-2, 115.0 cm.					
147.600	7.600			16H-6, 132.0 cm.					
147.800	7.800			16H-6, 152.1 cm.					
148.000	8.000	11		16H-7, 126.0 cm.					
148.200	8.200			16H-8, 0.0 cm.					
148.400	8.400			nanno, foram, spicule-bearing diatomaceous silty clay, the same lithology as 16H-1, 0.0–16H-2, 115.0 cm.					
148.600	8.600			16H-8, 52.1 cm. wavy contact.					
148.800	8.800	12		feldspar, hornblende. microscope slide: SS 16H-8, 53.0 cm.					
149.000	9.000			16H-8, 53.5 cm.					
149.200	9.200			nanno, foram, spicule-bearing diatomaceous silty clay, the same lithology as 16H-1, 0.0–16H-2, 115.0 cm.					
149.400	9.400								
149.600	9.600	CC		16H-CC, 20.0 cm.					
149.800	9.800								
150.000	10.000								
150.200	10.200								

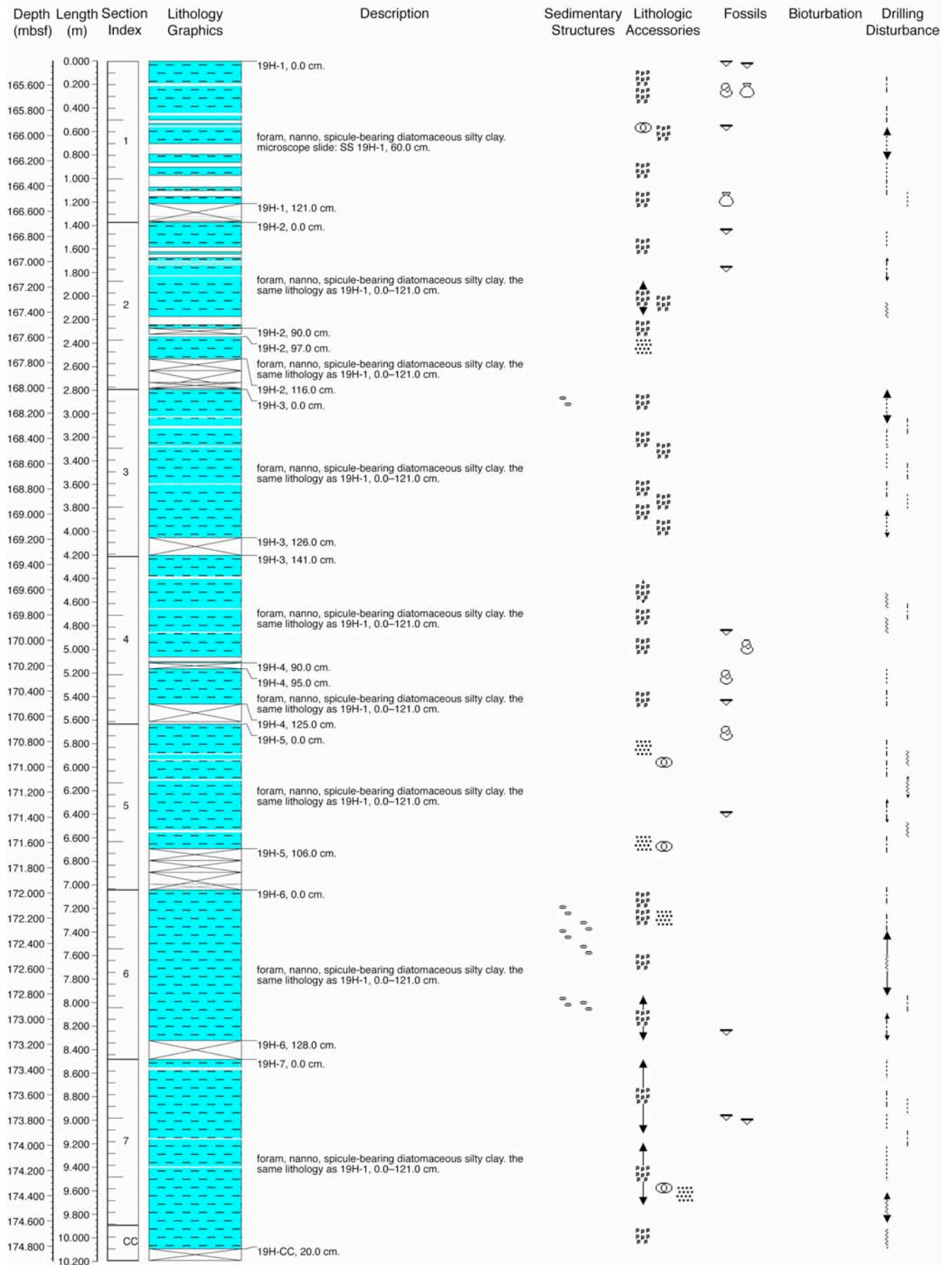
902-C9001C-17H (149.41–158.91 mbsf)



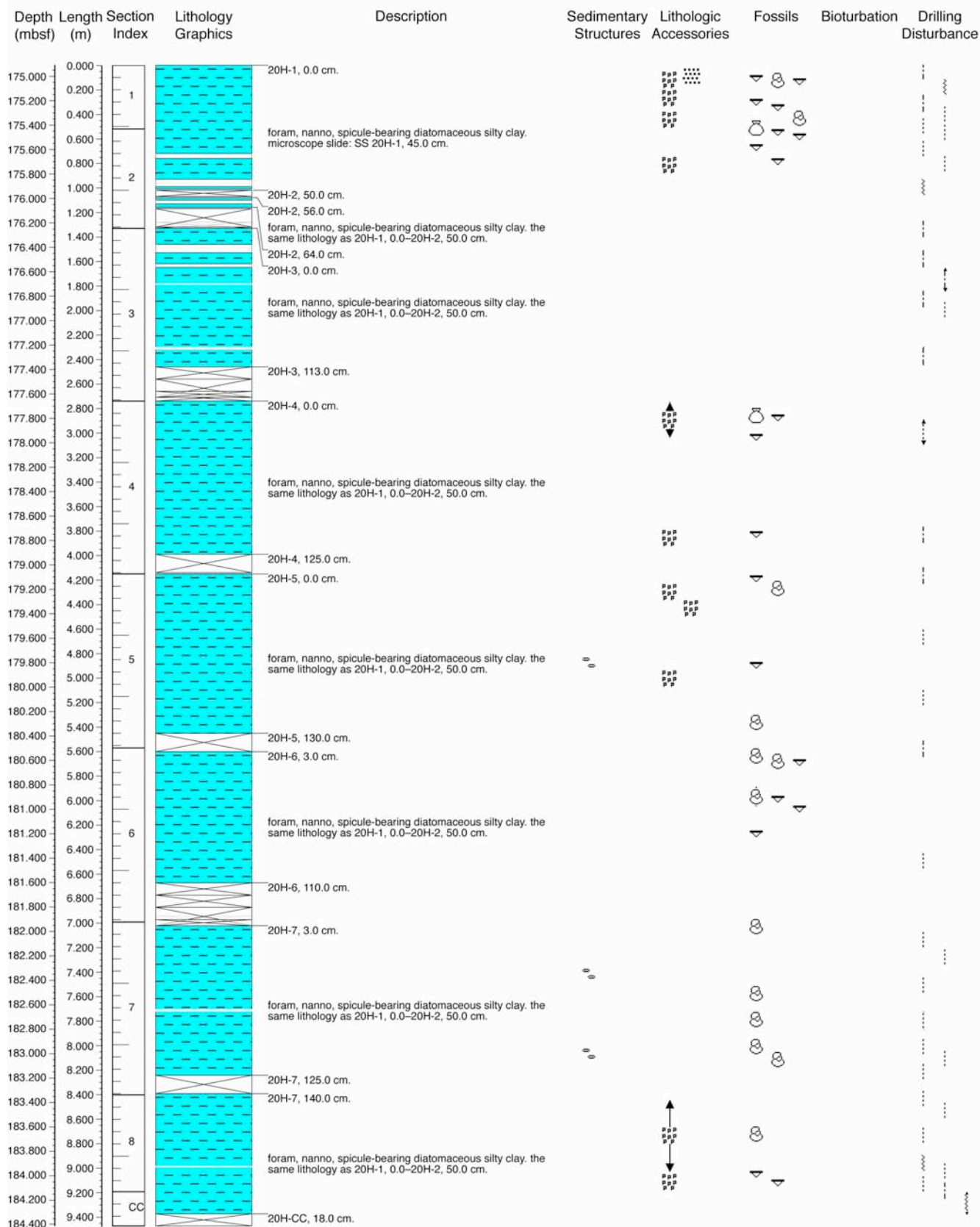
902-C9001C-18H (158.91–165.41 mbsf)



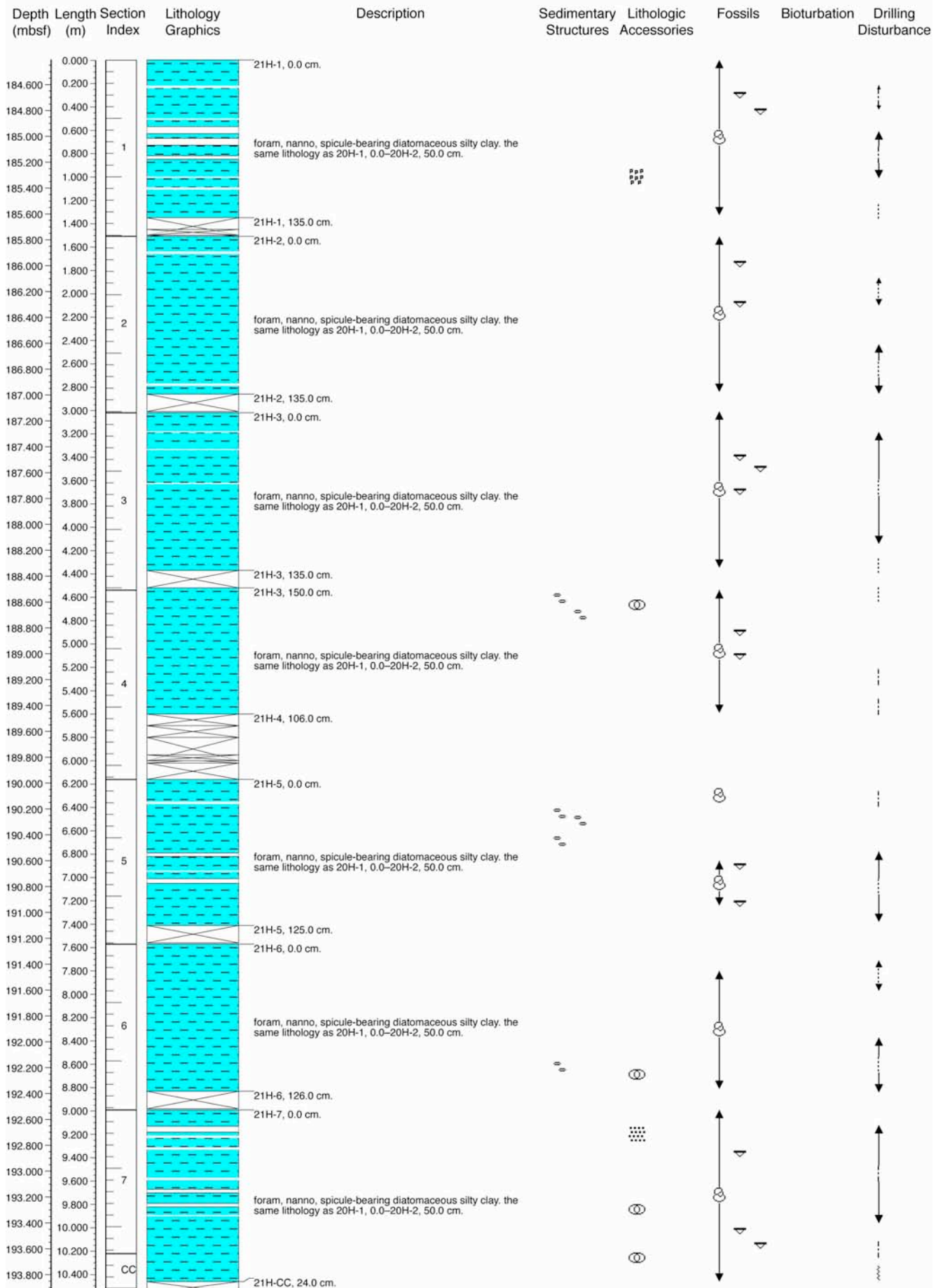
902-C9001C-19H (165.41–174.91 mbsf)



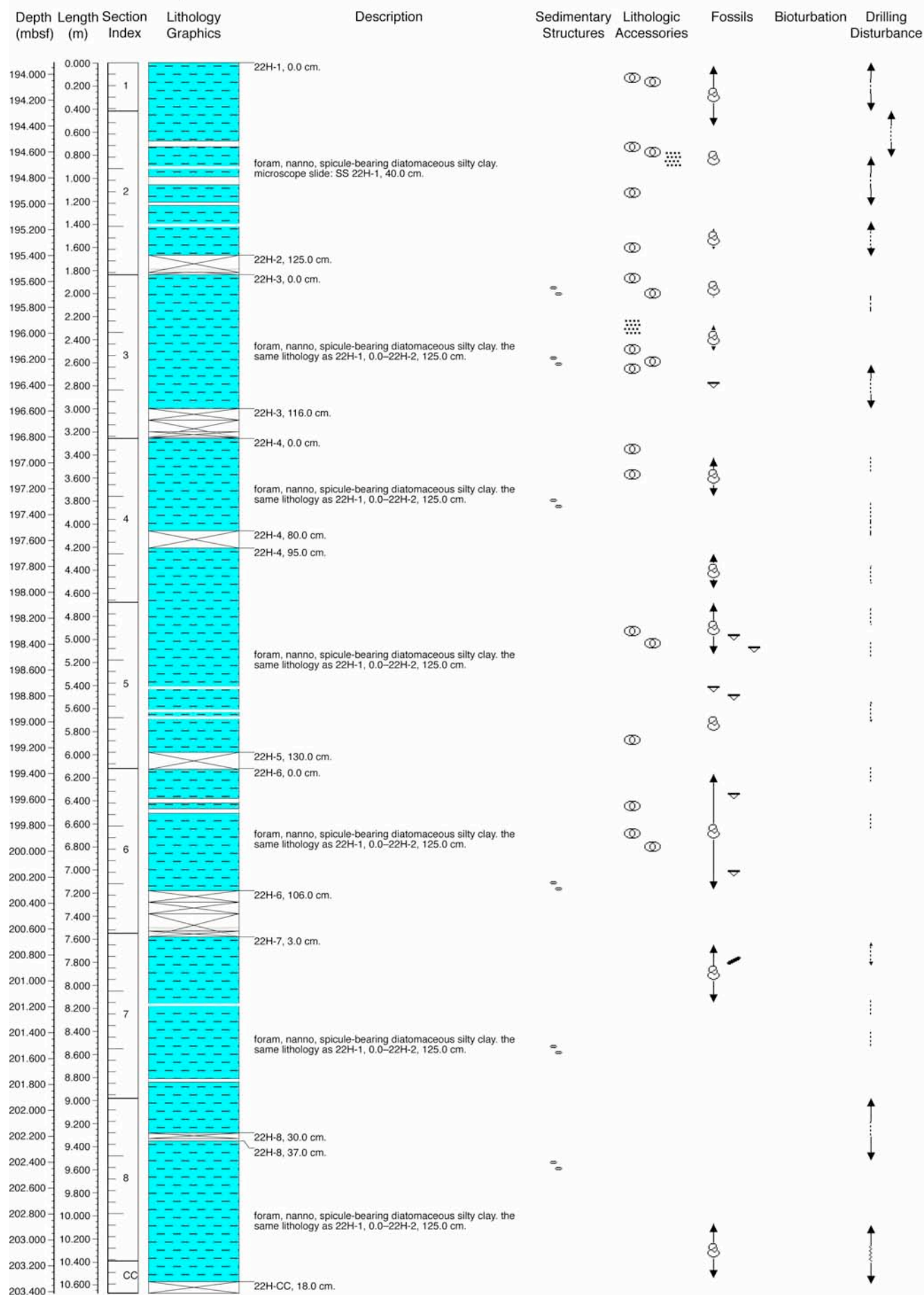
902-C9001C-20H (174.91–184.41 mbsf)



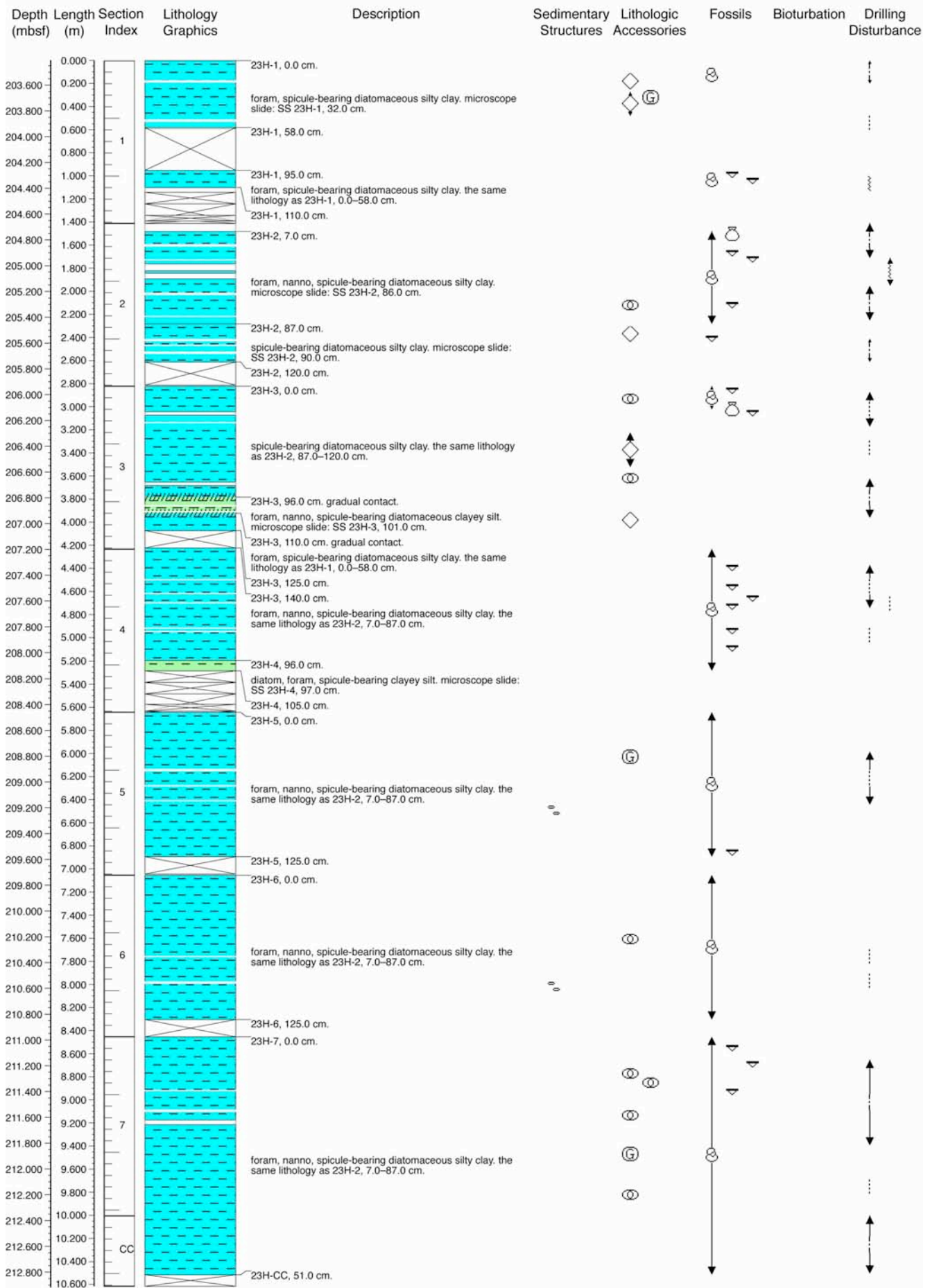
902-C9001C-21H (184.41–193.91 mbsf)



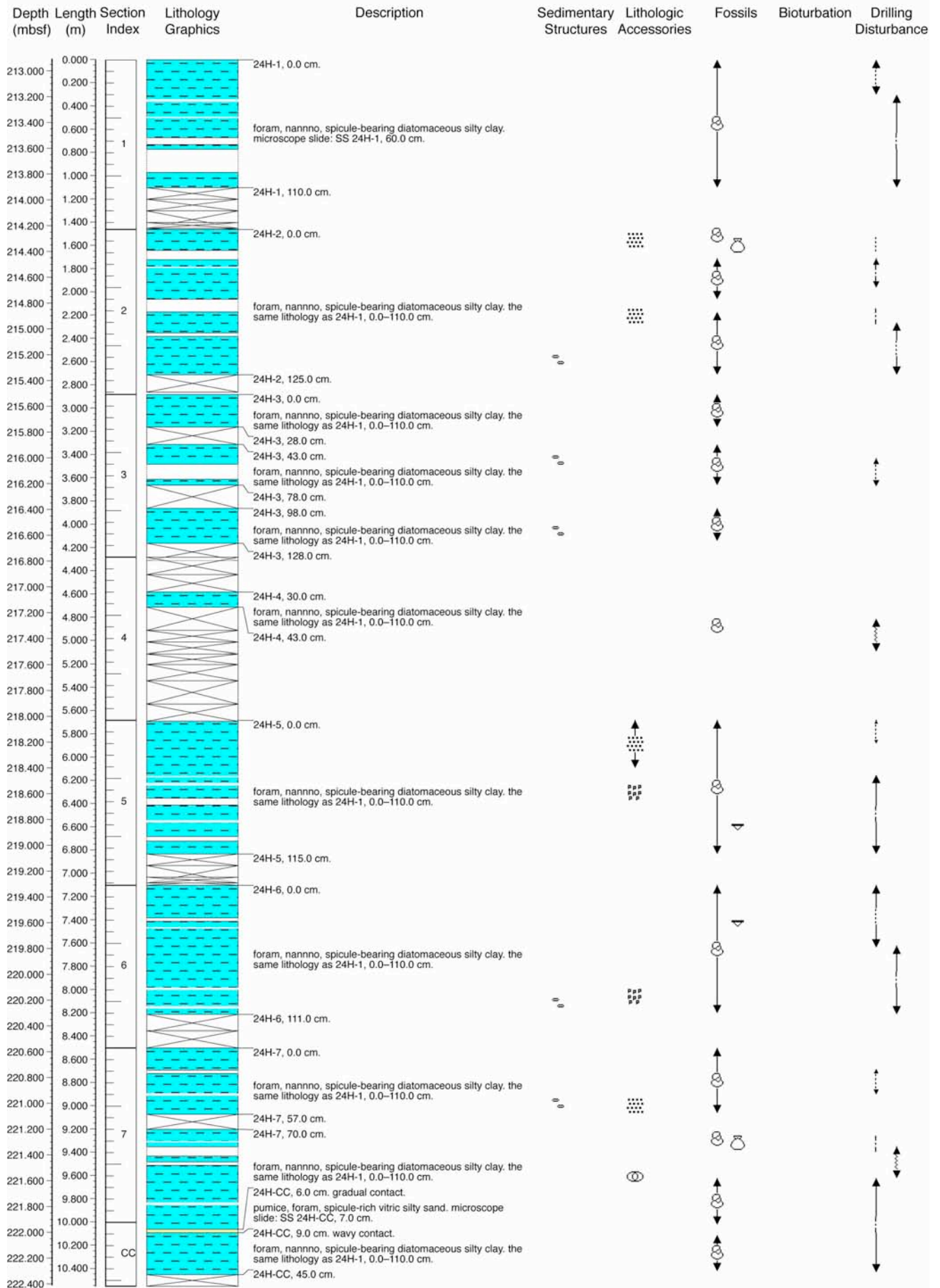
902-C9001C-22H (193.91–203.41 mbsf)



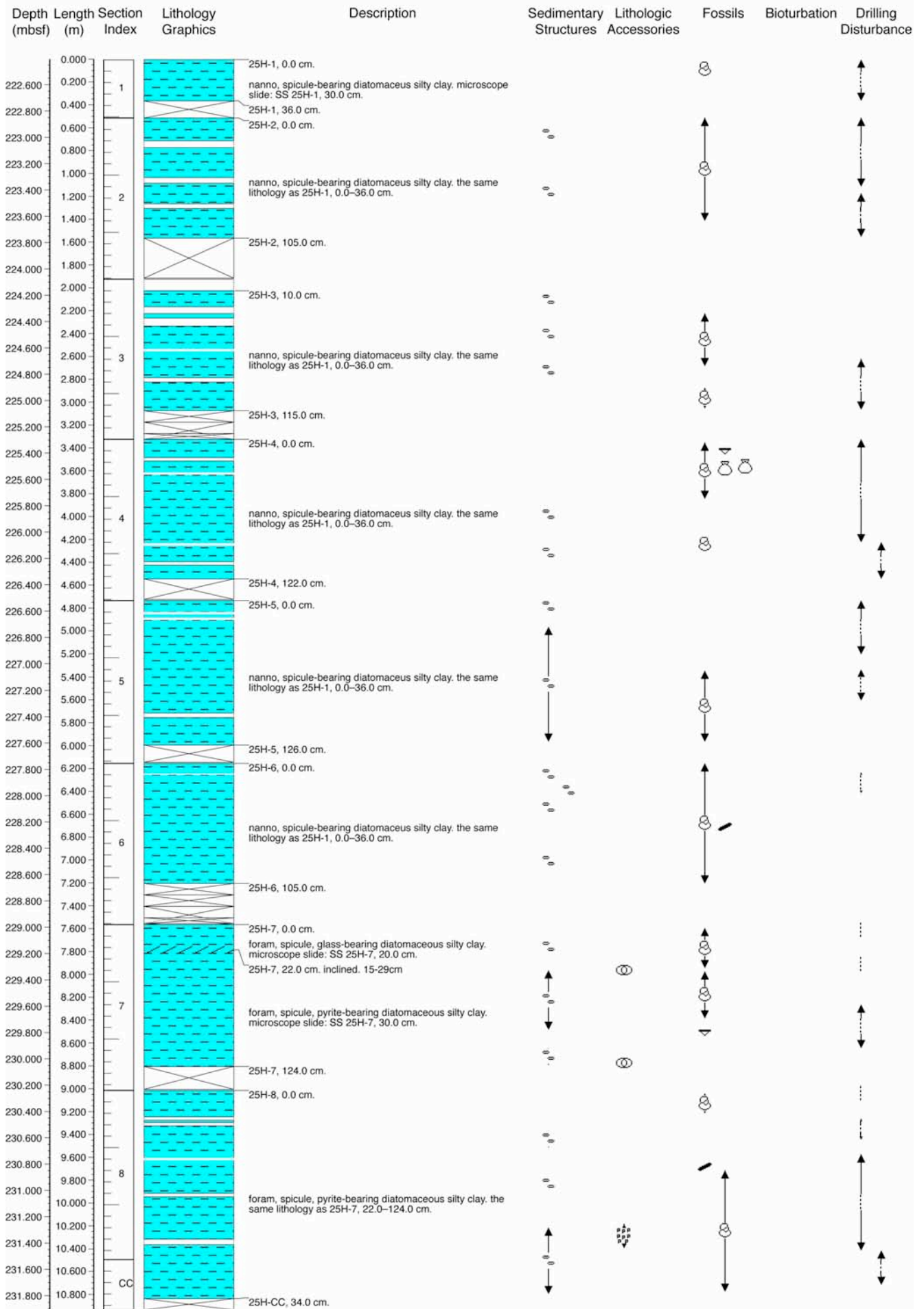
902-C9001C-23H (203.41–212.91 mbsf)



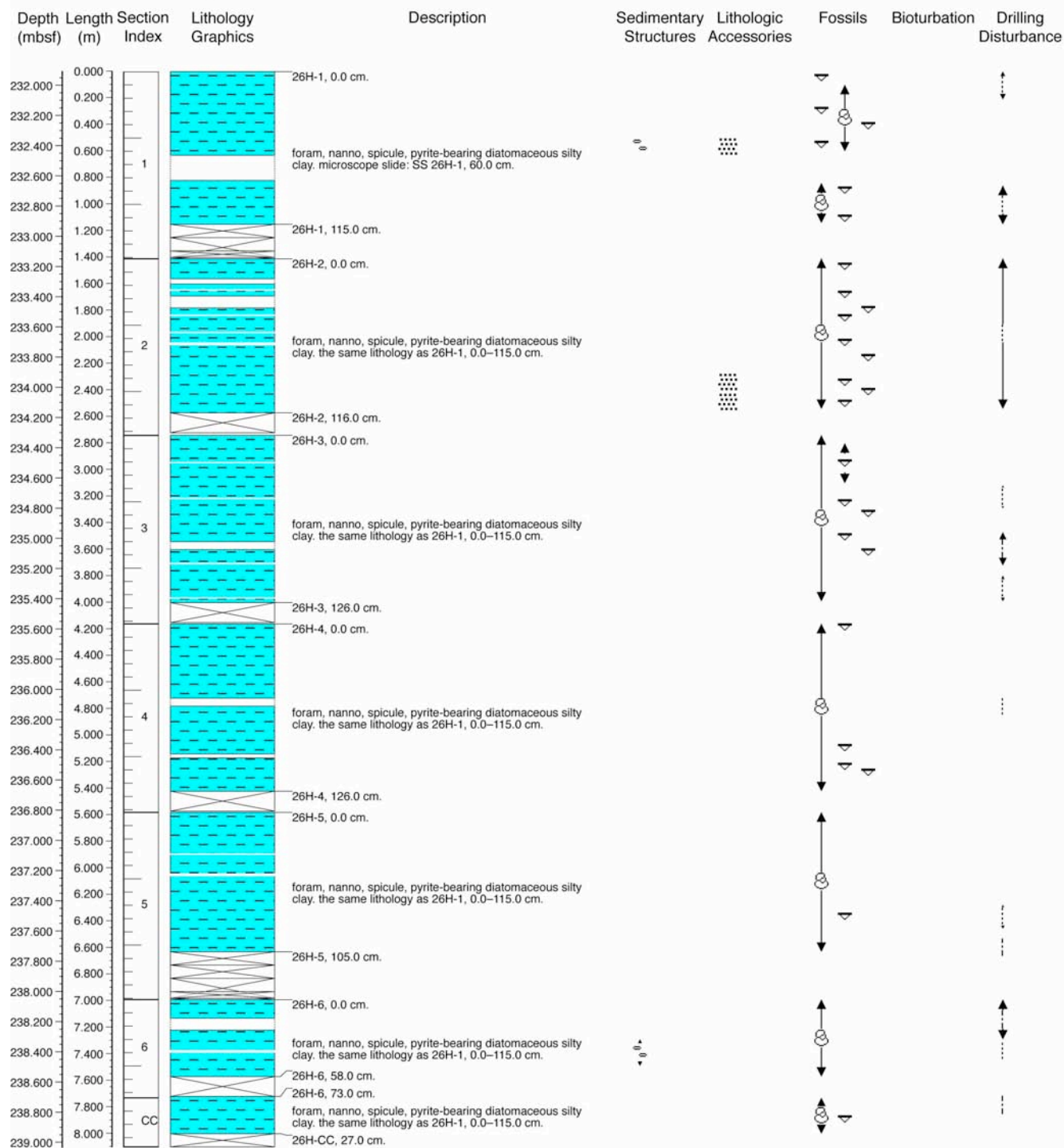
902-C9001C-24H (212.91–222.41 mbsf)



902-C9001C-25H (222.41–231.91 mbsf)



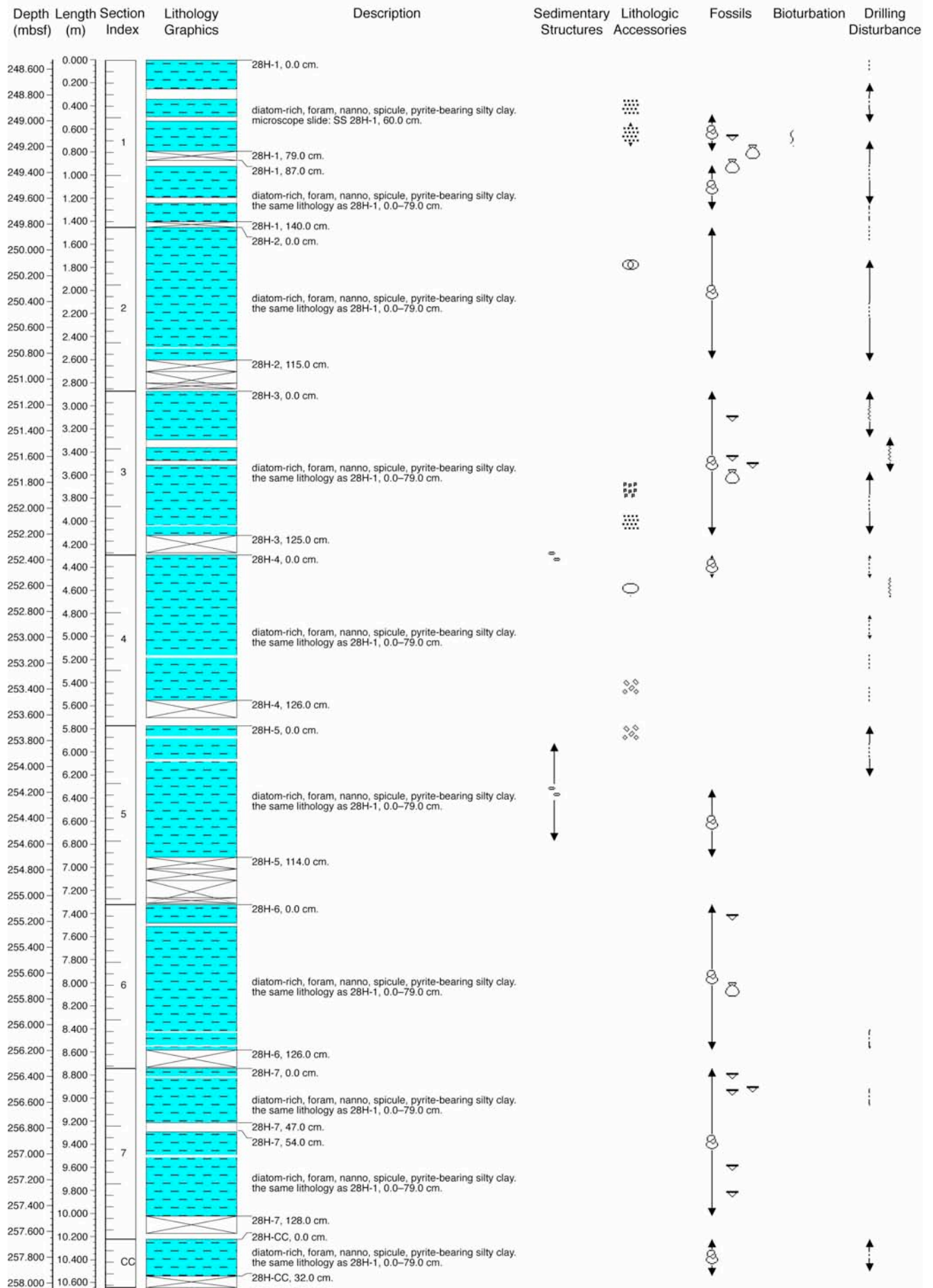
902-C9001C-26H (231.91–239.03 mbsf)



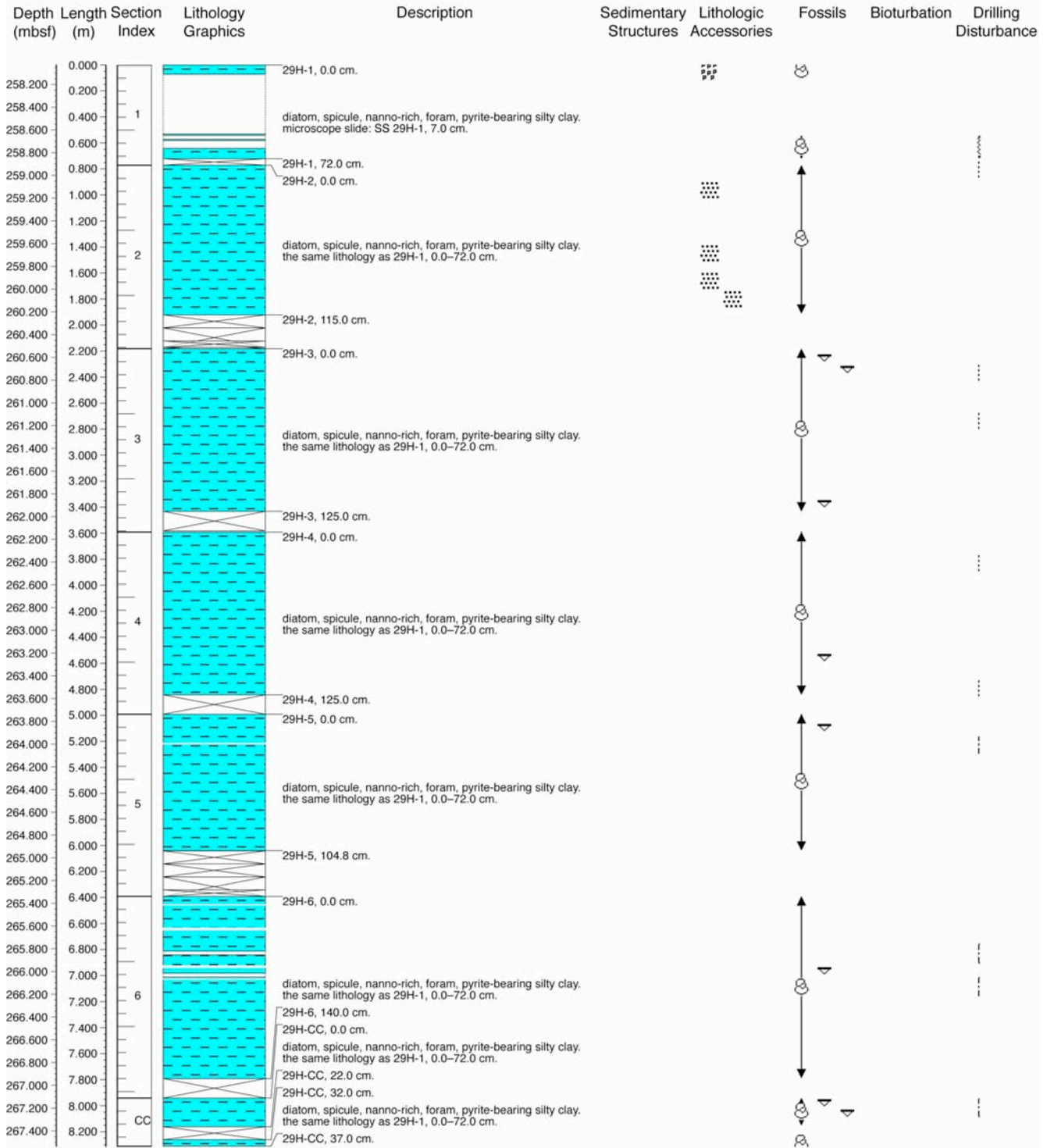
902-C9001C-27H (239.03–248.53 mbsf)



902-C9001C-28H (248.53–258.03 mbsf)



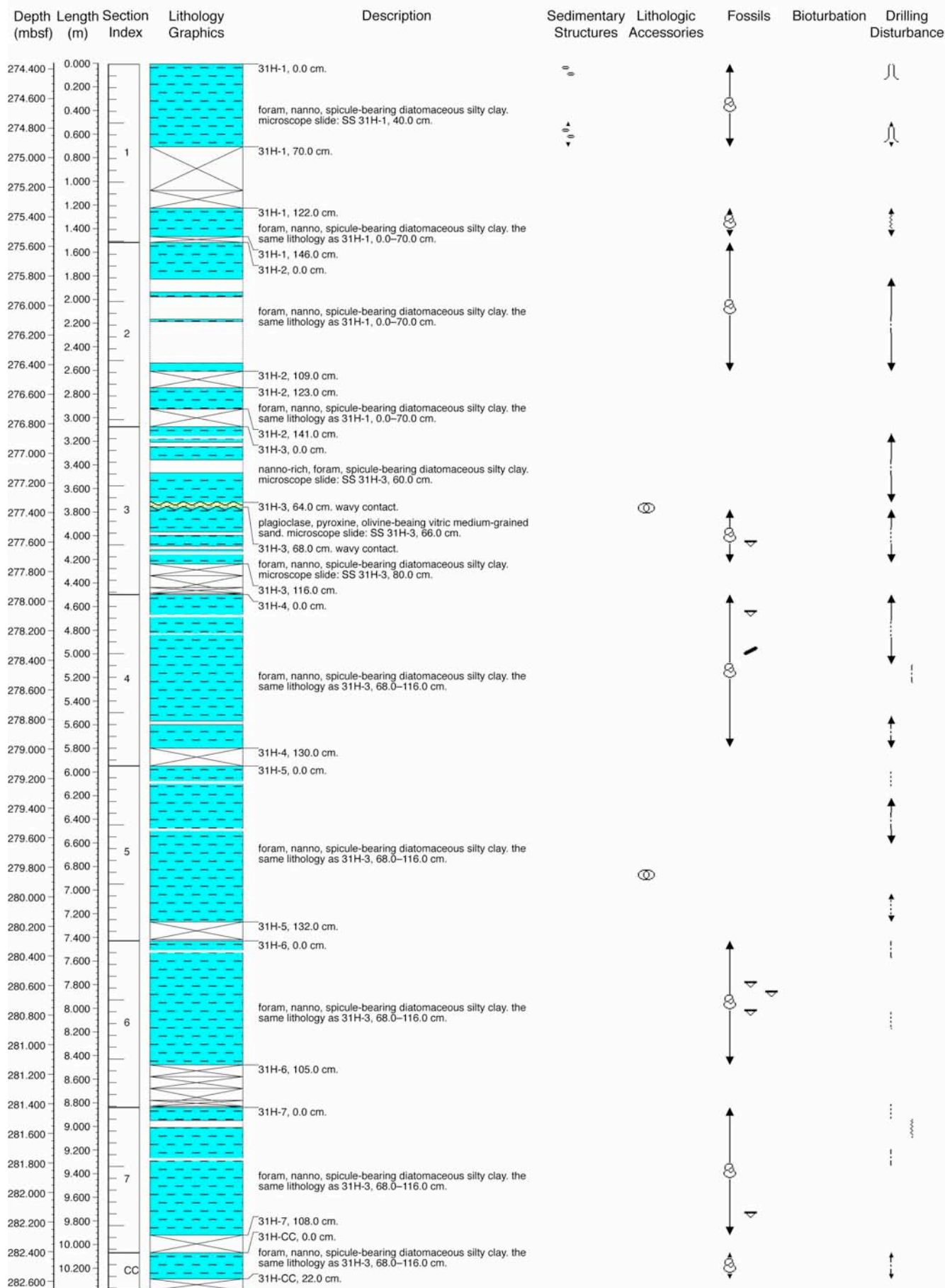
902-C9001C-29H (258.03–267.53 mbsf)



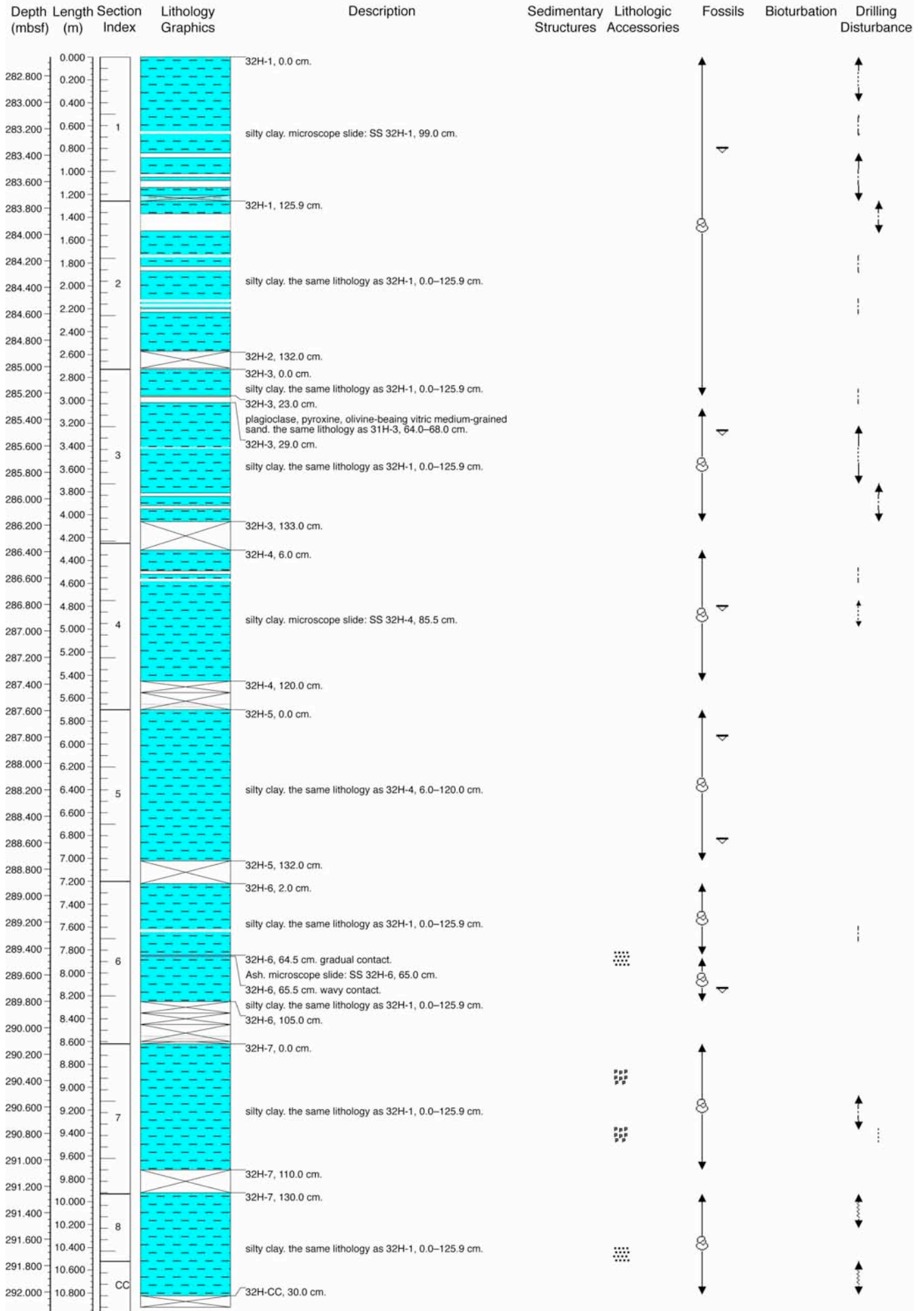
902-C9001C-30H (267.53–274.36 mbsf)



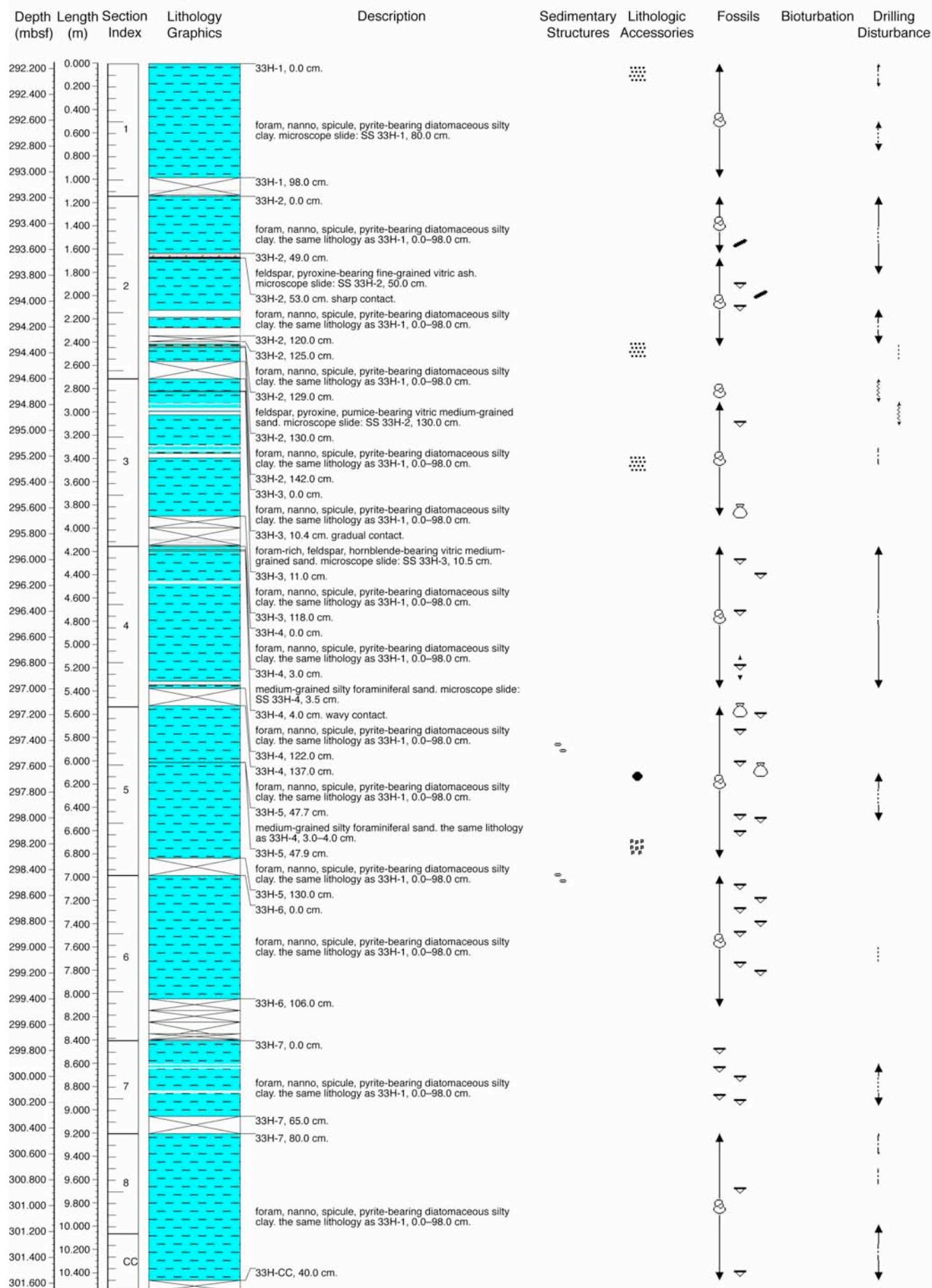
902-C9001C-31H (274.36–282.66 mbsf)



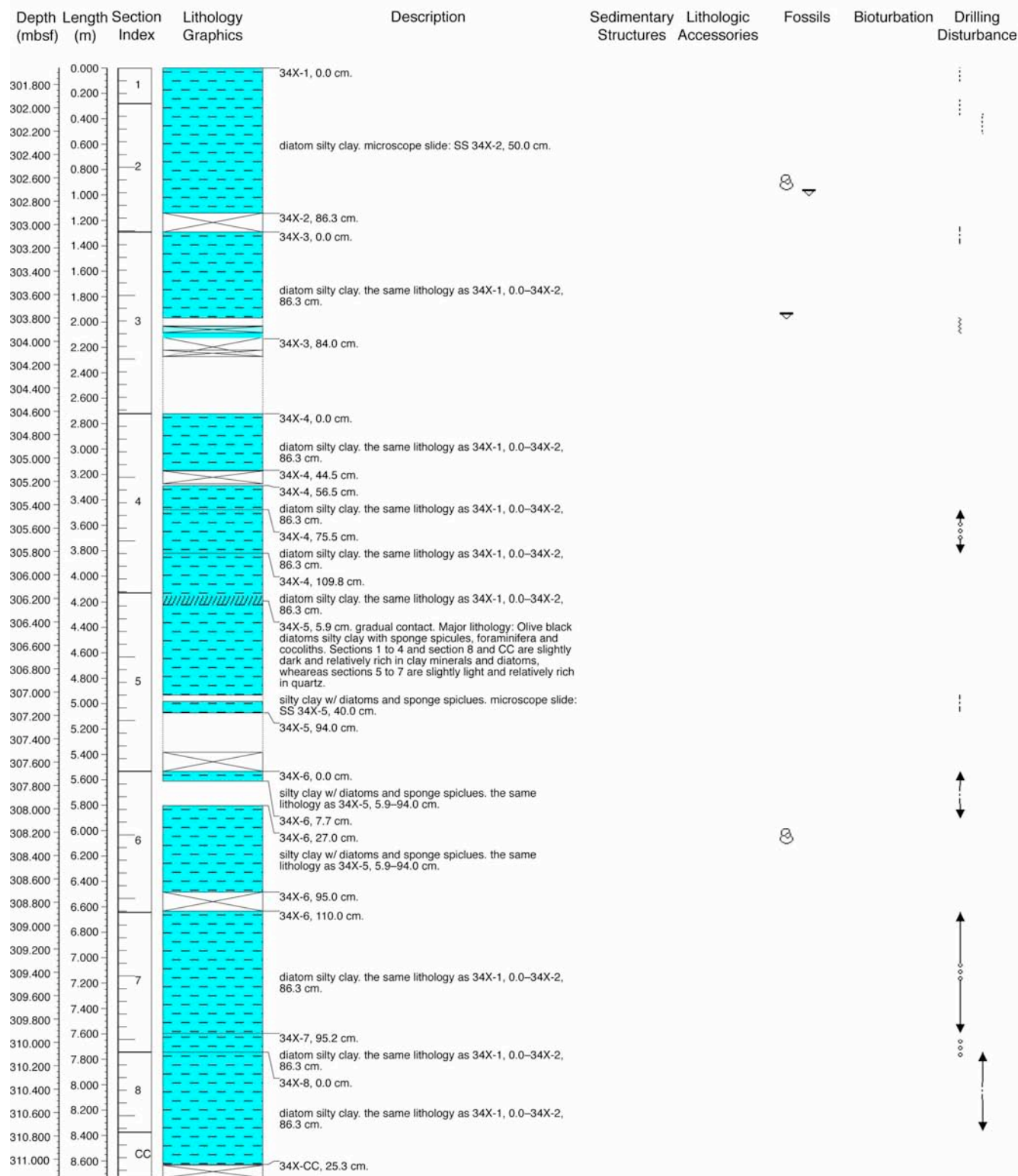
902-C9001C-32H (282.66–292.16 mbsf)



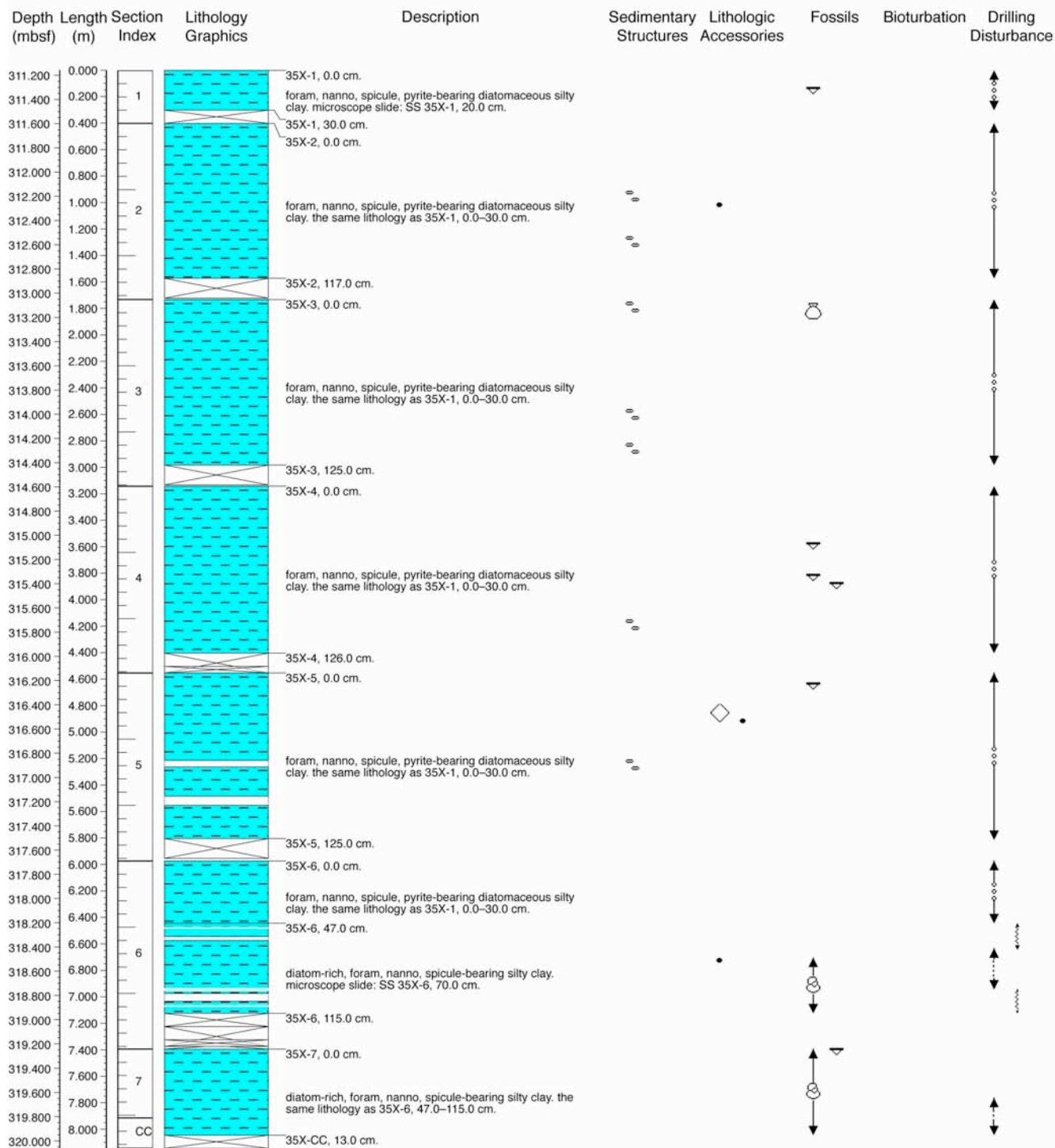
902-C9001C-33H (292.16–301.66 mbsf)



902-C9001C-34X (301.66–311.16 mbsf)



902-C9001C-35X (311.16–320.66 mbsf)



902-C9001C-36X (320.66–330.16 mbsf)

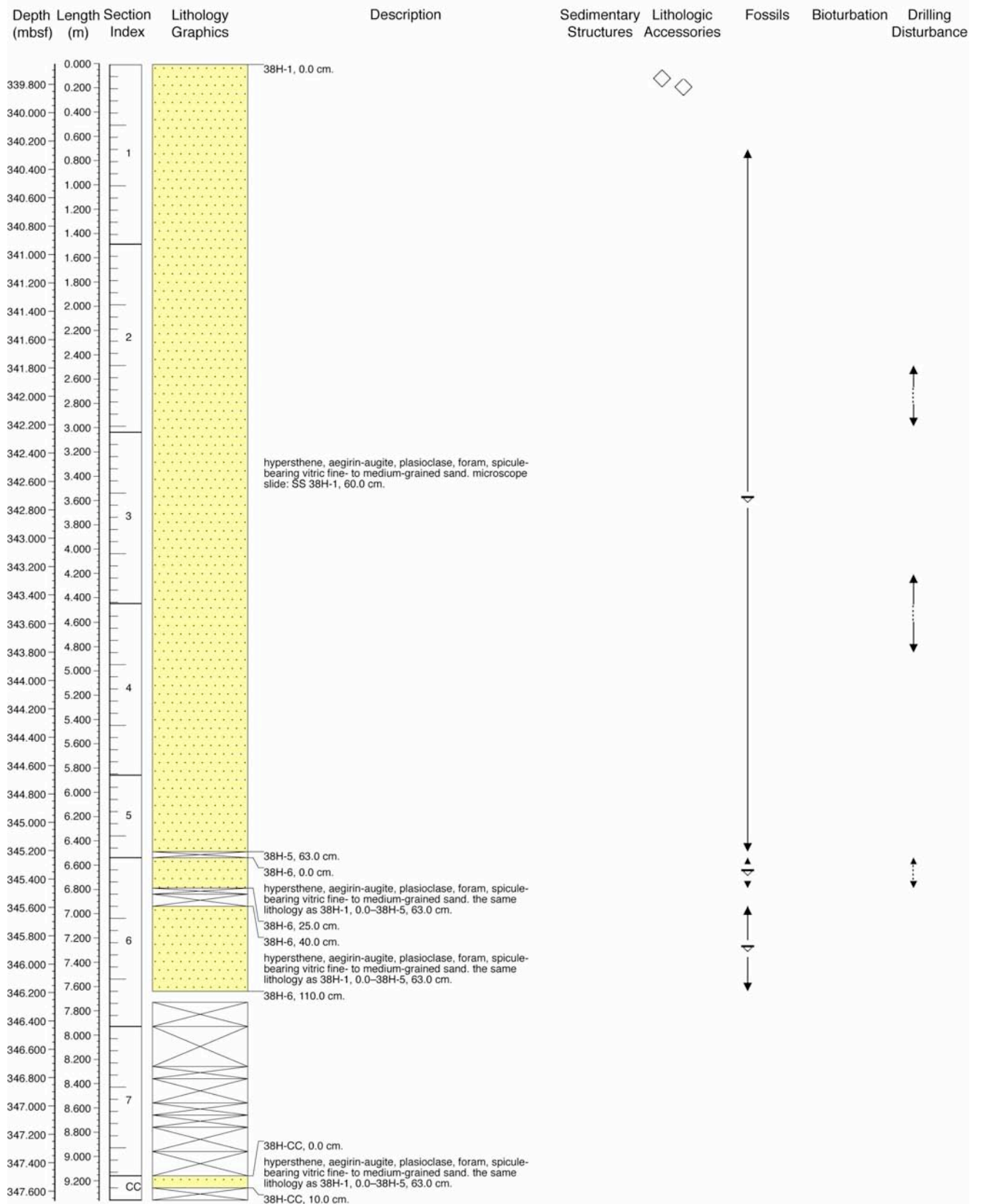
Depth (mbsf)	Length (m)	Section Index	Lithology Graphics	Description	Sedimentary Structures	Lithologic Accessories	Fossils	Bioturbation	Drilling Disturbance
-----------------	---------------	------------------	-----------------------	-------------	---------------------------	---------------------------	---------	--------------	-------------------------

Core Lost

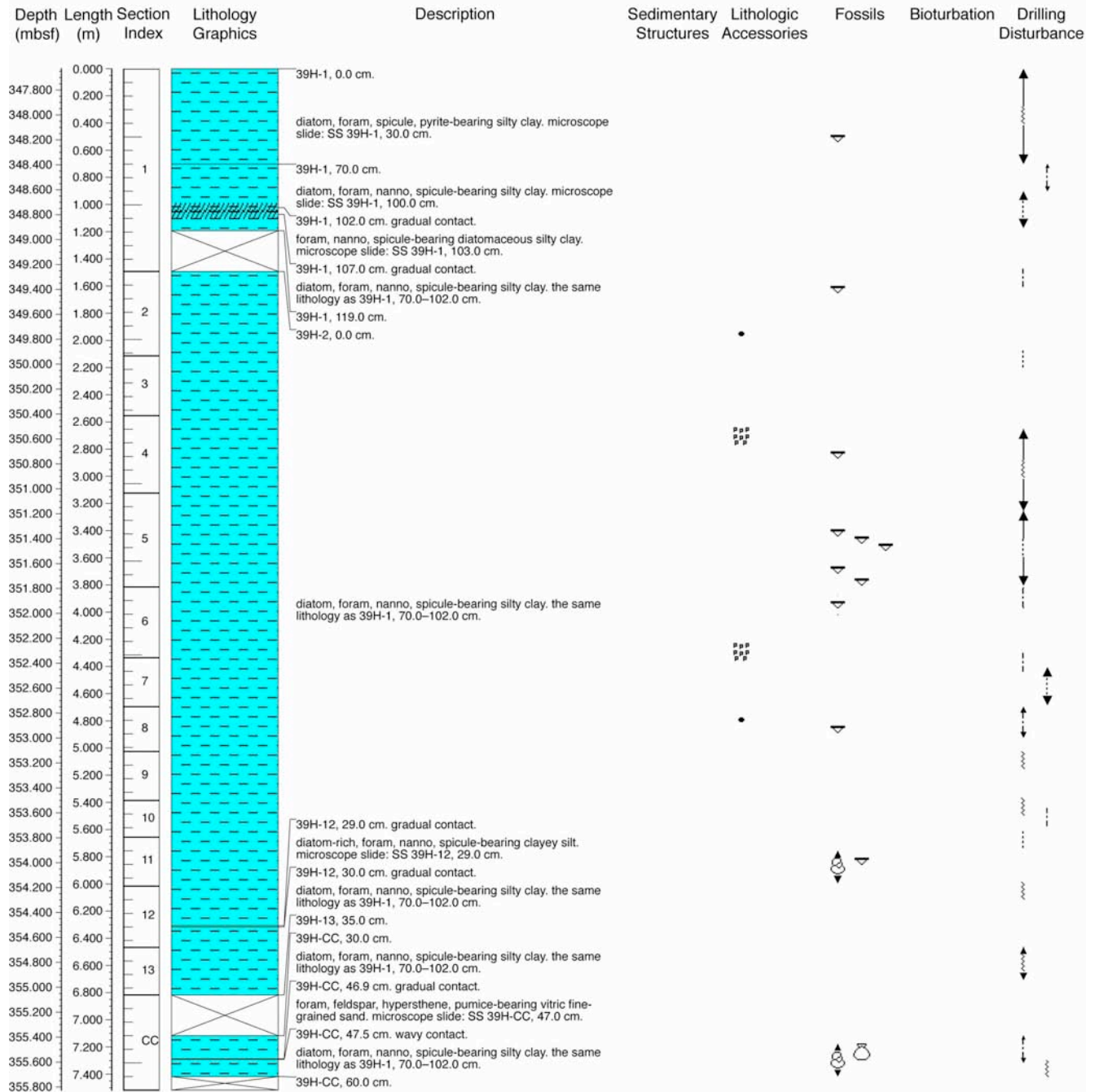
902-C9001C-37X (330.16–339.66 mbsf)

Depth (mbsf)	Length (m)	Section Index	Lithology Graphics	Description	Sedimentary Structures	Lithologic Accessories	Fossils	Bioturbation	Drilling Disturbance
330.200	0.000			37X-1, 0.0 cm.					
330.400	0.200								
330.600	0.400								
330.800	0.600			silty clay w/ diatom. microscope slide: SS 37X-1, 70.0 cm.					
331.000	0.800								
331.200	1.000	1							
331.400	1.200			37X-1, 100.0 cm. gradual contact.					
331.600	1.400			silt. the same lithology as 37X-4, 58.0–79.5 cm.					
331.800	1.600			37X-1, 104.5 cm. gradual contact.					
332.000	1.800			silty clay w/ diatom. the same lithology as 37X-1, 0.0–100.0 cm.					
332.200	2.000			37X-1, 114.0 cm.					
332.400	2.200			37X-2, 0.0 cm.					
332.600	2.400	2		silty clay w/ diatom. the same lithology as 37X-1, 0.0–100.0 cm.					
332.800	2.600								
333.000	2.800								
333.200	3.000			37X-2, 116.0 cm.					
333.400	3.200			37X-3, 0.0 cm.					
333.600	3.400			silty clay w/ diatom. the same lithology as 37X-1, 0.0–100.0 cm.					
333.800	3.600								
334.000	3.800			37X-3, 125.0 cm.					
334.200	4.000			silt. the same lithology as 37X-4, 58.0–79.5 cm.					
334.400	4.200	3		37X-3, 127.0 cm.					
334.600	4.400			silty clay w/ diatom. the same lithology as 37X-1, 0.0–100.0 cm.					
334.800	4.600			37X-4, 48.9 cm.					
335.000	4.800			gradation from silt to silty clay w/ diatom. silt (bottom end lithology). the same lithology as 37X-4, 58.0–79.5 cm. silty clay w/ diatom (top end lithology). the same lithology as 37X-1, 0.0–100.0 cm.					
335.200	5.000			37X-4, 58.0 cm. gradual contact.					
335.400	5.200			silt. microscope slide: SS 37X-4, 75.0 cm.					
335.600	5.400			37X-4, 79.5 cm. sharp contact.					
335.800	5.600			silty clay w/ diatom. the same lithology as 37X-1, 0.0–100.0 cm.					
336.000	5.800	4		37X-4, 125.3 cm.					
336.200	6.000			37X-5, 0.0 cm.					
336.400	6.200			silty clay w/ diatom. the same lithology as 37X-1, 0.0–100.0 cm.					
336.600	6.400			37X-5, 18.5 cm. gradual contact.					
336.800	6.600			silt. the same lithology as 37X-4, 58.0–79.5 cm.					
337.000	6.800			37X-5, 21.3 cm. gradual contact.					
337.200	7.000			silty clay w/ diatom. the same lithology as 37X-1, 0.0–100.0 cm.					
337.400	7.200			37X-5, 26.0 cm. gradual contact.					
337.600	7.400			silt. the same lithology as 37X-4, 58.0–79.5 cm.					
337.800	7.600	5		37X-5, 28.0 cm. gradual contact.					
338.000	7.800			silty clay w/ diatom. the same lithology as 37X-1, 0.0–100.0 cm.					
338.200	8.000			37X-5, 117.0 cm.					
338.400	8.200			37X-6, 0.0 cm.					
338.600	8.400			silty clay w/ diatom. the same lithology as 37X-1, 0.0–100.0 cm.					
338.800	8.600			37X-6, 6.5 cm.					
339.000	8.800	6		silt. the same lithology as 37X-4, 58.0–79.5 cm.					
339.200	9.000			37X-6, 8.7 cm.					
339.400	9.200			silty clay w/ diatom. the same lithology as 37X-1, 0.0–100.0 cm.					
339.600	9.400	CC		37X-CC, 14.0 cm.					

902-C9001C-38H (339.66–347.63 mbsf)



902-C9001C-39H (347.63–355.83 mbsf)



902-C9001C-40H (355.83–365.33 mbsf)

